

**ACNS 2006**

**American Conference  
on Neutron Scattering**

**Sponsored by the  
Neutron Scattering Society of America**

**Hosted by the  
Argonne Intense Pulsed Neutron Source**

**St. Charles, Illinois**

**June 18-22, 2006**

## **On the cover:**

Neutron data obtained with the General Purpose Powder Diffractometer (GPPD) at IPNS showing the phase evolution as a function of oxygen partial pressure of a Sr-Fe-Co mixed (ionic and electronic) conducting oxide membrane material.

**ACNS 2006**

**American Conference  
on Neutron Scattering**

**Sponsored by the  
Neutron Scattering Society of America**

**Hosted by the  
Argonne Intense Pulsed Neutron Source**

**St. Charles, Illinois**

**June 18-22, 2006**



---

**Table of  
Contents**

Welcome .....	1
General Information .....	2
NSSA Information.....	3
Special Thanks .....	3
Satellite Meeting.....	3
Conference Organization .....	4
Transportation to Pheasant Run .....	5
Layout of Pheasant Run Facilities.....	6
Lodging.....	8
Registration .....	8
Travel Reimbursement.....	9
Internet Access .....	9
Breakfasts, Lunches and Breaks .....	9
Receptions and Conference Banquet.....	10
Neutron Scattering Tutorials.....	10
Awards .....	13
Breakout Sessions.....	16
Tour of the IPNS Facility at Argonne National Laboratory.....	17
Neutron Scattering Facility Exhibits.....	17
Vendor Exhibits .....	17
Presenter Information .....	18
Invited Speakers.....	19
Comprehensive Program .....	21
<i>Meeting Schedule</i> .....	22
<i>Program</i> .....	23
Abstracts.....	29
Author Index.....	155
Vendor Ads .....	169



Welcome to the third *American Conference on Neutron Scattering*! Your enthusiastic response reflects the strength of the neutron scattering community in the U.S. and Canada. A total of 326 abstracts were received. Many of these abstracts represent the research work of young scientists, including over 36 abstracts from graduate students who are competing for the *Neutron Scattering Society of America Prize for Outstanding Student Research*.

---

## Welcome

The papers presented in this conference show the diversity in science that is directly impacted by the use of neutron scattering including: biology, chemistry and materials, engineering/applications, instrumentation, soft matter, condensed matter physics and fundamental physics.

Organizing a meeting like this takes an enormous amount of work. We especially wish to express appreciation to the Intense Pulsed Neutron Source for hosting the conference. Art Schultz and Bruce Gaulin have done an outstanding job in organizing the program, Angus Wilkinson has handled all of the finances, and Chuck Prokuski and Tom Worlton together with Maria Heinig have acted as local organizing committee. In addition, Rob Briber and Dave Belanger provided help and guidance based on their experience with ACNS 2004. For a meeting such as this one, these jobs take on a high level of time commitment and organizational ability and our extreme thanks goes to these people for their gargantuan efforts. We would also like to thank all those who have graciously given their time to serve on the meeting program committees and on the NSSA prize committees. Finally, we would like to thank our sponsors, without whom this meeting could not go ahead: the Intense Pulsed Neutron Source at Argonne National Laboratory, the High Flux Isotope Reactor and the Spallation Neutron Source at Oak Ridge National Laboratory, the Los Alamos Neutron Science Center at Los Alamos National Laboratory, the NIST Center for Neutron Research, and the Canadian National Research Council and the Institute for Neutron Scattering for generous financial support.

Most importantly, we express our appreciation to all of you for contributing such a large number of abstracts for oral presentations and posters. The presentation of great science is what makes a great meeting. There will certainly be a lot of great science presented at ACNS 2006. Enjoy the meeting!

### **Roger Pynn**

*President*

*Neutron Scattering Society of America*

### **Simon J. L. Billinge**

*Vice President*

*Neutron Scattering Society of America*

*General Chair of ACNS 2006*

---

## General Information

The third *American Conference on Neutron Scattering (ACNS 2006)* is hosted by the Intense Pulsed Neutron Source at Argonne National Laboratory and will be held at the Pheasant Run Conference Center in St. Charles, Illinois, June 18-22, 2006. The conference is being organized under the auspices of the *Neutron Scattering Society of America (NSSA)* and is sponsored by the North American neutron centers. The ACNS conferences are hosted by one of these centers and held every two years, in years that do not coincide with International Neutron Scattering Conferences.

The ACNS conferences are intended to showcase recent scientific results obtained by neutron scattering in a variety of research fields, including soft and hard condensed matter, biology, chemistry, engineering, geology, materials science, fundamental physics and neutron instrumentation. This is accomplished through a series of plenary, invited and contributed oral presentations as well as posters sessions. At ACNS 2006 several NSSA prizes will be presented to recognize important contributions to the field of neutron scattering. Dr. Jack Carpenter from Argonne National Laboratory will receive the second Cliff Shull prize for his outstanding contributions to neutron scattering; Dr. John Tranquada of Brookhaven National Laboratory will receive the 2006 Prize for Sustained Research; and Dr. Taner Yildirim of the National Institute of Standards and Technology will receive the 2006 Science Prize. The latter two prizes are being awarded for the first time this year. All three of the prize recipients will be giving presentations at ACNS 2006 during the award sessions.

The ACNS meetings are also intended to fulfill many of the objectives of individual facility “users” meetings, replacing multiple smaller meetings with an opportunity for broader interaction that encourages identification of common objectives and community building. Presentations of current and planned instrumentation at the major North American neutron centers will provide a forum for users and prospective users to ask questions and influence the future choices of the centers that provide the facilities which the whole community uses for its work.

The majority of neutron scattering research is publicly funded. For this reason, the neutron scattering community has a particular responsibility to ensure that it communicates clearly with the public and with political decision makers about the actual and potential benefits of neutron scattering research. For the first time at an ACNS meeting, the 2006 conference will feature a session in which such issues are aired for debate. Speakers will explain the ways in which decisions about federal funding are reached and discuss the responsibilities and opportunities that individual scientists have to contribute to the public discourse.

As in past years, the 2006 ACNS meeting particularly encourages the participation of early career scientists and is providing financial support to help defray travel costs for graduate students and postdocs, as well as presenting a prize for the best student poster.

Additional information about the conference is available at the ACNS 2006 web site at <http://acns2006.anl.gov/>.



The Neutron Scattering Society of America (NSSA) was formed in 1992 and is an organization of persons who have an interest in neutron scattering research in a wide spectrum of disciplines. Membership in the society is open to individuals in academia, industry, and government. Graduate students and recent Ph.D.s are especially encouraged to join. There is no cost to be a member, and all members receive a complementary copy of *Neutron News*. The NSSA website is <http://www.neutronsattering.org>. We encourage all conference attendees to stop by the NSSA booth during the ACNS meeting.

---

## **NSSA Information**

### **NSSA Executive Committee**

President	<i>Roger Pynn, Indiana University</i>
Vice-President	<i>Simon Billinge, Michigan State University</i>
Secretary	<i>Suzanne G.E. te Velthuis, Argonne National Laboratory</i>
Treasurer	<i>Angus P. Wilkinson, Georgia Institute of Technology</i>
Membership Secretary	<i>Gregory Smith, Oak Ridge National Laboratory</i>
Members at Large	<i>Shenda M. Baker, Harvey Mudd College</i> <i>John Root, National Research Council of Canada</i> <i>Brent Fultz, California Institute of Technology</i>

The ACNS Conference Committees would like to thank Matt Kwiatkowski and Conrad Zadlo who created the ACNS 2006 web site and abstract submission system. They also provided us with tools and reports which were needed to produce this program book. We would also like to thank Merlyn Faber of IPNS, Emily Young of Pheasant Run, and Felicia Brent and Anita Myers of Conferon. Melyn Faber planned and arranged for most of the audio visual equipment and has provided support in computers and networking. Emily Young was our conference coordinator at Pheasant Run and Felicia Brent and Anita Myers of Conferon have assisted in planning and arranging the conference.

---

## **Special Thanks**

### **The Eighth International Conference on Quasi-Elastic Neutron Scattering**

*June 14 to June 17, 2006 at the Bloomington Convention Center  
in Bloomington Indiana*

The QENS2006 conference will cover all aspects of quasi-elastic neutron scattering in fields ranging from physics to biology, as well as applications, instrumentation, theory and complementary techniques. Contact Moya Wright at [iucfconf@indiana.edu](mailto:iucfconf@indiana.edu).

---

## **Satellite Meeting**

---

## Conference Organization

### Sponsors

The ACNS has received generous support from the following sponsors:

- Spallation Neutron Source, Oak Ridge National Laboratory
- High Flux Isotope Reactor, Oak Ridge National Laboratory
- Canadian Institute for Neutron Scattering, McMaster University and the National Research Council of Canada
- Intense Pulsed Neutron Source, Argonne National Laboratory
- Manuel Lujan Center, Los Alamos National Laboratory
- Department of Commerce NIST Center for Neutron Research
- Indiana University Cyclotron Facility

### Organizing Committee

*General Chair and NSSA Vice-President*

Simon Billinge, Michigan State University

*Program Co-Chairs*

Bruce Gaulin, McMaster University

Arthur Schultz, Argonne National Laboratory

*NSSA President*

Roger Pynn, Indiana University

*NSSA Treasurer*

Angus Wilkinson, Georgia Institute of Technology

*NSSA Past President*

Robert Briber, University of Maryland

*NSSA Past Treasurer*

David Belanger, University of California, Santa Cruz

### Local Organizing Committee

Chuck Prokuski, Argonne National Laboratory

Tom Worlton, Argonne National Laboratory

Maria Heinig, Argonne National Laboratory

### Program Subcommittees

*Biology*

Susan Krueger, National Institute of Standards and Technology

Paul Langan, Los Alamos National Laboratory

P. Thiyagarajan, Argonne National Laboratory

*Chemistry and Materials*

Simon Billinge, Michigan State University

Thomas Koetzle, Argonne National Laboratory

Jack Rush, National Institute of Standards and Technology

*Condensed Matter Physics*

Meigan Aronson, University of Michigan

Charles Majkrzak, National Institute of Standards and Technology

Stephen Shapiro, Brookhaven National Laboratory

### *Engineering/Applications*

Mark Bourke, Los Alamos National Laboratory  
Ronald Rogge, National Research Council Canada  
Xunli Wang, Oak Ridge National Laboratory

### *Fundamental Physics*

Geoffrey Greene, Oak Ridge National Laboratory  
Fred Wietfeldt, Tulane University

### *Instrumentation/Software*

Brent Fultz, California Institute of Technology  
Kenneth Herwig, Oak Ridge National Laboratory  
Paul Sokol, Indiana University

### *Soft Matter*

John Katsaras, National Research Council Canada  
David Londono, DuPont Company  
Michael Mackay, Michigan State University

### ***From O'Hare International Airport***

Take the Northwest Tollway to Rt. 59 south. Continue south on Rt. 59 to North Avenue (Route 64). Go west on North Avenue approximately 3 miles. Pheasant Run is approximately three (3) miles west of Route 59 on North Avenue (Route 64) on the south side of the road.

### ***From Midway Airport***

Take Cicero Avenue north to I-55 south. Go west to I-355 north. Take I-355 north to I-88 west. Go west on I-88 to Farnsworth Ave. north. Take Farnsworth Ave north to North Ave (Route 64). Go east on North Avenue approximately one (1) mile. Pheasant Run is on the south side of the road.

### ***From Chicago***

Take I-290 west to I-88 west. Go west on I-88 to Farnsworth Ave. Take Farnsworth Ave. north to North Ave (Route 64). Go east on North Avenue approximately one (1) mile. Pheasant Run is on the south side of the road.

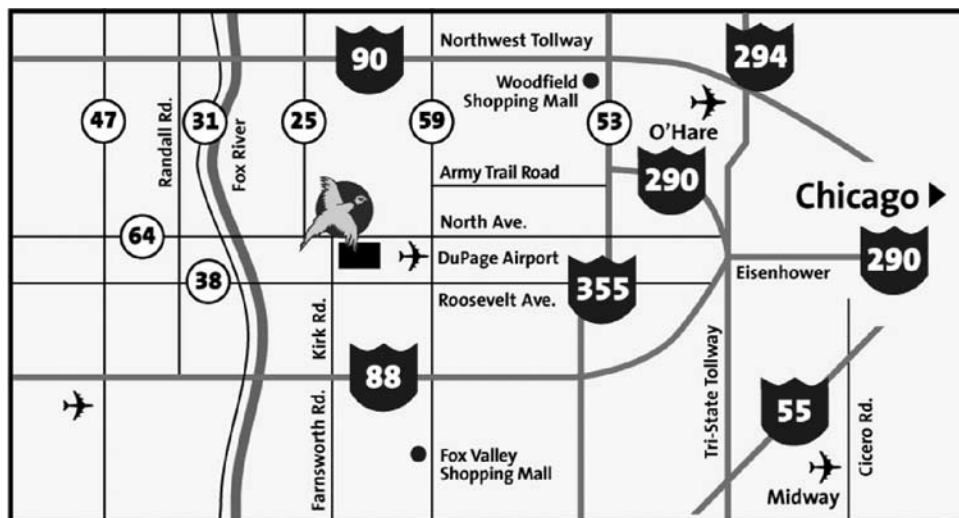
### ***Taxis***

There are many different taxi and limousine services available to get you from the airports to Pheasant Run and back. One company used by some patrons of Pheasant Run is A1 Limousine. Their phone number is 1-800-352-5849. The fare to O'hare is \$42 for the first person, and \$7 for each additional, and the ride takes about 45 minutes. The fare to Midway is \$57 for the first person and \$7 for each additional, and the ride takes about an hour.

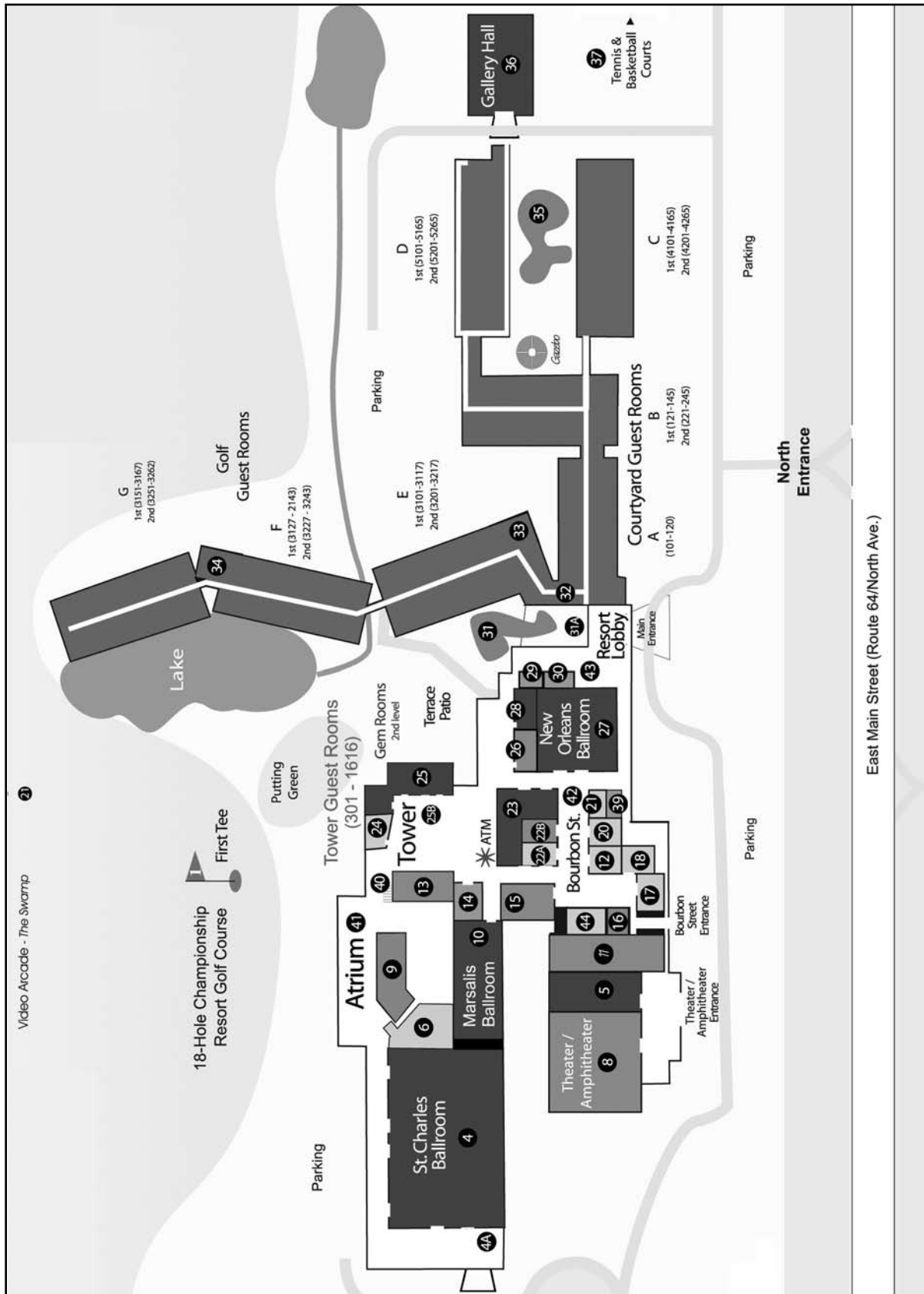
## **Transportation to Pheasant Run**

### ***Pheasant Run Resort***

4051 East Main Street,  
St. Charles, IL 60174  
1-800-474-3272  
[www.pheasantrun.com](http://www.pheasantrun.com)



***Located on North Avenue (Rt. 64) three miles west of Rt. 49***



## Guest Services & Offices

- 43 Activities Desk
- ★ ATM
- 29 Business Center
- 51a Executive Offices
- 38 Expo Center Offices
- 2 Expo Registration Desk
- 14 Food & Beverage Office
- 43 Front Desk
- 39 Hertz Rental Car
- 43 Kids Klub  
(Ask Front Desk for location)
- 30 Solarium Registration
- 51a Sales Office (2nd Floor)
- 44 St. Charles Registration

## Pools

- 9 Atrium Pool / Jacuzzi
- 35 Courtyard Pool
- 31 Indoor/Outdoor Pool

## Dining & Entertainment

- 42 Bourbon Street
- 11 Harvest Restaurant & Lounge
- 13 Clubhouse Lounge
- 15 Lilly's Lounge
- 28 Lucky Pierre's
- 23 Preservation Hall -  
Studio Theater
- 41 Sunday Brunch - Atrium
- 26 Terrace Cafe
- 8 Theater (Mainstage) / Amphitheater
- 16 Zanies Comedy Club

## Meeting Space

- 8 Amphitheater / Mainstage Theater
- 41 Atrium
- 42 Bourbon Street
- 5 Broadway Ballroom: A,B,C  
(Theater - 2nd Floor)
- 38 DuPage Expo Center
- 1 Mega Exposition &  
Conference Center  
Skyboxes
- 36 Gallery Hall  
Cezanne, Chagall, Corot, Gauguin,  
Matisse, Picasso, Rembrandt, Renoir,  
Robert Wood, Utrillo, Van Gogh, Vermeer
- 28 Gem Meeting Rooms  
(Tower - 2nd Floor)  
Coral, Jade, Ruby, Sapphire, Topaz,  
Turquoise A & B
- 8 Golf Meeting Rooms  
Augusta I & II  
Pinehurst I & II
- 34 Legends Meeting Rooms  
Arnold Palmer, Ben Hogan,  
Jack Nicklaus
- 10 Marsalis Ballroom: I & II
- 27 New Orleans Ballroom
- 23 Preservation Hall A&B
- 4 St. Charles Ballroom  
Salons I, II, III, IV, V, VI
- 44 St. Charles Registration
- 28 Terrace Boardroom

## Guest Rooms

- Courtyard Guest Rooms
- Golf Guest Rooms
- Tower Guest Rooms

## Recreation & Shopping

- 22a Art Gallery  
Orleans Street Gallery
- 18 Box Office - Ticket Master
- 40 Fitness Center & Locker Rooms  
(Tower - Lower Level)
- 12 Flower Shop - Designs, Etc.
- 17 Gift Shop - Thieve's Market
- 24 Golf Pro Shop
- 6 Hair Salon & Spa  
Mario Tricoci
- 44 Ice Cream Shop -  
Ben & Jerry's (coming 2006)
- 20 Jewelry/Gift Shop  
Tesoro's Boutique
- 32 Library
- 37 Tennis & Basketball Courts
- 21 Video Arcade - The Swamp

---

## Lodging

All technical sessions for ACNS 2006 will be held at the Pheasant Run Resort and Conference Center in St. Charles, IL. For detailed information on the meeting rooms, etc., see the **“Meeting Venue”** link on the ACNS web site, <http://acns2006.anl.gov/>. Plenary sessions will be held in the New Orleans Ballroom, and meals, exhibits, and poster sessions will be held in the St. Charles Ballroom. Parallel sessions will be held in the Amphitheater, New Orleans Ballroom, and the Gem rooms in the tower second floor. See the resort map or interactive online map for meeting room details.

We recommend that all attendees stay at Pheasant Run for the nights of the conference. Rooms for Sunday night through Wednesday night at Pheasant Run can be arranged at the Conference rate through the ACNS registration web site or by telephone or fax to Conferon at 330-425-9330 (8:30am - 5:00pm M-F EST), fax 330-963-0319 or email [NSSA@conferon.com](mailto:NSSA@conferon.com).

The conference rate for the hotel is \$99 single/double occupancy, plus applicable taxes. Room rates include wireless internet connection in all sleeping rooms and public spaces, excluding the hotel meeting rooms. Access and membership to the resort fitness center and all swimming pools during the stay is also complimentary. Rooms provide coffee and bottled waters during the stay, and complimentary USA Today (Monday-Friday). Parking is free in the hotel parking lots. Check in time is 4 pm, but guests may be checked in earlier if rooms are ready. Check out time is 12 pm.

---

## Registration

Registration for the 2006 American Conference on Neutron Scattering until June 1, 2006 was through the conference web site at <http://acns2006.anl.gov/>. Any additional registration after that date needs to be made on site at Pheasant Run and will incur a \$25 fee in addition to the normal registration fee. The normal registration fee is \$150 for students and \$400 for non-students. Cancellations received prior to June 1 are fully refundable. No refunds will be given for cancellations after that date. All cancellations must be in writing.

All registrants will receive a badge, a copy of the program book, a complimentary copy of Neutron News, a bag with the ACNS logo, and a USB memory device containing the program. Registration entitles attendees to the Sunday night reception, breakfast Monday through Thursday, lunch Monday through Wednesday, and daily refreshment breaks. Refreshments will also be served at the Monday night poster session. Each attendee will be issued two drink tickets for the Sunday reception and for the Monday poster session. Each ticket will entitle the attendee to a bottle of beer, a glass of wine, a soft drink, or a bottle of water. Tickets will only be good for the specified event.

On-site registration will be available at the Solarium registration desk on Sunday from 1 pm to 9 pm or at the St. Charles information desk on Monday through Wednesday from 9 am to 6 pm. No partial registration is offered.

Invited speakers and attendees who have been offered, in writing, partial support of their travel expenses should contact the information booth at the conference to obtain a travel reimbursement form. We anticipate being able to offer support of up to \$800 per person towards eligible travel and registration expenses. All attendees must have registered for the meeting and receipts must be provided for airline tickets, ground transportation, hotel, registration etc. along with proof of your identity and current address (driver's license etc.).

Questions concerning travel support may be directed to  
Prof. Angus Wilkinson (angus.wilkinson@chemistry.gatech.edu).

Wireless internet access will be available in all guest rooms at Pheasant Run as well as in the public areas as part of our contract with the hotel. Internet access will not be available in the meeting rooms. Please contact the hotel information desk if you have difficulty connecting to the network in your room. If you have no computer and need to access your electronic mail, there will be some computers in the ACNS office area that you can arrange to use.

Continental breakfast will be available daily Monday through Wednesday starting at 7:30 AM in the St. Charles Ballroom, and Thursday starting at 7:30 AM in the New Orleans Ballroom. Buffet lunch will be available in the St. Charles Ballroom Monday and Tuesday at 12:15 PM and Wednesday at 12:00 PM. Beverages and light snacks will be available for mid-morning and mid-afternoon breaks Monday through Wednesday.

---

## **Travel Reimbursement**

---

## **Internet Access**

---

## **Breakfasts, Lunches and Breaks**



---

## Receptions and Conference Banquet

### Receptions

There will be an evening welcome reception Sunday in the New Orleans Ballroom from 7:00 PM to 9:00 PM. There will also be a reception Monday evening from 8:00 PM to 10:00 PM in the St. Charles Ballroom concurrent with the poster session.

### Conference Banquet

The conference banquet will be held Tuesday evening in the Ginkgo Dining Room at the Morton Arboretum in Lisle, Illinois, beginning at 7:30 PM. Buses will begin departing Pheasant Run for the Arboretum at 6:15 PM. Ride time is about 30 minutes. The Arboretum features over 41,000 species of trees and plants from over 50 countries, and provides a beautiful, relaxing setting for the dinner. For more information, visit [www.mortonarb.org](http://www.mortonarb.org).

There will be three choices available for the dinner:

1. Grilled filet mignon with cabernet reduction
2. Stuffed chicken breast with apples and brie cheese
3. Layered eggplant with portabella mushrooms, spinach and red pepper coulis sauce

Wine and beer will also be served. Ticket prices are \$50.00 full fare, \$25.00 for students and \$60.00 for guests. Tickets are available online at [www.acns2006.anl.gov](http://www.acns2006.anl.gov) or at the registration desk on Sunday and Monday, contingent upon a maximum limit of 300 banquet attendees.

The Arboretum is located at 4100 Illinois Route 53 in Lisle, Illinois. If you are driving from Pheasant Run, turn left out of the lot and take North Ave. west one mile to Kirk Rd., turn left (south) on Kirk and proceed 8 miles to I88, which is a tollway. Be sure to bring coins for tolls. Take I88 eastbound about 11 miles and follow signs onto southbound I-355 and exit immediately to westbound Ogden Ave. (Route 34). Continue west on Ogden to Route 53 north. Proceed north less than one mile to the Arboretum entrance.

---

## Neutron Scattering Tutorials

We have arranged three tutorials to be held on Sunday, June 18, at Pheasant Run. Each tutorial is limited to 30 participants on a first come first serve basis. Please note the prerequisites on the tutorial descriptions before notifying the presenters that you are interested in attending. Please contact the presenters via the email links in the Tutorial Descriptions below, to notify them of your interest in attending or if you have questions.

It is Conference policy that tutorial participants will be asked to purchase their own food, refreshments, and coffee for breaks and lunch. There is a café and restaurant on the premises.



## **Neutron Scattering Fundamentals and Instrumentation as a Probe of Materials on the Nanoscale**

### **Contact and Information**

Mike Kotlarchyk  
Department of Physics, Rochester Institute of Technology  
mnksps@rit.edu, 585-475-6115

### **Description**

This is an intensive full-day tutorial that presents the basic background for understanding interactions between slow neutrons and materials, and describes a variety of neutron scattering instruments and techniques available to researchers in materials-related scientific and engineering disciplines. The presentation is primarily aimed at students and post-doctoral researchers who are relatively new to the field of neutron scattering. The tutorial will consist of a sequence of lectures delivered by researchers in various areas. Lecture notes from the tutorial will be made available to the participants.

### **Other Information**

Because of the rather ambitious scope of the tutorial material, it has been decided that incorporating hands-on computer exercises is difficult due to time constraints. Instead, presenters, at times, may briefly demonstrate some of the useful software modules available to participants for use outside of the tutorial. Therefore, bringing a laptop computer is not a requirement.

### **Tutorial Topics**

*Tutorial Overview/Interaction of Thermal Neutrons with Matter*  
(M. Kotlarchyk, RIT)

*Small-Angle Neutron Scattering (SANS)—Nanometer-Scale Structure*  
(B. Hammouda, NIST)

*Dynamic Structure Factors*  
(M. Kotlarchyk, RIT)

*Inelastic Scattering—Experimental*  
(C.K. Loong, Argonne National Laboratory)

*Quasielastic Neutron Scattering (QENS)—Molecular-Scale Dynamics*  
(K.W. Herwig, ORNL)

*Neutron Spin-Echo (NSE) Spectroscopy—Nanosecond-Scale Dynamics*  
(A. Faraone, NIST)

## **Magnetic Structure Analysis from Neutron Powder Diffraction Data Using GSAS**

*Presenters: Robert Von Dreele, Brian H. Toby, Laurent Chapon,  
and Bryan Chakoumakos*

Modeling and fitting magnetic scattering from powder diffraction data can provide unique information not easily available by other techniques.

Although the resulting magnetic spin lattice may not be unambiguous, it provides an important first step for magnetic structure analysis. Two approaches are used in the field for describing magnetic models: color space groups and representational analysis (“irreps”), with the latter method being more general, but more difficult to learn. Both approaches will be introduced, but this tutorial will concentrate on how to use color space groups within the GSAS software package for modeling and fitting of commensurate magnetic structures with neutron powder diffraction data.

Knowledge of crystallographic symmetry and Rietveld analysis is a prerequisite for obtaining any value from this tutorial. It will also be assumed that attendees have a basic familiarity with the GSAS package.

The tutorial will be in two parts: a series of lectures and an optional hands-on exercise.

1. Origins of magnetic scattering
2. Color symmetry & Shubnikov space groups
3. Magnetic extinctions classes & common magnetic structure types
4. Overview of representational analysis & FullProf implementation
5. Defining magnetic structures in GSAS
6. Viewing magnetic structures (possible)

Participants who wish to perform the hands-on exercise should bring a laptop for their own use. Windows and Macintosh software for the tutorial will be provided via CDROM and memory stick. Linux users will need to download files in advance; contact Brian Toby for information.

## **Neutron Scattering for Materials Study**

*Presenters: Peter K. Liaw and Hahn Choo , Department of Materials Science and Engineering, Rm. 427-B and 318, Dougherty Engineering Building, The University of Tennessee, Knoxville, Tennessee 37996-2200 Campus ext: 865-974-6356 and 3643, fax: 865-974-4115*

The application of neutron diffraction in studying engineering materials becomes increasingly important due to its unique ability to provide the microscopic information concerning the microstructural features and mechanical behaviors of advanced materials and composites. This tutorial will provide a forum for the presentation and discussion of recent experimental and modeling results.

### **Topics**

- Fundamentals of Neutron Studies – Ian Anderson
- Engineering Diffraction – Ron Rogge
- Small Angle Diffraction – Xun-Li Wang
- Theoretical Modeling – Mark Daymond
- Neutron Diffraction Applications – Cam Hubbard
- Neutron Studies of Materials Behavior – Don Brown



*Dr. John Carpenter*

**Dr. John M. Carpenter** is the recipient of the 2006 Clifford G. Shull prize of the Neutron Scattering Society of America with the citation:

*"For seminal contributions to the development of neutron sources and instrumentation that have had world-wide impact on neutron scattering across a broad range of scientific disciplines, culminating in the optimized design of the Spallation Neutron Source at Oak Ridge."*

The Neutron Scattering Society of America (NSSA) established the Clifford G. Shull Prize in Neutron Science to recognize outstanding research in neutron science and leadership promoting the North American neutron scattering community. The prize is named in honor of Prof. Clifford G. Shull, who received the Nobel Prize in 1994 with Prof. Bertram Brockhouse for seminal developments in the field of neutron science. The establishment of the prize was announced at the inaugural American Conference on Neutron Scattering (ACNS) in 2002.

The nominations were reviewed by a committee of experts in the field of neutron science and the NSSA is pleased to announce that the 2006 recipient of the Shull Prize is Dr. John M. Carpenter, Intense Pulsed Neutron Source Division of the Argonne National Laboratory. The prize and \$5000 honorarium will be awarded at the 2006 ACNS, St. Charles, IL, June 18-22, 2006 (<http://acns2006.anl.gov/>).

Dr. John (Jack) Carpenter has been a pivotal figure in the development of the next generation of neutron sources world-wide. Jack's work pioneered exploitation of the inherent efficiency of the spallation process for the production of neutrons together with the advantages of pulsed operation and time-of-flight measurements for the study of structure and dynamics of materials. His patented design for the moderator-reflector combination is at the heart of modern neutron source design and his creativity in matching the characteristics of neutron sources to the demands of the instrumentation and ultimately the scientific drivers continue to serve as an example to the international community. Jack's demonstrations of the advantages of the spallation process for neutron production led to the development of the Intense Pulsed Neutron Source at Argonne and KEK in Japan, the success of which paved the way for facilities such as ISIS in the United Kingdom and the Lujan Center at Los Alamos. The success of these facilities led to proposals for more advanced pulsed source facilities such as the Spallation Neutron Source (SNS) at Oak Ridge National Laboratory, AUSTRON in Austria, J-PARC (a KEK and JAERI collaboration) in Japan and the ESS project in Europe.

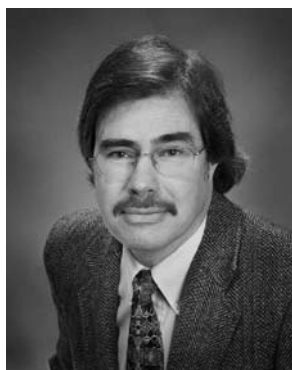
With a design power of 1.4 MW and an upgrade path to more than 2 MW, the SNS is DOE's flagship facility for neutron research and it will become the leading neutron facility worldwide when fully instrumented. It is fair to say that the US would not now be devoting \$1.4B to the construction of the

---

## Awards

SNS were it not for the groundbreaking work by Dr. Carpenter over a long productive career. In addition to his contributions to source technology, Jack has made seminal contributions to the development of pulsed source instrumentation such as focusing algorithms for time-of-flight powder and single crystal diffractometers and the design of converging multi-aperture collimator for SANS. Indeed Jack's emphasis on the coupled optimization of neutron source performance characteristics and instrument design has greatly increased our ability to exploit pulsed neutron sources as tools for a broad range of scientific endeavor. Jack's advice on technical and strategic issues is widely sought and his input into the design of the SNS, as well as new sources in Japan and Europe, has been invaluable.

In summary, his pioneering development of modern spallation neutron sources, their targets, the decoupled moderator reflector concept, cryogenic moderators, and time-of-flight instruments in general establish Jack Carpenter as a pivotal figure for the present and future of neutron scattering in North America and throughout the world.



*Dr. John Tranquada*

**Dr. John Tranquada** is the recipient of the 2006 Sustained Research Prize of the Neutron Scattering Society of America with the citation:

*"For his outstanding neutron scattering studies of the charge and spin ordering in the high  $T_c$  cuprates and related materials"*

The Neutron Scattering Society of America (NSSA) established the Sustained Research Prize to recognize a sustained contribution to a scientific subfield, or subfields, using neutron scattering techniques. Consideration is given to the impact

that the candidate's neutron scattering results have had on the subfield. Preference is given to applicants whose work was carried out predominantly in North America.

The nominations were reviewed by a committee of experts in the fields to which neutron scattering contributes and the NSSA is pleased to announce that the 2006 recipient of the Sustained Research Prize is Dr. John Tranquada, Leader of the Neutron Scattering Group at Brookhaven National Laboratory. The prize and a \$2,500 honorarium will be awarded at the 2006 ACNS, St. Charles, IL, June 18-22, 2006 (<http://acns2006.anl.gov/>).

Dr. Tranquada entered the field of neutron scattering in the late 1980s. Almost immediately he made important contributions to the field of high  $T_c$  superconductors. Indeed, his first paper in the field, which demonstrated antiferromagnetic order in the cuprate  $\text{YBa}_2\text{Cu}_3\text{O}_{6.8}$ , received over 500 citations. This observation provided a clear indication that the underlying antiferromagnetic order in the copper-oxygen planes is a characteristic common to all the cuprates. Subsequently, in a series of experiments performed in the mid-nineties, Tranquada and his co-workers

laid the experimental foundations for a revolution in our understanding of charge and spin ordering in strongly correlated materials. This work and Tranquada's subsequent explanation of the charge and spin phenomenology, has had a tremendous and sustained impact in the field of strongly correlated electron physics. It is universally recognized as one of the defining bodies of work in this field. Dr. Tranquada definitively established his impact on the field of superconductivity by conducting many of the critical experiments leading to the discovery of magnetic "stripes" that formed the basis of much of the theoretical work on the relationship of these stripes to superconductivity.

Dr. Tranquada is currently the Head of the Neutron Scattering Group at the Department of Energy's Brookhaven National Laboratory (BNL) on Long Island. In this capacity he has been responsible for overseeing the transition of this group to a new role following the closure of the High Flux Beam Reactor at Brookhaven. His group now functions as a scientific "user" group both at facilities within the U.S. and in Europe and Japan as well being heavily involved with designing an instrument providing new capabilities for the forthcoming Spallation Neutron Source at Oak Ridge National Laboratory. Tranquada's outstanding contributions to neutron scattering science have been previously recognized by the award of Fellowship in the American Physical Society and with the award of the BNL Research and Development Award, both in 1997.



*Dr. Taner Yildirim*

**Dr. Taner Yildirim** is the recipient of the 2006 Science Prize of the Neutron Scattering Society of America with the citation:

*"For his innovative coupling of first principles theory with neutron scattering to solve critical problems in materials science"*

The Neutron Scattering Society of America (NSSA) established the Science Prize to recognize a major scientific accomplishment or important scientific contribution within the last five years using neutron scattering techniques. Preference is given

to applicants whose work was carried out predominantly in North America.

The nominations were reviewed by a committee of experts in the scientific areas to which neutron scattering contributes, and the NSSA is pleased to announce that the 2006 recipient of the Science Prize is Dr. Taner Yildirim, from the NIST Center for Neutron Research. The prize and a \$2,500 honorarium will be awarded at the 2006 ACNS, St. Charles, IL, June 18-22, 2006 (<http://acns2006.anl.gov/>).

One of the hallmarks of neutron scattering, a powerful analytic method used in scientific research, is the inherent simplicity of the scattering process itself. This simplicity makes possible direct comparisons of theoretical calculations of the expected scattering with experimental observations

that can yield a wealth of information about the microscopic properties and structures of a wide variety of technologically important materials. Dr. Taner Yildirim, who is one of a very few neutron scattering practitioners possessing both strong theoretical skills and deft experimental talents, has used his unusual talents to couple theory and experiment closely and interactively to an unprecedented degree. He has the rare ability to make testable predictions about the properties of materials while simultaneously formulating elegant explanations of experimentally observed quantities in systems ranging from novel superconductors to high-capacity hydrogen storage materials. The power of Dr. Yildirim's approach, and the scientific insight that can be derived from it, is exceptionally well illustrated by a recent study of the important superconductor  $\text{MgB}_2$ , which has the highest transition temperature of any conventional superconductor. Dr. Yildirim combined first-principles calculations with neutron measurements to demonstrate that the high transition temperature is the result of a particularly anharmonic vibration of the atoms that couples strongly to the electronic states in the system. His results explain not only the origin of the large value of the superconducting transition temperature, but its pressure dependence as well. More recently Dr. Yildirim employed this approach to the problem of hydrogen storage and discovered ways to enhance the uptake of, and the capacity for, hydrogen in a variety of materials including alanates and carbon nanotubes. These results offer the promise of addressing what is widely considered to be the most serious obstacle in the road to the hydrogen economy.

Dr. Yildirim is currently the Team Leader for Computational Neutron Scattering at the National Institute of Standards and Technology Center for Neutron Research in Gaithersburg, Maryland. His outstanding contributions have been previously recognized by the NIST Chapter of Sigma Xi, which awarded him its Outstanding Young Investigator Award in 2002, and by the Department of Commerce, which awarded him a Bronze medal in 2005.

---

## Breakout Sessions

The afternoon of Wednesday, June 21, is being set aside to accommodate breakout sessions requested and organized by groups that want to plan, organize and discuss specific projects such as the development of a specific neutron instrument, data collection or analysis systems, etc. The topics of the breakout sessions are listed in the program, and the agendas will be distributed by the session organizers. All breakout sessions will run in parallel beginning at 4:15 pm in the designated rooms.

A tour of the IPNS facility at Argonne is planned for Thursday morning, June 22. Buses will be leaving Pheasant Run at 8:45 AM after breakfast. The ride to Argonne is about 35 minutes. IPNS is celebrating their 25<sup>th</sup> year of operation in 2006, and after the tour, there will be a brief ceremony followed by a buffet lunch. For those who wish to return to Pheasant Run, buses will depart Argonne at 1:30 PM. There will also be buses departing for the airports at the same time. Visitors to Argonne need to fill out the form on the ACNS website and be granted access approval before attending the tour.

Exhibit booths from each of the major neutron scattering facilities in North America will be located in the St Charles Ballroom Monday through Wednesday. These facilities are:

- Spallation Neutron Source, Oak Ridge National Laboratory
- High Flux Isotope Reactor, Oak Ridge National Laboratory
- Canadian National Research Council and the Institute for Neutron Scattering
- Intense Pulsed Neutron Source, Argonne National Laboratory
- Manuel Lujan Center, Los Alamos National Laboratory
- Department of Commerce NIST Center for Neutron Research

Exhibits from seven vendors will be available in the St. Charles Ballroom Monday through Wednesday.

Those vendors are:

**Blake Industries, Inc.**

660 Jerusalem Road  
Scotch Plains, NJ 07076  
1-908-233-7240  
email: blake4xray@worldnet.att.net

**Oxford Instruments**

300 Baker Avenue  
Suite 150  
Concord, MA 01742  
Rick Hapanowicz: 847-590-9581  
hapanowicz@ma.oxinst.co  
www.oxford-instruments.com1-

**Toshiba Electron Tubes  
& Devices Co., Ltd.**

1-1-1 Shibaura, Minato-ku  
Tokyo, 105-8001, Japan  
+81-(3) 3457-4870  
Hiroshi Saito  
email: hiroshi3.saito@toshiba.co.jp  
www.toshiba-tetd.co.jp/tetd/eng/

**Euro Collimators Ltd.**

T Booth works  
Elmstone Hardwicke  
Cheltenham, GL51 9TB  
United Kingdom  
+44 (0) 1242 242806  
email: sales@eurocollimators.com  
www.eurocollimators.com

**Kurt J. Lesker Company**

1925 Worthington Ave.  
Clairton, PA 15025  
John Lubic – 1-412-387-9200  
1-800-245-1656  
email: neutron@lesker.com

---

## **Tour of the IPNS Facility at Argonne National Laboratory**

---

## **Neutron Scattering Facility Exhibits**

---

## **Vendor Exhibits**



**Wiener Plein & Baus Elektronik**

300 E. Auburn Avenue  
Springfield, OH 45505  
1-937-324-2420  
email: sales@wiener-us.com  
www.wiener-us.com

**GE Energy**

1631 Bently Parkway South  
Minden, NV 89423  
phone: 1-775-215-2292  
fax: 1-775-215-2864

---

## **Presenter Information**

### **Oral Presentations**

Contributed oral presentations are 12 minutes plus 3 minutes for questions. Invited presentations are 25 minutes plus 5 minutes for questions. A computer projector will be available in each room for projecting PowerPoint presentations or Adobe pdf presentations. An overhead projector can be arranged by special request, but we encourage speakers to use the computer projectors. Speakers should bring their presentation on a USB drive or CD. Each room will also be equipped with a notebook computer with a CD-ROM, a USB port, and the following software installed:

- Windows XP
- Microsoft Office 2003
- Adobe Acrobat Reader 7.0
- Windows Media Player

We prefer that all computer-based presentations be in Microsoft PowerPoint 2000, or later, format. We prefer that speakers use the laptop provided by the ACNS and load their presentation onto the computer prior to the beginning of the session. If there is some reason the speaker wishes to use their own laptop, the staff will assist them in connecting to the projector. If presenters have additional technical requests, they should contact Tom Worlton at [tworlton@anl.gov](mailto:tworlton@anl.gov). The computers available in the Legends meeting rooms will have similar software to those in the Conference areas, and will be available for the speaker to check compatibility of the speaker's presentation with the available software.

### **Posters**

Poster sessions will be in the St. Charles Ballroom and poster spaces will be identified by number. Posters should be available for viewing in the morning prior to the start of the oral sessions so that they are available for viewing during the entire day. The presenter should stand by the poster throughout the Poster session. Posters should be attached with push pins, which will be provided. Dimensions of the usable poster display area are about 45 inches high by 45 inches wide.

Set up times for the posters.

Monday evening session: Set up no later than lunchtime on Monday

Tuesday morning session: Set up during breakfast time on Tuesday

Wednesday morning session: Set up during breakfast time on Wednesday

Posters should be taken down in the evening so that poster boards are available for the first session of the following morning.



### **Plenary Speakers:**

P. Dehmer (U.S. Department of Energy)  
J. Carpenter (Argonne National Laboratory)  
M. Arai (J-PARC)  
A. Taylor (Rutherford Appleton Laboratory)  
R. Pynn (Indiana University)  
T. E. Mason (Oak Ridge National Laboratory)  
G. Lander (Institute of Transuranium Elements)  
J. M. Tranquada (Brookhaven National Laboratory)  
T. Yildirim (NIST Center for Neutron Research)

---

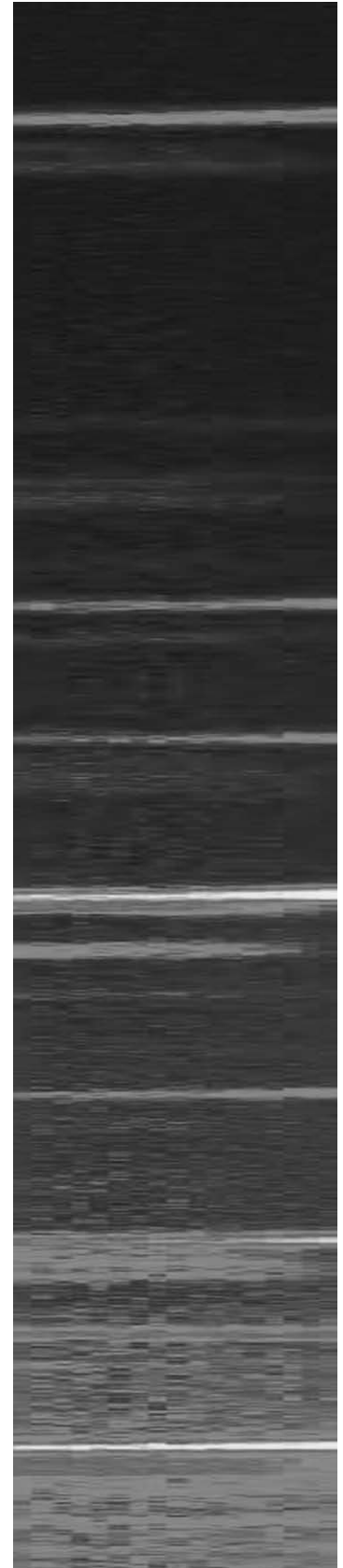
### **Invited Speakers**

### **Invited Speakers:**

R. Cava (Princeton University)  
G. Xu (Brookhaven National Laboratory)  
O. P. Vajk (NIST Center for Neutron Research)  
D. E. Moncton (Massachusetts Institute of Technology)  
D. V. Baxter (Indiana University Cyclotron Facility)  
N. Kucerka (NRC Chalk River Laboratories, Canada)  
T. A. Harroun (Brock University)  
J. E. Curtis (National Institute of Standards and Technology)  
D. G. Lynn (Emory University)  
T. Yildirim (NIST Center for Neutron Research)  
C. Y. Jones (Hamilton College)  
M. R. Eskildsen (University of Notre Dame)  
S. Kivelson (Stanford university)  
L. Clapham (Queen's University, Kingston, Canada)  
D. W. Brown (Los Alamos National Laboratory)  
M. R. Fitzsimmons (Los Alamos National Laboratory)  
G. L. Strycker (University of Michigan)  
R. Ham-Su (Defence R&D Canada – Atlantic)

Z. Feng (Oak Ridge National Laboratory)  
W. M. Snow (Indiana University, Bloomington)  
P. R. Huffman (North Carolina State University)  
V. Garcia Sakai (University of Maryland)  
N. Balsara (University of California, Berkeley)  
H. Lee (University of California, Davis)  
J. M. Lawrence (University of California, Irvine)  
D. Worcester (University of Missouri Biological Sciences)  
M. S. Kent (Sandia National Laboratories)  
C. J. Benmore (Argonne National Laboratory)  
L. Liu (Massachusetts Institute of Technology)  
T. M. Giebultowicz (Oregon State University)  
S. G. E. te Velthuis (Argonne National Laboratory)  
G. D. Smith (University of Utah)  
D. Louca (University of Virginia)  
G. J. Bunick (University of Tennessee, Knoxville)  
C. Dealwis (University of Tennessee, Knoxville)  
A. Zheludev (Oak Ridge National Laboratory)  
S. Lee (University of Virginia)  
H. Choo (University of Tennessee)  
R. Wenk (University of California, Berkeley)  
C. A. Tulk (Oak Ridge National Laboratory)  
G. P. Felcher (Argonne National Laboratory)  
G. Christou (University of Florida)  
H. M. Ronnow (Laboratory for Neutron Scattering,  
ETH Zurich and PSI Village)  
M. B. Stone (Oak Ridge National Laboratory)  
M. M. McKerns (California Institute of Technology)  
M. Nieh (NRC Chalk River Laboratories)  
B. J. Frisken (Simon Fraser University)

# Comprehensive Program



## Meeting Schedule

	Sunday	Monday	Tuesday	Wednesday	Thursday
<b>Morning</b>	Neutron scattering tutorials	Continental breakfast  Welcome and Keynote Speakers  Cliff Shull Prize Lecture  Break  Parallel scientific sessions	Continental breakfast  Neutron facilities – world wide status  Break  Parallel scientific sessions  Poster session	Continental breakfast  NSSA Sustained Research Prize Lecture  NSSA Science Prize Lecture  Break  Poster Session	Continental breakfast  Tour of the Argonne IPNS
		Lunch	Lunch	Lunch: Student awards Neutron advocacy discussion	Lunch at Argonne National Laboratory
<b>Afternoon</b>	Neutron scattering tutorials  Conference registration	Parallel scientific sessions  Breaks  Parallel scientific sessions	Parallel scientific sessions  Break  Parallel scientific sessions	Parallel scientific sessions  Break  Breakout sessions	Buses depart for Pheasant Run and airports
	Evening Welcome Reception	Student research award poster session	Conference banquet	Open	

## Sunday, June 18

---

## Program

- 9:00 am – 5:00 pm    **Neutron Scattering Tutorials**
- Neutron Scattering Fundamentals and Instrumentation as a Probe of Materials on the Nanoscale**  
Organizer: M. Kotlarchyk (*Jade Room*)
- Magnetic Structure Analysis from Neutron Powder Diffraction Data Using GSAS**  
Organizers: R. Von Dreele and B. Toby (*Coral Room*)
- Neutron Scattering for Materials Study**  
Organizers: P. K. Liaw and H. Choo (*Sapphire Room*)
- 1:00 pm – 8:30 pm    **Conference Registration**
- 7:00 pm – 9:00 pm    **Evening Welcome Reception** (*New Orleans Ballroom*)

## Monday, June 19

- 7:30 am    **Continental Breakfast** (*St. Charles Ballroom*)
- 8:30am    **M1-A, Opening Session** (*New Orleans Ballroom*)
- Welcome:**  
**S. Billinge**, General Chair of ACNS 2006, *NSSA Vice-President*  
**R. Pynn**, *NSSA President*
- 8:40 am    **Keynote Speaker:**  
**P. Dehmer**: *Energy Challenge in a New Era of Science: The Renewed Importance of Materials Probes*
- 9:20 am    **Cliff Shull Prize Lecture:**  
**J. M. Carpenter**: *Living with Neutrons: A Personal History – 40 Years or So in Neutron Scattering*
- 10:00 am    **Break**
- 10:30 am    **M2-A, Materials Chemistry and Earth Science**  
Chair: P. Woodward (*New Orleans Ballroom*)  
**R. Cava**, J. Johnson, J. Hill, D. Ma, R. Hjelm, B. Fultz
- 10:30 am    **M2-B, Multiferroics**  
Chair: J. Lynn (*Turquoise A-B Room*)  
**G. Xu**, **O. Vajk**, P. Gehring, M. Hagen, R. McQueeney
- 10:30 am    **M2-C, Instrumentation and Small Facilities**  
Chair: P. Sokol (*Amphitheater*)  
**D. Moncton**, **D. Baxter**, B. Micklich, C. Carlile, K. Littrell

10:30 am	<b>M2-D, Biomimetic Materials</b> Chair: B. Frisken ( <i>Ruby Room</i> ) <b>N. Kucerka, T. A. Harroun</b> , J. Katsaras, D. P. Bossev
12:15 pm	<b>Lunch</b> ( <i>St. Charles Ballroom</i> )
1:45 pm	<b>M3-A, Self Assembly, Interaction and Dynamics of Biological Systems</b> Chair: P. Thiyagarajan ( <i>Turquoise A-B Room</i> ) <b>J. Curtis, D. Lynn</b> , H. Kaiser, G. Thurston, S. Chen
1:45 pm	<b>M3-B, Energy Storage and Conversion</b> Chair: J. Fischer ( <i>Ruby Room</i> ) <b>T. Yildirim, C. Jones</b> , M. Hartl, C. Brown, A. Stowe
1:45 pm	<b>M3-C, Superconductivity</b> Chair: J. Tranquada ( <i>Amphitheater</i> ) <b>M. Eskildsen, S. Kivelson</b> , M. Laver, H. Mook, A. Shams
1:45 pm	<b>M3-D, Industrial Applications and Neutron Science</b> Chair: X.-L. Wang ( <i>New Orleans Ballroom</i> ) <b>L. Clapham, D. Brown</b> , W. Wagner, T. Watkins, T. Parikh
3:30 pm	<b>Break</b>
4:00 pm	<b>M4-A, Nanoscience with Neutrons</b> Chair: L. Horton ( <i>Amphitheater</i> ) <b>M. Fitzsimmons, G. Strycker</b> , H. Sha, G. Warren, V. Garlea
4:00 pm	<b>M4-B, In situ Experiments I: Deformation Mechanics</b> Chair: Mark Bourke ( <i>New Orleans Ballroom</i> ) <b>R. Ham-Su, Z. Feng</b> , Y. Sun, A. Stoica, Y. Wang
4:00 pm	<b>M4-C, Fundamental Physics</b> Chair: G. Greene ( <i>Ruby Room</i> ) <b>W. M. Snow, P. R. Huffman</b> , M. Leuschner, T. Ito, R. Moreh
4:00 pm	<b>M4-D, Polymeric Systems</b> Chair: M.-P. Nieh ( <i>Turquoise A-B Room</i> ) <b>V. Sakai, N. Balsara</b> , S. Titmuss, M. Foster, D. Perahia
8:00 – 10:00 pm	<b>MP, Reception and Poster Session: Student Research Award</b> ( <i>St. Charles Ballroom</i> )

## Tuesday, June 20

- 7:30 am     **Continental Breakfast** (*St. Charles Ballroom*)
- 8:30 am     **T1-A, Neutron Facilities – Worldwide Status**  
Chair: R. Teller (*New Orleans Ballroom*)  
**M. Arai:** *Neutron Scattering Developments and Initiatives in Asia and Australia*  
**A. Taylor:** *Neutron Scattering Developments and Initiatives in Europe*  
**R. Pynn:** *Neutron Scattering Developments and Initiatives in North America*  
**T. Mason:** *First Neutrons at SNS*
- 10:00am     **Break**
- 10:30 am     **TP, Poster session** (*St. Charles Ballroom*)
- 10:30 am     **T2-A, Heavy Fermions**  
Chair: R. Osborn (*Turquoise A-B Room*)  
**H. Lee, J. Lawrence, J. Hudis, V. Krishnamurthy, Y. Janssen**
- 12:15 pm     **Lunch** (*St. Charles Ballroom*)
- 1:45 pm     **T3-A, Biomembranes, Membrane Proteins and Functional Complexes**  
Chair: D. McGillivray (*New Orleans Ballroom*)  
**D. Worcester, M. Kent, S. Holt, F. Heinrich, K. Hristova**
- 1:45 pm     **T3-B, Structure and Dynamics of Hydrogen Bonded Systems**  
Chair: S.-H. Chen (*Amphitheater*)  
**C. Benmore, L. Liu, A. Kolesnikov, A. Acatrinei, E. Mamontov**
- 1:45 pm     **T3-C, Thin Film Magnetism**  
Chair: J. Borchers (*Ruby Room*)  
**T. Giebultowicz, S.G.E. te Velthuis, S. Watson, Z. Wiren, I. Zoto**
- 1:45 pm     **T3-D, Modeling and Simulation of Nanostructured Materials**  
Chair: N. Balsara (*Turquoise A-B Room*)  
**G. Smith, D. Louca, M. Nagao, E. Kintzel**
- 3:30 pm     **Break**
- 4:00 pm     **T4-A, Protein Structures, Mechanisms and Functional Complexes**  
Chair: D. Worcester (*Amphitheater*)  
**G. Bunick, C. Dealwis, L. Coates, W. Heller, C. Garvey**

- 4:00 pm    **T4-B, Low-D Magnetism**  
Chair: I. Zaliznyak (*Ruby Room*)  
**A. Zheludev, S. Lee**, S. Nagler, W. Ratcliff, T. Hong
- 4:00 pm    **T4-C, In situ Experiments: Emerging Applications**  
Chair: R. Rogge (*Turquoise A-B Room*)  
**H. Choo, R. Wenk**, D. Hussey, M. Ghargouri,  
D. Penumadu
- 4:00 pm    **T4-D, Instrumentation, Optics and Special Environments**  
Chair: K. Herwig (*New Orleans Ballroom*)  
**C. Tulk, G. Felcher**, A. Faraone, T. Krist, M. Bleuel
- 6:15 pm    **Buses begin departing to Morton Arboretum**
- 7:30 pm    **TB, Banquet at the Morton Arboretum**  
**G. Lander:** *From the Italian Navigator to SNS – the Saga of Neutrons in the US: a Personal View*

## Wednesday, June 21

- 7:30 am    **Continental Breakfast** (*St. Charles Ballroom*)
- 8:30 am    **W1-A, Plenary Session**  
Chair: R. Pynn (*New Orleans Ballroom*)
- NSSA 2006 Sustained Research Prize Lecture**  
**J. Tranquada:** *Twenty Years of Chasing Zurich Oxide*
- NSSA 2006 Science Prize Lecture**  
**T. Yildirim:** *Unravelling Secrets of Complex Materials Through First-Principles Computation, Theory and Neutron Scattering*
- TBA**
- 10:00 am    **Break**
- 10:30 am    **WP, Poster Session** (*St. Charles Ballroom*)
- 12:00 pm    **Lunch** (*St. Charles Ballroom*)
- Student Research Award Presentation**
- Neutron Advocacy Discussion**  
Chair: R. Pynn  
**S. Pierson:** *Grassroots Advocacy: Can scientists make a difference?*  
**J. Rush** (*to be confirmed*)  
**D. Koolbeck** (*to be confirmed*)



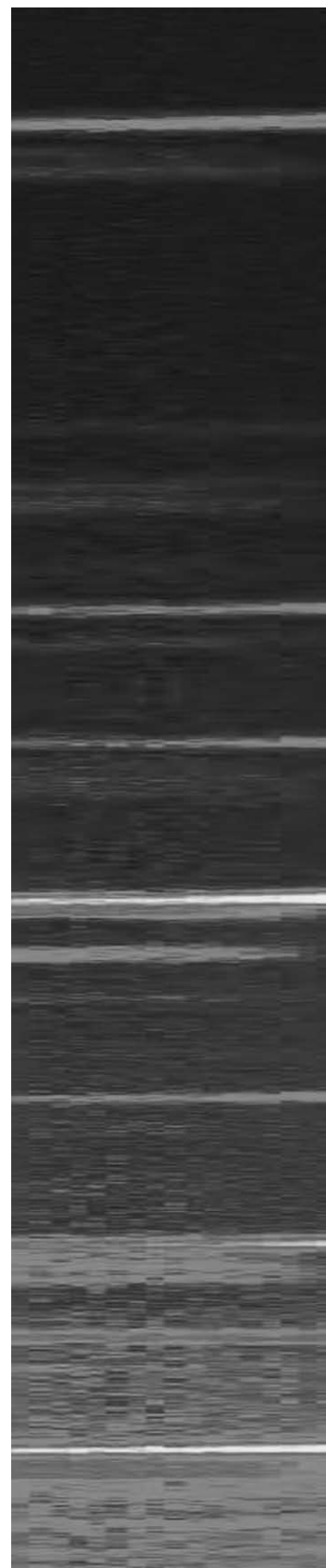
- 2:00 pm    **W2-A, Nanoclusters and Nanostructured Materials**  
Chair: J. Eckert (*New Orleans Ballroom*)  
**G. Christou**, C. Lo, W. Dmowski, P. Piccoli, F. Trouw,  
H. Wang
- 2:00 pm    **W2-B, Exotic Magnetism**  
Chair: C. Broholm (*Amphitheater*)  
**H. Ronnow**, **M. Stone**, W. Montfrooij, G. Gasparovic,  
J. Greedan
- 2:00 pm    **W2-C, Software and Methods**  
Chair: M. Aivazis (*Ruby Room*)  
**M. McKerns**, P. Willendrup, R. Rogge, N. Berk,  
C. Majkrzak
- 2:00 pm    **W2-D, Self-Assembled Nanoscopic Systems**  
Chair: J. Katsaras (*Turquoise A-B Room*)  
**M. Nieh**, **B. Frisken**, P. Thiyagarajan, D. McGillivray
- 3:45 pm    **Break**
- 4:15 pm    **W3-A, Breakout Sessions:**  
**SHUG Meeting**  
Organizer: D. Louca (*New Orleans Ballroom*)
- The Very Cold Neutron Source**  
Organizers: B. Micklich, J. Carpenter (*Ruby Room*)
- Topaz IDT Meeting**  
Organizer: C. Hoffmann (*Sapphire Room*)
- SEQUOIA IDT Meeting**  
Organizer: G. Granroth (*Coral Room*)
- Sample Environment at Neutron Scattering  
Facilities**  
Organizers: K. Volin, D. Dender, L. Santodonato  
(*Turquoise A-B Room*)

## Thursday, June 22

- 7:30 am    **Continental Breakfast** (*New Orleans Ballroom*)
- 8:45 am    **Buses depart for Argonne National Laboratory**
- 9:30 am    **Tour of the IPNS at Argonne National Laboratory**
- 11:00 am   **IPNS 25th Anniversary Ceremony**
- 12:00 pm   **Lunch at Argonne National Laboratory**
- 1:30 pm    **Buses depart for Pheasant Run and airports**



# Abstracts





**Sunday, June 18****9:00 am – 5:00 pm Neutron Scattering Tutorials**

- Neutron Scattering Fundamentals and Instrumentation as a Probe of Materials on the Nanoscale  
*Organizer: M. Kottlarchyk (Jade Room)*
- Magnetic Structure Analysis from Neutron Powder Diffraction Data Using GSAS  
*Organizers: R. Von Dreele and B. Toby (Coral Room)*
- Neutron Scattering for Materials Study  
*Organizers: P. K. Liaw and H. Choo (Sapphire Room)*

**1:00 – 8:30 pm Conference Registration****7:00 – 9:00 pm Evening Welcome Reception  
(New Orleans Ballroom)****Monday, June 19****M1-A (8:30–10:00 am)****Opening Session (New Orleans Ballroom)**

- Welcome  
*S. Billinge, General Chair of ACNS 2006, NSSA Vice-President*  
*R. Pynn, NSSA President*

**M1-A1 (8:40 am)****Energy Challenge in a New Era of Science:  
The Renewed Importance of Materials Probes (Plenary)**  
*P. Dehmer (U.S. Department of Energy)***Cliff Shull Prize Lecture****M1-A2 (9:20 am)****Living with Neutrons: A Personal History –  
40 Years or So in Neutron Scattering (Plenary)**  
*J. Carpenter (Argonne National Laboratory)*

I trace my involvement with neutrons and with some of the people that were significant in my education and work, and illustrate some of the steps along the way from small reactors to the big spallation neutron sources.

**M2-A (10:30 am – 12:15 pm)****Materials Chemistry and Earth Science**  
*Chair: P. Woodward (New Orleans Ballroom)***M2-A1 (10:30 am)****What's happening in Solid State Chemistry? (Invited)**  
*R. Cava (Princeton University)*

Solid State Chemists are a small, congenial community traditionally specializing in the synthesis of non-molecular solids. We are motivated by exploring new routes to synthesis, discovering and exploiting new chemical families, and, increasingly in the past decade, working with the materials physics community to elucidate the relationships between the structures and properties of solids. There are as many ways of looking at solid state chemistry as there are solid state chemists, which in my view is what makes it interesting. In this talk I will describe some of the current activities in our field.

**M2-A2 (11:00 am)****Neutron reflectivity on diamond-like carbon films under ambient and vacuum conditions**

*J. A. Johnson, S. Park, A. Erdemir, O. L. Eryilmaz, J. B. Woodford (Argonne National Laboratory)*

Carbon-based coatings exhibit many attractive properties that make them good prospects for a wide range of engineering applications. Tribological studies of the films revealed a close correlation between the chemistry of the hydrocarbon source gases and the friction and wear coefficients of the resultant diamond-like carbon films. Those films grown in source gases with higher hydrogen-to-carbon ratios had much lower friction and wear coefficients than did films derived from source gases with lower hydrogen-to-carbon ratios.

A series of three films were made with different ratios of C:H in the plasma; the deuterated counterparts were also synthesized. The films were structurally characterized under ambient conditions using neutron reflectivity, and thickness, density and roughness were determined. Modeling showed that more than one layer was required to obtain a good fit to the data. The measurements were repeated in vacuum. Considerable differences were obtained between the two sets of results and these differences will be the discussion points of our presentation.

M2-A3 (11:15 am)

**Crystal Structure and Magnetic Properties of the Oxygen Deficient  $n = 2$  Ruddlesden-Popper Phase  $\text{Sr}_3\text{Co}_2\text{O}_{7-\delta}$** 

J. M. Hill, J. F. Mitchell (Argonne National Laboratory, Material Science Division), B. Dabrowski (Northern Illinois University)

Interest in charge, orbital, and spin state phenomena in perovskite and related cobalt oxides is a growing area of transition metal oxide physics. Recently, J. Matsuno et al.<sup>1</sup> have found that epitaxial films of the  $n = 1$  Ruddlesden-Popper (R-P) phase  $\text{Sr}_2\text{CoO}_4$  are metallic ferromagnets with relatively high  $T_C \sim 250$  K. This is particularly interesting in light of the formal oxidation state of Co,  $\text{Co}^{4+}$ , offering no clear source of carriers. The accepted rules of superexchange predict an antiferromagnetic insulator if  $\text{Co}^{4+}$  is in the expected low-spin state ( $S=1/2$ ).

To extend the materials chemistry and physics of the R-P series of cobaltites, we have synthesized the  $n = 2$  R-P phase  $\text{Sr}_3\text{Co}_2\text{O}_{7-\delta}$  in bulk polycrystalline form. The strategy is to exploit the oxygen-defect to both tune the  $\text{Co}^{2+}/\text{Co}^{3+}$ - $\text{Co}^{3+}/\text{Co}^{4+}$  ratio and the coordination geometry (and potentially the spin-state) of the Co ion. Additionally, this compound allows us to study the properties of oxygen vacancy defect structures, which play an important role in the properties of other cobaltites, such as  $\text{GdBaCo}_2\text{O}_{5+\delta}$ .

We have combined laboratory x-ray (XRD), synchrotron x-ray (SXRD) and neutron powder diffraction (NPD) to map out changes in the crystal structure as a function of oxygen content  $\delta$ . Samples with oxygen contents of  $1.21 \leq \delta \leq 1.33$  exhibit a defect orthorhombic crystal structure in the space group  $Immm$ . Additionally, magnetization measurements show two composition-dependent transitions. To further elucidate the magnetic properties of this  $\text{Co}^{2+}/\text{Co}^{3+}$  material, we have conducted a temperature-dependent NPD study. The low temperature antiferromagnetic structure is surprisingly complex and suggestive of an incommensurate ordering wave vector.

By contrast, samples made with  $\delta \approx 0.5$  are ferromagnetic ( $T_C \sim 120$  K). These  $\text{Co}^{3+}/\text{Co}^{4+}$  compounds are made by annealing the above low-oxygen-content material at low temperatures ( $\sim 300^\circ\text{C}$ ) in 1 atm  $\text{O}_2$ . Both SXRD measurements on a quenched sample and XRD patterns collected *in situ* during oxidation clearly show that the first-formed

oxygenated material is tetragonal and indexes in the ideal R-P  $I4/mmm$  space group. Additionally, *in situ* XRD oxidation experiments also show that, upon slow cooling, the sample transforms back into the orthorhombic structure, indicating that the oxygen vacancies preferentially lie (at least partially) along one axis in the plane at room temperature. To more accurately characterize the structure of this annealed material, we have collected NPD data on a slow-cooled annealed sample. However, our data do not suggest any long-range oxygen vacancy ordering in the plane.

<sup>1</sup>J. Matsuno et al., *Phys. Rev. Lett.* **93**, 167202 (2004).

M2-A4 (11:30 am)

**Nearest neighbor chemical bond ordering in a multi-component Zr-based bulk metallic glass**

D. Ma, L. Yang, A. D. Stoica, X. L. Wang (Oak Ridge National Laboratory), M. J. Kramer (Iowa State University), T. Proffen (Los Alamos Neutron Science Center, Los Alamos National Laboratory), J. Neumeier (Oak Ridge National Laboratory)

Since the discovery in the early 1990s, bulk metallic glasses (BMGs) have been emerging as the promising structural materials for engineering applications due to their superior mechanical properties originating from the amorphous nature of their structures. However, the local atomic structure and chemical bonding, particularly in multi-component bulk metallic glasses, are far from well understood as a result of the complexity of the multiple chemical interactions among the constituent species. Here we report the use of synchrotron X-ray and neutron diffraction to investigate the chemical bond ordering in a quinary Zr-based bulk metallic glass. The diffraction data were analyzed in terms of pair-distribution-functions (PDF). Based on a simple cluster model and by exploring the scattering contrast, we are able to identify the correlation functions for the nearest neighboring Zr-Zr pair and the major Zr-metal pairs out of the 15 possible atomic pairs. We will also present the anisotropic responses of the identified pairs under in-situ uni-axial loading.

*This research was supported by Division of Materials Sciences and Engineering, Office of Basic Energy Sciences, U.S. Department of Energy under Contract DE-AC05-00OR22725 with UT-Battelle, LLC.*

M2-A5 (11:45 am)

**Investigation of the Structural Evolution of  $\beta$ -Phase Erbium Tritide with Small Angle Neutron Scattering**

R. P. Hjelm (Los Alamos Neutron Science Center, Los Alamos National Laboratory), J. F. Browning (Sandia National Laboratories), G. M. Bond (New Mexico Tech)

The trapping and behavior of  $^3\text{He}$  in metal hydride systems in which tritium is at appreciable concentration is of particular interest both from a fundamental perspective as well as a broad range of applications. In the erbium ditritide system,  $^3\text{He}$  is generated due to beta decay of the tritium. It is well known that much of the helium generated does not readily diffuse from the hydride system but becomes trapped or bound in low energy sites, such as interstices, defects, etc. within the crystal. Due to its limited solubility, helium tends to cluster at these sites subsequently forming high-density, high-pressure bubbles.  $^3\text{He}$  bubble formation and kinetics in erbium ditritide is poorly understood. Our goal is to understand of the behavior of radiogenically produced  $^3\text{He}$  in erbium ditritide films and determine how the structure of these films evolve as a function of time, i.e., helium concentration. We use small-angle neutron scattering (SANS) as a nondestructive probe to study the long-term structural evolution, arrangement and morphology of  $^3\text{He}$  in the  $\text{ErT}_2\text{-x}_3\text{Hex}$  system, by making repeated measurements of the same samples at different times after tritium loading. The SANS data provides for first time evidence of disk-like  $^3\text{He}$ -bubbles with long-length scale ordering along the various crystallographic axes of the  $\text{CaF}_2$ -like unit cell. Transmission electron microscopy confirmed this result and the disk-like morphology. The spacing between the disks decreased with time. It is likely that the positions of the disks result from defects introduced in the Erbium lattice on loading with tritium.

M2-A6 (12:00 pm)

**Anharmonic Phonon Thermodynamics in Transition Metal Alloys at High Temperatures**

B. Fultz, O. Delaire, M. Lucas, T. Swan-Wood, M. Kresch (California Institute of Technology)

Inelastic neutron scattering has proved invaluable for showing how and why there are differences in phonon entropies of different materials. These differences are usually important for the

thermodynamic stability of crystalline phases.

With goals of phase diagram determinations and calculations of equations of state, often for materials under extreme conditions, there is now an increasing theory activity to calculate phonon entropy with electronic structure codes based on density functional theory. The agreement between theoretical and experimental phonon dynamics is frequently satisfactory at low temperatures. It is often practical to extend these computations to higher temperature using the quasi-harmonic approximation, in which the phonon frequencies soften with temperature, but dynamics can be understood with a Born-von Karman model, for example. The quasi-harmonic approximation has had successes, but interesting failures seem common. These will be reviewed for FeAl and for vanadium alloys at high temperatures, where the experimental phonon densities of states are quite different from those predicted with the quasi-harmonic approximation. This talk will explain our approaches and early results on interpreting these anharmonic effects in term of electron-phonon and phonon-phonon interactions.

M2-B (10:30 am – 12:15 pm)

**Multiferroics**

Chair: J. Lynn (Turquoise A-B Room)

M2-B1 (10:30 am)

**Competition of long- and short-range polar order in relaxor ferroelectrics (Invited)**

G. Xu (Brookhaven National Laboratory), C. Stock (Johns Hopkins University), P. M. Gehring (National Institute of Standards and Technology)

Neutron and x-ray diffraction have been used to study the competing long- and short-range polar orders in the relaxor ferroelectrics  $\text{Pb}(\text{Mg}_{1/3}\text{Nb}_{2/3})\text{O}_3$  (PMN) and  $\text{Pb}(\text{Zn}_{1/3}\text{Nb}_{2/3})\text{O}_3$  (PZN) under an [111] electric field. The results from the two relaxor systems are distinctively different. In PZN, the field induces long-range polar order, without being able to suppress the (overall) short-range polar order, measured with diffuse scattering intensities. The structure (long-range order) and diffuse scattering (short-range order) both have a strong field memory effect, associated with ferroelectric domain formations. In PMN, the unit cell shape in the bulk volume remains cubic for E up to 8 kV/cm,



while a clear suppression of the diffuse scattering and concomitant enhancement of the Bragg peak intensity is observed, indicating a more ordered structure with increasing E field. However, the absence of hysteresis of these changes suggests that the ground state is not a frozen glassy phase as previously postulated.

M2-B2 (11:00 am)

**Neutron Scattering Studies of Multiferroic  $\text{HoMnO}_3$**   
(Invited)

O. P. Vajk, M. Kenzelmann, J. W. Lynn (NIST Center for Neutron Research), S. B. Kim, S. W. Cheong (Rutgers University)

Hexagonal rare-earth manganites of the form  $\text{RMnO}_3$  exhibit simultaneous ferroelectric and antiferromagnetic order. Much of the interest in these materials has been focused on  $\text{HoMnO}_3$ , which exhibits particularly strong coupling between the ferroelectricity and magnetism. Neutron diffraction measurements of  $\text{HoMnO}_3$  in a magnetic field reveal a complex phase magnetic diagram as a function of temperature and magnetic field. Inelastic measurements of the spin wave spectrum indicate that the magnetism of the spin-2  $\text{Mn}^{3+}$  ions is dominated by a nearest neighbor antiferromagnetic Heisenberg exchange with  $J = 2.44$  meV and a temperature-dependent easy-plane anisotropy. Our neutron scattering measurements also reveal dispersionless magnetic excitations which we attribute to crystal field levels of the  $\text{Ho}^{3+}$  ions. These crystal field levels show temperature- and magnetic field-dependent changes across phase boundaries, as well as signs of coupling between these excitations and the magnon dispersion.

M2-B3 (11:30 am)

**Evolution of the Diffuse Scattering Across the Morphotropic Phase Boundary in the Relaxor  $\text{Pb}(\text{Mg}_{1/2}\text{Nb}_{2/3})\text{O}_3$  doped with Ferroelectric  $\text{PbTiO}_3$**

P. M. Gehring (National Institute of Standards and Technology), M. Matsuura, K. Hirota (Institute for Solid State Physics, The University of Tokyo), Z. G. Ye, W. Chen (Simon Fraser University), G. Shirane (Brookhaven National Laboratory)

We have characterized the evolution of the diffuse scattering in the prototypical relaxor compound  $\text{Pb}(\text{Mg}_{1/3}\text{Nb}_{2/3})\text{O}_3$  (PMN) as the material is doped with  $\text{PbTiO}_3$  (PT), a displacive ferroelectric with  $T_c = 763$  K. Single crystals of PMN-xPT with x=0, 10, 20, 30, and 40% were examined using neutron diffraction. The addition of ferroelectric  $\text{PbTiO}_3$  modifies

the well-known butterfly and ellipsoidal diffuse scattering intensity contours that are observed in pure PMN, and which are believed to result from the presence of randomly oriented, polar nanoregions (PNR) that form at high temperature. The spatial correlation length derived from the width of the diffuse scattering increases from 13 Angstroms for PMN to 350 Angstroms for PMN-20%PT, which suggests a substantial enlargement of the PNR. The  $q$ -integrated diffuse scattering intensity, which is proportional to  $X''$ , increases with doping and is largest in the PMN-20%PT sample. Beyond 30% PT, a concentration very close to the morphotropic phase boundary, no diffuse scattering is observed below  $T_c$  and well-defined critical behavior is observed. By contrast, the diffuse scattering for the 0, 10, and 20% samples persists to low temperatures, where each crystal retains an average cubic structure.

M2-B4 (11:45 am)

**Anomalous phonon behavior in the negative thermal expansion material Cuprite ( $\text{Cu}_2\text{O}$ )**

M. E. Hagen (Oak Ridge National Laboratory), S. M. Shapiro (Brookhaven National Laboratory), A. Goodwin, M. Dove (University of Cambridge, Cambridge, England)

It is known from both neutron and x-ray diffraction work that the semiconductor cuprite ( $\text{Cu}_2\text{O}$ ) displays negative thermal expansion (NTE) at temperatures below 300K and (conventional) positive thermal expansion (PTE) above 300K. The linear coefficient of thermal expansion can, in a quasi-harmonic approximation, be associated with a thermally weighted sum over the (mode) Gruneisen parameters for the various modes in the material. As a consequence, the change from NTE to PTE behavior in cuprite should arise from a balancing, as a function of temperature, of phonon modes with negative and positive mode Gruneisen parameters. In order to examine this we carried out a detailed study of the phonon modes in single crystal samples of cuprite. Our preliminary work suggests that the TA modes along the  $[\pi, 0, 0]$  direction in cuprite show a small, anomalous softening on decreasing temperature over the range  $8\text{K} < T < 300\text{K}$ , whereas the lowest lying TO mode along  $[\pi, 0, 0]$  shows a conventional hardening. Over this temperature range the zone boundary TA mode shows a large amount of damping. We will describe the general background to the behavior in cuprite



and the results of our preliminary inelastic neutron scattering work.

*Work at Brookhaven and Oak Ridge supported by the Division of Materials Sciences at the US Department of Energy.*

M2-B5 (12:00 pm)

### **Optical spin waves in magnetite**

R. J. McQueeney (Iowa State University), M. Yethiraj (Oak Ridge National Laboratory), W. Montfrooij (University of Missouri), S. Chang (Ames Laboratory), T. G. Perring (ISIS Pulsed Neutron Facility), J. Honig, P. Metcalf (Purdue University)

Magnetite ( $\text{Fe}_3\text{O}_4$ ) is well-known for its metal-insulator transition, called the Verwey transition. For the last 70 years, the microscopic origin of the Verwey transition was thought to be charge-ordering, although this has been disputed of late, bringing renewed interest in this system. We measured the optical spin wave dispersions of magnetite above and below the Verwey transition using the MAPS spectrometer at ISIS. Any changes in the spin wave dispersion may indicate charge ordering, due to the dependence of the superexchange on orbital occupancy. The spinel structure of magnetite contains two different iron sites; A (stable valence,  $\text{Fe}^{3+}$ ) and B (mixed valence,  $\text{Fe}^{2.5+}$ ), with charge ordering of  $\text{Fe}^{2+}/\text{Fe}^{3+}$  species occurring on the B-site. The optical spin waves propagating on the A-site sublattice ( $\sim 115$  meV) are unchanged at the transition. The spin waves propagating in the B-site sublattice ( $\sim 70$  meV) are  $\sim 5$  meV softer in the metallic phase. We discuss the possibility that the B-site optic spin waves are damped by charge fluctuations in the metallic phase.

M2-C (10:30 am – 12:15 pm)

### **Instrumentation and Small Facilities**

*Chair: P. Sokol (Amphitheater)*

M2-C1 (10:30 am)

#### **Neutron Research at the MIT Reactor (Invited)**

D. E. Moncton (Massachusetts Institute of Technology)

Neutron scattering research at the 5MW MIT reactor ceased with Professor Cliff Shull's retirement over a decade ago. However, it has become increasingly clear that this reactor can make a significant contribution to education and research as the US neutron community expands to take full advantage of the upcoming Spallation

Neutron Source. I will describe the overall program at the MITR, which is evolving to a major mission in nuclear engineering, but focus on the installation of a new instrument for neutron scattering aimed at three missions: (1) the development of focusing optics and new methods for imaging; (2) sample preparation and initial studies for on-going experiments at major facilities; and (3) supporting education at both the graduate and undergraduate levels. The instrument will be available to both internal and external users.

M2-C2 (11:00 am)

#### **The Low Energy Neutron Source at IUCF: Design and Instrumentation (Invited)**

D. V. Baxter (Indiana University Cyclotron Facility)

The Low Energy Neutron Source (LENS) is a novel neutron scattering facility that is being constructed at the Indiana University Cyclotron Facility. This facility makes use of pn reactions in Be to produce neutrons with relatively little activation near the target and a solid methane moderator operating at temperatures below 10 K to produce beams of cold neutrons for a number of scattering instruments. The facility has a three-fold mission for education, materials research, and the development of new instrumentation. LENS produced its first neutron beam in late 2004 and is presently being used for education and moderator development while running at less than 1% of its eventual power. Accelerator and RF power upgrades over the next year will increase the available neutron flux by roughly two orders of magnitude, to a point where scattering experiments become possible. The talk will describe the design and status of the facility, the plans for its instrumentation, and the results obtained to date.

*The LENS project is supported by the National Science Foundation (under grants DMR-0220560 and DMR-0320627), the 21<sup>st</sup> Century Science and Technology fund of Indiana, Indiana University, and the Department of Defense.*

M2-C3 (11:30 am)

#### **Concepts for a Very Cold Neutron Source**

B. J. Micklich, J. M. Carpenter (Argonne National Laboratory)

Long-wavelength neutrons are of increasing interest for a broad variety of neutron scattering applications, including characterization of biological and nanoscale materials, magnetic materials, fundamental physics, direct neutron imaging, and applications in medicine, energy, and

the environment. We are studying the feasibility of a neutron source having a peak wavelength distribution in the range 10-20 Å, with usable flux out to 100 Å. The present concept consists of a long-pulse linear accelerator operating at 1000 MeV and 5 pulses/second, a liquid lead target, and cryogenic moderators in the form of pellets cooled by superfluid helium at 2 K. We will discuss some of the scientific applications and some experiments to demonstrate instrument concepts for long-wavelength neutrons.

M2-C4 (11:45 am)

### **The development of Neutron Facilities across the Atlantic**

C. J. Carlile (Institut Laue-Langevin, France)

Neutron scattering around the world is undergoing something of a renaissance with the imminent operation of the SNS and JPARC. Across the Atlantic there is also significant progress, less dramatic maybe but significant nevertheless. The ILL in Grenoble has invested \$70 M in the last 5 years to rebuild its instrument suite and the delivery systems for the neutron beams and to retrofit the nuclear installation surrounding buildings to be fit for purpose for the next 20 years. ILL has developed a strategy plan of additional investment in key reactor component and instruments for the next 10 years and is working energetically to obtain funding for this. Elsewhere in Europe the FRM-II reactor is fully commissioned and the User programme is starting and the ISIS second target station particularly aimed at cold neutron science will generate its first beams next year. The long debated European Spallation Source having had many set backs is also entering a new phase. Serious bids to locate the ESS are now being debated and there is room for optimism that visible progress will be made in the next few years. I will present the view from the other side of the Atlantic.

M2-C5 (12:00 pm)

### **A compound refractive magnetic lens for cold neutrons**

K. C. Littrell (Argonne National Laboratory, Intense Pulsed Neutron Source), S. G. E. te Velthuis, G. P. Felcher (Argonne National Laboratory, Material Science Division), S. Park, B. Kirby, M. Fitzsimmons (Los Alamos Neutron Science Center, Los Alamos National Laboratory)

The recent surge of interest for cold neutrons for reflectometry and small angle scattering has

spurred the development of optical elements to concentrate the neutron flux. It is well-known that biconcave cylindrical lenses focus a cold neutron beam within a plane perpendicular to the cylinder's axis. Analogously, a magnetic field  $\mathbf{H}$  restricted to a cylindrical region constitutes a birefringent cylindrical lens for a neutron beam. This magnetic lens focuses neutrons with moment  $\mu$  antiparallel to  $\mathbf{H}$  and diverges those with moment parallel to  $\mathbf{H}$ , thereby creating a polarized beam. As the beam does not pass through any material, flux losses due to absorption or scattering are eliminated. This concept was tested using a compound lens consisting of N=99 pairs of cylindrical magnets. The magnets of each pair, with a 1.2 cm diameter, had a 0.3 cm gap with a magnetic field  $\mathbf{H}$ = 1 Tesla. The assembly was found to perform exactly as expected, selectively focusing a white beam of cold neutrons of one spin state at the detector, which was located at 2.1 m from the lens. This experiment confirmed that a lens of this nature may boost the flux by almost an order of magnitude and create a polarized beam. The one-directional character of the focusing along with its polarizing capability make a scaled-up version of this lens very suitable for incorporation into polarized neutron reflectometers and spin-echo resolved grazing incidence scattering instruments.

---

M2-D (10:30 am – 12:00 pm)

### **Biomimetic Materials**

Chair: B. Frisken (Ruby Room)

M2-D1 (10:30 am)

### **Structure of Fully Hydrated $L_\alpha$ Phase Lipid Bilayers and Biomembranes (Invited)**

N. Kucerka (NRC Chalk River Laboratories, Canada)

The title emphasizes the biologically relevant state of lipid bilayers – those that are fully hydrated and in the fluid  $L_\alpha$  phase. I will review the different approaches used to obtain the structure of  $L_\alpha$  phase bilayers and describe a new method providing more detailed information regarding bilayer structure. Specifically, I will talk about small-angle neutron scattering from a system of unilamellar vesicles and the corresponding simple models, which were found suitable for analysis of such data. Functional forms of these models, guided by extended molecular dynamics

simulations, are reasonable approximations of lipid bilayers, while at the same time not employing an inordinate number of parameters. However, for more advanced structural models it is necessary to increase the amount of experimental data, achieved by combining several data sets from independent experiments (e.g.: scattering data obtained from unoriented unilamellar vesicles and oriented multilamellar stacks, along with volume measurements).

*M2-D2 (11:00 am)*

### **Deuterium labeling of bio-molecules for neutron diffraction** *(Invited)*

T. A. Harroun (Brock University), J. P. Bradshaw (University of Edinburgh), S. R. Wassall (Indiana University Purdue University Indianapolis), J. Katsaras (National Research Council Canada)

Isomorphous replacement of atoms within molecules is a method whereby individual atoms or groups can be located with high precision in the unit cell. For crystallography, this may assist in solving the phase problem. In other cases, it is enough to determine the location of the replaced group within a larger macromolecular context. Perhaps the best isomorphous replacement available is that of replacing deuterium for hydrogen.

In a lipid membrane and water environment, deuterium labeling has been used in several modalities. By labeling components of the lipid, the sub-structure of the bilayer can be determined. Selective labeling of small molecules can reveal their location embedded in the membrane environment. Several labels of protein residues can yield the 3D orientation of the whole peptide for molecular modeling. Finally, heavy water can reveal the penetration of the aqueous environment into the membrane. We will review some recent examples in each of the cases, and explore the difficulties and successes associated with these types of experiments.

*M2-D3 (11:30 am)*

### **A Comprehensive Examination of Mesophases Formed by DMPC/DHPC Lipid Mixtures**

J. Katsaras (National Research Council Canada), T. A. Harroun (Brock University), M. P. Nieh (National Research Council Canada), V. A. Raghunathan (Raman Research Institute)

Mixtures of long- and short-chain phospholipids, specifically 14:0 and 6:0 phosphatidylcholines

(DMPC and DHPC), have been used successfully in NMR studies as magnetically alignable substrates for membrane associated proteins. However, recent publications have shown that the phase behavior of these mixtures is much more complex than originally thought. Using small-angle neutron scattering and polarized light microscopy the various morphologies of DMPC/DHPC mixtures at molar ratios of 2, 3.2, and 5 have been determined. Generally, at temperatures below the DMPC main-chain melting transition ( $T_M = 23^\circ\text{C}$ ), an isotropic phase of disk-like micelles is found. At high temperatures ( $T > 50^\circ\text{C}$ ), a lamellar phase consisting of either multilamellar vesicles (MLV) or extended lamellae is formed, which at low lipid concentrations (e.g., MLV) coexists with an excess of water. At intermediate temperatures and lipid concentrations, a chiral nematic phase made up of wormlike micelles is observed.

*M2-D4 (11:45 am)*

### **Determining the bending rigidity of bio-membranes by Neutron Spin-Echo Technique**

D. P. Bossev, Z. Yi (Indiana University, Bloomington, IN)

NSE is the most direct method to probe the thermal undulations of the lipid bilayers in solution because it is a unique scattering technique that covers the time scale of 0.01 – 100 ns, characteristic of these motions. Following Zilman-Granek approach one can interpret the decay of the intermediate scattering function and to evaluate the bending modulus of elasticity,  $k$ , of the lipid bilayers. Experimental studies, however, show that the obtained  $k$  values are consistently higher than the predicted ones. These observations have been attributed to the presence of internal friction of the lipid bilayer that is not accounted as a damping mechanism by Zilman-Granek theory. To shed light on this discrepancy we have studied the bending elasticity of well studied lipid, DMPC, in D<sub>2</sub>O with addition of deuterated glycerol to modify the solvent viscosity. We found that addition of 30% glycerol resulted in a decrease of the bending modulus of the DMPC bilayers at  $T_c$ . The results are compared to those obtained by other methods and discussed in perspective of the Zilman-Granek theory.

M3-A (1:45 – 3:30 pm)

## **Self Assembly, Interaction and Dynamics of Biological Systems**

*Chair: P. Thiyagarajan (Turquoise A-B Room)*

M3-A1 (1:45 pm)

### **Relaxation processes and coarse grain dynamics: A neutron perspective (Invited)**

J. E. Curtis, H. Nanda (National Institute of Standards and Technology)

The development of coarse-grain simulation methods is a major advancement in the simulation of large macromolecular systems. The underlying principle used in these strategies is to use a reduced number of atoms and soft-potentials that allow one to obtain structures of large macromolecular systems with a greatly reduced simulation time. We are interested in the use of coarse-grain simulations to study the structure and dynamics of lipid membranes. The purpose of this talk is to describe our efforts to validate the semi-quantitative nature of the dynamics of DPPC and DOPC lipid membrane bilayers by comparison of coarse-grain simulations to previously validated all-atom simulations. We find, that at least in one coarse-grain methodology, that the relaxation of individual beads on the nanosecond time-scale does not match all atom simulations. Examples of neutron scattering observables for all-atom and coarse-grain simulation will be shown to highlight the similarities and differences as well to stimulate future neutron scattering experiments.

M3-A2 (2:15 pm)

### **Conformational Genomics: The Wiggling of Peptides into Amyloid (Invited)**

D. G. Lynn, A. Mehta, Y. Liang, K. Lu, J. Dong, W. S. Childers, P. Liu (Emory University), S. V. Pingali, P. Thiyagarajan (Argonne National Laboratory, Intense Pulsed Neutron Source)

The peptide self-assemblies found in very different amyloid morphologies can range from toxic, e.g. Alzheimers Disease and Mad Cow Disease, to quite beneficial, e.g. yeast prions. In addition, these assemblies are proving to be robust structures for nanotechnology. We will show that long fibrils, robust ribbons, and homogeneous nanotubes are all readily accessible from simple peptide building blocks. Very subtle differences in the assembly conditions can result in huge overall changes in assembly morphology. These differences range

from the incorporation of specific metal ions, the hydrogen bond registry within the sheets, the packing arrangements of the sheets, and the side chain compatibilities along and between individual sheets. Now the combination of various scattering, imaging, spectroscopic and modeling approaches provides a robust approach to both define self-assembly morphology and predict the pathways for their assembly. These approaches have now produced a tool box for the generation of various nano- and micro-scale molecular assemblies and devices.

M3-A3 (2:45 pm)

### **SANS Study of $\alpha$ -Synuclein**

H. Kaiser, N. L. Armstrong, D. Bossev, P. E. Sokol (Indiana University, Bloomington, IN), B. Hammouda (NIST Center for Neutron Research, Gaithersburg, MD), V. N. Uversky, A. K. Dunker (Indiana University, Indianapolis, IN)

Intrinsically disordered proteins, such as  $\alpha$ -synuclein, are thought to be responsible for the development of various protein deposition disorders. In particular, aggregation and fibril formation of  $\alpha$ -synuclein has been implicated as a causative factor in Parkinson's disease, as well as in several other neurodegenerative disorders, including Alzheimer's disease.  $\alpha$ -Synuclein is a natively unfolded protein and can adopt a series of different conformations and structures, highly dependent on the effect of environmental factors such as pH, temperature, different organic solvents, etc. Thus, SANS provides an ideal tool to characterize the behavior of this important class of proteins and to study the protein non-folding problem, complementing other biophysical analysis methods, such as circular dichroism, SAXS, FTIR, NMR, light scattering, fluorescence, gel-filtration, etc. Preliminary SANS data, taken with the NG3 SANS instrument at NIST, show a shift of scattered intensity to higher Q's when the temperature is increased at pH 6.0, implying that  $\alpha$ -synuclein is going through a transition from an extended unfolded state to a more compact partially folded conformation. The opposite behavior is observed at pH 2.0. Data for various concentrations (0.1 % - 0.5 % of  $\alpha$ -synuclein in D<sub>2</sub>O) and various pH (2.0 – 6.0) over a temperature range of 25° C to 95° C are presented. Preliminary data analysis shows a distinct structural transition of  $\alpha$ -synuclein in this temperature range.



M3-A4 (3:00 pm)

**Small angle neutron scattering studies of eye lens gamma crystallin vs. charge and ionic strength**

G. M. Thurston, K. Desmond (Rochester Institute of Technology), A. Stradner, P. Schurtenberger (U. Fribourg)

We are using small-angle neutron scattering to study the liquid structure of concentrated aqueous solutions of the eye lens protein, gammaB crystallin, as functions of charge and ionic strength. The gamma crystallins exhibit liquid-liquid phase separation in aqueous solution that has been linked to cataract disease. The role of charge in mediating this phase separation is unknown, and is of potential importance since lens protein charge can change during aging. We have obtained small-angle neutron scattering data from dilute and concentrated gammaB crystallin solutions at ionic strength 0.24M at pH values from 4.5 to 7.4, in which net protein charge changes from +8 to nearly 0 electronic units. At pH 4.5 we have also varied ionic strength down to 0.02M. Protein concentrations ranged from 6 to 370 mg protein/ml solution and the scattering vector magnitude ( $q$ ) ranged from 0.004 to 0.45 inverse Angstroms. At pH 5.5 to 7.4 gammaB crystallin exhibits pH-dependent liquid-liquid phase separation and liquid structure factors vs. concentration and temperature near the cloud point are well represented, in general, by the Baxter sticky sphere model. In contrast, at pH 4.5, concentrated gammaB has a very different liquid structure indicating highly repulsive interprotein interactions, consistent with both high net protein charge and reduced screening. At pH 4.5 the scattering also exhibits features consistent with repulsive interactions between clusters of gammaB crystallin, qualitatively similar to those recently observed for lysozyme.

M3-A5 (3:15 pm)

**Observation of Fragile-to-Strong Dynamic Crossover in Protein Hydration Water**

S. Chen, L. Liu (Massachusetts Institute of Technology), E. Fratini, P. Baglioni (University of Florence, Italy), A. Faraone (NIST Center for Neutron Research), E. Mamontov (Spallation Neutron Source, Oak Ridge National Laboratory)

Without water, a biological system would not function. Dehydrated enzymes are not active, but a single layer of water surrounding them restores their activity. It has been shown that the enzymatic activity of proteins depends crucially on the

presence of at least a minimum amount of solvent water. It is believed that about 0.3 g of water per g of protein is sufficient to cover most of the protein surface with one single layer of water molecules and to fully activate the protein functionality. Thus, biological functions, such as enzyme catalysis, can only be understood with a precise knowledge of the behaviour of this single layer of water and how that water affects conformation and dynamics of the protein. The knowledge of the structure and dynamics of water molecules in the so-called hydration layer surrounding proteins is, therefore, of utmost relevance to the understanding of the protein functionality. It is well documented that at low temperature proteins exist in a glassy state, which has no conformational flexibility. As the temperature is increased, the atomic motional amplitude increases linearly initially, as in a harmonic solid. In hydrated proteins, at approximately 220 K, the rate of the amplitude increase suddenly becomes enhanced, signalling the onset of additional anharmonic and diffusive motion. This 'dynamical' transition of proteins is believed to be triggered by its strong coupling through hydrogen bonding with the hydration water, which also shows some kind of dynamic transition at the similar temperature. In this talk, we shall show, using a high-resolution quasi-elastic neutron scattering (QENS) experiment, that this dynamic transition of hydration water on lysozyme protein is in fact the Fragile-to-Strong (FS) dynamic crossover at 220 K. This crossover signals a transition of water structure from predominantly high-density liquid (HDL, more fluid) to low-density liquid (LDL, less fluid), emanating from existence of the second low-temperature critical point, similar to that recently observed in confined water in cylindrical nanopores of silica material [1, 2].

[1] L. Liu, S.-H. Chen, A. Faraone, C.W. Yen, C. Y. Mou, "Pressure Dependence of Fragile-to-Strong Transition and a Possible Second Critical Point in Supercooled Confined Water," *Phys. Rev. Lett.* **95**, 117802-1-117802-4 (2005).

[2] S.-H. Chen, L. Liu, E. Fratini, P. Baglioni, A. Faraone, E. Mamontov, "Observation of Fragile-to-Strong Dynamic Crossover in Protein Hydration Water," to be published.

M3-B (1:45 – 3:30 pm)

**Energy Storage and Conversion***Chair: J. Fischer (Ruby Room)*

M3-B1 (1:45 pm)

**Combined Neutron Scattering and First-Principles Study of Novel Hydrogen Storage Materials (Invited)**

T. Yildirim (NIST Center for Neutron Research)

We present a brief review of several projects in which we use neutron scattering and first-principles calculations to characterize and predict novel hydrogen storage materials. In particular we will discuss our new results on the transition metal doped aluminates and several nanostructures such as SWNT/C60 and CDC (carbide derived carbons), metal-organic frameworks (MOF), and novel metal hydrides where very short H-H distance was observed. Particular attention will be given to our recent study of structure and quantum dynamics of hydrogen and methane in MOFs. More information about these projects can be obtained at <http://www.ncnr.nist.gov/staff/taner/h2>

M3-B2 (2:15 pm)

**Orientation Dependence of the Interaction Energy of Propylene Oxide and the 5(12)6(4) Clathrate Hydrate Cage (Invited)**

C. Y. Jones, N. Banishki (Hamilton College)

Quasielastic neutron scattering experiments on propylene oxide (PO) clathrate hydrate (CH) have revealed a complex set of PO guest dynamics involving multiple temperature regimes and time scales. This behavior is not surprising, because for a molecule of its size, PO ( $C_3H_6O$ ) is quite complex; it has a permanent dipole and contains an oxirane ring, a methyl group, a chiral center, and three types of hydrogen atoms. Uniaxial whole-molecule motions take place below 50 K, but above 50 K methyl rotation and whole-molecule rotations about multiple molecular axes occur with increasing probability. These dynamics occur over multiple time scales, depending on the temperature but also because whole-molecule reorientation is slower than rotation of the methyl group, which MD simulations show to become freely rotating above 200 K. The presence of three types of hydrogen atoms makes the finer details of quasielastic neutron scattering experiments and MD simulations difficult to compare and interpret. Furthermore,

the highly asymmetric shape of PO makes it one of the largest guests for a structure II CH; it has a lattice parameter and thermal expansivity closer to that of tetrahydrofuran ( $C_4H_8O$ ) CH than to trimethylene oxide ( $C_3H_6O$ ) CH. In fact, the large size of PO allows it to interact strongly with the host and causes a non-monotonic change in the volume of the 5(12)6(4) cage with temperature. All of this complex behavior of PO takes place within a highly orientation-dependent “cavity potential” created by the 5(12)6(4) cage. Because of the large size and highly asymmetric shape of PO, this potential should show a dramatic dependence on both whole-molecular orientation and the methyl-oxirane dihedral angle. This talk presents recent results from ab initio calculations of the potential energy surfaces of the PO methyl group and whole molecule as a function of orientation of the PO molecule within the cage, and discusses these results in terms of recent QENS and MD work and the possibility of guest-host binding interactions and preferred orientation of PO within the cage.

M3-B3 (2:45 pm)

**Powder neutron diffraction structure of ammonia-borane**

M. Hartl, L. Daemen (Los Alamos Neutron Science Center, Los Alamos National Laboratory), A. Stowe, N. Hess, T. Autrey (Pacific Northwest National Laboratory)

Ammonia-borane,  $NH_3BH_3$ , was first synthesized by Shore and Parry at the University of Michigan in 1955 [S.G. Shore and R.W. Parry, J. Am. Chem. Soc., **77**, 6084 (1955)]. It has drawn considerable attention lately as a possible hydrogen storage medium in view of its large hydrogen content (19.6% by weight). The molecule of ammonia-borane can be viewed as a Lewis acid-base adduct with a coordinate (covalent dative) bond between boron and nitrogen. At room temperature the material is tetragonal (14mm,  $a=5.240$ ,  $c=5.028$ ); it undergoes a phase transition to an orthorhombic unit cell (Pmn21,  $a=5.517$ ,  $b=4.742$ ,  $c=5.020$ ) at 225 K. Both phases exhibit a network of dihydrogen bonds that have a significant impact on the physical and chemical properties of these hydrogen rich materials. At higher temperatures the interaction of these intermolecular dihydrogen bonding is believed to be involved in the mechanistic pathway leading to the formation of molecular hydrogen from solid state ammonia-borane. Dihydrogen bonds, X-H...H-Y are unconventional hydrogen

bonds in which X represents an element less electronegative than hydrogen, whereas Y is a conventional electronegative atom (or group of atoms). One hydrogen exhibits a marked protonic character (as in a conventional hydrogen bond) while the other one displays hydridic character. The fact that the dihydrogen bonds are bifurcated and the rotational disorder of  $\text{NH}_3$  (and perhaps  $\text{BH}_3$ ) complicate significantly the task of elucidating the details of the structure of ammonia-borane. Most of the crystallographic work to date has been performed with powder x-ray diffraction (low Z elements, poor contrast) or neutron single crystal diffraction (with natural boron and hydrogen). We recently developed a simple and efficient method for the laboratory-scale synthesis of ammonia-borane in good yields and high purity and proceeded to synthesize enough  $\text{ND}_3$ ,  $^{11}\text{BD}_3$  for neutron powder diffraction. We collected diffraction patterns at three different temperatures on the Neutron Powder Diffractometer, NPDF -a high resolution total scattering powder diffractometer at LANSCE. We report on a new phase transition in ammonia-borane and discuss the nature of disorder in the material and its effect on dihydrogen bonding.

M3-B4 (3:00 pm)

### Hydrogen rotation in carbon materials

C. M. Brown (Indiana University Cyclotron Facility), Y. Liu (University of Maryland), D. A. Neumann (National Institute of Standards and Technology)

Hydrogen adsorption on nanoporous carbons has received considerable attention since the early report of as much as 10 weight percent hydrogen reversibly stored on single-walled carbon nanotubes (SWNTs) near room temperature [1] coupled with the interest in moving to a hydrogen-based economy. This interest persists because carbon is a light element, cheap, available in bulk and able to be produced with very high specific surface areas ( $\approx 3000 \text{ m}^2/\text{g}$ ). A consensus seems to be forming in the research community that if carbon is going to be technologically useful in storing hydrogen, methods must be developed that can enhance the binding energy of  $\text{H}_2$  to the carbon framework while maintaining the high specific surface area. Theoretical approaches recently proposed to increase the binding potential of hydrogen to carbons include decorating with metal catalysts [2] and substituting carbon for boron

[3]. We present results from inelastic neutron scattering of hydrogen adsorbed upon carbon materials synthesized with the aim of increasing the binding potential.

[1] A.C. Dillon, K.M. Jones, T.A. Bekkedahl, C.H. Kiang, D.S. Bethune, M. J. Heben, *Nature* **386** (1997) 377.

[2] T. Yildirim, S. Ciraci, *Phys. Rev. Lett.* **94** (2005) 5501.

[3] Y.H. Kim, Y. Zhao, A. Williamson, M.J. Heben, S.B. Zhang, *Phys. Rev. Lett.* **96** (2006) 016102.

M3-B5 (3:15 pm)

### Vibrational Density of States of Ammonia-Borane and Ammonia Borane Adsorbed into Mesoporous Silica

A. C. Stowe (Pacific Northwest National Laboratory), M. Harlt, L. L. Daemen (Los Alamos National Laboratory), C. Brown, T. Udovic (National Institute of Standards and Technology), N. Hess, M. Gutowski, T. Autrey (Pacific Northwest National Laboratory)

Inelastic neutron scattering studies have been conducted to explore the dihydrogen bonding nature of ammonia borane ( $\text{NH}_3\text{BH}_3$ ) in the low temperature orthorhombic phase. Eight soft dihydrogen vibrational modes as well as the torsional modes which are optically inactive, may be observed in the low frequency neutron vibrational spectrum of  $\text{NH}_3\text{BH}_3$ . DFT and MP2 calculations of the linear and cyclic AB dimer were used to enhance the identification of the intermolecular dihydrogen bonding modes. The neutron vibrational spectrum for ammonia borane adsorbed into a mesoporous silica substrate (nano-phase AB) was measured to gain insight into the interfacial interactions. Nano-phase AB has been shown to have enhanced thermodynamics and kinetics for dehydrogenation.

M3-C (1:45 – 3:30 pm)

### Superconductivity

Chair: J. Tranquada (Amphitheater)

M3-C1 (1:45 pm)

### Vortex Studies in Type-II Superconductors by Small-Angle Neutron Scattering (Invited)

M. R. Eskildsen (University of Notre Dame)

We have used SANS to study the flux-line lattice (FLL) in a range of unusual superconductors, with the emphasis on investigating the detailed nature of the superconducting state in the host material. This talk will focus on measurements of the FLL form factor in  $\text{MgB}_2$  and  $\text{CeCoIn}_5$ , which in both of these

compound deviate from the usual exponential field dependence although for different reasons. In  $\text{MgB}_2$  the rapid suppression of superconductivity on the  $\pi$ -band, leads to a reduction of the superfluid density which in turn trigger a reorientation of the FLL. In  $\text{CeCoIn}_5$  the form factor is found to be independent of the applied field. This result is consistent with a strongly field-dependent coherence length in  $\text{CeCoIn}_5$ , in qualitative agreement with recent theoretical predictions for superclean, high- $\kappa$  superconductors.

M3-C2 (2:15 pm)

### **Optimal Inhomogeneity for High Temperature Superconductivity (Invited)**

S. Kivelson (Stanford university)

It is widely believed that the phrases “mechanism of superconductivity” and “BCS theory” are synonymous, and that all that needs to be identified in any particular material is the character of the “glue,” i.e. the nature of the intermediate boson. However, the BCS mechanism derives from a Fermi surface instability, and therefore presupposes (as has often been stressed by Schrieffer) an accurate description of the normal state in terms of Fermi liquid theory. Contrary to popular belief, it is possible to have circumstances in which the normal state is highly incoherent down to  $T_c$ , so BCS theory does not apply. I will illustrate a non-BCS mechanism in a solvable highly inhomogeneous Hubbard model. On a more speculative note, I will present arguments that there exists an optimal inhomogeneity for superconductivity, and suggest that the various sorts of self-organized inhomogeneous structures that are seen in the cuprates may be essential to the mechanism of high temperature superconductivity.

M3-C3 (2:45 pm)

### **Spontaneous Symmetry-Breaking Transitions and Glassy Phases of the Flux Line Lattice in Superconducting Niobium**

M. Laver (Institut Laue-Langevin, France), E. M. Forgan (University of Birmingham, UK)

The lattice of magnetic flux lines formed in Type-II superconductors provides an ideal system with which to investigate the effects of underlying weak quenched disorder, since the concentration of disorder can be “tuned” not only by the addition of impurities to the crystal, but the flux line lattice

spacing can be adjusted by varying the applied field. In a popular recent theory, weak disorder is believed to result in a phase which is nearly as ordered as a perfect crystal - the so-called Bragg glass. This novel phase, exhibiting divergent Bragg peaks, is unexpected by previous theoretical treatments that anticipate the destruction of true long-range order. Here we report on extensive small-angle neutron scattering (SANS) studies of the flux line lattice (FLL) in high-quality single crystals of niobium, some with known amounts of impurities added, using a high-resolution technique that measures *directly* the relevant (in-plane) correlations between flux lines. Our results may have some general relevance in other quasi-2D systems including liquid crystals, spin glasses, crystal growth on substrates and 2D electron hole systems. The *morphology* of the flux line lattice also gives valuable information about the nature of the superconducting state. The structure of the FLL typically reflects the anisotropies present in the superconducting gap or in the Fermi surface. We explore in detail the situation in *pure* niobium with field applied parallel to a fourfold-symmetry crystal axis, so inducing frustration between the crystal symmetry and the hexagonal FLL coordination expected from an isotropic situation. We observe that all of the FLL phases spontaneously *break* some crystallographic symmetry, which is quite unlike the situation in the high- $T_c$  or borocarbide superconductors where the FLL structures align with the underlying crystal. The causes of this behavior are discussed.

M3-C4 (3:00 pm)

### **The Origin of the Pseudogap in High $T_c$ Superconductors**

H. A. Mook (Oak Ridge National Laboratory), P. Dai (University of Tennessee), H. J. Kang, J. W. Lynn (NIST Center for Neutron Research)

The origin of the pseudogap is one of the most important questions in high  $T_c$  superconductors. The idea of the pseudogap will be introduced and methods of determining it will be discussed. The idea of circulating currents as being responsible for the pseudogap will be considered and various current paths through the Cu-O plane examined in the light of recent neutron scattering experiments.



M3-C5 (3:15 pm)

**Localization of Bose-Einstein condensation in liquid helium confined in nanoporous media**

A. Shams, H. Glyde (University of Delaware)

We have made inelastic neutron scattering measurements of the elementary phonon-roton (P-R) excitations and of Bose-Einstein condensation (BEC) of liquid  $^4\text{He}$  confined in porous media. The aim is to explore the interdependence of BEC, the P-R modes and superfluidity in  $^4\text{He}$  confined to nanoscale dimensions and in disorder. Specifically, the goal is to determine whether, at finite size and in disorder, superfluidity depends on the existence of BEC or on the existence of well-defined P-R modes, as proposed by Landau. We find that in all porous media investigated to date that we observe well-defined excitations and BEC at temperatures above the superfluid-normal transition temperature,  $T_c$ , in the “normal” phase. Contrary to expectations, there can be BEC and well defined modes but no superfluidity. This BEC above  $T_c$  is interpreted as BEC that is localized to specific regions in the sample separated by regions of normal fluid. Above  $T_c$ , there is localized phase coherence only rather than phase coherence extended across the sample as needed for observable superflow in 3D. In this talk we present a Monte Carlo calculation of BEC in porous media. The goal is to demonstrate that BEC can be separated (localized) by regions of strong attractive potential. We represent the media by two regions separated by a strip of attractive potential. We show that an initially continuous condensate can be divided into two parts by the strip of high potential where the condensate fraction is driven to zero. In this way we show that a condensate can be localized or separated into isolated regions by a spatially varying external potential.

[1] H. R. Glyde, O. Plantevin et al. *Phys. Rev. Lett.* **84**, 2646 (2000)[2] O. Plantevin, H. R. Glyde, et al. *Phys. Rev.* **B65**, 224505 (2002)[3] F. Albergamo, H. R. Glyde, et al. *Phys. Rev.* **B69**, 014514 (2004).[4] J. V. Pearce, J. Bossy, et al., *Phys. Rev. Lett.* **93**, 145303 (2004).

M3-D (1:45 – 3:30 pm)

**Industrial Applications and Neutron Science**

Chair: X.-L. Wang (New Orleans Ballroom)

M3-D1 (1:45 pm)

**Of Pigs, Pipes and Particles: Neutrons in the Oil Patch (Invited)**

L. Clapham (Queen's University, Kingston, Canada)

Neutron diffraction can be applied to many different industrial situations. Strain in engineering materials can be complex and very difficult to measure non-destructively, yet an understanding of strain distributions is critical in evaluating the remaining lifetime of a material and in some cases the mechanisms of failure. This talk will focus on applications relevant to the oil patch and oil and gas industry, and will cover a range from highly applied contract work, through to more fundamental studies. Three examples taken from the author's contracts and research will be discussed.

Using neutron diffraction to investigate the origins of cracking in pump components used for well fracturing. Using neutron diffraction to calibrate and understand magnetic signals obtained from dent defects during non-destructive testing of oil and gas pipelines. A more fundamental investigation using neutron diffraction to study how intergranular stresses affect magnetic behaviour in steels.

M3-D2 (2:15 pm)

**Beyond Slip : Using Neutron Diffraction and Polycrystalline Plasticity Models to Understand Plastic Deformation in Anisotropic Materials (Invited)**

D. W. Brown, W. R. Blumenthal, M. A. Bourke, C. N. Tome, S. C. Vogel (Los Alamos National Laboratory), S. R. Agnew (University of Virginia)

Plastic deformation in cubic metals is relatively simple due to the high crystallographic symmetry of the underlying structure. Typically, one unique slip mode can provide arbitrary deformation. This is not true in lower symmetry hexagonal metals, for instance, where prismatic and basal slip (the usual favored modes) are insufficient to provide arbitrary deformation. Often, through control of the crystallographic texture, non-slip deformation modes, such as twinning and/or deformation induced martensitic phase transformations may be activated, resulting in

novel mechanical properties that may be exploited. For instance, the pseudo-elastic and thermo-elastic shape memory effects are associated with deformation induced transformation and twinning, respectively. Deformation induced twinning and martensitic phase transformations are mechanistically similar and may be discussed in parallel. This talk highlights studies undertaken by several researchers at the Los Alamos Neutron Scattering Center (LANSCE) over the past two years focused on the combined use of neutron diffraction measurements and polycrystalline plasticity models to better understand these atypical deformation mechanisms. Examples of both industrial (magnesium and nickel-titanium) and weapons (beryllium and uranium-niobium) significant alloys will be presented to highlight the techniques as well as summarize general results.

M3-D3 (2:45 pm)

### **The Potential of Neutrons for Industrial Research – Examples from SINQ illustrating opportunities and challenges**

W. Wagner, E. Lehmann (Paul Scherrer Institute), M. Grosse (Forschungszentrum Karlsruhe), J. Kohlbrecher (Paul Scherrer Institute)

SINQ is a continuous spallation neutron source, driven by PSI's 590 MeV proton accelerator. Receiving a stable proton current of 1.3 mA, SINQ is the presently most powerful accelerator driven facility worldwide. The primary designation of SINQ is to serve as user facility for neutron scattering and neutron imaging. Within the user program, SINQ is aspiring to attract an appropriate contingent of industrial applications. The paper highlights the potential for industrial research by means of selected experiments conducted at SINQ, addressing different fields of application: non-destructive inspection by neutron radiography and tomography, strain mapping for transportation systems, SANS studies on dispersions and suspensions, and time resolved or *in-situ* radiography following dynamic processes.

M3-D4 (3:00 pm)

### **Residual Stresses due to Explosive Welding in Pressure Vessels**

T. Watkins (Oak Ridge National Laboratory), D. J. Taylor (TPL, Inc.), C. R. Hubbard, F. Tang, W. B. Bailey (Oak Ridge National Laboratory)

Refractory metal liners are explosively welded into pressure vessels made of mild steel to increase wear and erosion resistance. The cladding increases the useful lifetime of these vessels by a factor of 3 to possibly 10, which represents a cost savings not only in fewer vessels, but in time, logistics and labor to replace vessels less frequently. Since the residual stress profile of these vessels is important to their use and lifetime, the effect of the explosive cladding process on residual strain must be determined in order to compensate for it in production. Three samples were examined using neutron diffraction: (1) non-clad (stress-free), (2) clad in a stress-free vessel, and (3) clad in a pre-stressed vessel. The corresponding residual stress analyses will be presented.

*Research sponsored by the Assistant Secretary for Energy Efficiency and Renewable Energy, Office of FreedomCAR and Vehicle Technologies, as part of the High Temperature Materials Laboratory User Program, Oak Ridge National Laboratory, managed by UT-Battelle, LLC, for the U.S. Department of Energy under contract number DE-AC05-00OR22725.*

M3-D5 (3:15 pm)

### **Determination of residual stress in Nb<sub>3</sub>Sn superconducting wire**

T. S. Parikh, N. A. Fellows, J. F. Durodola (Oxford Brookes University, UK)

The main goal of this work is to develop suitable techniques for predicting and measuring residual stress in the Nb<sub>3</sub>Sn wires used in high field superconducting magnets. Knowledge of the residual stress state is required to improve the current and load carrying capacity of these wires and predict wire failure. The specimen involved in this work is a niobium tin (Nb<sub>3</sub>Sn) wire, which is 1.5 mm in diameter and very brittle in nature. It consists of a copper core, which is covered by very thin niobium (Nb) and tantalum (Ta) layers. Outside these two thin layers, there are niobium filaments surrounded by a bronze matrix. The figure below shows the cross sectional view of Nb<sub>3</sub>Sn wire. Overall, there are about 10000 filaments in the wire, each around 3 μm in diameter. After the fabrication of Nb<sub>3</sub>Sn, the wire is given a prolonged heat treatment, typically for 1-10 days

at 700° C. During this heat treatment, tin diffuses through the bronze and reacts with the niobium to form Nb<sub>3</sub>Sn. Residual thermal stresses develop in the composite because of the different coefficients of thermal expansion of the components. We are interested in the residual stress in axial, radial, and hoop directions in the different materials, particularly in the Nb<sub>3</sub>Sn filaments. We are developing a chemical etching method for use in the laboratory, in which HNO<sub>3</sub> is used to etch the outer layers by 0.1mm and strain readings are measured. Results from chemical etching will be compared with those from neutron diffraction work to be done at FRM-II, Munich. We hope this work will lead to a novel non-destructive experimental method for determining residual stresses in composite superconducting wires, enabling better superconducting magnet design. The combination of the chemical etching method, analytical calculations, finite element modelling and neutron/synchrotron diffraction will validate each result.

M4-A (4:00 – 5:45 pm)

### **Nanoscience with Neutrons**

*Chair: L. Horton (Amphitheater)*

M4-A1 (4:00 pm)

#### **The vector magnetization depth profile of a Laves phase exchange-coupled superlattice obtained using a combined approach of micromagnetic simulation and neutron reflectometry (Invited)**

M. R. Fitzsimmons, S. Park (Los Alamos National Laboratory), K. Dumesnil, C. Dufour (Laboratoire de Physique des Matériaux, Université H. Poincaré Nancy I, BP 239, 54506 Vandœuvre les Nancy Cedex, France), R. Pynn (University of Indiana, Bloomington, IN), J. A. Borchers (NIST Center for Neutron Research), J. J. Rhyne (Los Alamos National Laboratory), P. H. Mangin (Laboratoire Léon Brillouin (UMR 12 CNRS/CEA) CEA-Saclay 91191 Gif sur Yvette France)

Owing to the coexistence of ferromagnetic and antiferromagnetic exchange coupling in an exchange-coupled Laves phase superlattice composed of DyFe<sub>2</sub> and YFe<sub>2</sub> layers, the field dependence of the magnetization depth profile is complex. Using a novel approach that combines micromagnetic simulation and analysis of neutron scattering data, we have obtained the depth dependence of magnetization across the DyFe<sub>2</sub>/YFe<sub>2</sub> interfaces. We find that the exchange interaction

across the interface is reduced compared to the exchange interaction of the constituent layers; therefore, compromising the ability of this system to resist magnetization reversal in large applied fields.

M4-A2 (4:30 pm)

#### **Diffraction and Inelastic Neutron Scattering Measurements on Exchange-Biased Co/CoO Core-Shell Nanoparticles (Invited)**

G. L. Strycker, S. E. Inderhees, M. C. Aronson (University of Michigan), Y. Qiu, J. A. Borchers (NIST Center for Neutron Research)

We report results of diffraction and inelastic neutron scattering measurements on exchange biased Co/CoO core-shell nanoparticles. Electron microscopy experiments show that these surfactant coated particles have a Co core which is 5 +/- 2 nm, and a uniform CoO shell thickness of 2 nm. Magnetization measurements indicate that the core dynamics are blocked at ~ 230 K, while the exchange field emerges at 190 K. Diffraction experiments found the antiferromagnetic ( $\frac{1}{2} \frac{1}{2} \frac{1}{2}$ ) peak of bulk CoO, albeit with a reduced Neel temperature of 250 K. For temperatures below 330 K, we also found a broad magnetic peak at the CoO (100) which we ascribe to ferromagnetically aligned moments at the interface of the core and shell. These data indicate that the interface moments align first, and that antiferromagnetic order of the shell triggers the blocking of the core dynamics. We used inelastic neutron scattering measurements, obtained using the DCS time of flight spectrometer at NIST, to explore the exchange blocking mechanism further. At high temperatures, the scattering is broad and quasielastic with an amplitude adequately described by short range magnetic interactions consistent with the CoO magnetic structure. The quasielastic linewidth is approximately linear with wave vector, and decreases markedly with reduced temperature, signaling that longitudinal fluctuations of the core moment are increasingly frozen out near the magnetization blocking temperature. The scattering is qualitatively different below the Co core blocking temperature and the CoO Neel temperature. At low temperature, an almost dispersionless inelastic peak emerges from the quasielastic scattering. We ascribe this feature to the transverse fluctuations of the interface moments, in a field which tracks the antiferromagnetic ( $\frac{1}{2} \frac{1}{2} \frac{1}{2}$ ) order parameter of the CoO shell. Our results indicate that the

magnetic structure of the Co/CoO core shell nanoparticles is complex, with magnetic order occurring independently in both the CoO shell and interface regions. The staggered field created by conventional antiferromagnetic order in the CoO shell seems to have dual purposes in establishing the exchange bias effect. First, the onset of antiferromagnetic order leads almost immediately to freezing of the longitudinal fluctuations. Further growth of the antiferromagnetic order parameter results in the establishment of a quasi-static field in both the core and the interface, reflected in the emergence of a macroscopic exchange field in magnetization measurements.

*Work at the University of Michigan performed under the auspices of the Department of Energy, Office of Basic Energy Science.*

M4-A3 (5:00 pm)

### **An Observation of Nanoscale Spin Clusters in a Single Crystal $\text{Pr}_{0.7}\text{Ca}_{0.3}\text{MnO}_3$**

H. Sha (Florida International University), F. Ye, J. A. Fernandez-Baca (Oak Ridge National Laboratory), P. Dai, E. W. Plummer (University of Tennessee), Y. Tomioka (CERC, Japan), Y. Tokura (University of Tokyo, Japan), J. Zhang (Florida International University)

Colossal magnetoresistive manganite  $\text{Pr}_{0.7}\text{Ca}_{0.3}\text{MnO}_3$  (PCMO30) is an ideal system to test the microscopic phase separation scenario because it has an inhomogeneous low-temperature insulating metastable state where ferromagnetic (FM), antiferromagnetic (AF), and charge/orbital (CO-OO) phases coexist. On cooling from room temperature, a CO-OO state occurs below  $T_{\text{CO-OO}} \sim 200$  K, followed by AF ordering below  $T_N \sim 140$  K. Below  $T_C \sim 110$  K, the magnetic structure develops a FM component coexisting with AF ordering. We have used neutron scattering to study FM, AF and CO-OO phase transitions in a single-crystal PCMO30. The diffuse scattering of FM component demonstrates the presence of short-range ferromagnetic clusters both above and below  $T_C$ , while no diffuse component in the CO-OO scattering peaks has been observed near  $T_{\text{CO-OO}}$ . Interestingly, the short-range AF correlations associated with  $\text{Mn}^{4+}$  sites but not with  $\text{Mn}^{3+}$  sites are observed for both above and below  $T_N$ , indicating that the local AFM clustering is directly associated with doped holes in this system.

*The work was supported by NSF-DMR0453804, NSF-DMR0346826, DE-FG02-05ER46202, and DOE DE-FG02-04ER46125. ORNL is managed by UT-Battelle, LLC, for the U.S. DOE under contract DE-AC05-00OR22725.*

M4-A4 (5:15 pm)

### **SANS study on structures and counterion binding in anionic perfluorinated surfactant systems**

G. T. Warren, D. P. Bossev (Indiana University, Bloomington, IN)

Tetraethylammonium ( $\text{TEA}^+$ ) counterions, in contrast to lithium ( $\text{Li}^+$ ) counterions, induce high viscosity in aqueous solutions of perfluorooctylsulfonate (FOS) surfactant ions. This phenomenon was attributed to the degree and mechanism of counterion binding. The  $\text{TEA}^+$  counterion was found by using NMR to be preferentially bound to the micellar surface in mixtures of TEAFOS/LiFOS. In this work we have chosen small angle neutron scattering technique (SANS) to investigate the structures formed by the anionic perfluorooctylsulfonate surfactant ion in combination with various counterions. SANS is an ideal method to characterize the morphology of the micellar aggregation phase behavior, in providing answers to questions regarding structure, counterion binding, formation of Stern layer, and effective range of the diffuse double-layer with respect to the two counterion species of our perfluorinated surfactant system. We have taken advantage of the contrast variation techniques to obtain separate scattering curves from the micellar core and the counterion atmosphere. Based on the SANS data we determined the structures and the mechanism of the spherical to threadlike micellar transition in the presence of two different counterions at different ratios.

M4-A5 (5:30 pm)

### **Magnetic excitations in the magnetic molecule $\{\text{Cr}_8\}$**

V. O. Garlea, S. E. Nagler (Oak Ridge National Laboratory), J. Li, P. Kögerler, L. Engelhardt, M. Luban (Ames Laboratory), Y. Qiu (NIST Center for Neutron Research and University of Maryland), D. Vaknin (Ames Laboratory)

Inelastic neutron scattering studies of the cubane-like cluster  $\{\text{Cr}_8\}$  reveal two prominent magnetic excitations that are strongly dependent on both magnetic-field and temperature. The  $\{\text{Cr}_8\}$  cluster consists of eight  $s = 3/2$   $\text{Cr}^{\text{III}}$  paramagnetic centers arranged as a central  $\text{Cr}_4\text{O}_4$  cube-like structure surrounded by four outer Cr ions that occupy the vertices of a tetrahedron. To model the spin system, we assume three distinct isotropic exchange couplings among nearest and next nearest neighbors. Numerical diagonalization of the Hamiltonian with the three distinct



antiferromagnetic exchange couplings yields a singlet ground state ( $S = 0$ ) and two distinct triplet excited states ( $S = 1$ ) consistent with the two excitations observed experimentally. The change in intensity of the two excitation peaks as a function of magnetic field at base temperature ( $\sim 100$  mK) can be explained by the theoretical predictions. Furthermore, the neutron scattering data also indicate a level-crossing just below 2 Tesla that can also be explained qualitatively by the theoretical spectrum scheme.

M4-B (4:00 – 5:45 pm)

### ***In situ* Experiments I: Deformation Mechanics**

**Chair: Mark Bourke (New Orleans Ballroom)**

M4-B1 (4:00 pm)

#### **Neutron diffraction used for the development of energy harvesting and actuator magnetic polymer matrix composites (Invited)**

R. Ham-Su (Defence R&D Canada - Atlantic), M. A. Gharghouri (National Research Council Canada), S. P. Farrell (Defence R&D Canada - Atlantic)

Magnetic shape memory alloys (MSMA's) can convert magnetic energy into mechanical energy and vice versa. NiMnGa-based MSMA's have attained magnetic field induced strains up to approximately 10% at temperatures ranging from well below 0°C to above room temperature, making them very attractive for a variety of applications. Current MSMA's suffer from low toughness. In addition, eddy currents are established under oscillating magnetic fields, resulting in significant energy losses. Using these alloys in composites, dispersed in a polymer, could overcome or mitigate these shortcomings. The magnetic shape memory effect is due to magnetic domain changes that accompany twin boundary motion in a single crystal subjected to a magnetic field. The material changes shape as a result of the twin boundary motion, performing work and acting as an actuator. The complementary effect occurs when work is done on the MSMA: twin boundaries move, giving rise to magnetic domain changes and thus fluctuating magnetic fields that can be used for energy harvesting. For a particle composite to work as actuator or energy harvester, the twin boundary motion must be harmonious throughout the sample: the effect from each particle must

add rather than cancel out. In this paper, the fabrication and characterization of MSMA/polymer matrix composites are described, with special emphasis on the role of neutron diffraction in the design and development of these materials. Of particular interest are the crystallographic texture measurements on MSMA particles embedded in a polymer matrix and the role of *in-situ* testing.

M4-B2 (4:30 pm)

#### ***In-Situ* Neutron Diffraction Measurement of Rapid Transient Temperature and Stress Fields (Invited)**

Z. Feng (Oak Ridge National Laboratory), W. Woo (University of Tennessee), X. Wang (Oak Ridge National Laboratory), D. W. Brown, B. Clausen (Los Alamos National Laboratory), K. An, C. Hubbard, S. A. David (Oak Ridge National Laboratory)

We present a novel experimental approach and results of direct experimental measurement of the temperature and thermal stress during thermomechanical processing of 6061-T6 aluminum plate using *in-situ* neutron diffraction measurements. This novel technique is based on the "quasi-steady state" phenomenon induced by moving, localized thermomechanical processing of the material of interest. The quasi-steady state circumvents the neutron flux limitation for studying the rapid transient material behavior. The principle of the quasi-steady state will be presented. The experimental set-up to achieve such quasi-steady state will be described. Decomposition of the thermal and elastic strains from the lattice spacing changes measured using the neutron diffraction will be discussed.

*This research is sponsored by the Laboratory Directed Research and Development program of Oak Ridge National Laboratory (ORNL), managed by UT-Battelle, LLC for the U. S. Department of Energy under Contract No. DE-AC05-00OR22725.*

M4-B3 (5:00 pm)

#### **Evaluation of the Dislocation Arrangement near the Crack Tip Region of 316LN Stainless Steel by Neutron and X-ray Diffraction**

Y. Sun (University of Tennessee), R. Barabash (Oak Ridge National Laboratory), H. Choo, P. K. Liaw, Y. L. Lu (University of Tennessee), D. W. Brown (Los Alamos Neutron Science Center, Los Alamos National Laboratory), G. Ice (Oak Ridge National Laboratory)

The deformation in the vicinity of the crack tip was studied with neutron diffraction and microbeam diffraction. From neutron diffraction measurements, anisotropic line broadening was observed at different distances from the crack

tip. The dislocation density and arrangement were studied from the diffraction peak width change behavior for several crystallographic families. Lattice strains were also measured. Non-random dislocation arrangement was obtained by observing the orientation dependence of both strain and diffraction peak broadening on (hkl). The comparison of the lattice strain profiles and peak-width change facilitate the understanding of the change of dislocation densities and strains in the plastic zone. Laue patterns from microbeam results were obtained at different locations near the crack. The analysis of these Laue patterns demonstrates that plastic-deformation results in the formation of the alternating regions with high and low dislocation densities. Over all the dislocation density was found to decrease with the distance from the crack tip.

*M4-B4 (5:15 pm)*

#### **Lattice strains representation for cubic polycrystalline materials as applied to cyclic deformation of stainless steel**

A. D. Stoica, X. L. Wang (Spallation Neutron Source, Oak Ridge National Laboratory), M. L. Benson (University of Tennessee), B. Clausen, D. W. Brown (Los Alamos Neutron Science Center, Los Alamos National Laboratory), M. R. Daymond (Queen's University, Kingston, Canada), P. K. Liaw (University of Tennessee)

The lattice strains measured by diffraction in a polycrystalline material can be related to the general concept of strain or stress orientation distribution function (SODF). However, in practice, finding the SODF is a laborious process, since the directional dependences of the lattice strain in both real space and reciprocal space are required. Furthermore, the solution is not unique because of the symmetry restrictions. We analyze the case of uniaxial loading and cubic crystal symmetry in an attempt to simplify the interpretation of in-situ loading experiments at a phenomenological level. In this case, a reciprocal space representation for longitudinal and transversal direction allows separation of the effects of elastic and plastic deformation on grain interaction. As an example, the lattice-strain development in 316LN stainless steel during cyclic deformation is characterized using this approach. Different experimental procedures are compared to assess the optimum way to study the fatigue behavior. It is shown that the evolution of the residual intergranular

strains during fatigue life provides insights on the nucleation and growth of cracks in a late stage of fatigue life.

*This research was supported by Division of Materials Sciences and Engineering, Office of Basic Energy Sciences, U.S. Department of Energy under Contract DE-AC05-00OR22725 with UT-Battelle, LLC.*

*M4-B5 (5:30 pm)*

#### **Phase Transformation in Ferromagnetic Shape-Memory Alloys**

Y. Wang (University of Tennessee and Northeastern University), D. Brown (Los Alamos Neutron Science Center, Los Alamos National Laboratory), Y. Ren (Argonne National Laboratory), H. Choo, M. L. Benson (University of Tennessee), Y. D. Liu (Northeastern University (China)), P. K. Liaw (University of Tennessee), L. Zuo (Northeastern University (China))

Materials that can reversibly change their dimension upon the application of external fields, such as magnetic or electric fields, have been used as actuators or sensors in many applications. Among them are magnetic-driven shape-memory alloys (SMAs), which can be deformed by a magnetic field. The possibility of a magnetic-field control of the shape-memory effect has been demonstrated in the ferromagnetic Ni-Mn-Ga and Ni-Co-Mn-In alloys with a composition close to the Heusler structure [1-5]. Although considerable attention has been devoted to the processing of ferromagnetic materials for optimal performance properties, the underlying mechanism that controls the shape-memory effect (SME) remains unclear. In particular, the interactions between crystallographic textures and stresses and their influences on the functional performance in polycrystalline SMAs are less understood. The neutron-diffraction technique based on the pulsed neutron source, in combination of the synchrotron X-ray diffraction method, provides the ability to trace in-situ changes in the detailed local and global information on the stress and orientation under the application of the temperature and high magnetic fields. The full information on crystallographic aspects during the phase transformation is essential for understanding the 'memory' characteristics in the ferromagnetic SMAs related to the texture and stress. In this presentation, some new progresses on the *in-situ* investigations of the phase transformation in the Ni-Mn-Ga and Ni-Mn-Ga-Co alloys [6] will be shown in all aspects, covering from the phase-transformation kinetics of bulk samples and nano-particles, the

influence of various stresses on the microstructural characteristics of SME, to the transformation behaviors under the stress and magnetic fields. The experimental investigations on the pre-transformation phenomena of ferromagnetic SMAs by neutron and X-ray diffuse scattering techniques are also presented.

*We greatly appreciate the National Science Foundation for the financial support of (1) the Integrative Graduate Education and Research Training (IGERT) Program (DGE-9987548), with Drs. C. J. Van Hardsveldt and D. Dutta as program directors; (2) the International Materials Institutes (IMI) Program (DMR-0231320), with Dr. C. Huber as the program director; and (3) the Combined Research-Curriculum Development Program (EEC-9527527 and EEC-0202415), with Ms. M. Poats as the program director. Additional financial support was gratefully received from the Tennessee Advanced Materials Laboratory, with Dr. E. W. Plummer as the director. The authors are also grateful to the National Natural Science Foundation of China (Grant No.s 50531020, 50325102 and 50528102). Use of the Advanced Photon Source was supported by the U.S. Department of Energy, Office of Science, Office of Basic Energy Science, under Contract No. W-31-109-ENG-38.*

- [1] V.A. Chernenko, V. L'vov, J. Pons, E. Cesari, *J Appl Phys* **93**, 2394 (2003).
  - [2] A. Sozinov, A.A. Likhachev, N. Lanska, K. Ullakko, *Appl Phys Lett* **80**, 1746 (2002).
  - [3] C.P. Henry, D. Bono, J. Feuchtwanger, S.M. Allen, R.C. O'Handley, *J Appl Phys* **91**, 7810 (2002).
  - [4] K. Ullakko, Y. Ezer, A. Sozinov, G. Kimmel, P. Yakovenko, V.K. Lindroos, *Scripta Mater* **44**, 475 (2001).
  - [5] R. Kainuma, Y. Imano, W. Ito, Y. Sutou, H. Morito, S. Okamoto, O. Kitakami, K. Oikawa, A. Fujita, T. Kanomata, K. Ishida, *Nature* **439**, 957 (2006).
  - [6] Y.D. Wang, D.Y. Cong, R. Lin Peng, P. Zetterström, Z.F. Zhang, X. Zhao, L. Zuo, *J. Mater. Res.* **21**, 691 (2006).
- \* To whom correspondence should be addressed,  
e-mail: ydwang@mail.neu.edu.cn

**M4-C (4:00 – 6:00 pm)**

## **Fundamental Physics**

**Chair: G. Greene (Ruby Room)**

**M4-C1 (4:00 pm)**

### **Nuclear, Particle, and Astrophysics with Low Energy Neutrons (Invited)**

**W. M. Snow (University of Indiana, Bloomington, IN)**

Measurements using low energy neutrons can address a number of important scientific questions in nuclear, particle, and astrophysics. Most of the experiments can be classified into three broad categories: (1) investigations of the strong interaction, (2) tests of the theory

of the electroweak interaction, (3) searches for phenomena beyond the “Standard Model” of particle physics and Big Bang cosmology. In this talk I will describe examples of experiments from each of these areas either in progress or planned at US neutron facilities

**M4-C2 (4:30 pm)**

### **Fundamental physics with ultracold neutrons (Invited)**

**P. R. Huffman (North Carolina State University)**

Ultracold neutrons (UCN) are a valuable tool used to investigate the weak interaction and to search for physics beyond the Standard Model. With energies of order 100 neV, UCN have energies comparable to the energies of material interactions, gravitational interactions, and magnetic interactions. Each of these types of interactions are currently used by experimentalists to confine UCN for extended periods of time, some as long as their beta-decay lifetime (~15 minutes). Experiments utilizing these confined neutrons include measurements of the neutron lifetime, the beta-decay asymmetry coefficient, and a search for the neutron electric dipole moment. I will present a survey of recent and proposed fundamental neutron physics measurements utilizing UCN. I will also report on future prospects, especially once new sources presently under construction become available.

**M4-C3 (5:00 pm)**

### **Contradictions of quantum scattering theory**

**V. K. Ignatovich (Joint Institute for Nuclear Research)**

The standard scattering theory (SST) in non relativistic quantum mechanics is analyzed. Contradictions of SST are revealed. Justification of SST in textbooks with the help of fundamental scattering theory (FST) is shown to be unconvincing. A theory of wave packets scattering on a fixed center is presented, and its similarity to plane wave scattering is demonstrated. The neutron scattering in a monatomic gas is investigated, and ambiguity of the cross section is found. The ways to resolve contradictions and ambiguity is suggested, and experiments to explore properties of the neutron are discussed.

M4-C4 (5:15 pm)

**aCORN: A New Measurement of the Electron-antineutrino Correlation Coefficient in Neutron Decay**

M. Leuschner (Indiana University Cyclotron Facility), G. L. Jones (Hamilton College), A. Komives (DePauW University), F. E. Wietfeldt (Tulane University, New Orleans, LA)

The aCORN collaboration plans to measure the electron-antineutrino correlation coefficient ("little a") in neutron decay. "a" is the least well known of the neutron decay coefficients. Its value, when combined with other neutron decay parameters, can be used to determine the weak vector and axial vector coupling constants and to test the validity and self-consistency of the Electroweak Standard Model.

The present accepted value for "a" is  $-0.103 \pm 0.004$ . Previous experiments that measured it relied on precise proton spectroscopy and were limited by systematic effects at about the 4% level. We propose a new approach to measuring "a" that uses an experimental asymmetry for which systematic uncertainties promise to be much smaller. The aCORN collaboration plans to reduce the uncertainty in "a" to less than 1%.

The experiment will be constructed and tested at the new LENS pulsed neutron source at IUCF. After commissioning in the spring and summer of 2007 it will be moved to the NG6 beamline at NIST where production running will occur. Detailed design and optimization results of the experimental apparatus will be presented

*The aCORN project is supported by the National Science Foundation MRI grant PHY-0420563.*

M4-C5 (5:30 pm)

**Search for the Electric Dipole Moment of the Neutron at SNS**

T. M. Ito (Los Alamos National Laboratory)

*(The listed author is giving the presentation representing the EDM collaboration)*

Physicists have been trying for 50 years now to detect the possible separation of positive and negative electric charges inside the neutron. This quantity, called the Electric Dipole Moment (EDM), is known to violate some of the basic symmetries, and if found to have a finite value, has a large implication for the fundamental theory of elementary particle physics. A new experiment to search for the neutron EDM with a sensitivity more than 2 orders of magnitude higher than the present

limit is planned to run at the Fundamental Neutron Physics Beamline at SNS. In this talk, the principle of the experiment, and the status of ongoing R&D will be reviewed and discussed.

M4-C6 (5:45 pm)

**Neutron-proton Scattering and Quantum Entanglement**

R. Moreh (Ben-Gurion University, Beer-Sheva, Israel), R. Block, Y. Danon, M. Neuman (Gaerttner LINAC Laboratory, Rensselaer Polytechnic Institute, Troy, New York 12180)

Recently, several experiments were reported concerning the observation of a strong anomalous drop,  $\sim 40\%$ , in the n-p scattering cross section compared to conventional values. The anomalies were reported in  $\sim 10$  different H-containing samples (such as  $H_2O$ , etc.), at room temperature, using 10 eV - 200 eV neutrons. All samples revealed more or less the same effect. This anomaly was explained in terms of short lived ( $10^{-15}$  to  $10^{-16}$ s) quantum entanglement of protons. It was suggested that during the very short times of the scattering process, no quantum decoherence is expected to take place. To test the above findings, we used neutrons generated from the RPI electron Linac and the final energy of the scattered neutrons was fixed at 24.3 keV using a pure iron filter. The scattering intensity ratios from  $H_2O$  and  $D_2O$  were found to agree with conventional values and no anomaly was observed [1]. In another experiment, the n-scattering intensities from  $CH_2$  and C (graphite) were compared at several discrete final energies, of narrow widths between 64 eV and 3 keV. The final energies were selected using a  $^{238}U$  filter. Here we searched for an anomaly in the n-p scattered intensities from  $CH_2$  caused by the neutron coherence length. At such energies and short scattering times ( $10^{-17}$  to  $10^{-18}$ s), decoherence is not likely to occur, and proton quantum entanglement was expected to show up clearly. Here again the scattering intensity ratios were found to conform to conventional values and no anomaly was observed [2]. Possible reasons for the above results will be discussed.

[1] R. Moreh, R. C. Block, Y. Danon, and M. Neuman, *Phys. Rev. Lett.* **94**, 185301 (2005).

[2] R. Moreh, R. C. Block, Y. Danon, and M. Neuman, *Phys. Rev. Lett.* **96**, 055301 (2006).



M4-D (4:00 – 5:45 pm)

**Polymeric Systems***Chair: M.-P. Nih (Turquoise A-B Room)*

M4-D1 (4:00 pm)

**The effect of environment on dynamics as probed by QENS (Invited)**

V. Garcia Sakai (University of Maryland)

The objective of this presentation is to address how quasi-elastic neutron scattering can help us understand how the environment affects the dynamics of components in macromolecular systems. The presentation will focus on an intriguing polymer blend, that of poly(ethylene oxide) and poly(methyl methacrylate), one whose behavior is still far from understood. These two polymers have widely differing glass transition temperatures and show distinct dynamic behavior in the blend system. Although the mobility of PMMA is greatly reduced in the presence of PEO, that of PEO is not so much affected. The results will be discussed in the context of the current models on blend dynamics. QENS data on the changes in the dynamics of biological macromolecules due to environment will also be addressed.

M4-D2 (4:30 pm)

**Minimizing the Concentration of Diblock Copolymer Needed to Obtain Polymeric Lamellar Phases (Invited)**

N. Balsara, M. L. Ruegg (University of California, Berkeley)

We propose a new strategy for stabilizing the interface between immiscible polymers. Organized microphases are obtained when an A-C diblock copolymer is added to mixtures of A and B homopolymers. The C-block exhibits attractive interactions with B and repulsive interactions with A. In contrast, previous studies have focused on A-B block copolymers wherein the inter-chain interactions are purely repulsive. Using neutron scattering and self-consistent field theory, we show that organized lamellar microphases are obtained when as little as 1% of the A-C copolymer is added to a 50/50 A/B mixture.

M4-D3 (5:00 pm)

**Adsorption of polymer/surfactant mixtures at the air-water and sapphire-water interfaces: poly(dimethyl aminoethylmethacrylate) and sodium dodecyl sulphate**

S. Titmuss, M. Moglianetti (University of Oxford), S. P. Armes (University of Sheffield), P. Li, R. K. Thomas (University of Oxford)

The adsorption of the polymer/surfactant mixture mispoly(dimethyl aminoethylmethacrylate) (poly-(DMAEMA)) and sodium dodecyl sulphate (SDS) has been studied at the air-water interface using specular neutron reflectivity and surface tension and at the sapphire-water interface using X-ray reflectivity and AFM.

At the air-water interface, surface tension measurements and neutron reflectivity from null reflecting water provide two independent measures of surface coverage. We outline the considerations necessary to rationalise these independent measurements.

The use of different combinations of perdeuterated polymer and surfactant and suitable contrast conditions, enable the distributions of polymer, surfactant and water through the interfacial region to be elucidated.

The addition of a negatively charged, short-chain, surfactant SDS, results in the formation of multilayer structures as signified by the emergence of characteristic Bragg-peaks in the reflectivity profiles.

Comparisons will be drawn with the interaction behaviour of SDS and brushes of poly(DMAEMA) grown at the sapphire-water interface by surface-initiated atom-transfer radical polymerization.

M4-D4 (5:15 pm)

**Internal Morphology of Diblock Copolymer Brushes Determined by Neutron Reflectivity**

M. D. Foster, B. Akgun, W. J. Brittain (University of Akron), C. F. Majkrzak (National Institute of Standards and Technology)

Although diblock copolymer brushes (BCB) have been extensively studied in recent years, their internal structure is still unknown. To elucidate the interface width and internal structure of BCBs, neutron reflectivity (NR) has been used. BCBs of deuterated polystyrene (dPS) and poly(methyl acrylate) (PMA) with dPS adjacent to the surface (d-PS-b-PMA) or with PMA adjacent to the surface (PMA-b-dPS) and having different thicknesses were synthesized using atom transfer radical

polymerization. In ultrathin BCBs a gradient in composition perpendicular to the surface extends essentially through the entire thickness of the brush. The interface width, defined as the full-width at half-maximum of a Gaussian function needed to represent the broadening of the step interface profile, is found to be smaller for PMA-b-dPS than for dPS-b-PMA brushes. The interface width for a film spun from untethered chains of dPS-b-PMA has been measured and the results compared with those for the BCBs. BCBs have been measured in both good solvent and poor solvent vapors with NR and the concentration profiles and extent of swelling determined.

*M4-D5 (5:30 pm)*

### **Structural and Collective Dynamics Studies of Highly Rigid polymers in Solutions**

D. Perahia, Y. Jiang, U. H. Bunz (Clemson University)

The chemical structure together with association modes and the dynamics of polymers define their properties. Numerous neutron based studies have targeted the structure and dynamics in co-polymers and blends, where the experimental results have been analyzed in view of current theories. In this study we report a small angle neutron scattering (SANS) and neutron spin echo (NSE) studies of a highly rigid polydispersed polymer, 2,5-Dialky-Poly(p-phenyleneethynylene (PPE) in solutions. Alkyl substituted PPEs are conjugated polymers with well define fluorescence characteristics that are directly correlated with the degree of conjugation of the backbone. These polymers are inherently semiconducting and their association mode and dynamics are directly coupled to their electro-optical response. The degree of conjugation depends on the association of the PPE into aggregates and dynamics of the backbone and the side chains. SANS provided the length scale needed to study the structure of the polymer solutions and NSE the dynamics of the polymer on multiple length scales. SANS studies identifies three phases, a molecular solution in which the polymer molecules are isolated and fully stretched, a micellar solution that consists of flat aggregates and a gel phase, formed as a result of jamming of aggregates into each other. These measurements have shown that an equilibrium between the stacking of the backbone and the solubility of the side chains results in well

defined aggregates. NSE studies have provided an insight into collective dynamics of the aggregates as affected by the motion of the individual chain and the side chains. New models are currently being developed to correlate these processes. The combination of elastic and inelastic scattering in polymer solution of these highly rigid polymers, provide a comprehensive understanding of the correlation between aggregation and the dynamics within a polymer solution.

---

*MP (8:00 – 10:00 pm)*

### **Reception and Poster Session: Student Research Award (St. Charles Ballroom)**

*MP01*

#### **Addition of hydrogen to Ni-Ti multilayers: Implications for improved neutron monochromator and neutron supermirror performance**

H. Ju, B. J. Heuser (University of Illinois)

Ni-Cr supermirror coatings extend the range of total external reflection and find application as neutron optical elements. In principle, the addition of hydrogen to Ti should increase the scattering length density contrast between the Ti and Ni, thereby improving the neutron reflectivity response. This has never been documented in the published literature, however. We have investigated the effect of incorporating hydrogen into the Ti component of multilayer (ML) depositions with a variety of experimental techniques. Two series of ML depositions, with and without hydrogen, were fabricated by magnetron sputtering. The number of bilayers (BL) in each series was varied from 1 to 40, with a typical bilayer spacing of 80 Angstroms. The effect of hydrogen addition on the first-order ML diffraction peak was characterized with neutron reflectometry (NR) and x-ray reflectometry. The effect of hydrogen addition was to increase the peak neutron reflectivity by ~50% for all samples. Such an improvement would correspond to a ~2 increase in end-of-guide intensity. The crystal structure and texture were characterized with x-ray diffraction. Results of this analysis indicated the expected (111) and (001) texture of the Ni and Ti, respectively, and the existence of TiH<sub>2</sub> hydride when hydrogen was added to Ti. The TiH<sub>2</sub> stoichiometry was also confirmed with temperature programmed desorption analysis.

Fits to the NR data are also consistent with TiH<sub>2</sub>. Surface roughness was quantified with atomic force microscopy (AFM). A correlation between the first-order ML diffraction peak intensity and the RMS roughness from AFM has been established and explain the general trend of fall of in peak reflectivity for greater BL values. The presentation of this work will focus on the neutron reflectivity response, including data fitting, and the correlation between the NR response, hydrogen incorporation, the XRD measurements, and the AFM results.

#### MP02

##### **Development of a High Temperature Furnace for *In-situ* Neutron Studies**

J. J. Wall, H. M. Reiche, S. C. Vogel (Los Alamos National Laboratory), B. Winkler (Universität Frankfurt, Institut für Mineralogie, Abteilung Kristallographie, Frankfurt, Germany)

A furnace with the capacity to heat samples in excess of 2,500°C in vacuum is currently being developed at the Los Alamos Neutron Science Center for the High Pressure Preferred Orientation (HIPPO) diffractometer. The furnace design allows rapid heating (~100K/min), and subsequent quenching, of samples *in-situ*. PC controlled motion in both vertical translation and rotation will enable sample alignment and automated texture measurements. This device is scheduled to become available as part of the HIPPO user program in 2007 and is expected to benefit a range of studies that could not be accommodated previously. Specifically, for the commissioning phase of this device we plan to investigate (1) thermal expansion coefficients from crystal lattice expansion in temperature ranges beyond the accessibility of dilatometers, (2) phase transitions in refractory materials and (3) phase formation and texture development during solidification of metal melts. By utilizing the exceptionally high data rates available on HIPPO, quantitative phase analysis during complex heat treatment schedules (heating & quenching), and solidification from the melt will now be possible in situ and in close to real time temporal resolution (< 1 minute). Future enhancements of the device include setup for controlled atmospheres, rapid quenching and a combination of DSC and neutron diffraction experiments. Preliminary neutron scattering results on standard samples and the current state of development are presented.

#### MP03

##### **Quantum Mechanical Analysis and Numerical Optimization of a "Zero-Field" Spin Echo Small Angle Neutron Scattering instrument**

G. Danagouliau, B. J. Heuser (University of Illinois), M. B. Leuschner, R. Pynn, W. M. Snow (University of Indiana, Bloomington, IN)

The interaction between the neutron magnetic moment with magnetic fields can be used to construct high resolution neutron spin echo spectrometers to encode small energy and momentum transfers. Spin echo techniques measure correlation functions in real space rather than reciprocal space, and can resolve smaller scattering angles than conventional pinhole SANS instruments. A new spin-echo small angle neutron scattering (SESANS) instrument is currently planned at the Indiana University Cyclotron Facility (IUCF) in Bloomington, Indiana. The instrument, combined with the Low Energy Neutron Source (LENS), will be able to probe the structure of complex materials over the length scales from 10 to 1000 nm. The instrument will be optimized for a long pulsed source such as LENS. The instrument will feature oppositely directed magnetic fields in the incident and scattered flight path of the spectrometer, with the fields arranged normal to the neutron spin with field boundaries tilted with respect to the beam momentum. In addition, a RF field will be added as a perturbation to the static magnetic fields, to increase the spatial and time separation of the splitted beams corresponding to the two final neutron spin states. We will present a quantum mechanical analysis and a numerical optimization of the design of a "zero-field" spin echo small angle neutron scattering instrument.

#### MP04

##### **Neutron Scattering Measurements on the Dilute Singlet Ground State System $\text{SrCu}_{2-x}\text{Mg}_x(\text{BO}_3)_2$**

S. Haravifard, S. R. Dunsiger, B. D. Gaulin, H. A. Dabkowska (McMaster University), S. El Shawish, J. Bonca (J. Stefan Institute), M. T. Telling (ISIS Pulsed Neutron Facility)

We have carried out high resolution time-of-flight neutron scattering measurements on a new high quality single crystal of  $\text{SrCu}_{2-x}\text{Mg}_x(\text{BO}_3)_2$  with  $x=0.1$ . These studies revealed the presence of new spectral weight within the singlet-triplet gap of this quasi-two dimensional, dilute, singlet ground state system. In addition, we observed substantial broadening of the three triplet excitations in

the dilute single crystal, as compared with pure  $\text{SrCu}_2(\text{BO}_3)_2$  [1,2]. Therefore, the triplet excitations in doped  $\text{SrCu}_{2-x}\text{Mg}_x(\text{BO}_3)_2$  possess finite lifetimes at low temperatures in the range that can be measured with cold neutron spectroscopy. We have also calculated the dynamical spin structure factor using the zero temperature Lanczos method on a finite 20 spin lattice, and solved a Shastry-Sutherland model at zero and finite doping for different strengths of external magnetic field. These calculations reproduce the qualitative features observed in the experiments on  $\text{SrCu}_{2-x}\text{Mg}_x(\text{BO}_3)_2$ .

[1] H. Kageyama *et al.*, *Phys. Rev. Lett.*, **84** (2000) 5876

[2] B.D. Gaulin *et al.*, *Phys. Rev. Lett.*, **93** (2004) 267202.

#### MP05

### Neutron Incoherent Scattering Studies of Hydrogen Distribution in Hydrogenated Zircaloy-4 Alloys

E. Garlea (University of Tennessee), V. O. Garlea (Oak Ridge National Laboratory), H. Choo (University of Tennessee), C. R. Hubbard (Oak Ridge National Laboratory), P. K. Liaw (University of Tennessee)

Neutron incoherent scattering measurements were conducted on Zircaloy-4 round bars. The specimens were charged in a tube furnace at 430 °C, using a 12.5 vol. % hydrogen in an argon mixture for 30, 60, and 90 minutes at 13.8 kPa pressure. The neutron diffraction measurements, with the beam illuminating the entire sample, showed the presence of the face-centered-cubic delta zirconium hydride ( $\delta\text{-ZrH}_2$ ) phase in the hydrogenated specimens. The assessment of the background in the diffraction profiles due to the incoherent scattering from the hydrogen atoms was carried out by performing inelastic scans around zero energy transfer at a fixed two-theta value for which there was only flat background and no coherent scattering. To estimate the relative amount of hydrogen in the Zircaloy-4 samples, the increase in incoherent scattering intensities with hydrogen content was calibrated using samples for which the hydrogen content was known. Measurement of the background scattering from locations within the round bar was also performed using strain mapping methods to determine the spatial distribution of hydrogen content as a function of radius. The qualitative study was extended to a quantitative investigation by means of combined bulk and spatially-resolved neutron incoherent scattering experiments and detailed numerical analyses.

*Acknowledgements – The authors acknowledge the support of the National Science Foundation (NSF) International Materials Institutes (IMI) Program (DMR-0231320). E. Garlea acknowledges the support of Tennessee Advanced Materials Laboratory (TAML) Fellowship Program. Portion of the research was sponsored by the Assistant Secretary for Energy Efficiency and Renewable Energy, Office of FreedomCAR and Vehicle Technologies as part of the High Temperature Materials Laboratory User Program, Oak Ridge National Laboratory, managed by UT- Battelle, LLC, for the U.S. Department of Energy under contract number DE - AC05-00OR22725. Ames Laboratory is operated by Iowa State University for the U.S. DOE under Contract No. W-7405-ENG-82 at the HFIR Center for Neutron Scattering which is supported by the DOE's Office of Basic Energy Sciences Materials Sciences Division under Contract No. DE-AC05-00OR22725 with UT-Battelle, LLC.*

#### MP06

### A New Approach for a Gravitationally-Induced Quantum Interference Experiment

N. L. Armstrong, H. Kaiser (Indiana University, Bloomington, IN), M. Huber, F. E. Wietfeldt (Tulane University, New Orleans, LA), T. C. Black (University of North Carolina, Wilmington, NC), M. Arif, D. L. Jacobson, S. A. Werner (NIST Center for Neutron Research, Gaithersburg, MD)

The influence of Earth's gravity on the phase of a neutron de Broglie wave has been measured in a series of increasingly sophisticated and precise neutron interferometry experiments over a period of more than 20 years. In these gravitationally-induced quantum interference experiments, gravity and quantum mechanics simultaneously play important roles and test the equivalence principle at the quantum limit. A ~1% discrepancy between the measured phase shift and that predicted by theory is still unresolved and is thought to be due to the difficulty of exactly determining the contribution of the bending of the blades, when the interferometer crystal is rotated. In this new approach, we will test this assumption and try to eliminate the bending effect by submersing the interferometer crystal in a solution with a density equal to that of silicon, i.e. a mixture of 60.4%  $\text{D}_2\text{O}$  + 39.6%  $\text{ZnBr}_2$ . This experiment will be performed at the Neutron Interferometer and Optics Facility at NIST. The status of the experiment and initial contrast measurements testing the influence of the  $\text{D}_2\text{O}$  +  $\text{ZnBr}_2$  mixture will be discussed.

*This work is supported by the U. S. National Science Foundation under grant no. PHY-0245679.*



MP07

### Structure of Polymer Brushes Under Confinement Using Contrast Matching

D. J. Mulder, C. F. Laub (University of California, Davis), G. S. Smith, W. A. Hamilton (Oak Ridge National Laboratory), T. L. Kuhl (University of California, Davis)

Polymer molecules at solid or fluid interfaces and their corresponding interactions have a vast importance in technological applications. Knowledge of the interaction forces and rheological properties of these polymer molecules are required to design and produce such effective applications. The system of study is tethered diblock chains in selective solvents under confinement. When two of these polymer brushes come into contact, either interpenetration, compression, or both concurrently can occur. Depending on this outcome, the resulting adhesion, lubrication, and shearing behavior will be greatly influenced. Using neutron reflectivity and contrast matching procedures, one side of the polymer brush has been screened out so an accurate density distribution profile of the other highlighted brush under confinement is obtained. Coupling the detailed density profile with Surface Force Apparatus (SFA) measurements of the extension of the polymer brushes and interaction forces, an understanding on how polymer brushes under confinement has been obtained.

MP08

### Octahedral Tilting in Triple Layer Dion-Jacobson Layered Perovskites: Neutron Powder Diffraction and Raman Spectroscopy of $\text{RbCa}_{2-x}\text{Sr}_x\text{M}_3\text{O}_{10}$ ( $\text{M} = \text{Nb, Ta, } x = 0, 1, \text{ and } 2$ )

J. A. Kurzman, M. J. Geselbracht (Reed College)

Layered perovskites provide a rich diversity of structures, compositions, chemical reactivity, and physical properties. Yet unlike the wealth of information that exists for three-dimensional perovskites, there is a paucity of detailed structural analyses of layered perovskites, particularly those containing early transition metals. Distortions and tilting in the octahedral framework characterize the single crystal X-ray structure of the Dion-Jacobson type phase  $\text{CsCa}_2\text{Nb}_3\text{O}_{10}$ , however the structures of all other related phases have been modeled with no octahedral tilting. We will present for the first time, neutron powder diffraction studies of  $\text{RbCa}_{2-x}\text{Sr}_x\text{M}_3\text{O}_{10}$  ( $\text{M} = \text{Nb, Ta, } x = 0, 1, \text{ and } 2$ ),

triple layer Dion-Jacobson layered perovskites with different degrees of octahedral tilting in the perovskite slab. The refined structural models of the strontium phases,  $\text{RbSr}_2\text{Nb}_3\text{O}_{10}$  and  $\text{RbSr}_2\text{Ta}_3\text{O}_{10}$ , exhibit a slight twist in the central octahedra of the perovskite slab. Preliminary results on the structures of the calcium analogs,  $\text{RbCa}_2\text{Nb}_3\text{O}_{10}$  and  $\text{RbCa}_2\text{Ta}_3\text{O}_{10}$ , indicate lower symmetries and presumably more extensive octahedral tilting with a smaller cation on the A-site. Vibrational modes of the perovskite slab observed using Raman spectroscopy show subtle changes as a function of calcium/strontium content and more intriguing differences between the niobates and tantalates. A long-term goal of this work is to correlate the Raman spectral bands with the neutron structures so that Raman studies could be used to monitor structural changes in experimental settings that are not amenable to diffraction studies.

MP09

### Neutronic Performance of the LENS Moderator – Simulation and Measurement

C. M. Lavelle, D. V. Baxter, H. Kaiser, M. B. Leuschner, W. R. Lozowski, N. B. Remmes, T. Rinckel, M. A. Lone, P. E. Sokol (University of Indiana, Bloomington, IN)

The Low Energy Neutron Source (LENS) is a long pulse neutron source based on  $\text{Be}(p,xn)$  reactions at proton energies up to 13 MeV. Its novel design employs a cylindrical light water reflector/moderator surrounding the Be target primary neutron source and a  $\text{CH}_4$  cold neutron moderator downstream from the Be target. The moderator is strongly coupled to the thermal flux produced in the reflector and has achieved moderator temperatures as lower than 4 K during operation of the neutron source. The neutron spectrum for the cold methane moderator is measured at the SANS instrument sample position by time of flight neutron spectroscopy with a thin  $^3\text{He}$  detector normalized to a simultaneously activated gold foil. The gold foil activity was measured on a high sensitivity beta-gamma coincidence setup. The resulting neutron spectra are well fit to a sum of a thermal and a cold Maxwellian, a feature reproduced in the MCNP simulations. The integrated yields of cold and thermal neutrons are 60-70% of the yields predicted by the MCNP simulation of the constructed geometry. Possible modifications to the design that would increase the cold flux of the source will also be presented.

*The LENS project is supported by the National Science Foundation (under grants DMR-0220560 and DMR-0320627), the 21<sup>st</sup> Century Science and Technology fund of Indiana, Indiana University, and the Department of Defense.*

#### MP10

### **Porogen/matrix effect on the microstructure of Nanoporous Poly(methylsilsesquioxane) Thin Films**

Z. Lin, R. M. Bribe (University of Maryland), H. Kim, W. Volksen, R. D. Miller (IBM Almaden Research Center)

Nanoporous poly(methylsilsesquioxane) (PMSSQ) thin films are one of the promising materials for ultra low dielectric constant interconnect material for next generation microchips. A viable route to nanoporous PMSSQ films is to spin-cast thin film of PMSSQ (matrix) with an organic polymer (porogen). The films are then cured at high temperature and a concomitant degradation of the porogen occurs resulting in a nanoporous structure. In this study, we examine the effect of matrix/porogen miscibility, and porogen molecular architecture on the phase behavior and final pore morphology using small angle neutron scattering (SANS) as a function of cure of the material. The work will compare materials produced from low -OH and high -OH content precursor PMSSQ materials (PMSSQ-LO and PMSSQ-HI, respectively). PMSSQ-HI materials showed better miscibility, more controlled microphase separation and smaller pores. Linear and star-shaped polymers were used as porogens and two pore formation mechanisms were found for these different porogens.

#### MP11

### **Field Dependence of the Vortex Core Size in CeCoIn<sub>5</sub>**

L. M. DeBeer-Schmitt (University of Notre Dame), C. D. Dewhurst (Institut Laue-Langevin, France), B. W. Hoogenboom (University of Basel), C. Petrovic (Brookhaven National Laboratory), M. R. Eskildsen (University of Notre Dame)

Using Small-Angle Neutron Scattering, we have imaged the flux-line lattice (FLL) in the d-wave heavy fermion superconductor, CeCoIn<sub>5</sub>. At low fields, we observe a hexagonal lattice. As the field is increased above 0.55 T, the FLL goes through a first order transition to a distorted rhombic lattice. Also, measurements of the reflectivity yields a constant form factor independent of the applied magnetic field which is in stark contrast to the exponential dependence usually observed in superconductors. One way to account for this is for the vortex core size to have a field dependence of  $1/q$ .

#### MP12

### **Influence of temperature on protein dynamics**

J. H. Roh, A. P. Sokolov (University of Akron), J. E. Curtis, I. Peral, Z. Chowdhuri, V. Garcia-Sakai (NIST Center for Neutron Research, Gaithersburg, MD), S. Azzam, R. Gregory (Kent State University), V. N. Novikov (Russian Academy of Sciences)

Protein dynamics and functions are strongly influenced by temperature. Dynamic transition of protein is believed to be closely related to onset of protein function since many protein functions activate at dynamic transition temperature,  $T_D \sim 180 - 230$  K [1]. Our previous results of hydration dependence of protein dynamics showed slow relaxation process is the mode that activates dynamic transition and seems to be closely related to enzymatic activity [2,3]. However, understanding of the nature of the dynamic transition and of the microscopic mechanism of the slow relaxation process is still a subject of discussion. We performed neutron scattering measurements (HFBS and DCS) for dry and wet lysozyme at  $T$  up to 300 K in order to understand temperature dependence of the slow relaxation process. Our detailed analyses of protein dynamics provide temperature dependence of slow relaxation process exhibits Arrhenius-like behavior with its activation energy  $\sim 36$  kJ/mol at  $T > T_D$ . This observation suggests that the dynamic transition of protein seems to originate from the slow relaxation process that simply moves into the given experimental energy window, (i.e. pico- to nano-second time scale), at  $T > T_D$ .

[1] R. M. Daniel, R. V. Dunn, J. L. Finney, and J. C. Smith. *Ann. Rev. Biophys. Biomol. Struct.* 2003, **32**, 69.

[2] J. H. Roh, V. N. Novikov, R. B. Gregory, J. E. Curtis, Z. Chowdhuri, and A. P. Sokolov, *PRL*, 2005, **95**, 038101.

[3] J. H. Roh, J. E. Curtis, S. Azzam, V. N. Novikov, I. Peral, Z. Chowdhuri, R. B. Gregory, and A. P. Sokolov, submitted to *Biophys. J.* Jan. 2006.

#### MP13

### **Effect of nanoparticle addition on the properties of linear polymers: non-Einstein like behavior**

A. Tuteja, M. E. Mackay (Michigan State University), C. J. Hawker (University of California, Santa Barbara)

In recent times, nanofillers have attracted the interest of a variety of research groups as these materials can cause unusual material property enhancements. These enhancements are induced by the presence of the nanoparticles, their interaction with the host matrix, and also quite

critically, by their state of dispersion. In this work we find that nanoparticles can be dispersed in linear polymers, despite chemical dissimilarity, when the nanoparticle is smaller than the linear polymer, as demonstrated by the miscibility of polyethylene nanoparticles in linear polystyrene (polystyrene and polyethylene is a classical phase separating system; the miscibility is determined through small angle neutron scattering, SANS). If the particle becomes larger than the polymer, phase separation occurs with even polystyrene nanoparticles phase separating from linear polystyrene. In addition, other SANS experiments show that the linear polymer becomes distorted on the addition of nanoparticles in the stable systems and is far from its equilibrium conformation. This aspect demonstrates the uniqueness of nanoscale thermodynamics as phase separation is expected (i.e. depletion flocculation) and we believe that the nanoparticles are stabilized by enthalpic gain. When properly dispersed, the addition of nanoparticles causes a large reduction (up to 90%) in the melt viscosity of the system, a result at odds with Einstein's century old prediction and experimental observations of the viscosity increase particles provide to liquids and melts. Also, the addition of specific nanoparticles, apart from improving the polymer processing by reducing the viscosity, can simultaneously lead to enhanced electrical conductivity, enhanced mechanical damping, enhanced thermal stability, and can even make the polymers magnetic.

MP14

**Micro to Nano Scale Structure and Mechanical Properties of Hydrogels of Poly (lactide)-Poly (ethylene oxide)-Poly (lactide) Triblock Copolymer**

S. K. Agrawal, N. Sanabria-DeLong, G. N. Tew, S. R. Bhatia (University of Massachusetts, Amherst, MA)

Biodegradable and biocompatible polymers made from poly(lactide)-poly(ethylene glycol)-poly(lactide) have attracted attention recently because of their property to form hydrogels, which has potential applications in drug delivery and tissue engineering. We have performed for the first time a complete structural characterization of PLA-PEO-PLA in the solution and hydrogel states. Previous studies on hydrogels of these polymers have shown that these gels have excellent

mechanical properties suitable for possible application in tissue engineering and drug delivery. To obtain further insight into the structure-property relationships for these materials, we have performed SANS to understand the self-assembly of these polymers in aqueous solution with change in the block length and stereospecificity of the PLA block. A significant difference in structure and association behavior was seen between the polymers made from amorphous D/L-lactide as compared to those with crystalline L lactide blocks. In the former case spherical micelles were seen to form which pack regularly at higher concentrations leading to formation of a correlation peak in the SANS spectra whereas the latter forms nonspherical polydisperse micellar assemblies and thus show no correlation peak in the SANS spectra at high concentrations. Despite the difference, both polymers were seen to form an associative network structure leading to gelation at high concentration. The size of structural moieties formed was also comparable and was about 7-14 nm in both cases. The PLA block length was also seen to directly influence the sizes and association number of the nanodomains forming the hydrogels. This difference in microstructure has important implications for use of these polymers in drug delivery applications. We also performed ultra small angle x-ray scattering (USAXS) and confocal microscopy on these polymer gels to look at their structure from nanometer to micron length scales. Polymers made from both D/L lactide and L-lactide blocks showed the presence of large-scale fractal aggregates in the hydrogels with water channels running between them. Also, the fractal structure was denser for the D/L lactide series polymers as compared to the L-lactide series polymers. These results show that we can tune the microstructure and thereby the mechanical strength of these gels depending upon the specific application we need it for. The value of elastic moduli of these gels is in the same range as several soft tissues, making these materials excellent candidates for a variety of tissue engineering applications.

MP15

**Consecutive Nucleation Events during Devitrification of  $\text{Zr}_{52.5}\text{Cu}_{17.9}\text{Ni}_{14.6}\text{Al}_{10}\text{Ti}_5$  Bulk Metallic Glass**

L. Yang (University of Cincinnati), W. D. Porter, Z. P. Lu (Oak Ridge National Laboratory), D. Ma, A. D. Stoica, X. L. Wang (Spallation Neutron Source, Oak Ridge National Laboratory), E. Z. Payzant (Oak Ridge National Laboratory), T. Proffen (Los Alamos National Laboratory), D. Shi (University of Cincinnati)

Through careful measurements of isochronal and isothermal DSC traces, we identified two consecutive exothermal peaks in  $\text{Zr}_{52.5}\text{Cu}_{17.9}\text{Ni}_{14.6}\text{Al}_{10}\text{Ti}_5$  bulk metallic glass during devitrification. Examination of the X-ray diffraction patterns at various stages of isothermal annealing confirms that the exothermal peaks correspond to two different nucleation events, with different local atomic structures. Modeling of the DSC data indicates that the devitrification of  $\text{Zr}_{52.5}\text{Cu}_{17.9}\text{Ni}_{14.6}\text{Al}_{10}\text{Ti}_5$  bulk metallic glass is adequately described by Johnson-Mehl-Avrami theory with a two-step consecutive reaction model, so long as the heating rate is  $< 10$  K/min. *In-situ* neutron diffraction study was carried out using NPDF at Los Alamos National Laboratory to determine the structure and transformation kinetics during isothermal annealing. Preliminary analysis results of the neutron diffraction data will be presented.

MP16

**Phase Transformation and Lattice-Strain Evolution in a Cobalt-Based Superalloy during Low-Cycle Fatigue**

M. L. Benson, P. K. Liaw, H. Choo (University of Tennessee), A. D. Stoica (Oak Ridge National Laboratory), M. R. Daymond (Queen's University, Kingston, Canada), T. A. Saleh (Los Alamos Neutron Science Center, Los Alamos National Laboratory), X. L. Wang (Oak Ridge National Laboratory), D. L. Klarstrom (Haynes International, Inc.)

The cobalt-based ULTIMET® superalloy partially undergoes a strain-induced phase transformation from the parent face-centered-cubic (fcc) phase to the daughter hexagonal-close-packed (hcp) phase. The material was studied under low-cycle fatigue loading at room temperature with a total strain range of  $\Delta\epsilon = \epsilon_{\text{max}} - \epsilon_{\text{min}} = 2.5\%$  and a strain ratio of  $R = \epsilon_{\text{min}} / \epsilon_{\text{max}} = -1$  (where  $\epsilon_{\text{max}}$  and  $\epsilon_{\text{min}}$  are the applied maximum and minimum strains, respectively). A method is presented here whereby hkl-dependent lattice strains in the fcc phase are used to calculate an effective macroscopic stress. Any deviations of the effective stress from the applied macroscopic

stress are considered to be indicative of load sharing by the developing hcp phase. The load-partitioning characteristics of the material during low-cycle fatigue are then discussed in context of weight fraction of hcp phase from Rietveld refinements. The evolution of the intergranular strain during fatigue is also reported.

*Acknowledgements* – We greatly appreciate the National Science Foundation for the financial support of (1) the Integrative Graduate Education and Research Training Program (DGE-9987548), with Drs. C. J. Van Hardeveldt and D. Dutta as program directors; (2) the International Materials Institutes Program (DMR-0231320), with Dr. C. Huber as program director; and (3) the Combined research-Curriculum Development Program (EEC-9527527 and EEC-0202415), with Ms. M. Poats as the program director. Additional financial support was gratefully received from the Tennessee Advanced Materials Laboratory, with Dr. E. W. Plummer as director. This work benefited from the use of the ISIS Pulsed Neutron and Muon Source.

MP17

**Contrast Variation SANS of NiO nano particles supported on porous  $\text{Al}_2\text{O}_3\text{-SiO}_2$** 

S. R. Kirumakki, H. P. Perry, A. Clearfield (Texas A&M University), S. V. Pingali, P. Thiyagarajan (Intense Pulsed Neutron Source, Argonne National Laboratory)

A series of  $\text{NiO}/\text{Al}_2\text{O}_3\text{-SiO}_2$  synthesized by sol-gel process was studied by SANS to obtain information on the structure and size of the pores. Accurate determination of pore sizes in microporous and mesoporous compounds has been a challenge for materials chemists. Gas adsorption methods have long been employed for this purpose but their interpretation has been a subject of ongoing debate. The SANS data was utilized to complement and validate the pore sizes determined by  $\text{N}_2$ -sorption technique. Experiments on powders revealed two distinct length scales, one in 8-16 Å range and the other an order of magnitude higher in the 8-10 nm range. By contrast matching using  $\text{D}_2\text{O}/\text{H}_2\text{O}$  mixtures we identified that the smaller length scale corresponds to open pores that are accessible to solvent while that with a larger size corresponds to NiO particles. The transmission electron microscopy (TEM) images of these samples show that NiO is present as nano particles on the surface of  $\text{Al}_2\text{O}_3\text{-SiO}_2$  matrix. The large size and the high scattering length density together produce strong scattering intensity from the NiO nanoparticles. We will present the pore size distribution data and correlate the variation in the pore size to the amine used in the preparation.

*This work was supported by the IPNS funded by DOE-BES under contract #W-31-109-ENG-38 and by the NSF under Grant No.DMR-*



0332453. \*Authors to whom correspondence may be addressed  
clearfield@mail.chem.tamu.edu (A. Clearfield), thiyaga@anl.gov  
(P. Thiyagarajan).

MP18

### Inelastic Neutron Scattering and Crystal Polymorphism: The Thermodynamics of Polymorphic Forms

S. A. Rivera, D. G. Allis, B. S. Hudson (Syracuse University)

Polymorphism has been widely explored and has recently received increased attention due to its importance to the pharmaceutical industry and crystal engineering. Inelastic neutron scattering (INS) spectroscopy provides a useful test of the reliability of computations of crystal vibrations, which can be used to estimate vibrational contributions to the thermodynamic properties of polymorphic forms. Calculations can be performed with periodic density functional methods that provide both crystal energies and dynamical matrices. The comparison of the INS spectra with that calculated by DFT can be used in an empirical fashion to establish the full density of states of the crystal. Two examples of hydrogen-bonding polymorphism will be studied in detail in this work. First, glycine polymorphs,  $\alpha$ ,  $\beta$ , and  $\gamma$ , differ in their intermolecular hydrogen bonding. This results in a difference in crystal packing and thermodynamic stability. They have been previously investigated experimentally in terms of the enthalpy differences based on heats of solution. In this work we present the INS spectra and DMol<sup>3</sup> calculations of the crystal lattice structure, energy and harmonic vibrational frequencies for the  $\alpha$  and the more stable  $\gamma$  form of glycine. The computed vibrational levels are used to determine zero point energy differences and vibrational contributions to the enthalpy difference. Second, the strong hydrogen bonded complex of 4-methylpyridine and pentachlorophenol drastically changes the unit cell packing when the hydrogen-bonded hydrogen is substituted with deuterium. This is of interest because isotope exchange is usually assumed not to affect the crystal structure. This observation must be related to the contributions of crystal vibrations to the free energy since the lattice energy is independent of the isotopic replacement. INS spectra of these two materials will be presented and their interpretation discussed in terms of DMol<sup>3</sup> calculations.

MP19

### An *In-Situ* Neutron-Diffraction Tension Study of a HASTELLOY C-22HS™ Superalloy

E. Huang, M. L. Benson, K. Tao (University of Tennessee), B. Clausen (Los Alamos Neutron Science Center, Los Alamos National Laboratory), Y. Wang (Northeastern University (China)), P. K. Liaw, H. Choo (University of Tennessee), D. L. Klarstrom (Haynes International, Inc.)

Corrosion-resistant nickel-based superalloys are widely used in engineering applications because of their excellent resistance to a wide variety of corrosive environments. The HASTELLOY C-22HS superalloy is an aged-hardened, nickel-based, corrosion-resistant superalloy, which is strengthened by Ni<sub>3</sub>(Cr,Mo) long-range ordered precipitates in a face-centered cubic matrix. In the present study, the tension behavior of HASTELLOY C-22HS superalloy was examined by the in-situ neutron diffraction at room temperature to study the mechanical-deformation characteristics. The hkl-dependent internal strains were determined as a function of strain levels. The behavior of the elastic lattice strains during *in-situ* tension loading clearly showed the anisotropy. The hkl-dependent stress-strain curve was the focus of this study.

MP20

### Inelastic neutron scattering study of the spin dynamics and quantum fluctuations in antiferromagnetic molecular rings

T. Guidi (NIST Center for Neutron Research), R. Caciuffo (Institute for Transuranium Elements, Germany), S. Carretta, P. Santini, G. Amoretti (University of Parma, Italy), J. R. D. Copley, Y. Qiu (NIST Center for Neutron Research), G. Timco, R. E. P. Winpenny (University of Manchester, UK)

Molecular Nano-Magnets (MNMs) comprise clusters of strongly exchange-coupled transition-metal ions, linked by organic ligands and arranged on a regular crystal lattice. Since the intermolecular magnetic interaction is negligible as compared with the intramolecular interaction, MNMs may be regarded as collections of identical isolated magnetic units. In such systems the macroscopic quantum phenomenon of quantum tunneling of the magnetization may be observed. "Magnetic wheels" constitute a particular class of MNMs having a ring-shaped cyclic structure and a dominant antiferromagnetic (AF) coupling between nearest-neighbour ions, resulting in a singlet ground state. In antiferromagnets the rate of tunnelling between

classically degenerate spin configurations can be large compared with the spin decoherence rate, in which case coherent tunnelling may be observed. The most promising candidates for the observation of this phenomenon are heteronuclear AF wheels, i.e. AF ring-shaped clusters with uncompensated spin sublattices. Here we report the results of inelastic neutron scattering (INS) experiments on several AF ring-shaped molecules that allowed us to precisely determine zero-field anisotropy and exchange interaction parameters [1]. In addition, the spin dynamics of the heterometallic Cr<sub>7</sub>Ni ring in an external magnetic field has been studied. INS has been used to investigate the total-spin composition of the molecular spin wave function as the magnetic field is varied near the value corresponding to the anti-crossing between  $S = 1/2$  and  $S = 3/2$  spin states, where coherent oscillations of the total spin length can occur [2].

[1] R. Caciuffo, T. Guidi, G. Amoretti, S. Carretta, E. Livioti, P. Santini, C. Mondelli, G. Timco, C. A. Muryn, R. E. P. Winpenny, *Phys. Rev. B* **71**, 174407 (2005)

[2] S. Carretta, P. Santini, G. Amoretti, M. Affronte, A. Ghirri, I. Sheikin, S. Piligkos, G. Timco, and R. E. P. Winpenny, *Phys. Rev. B* **72**, 060403 (2005)

#### MP21

### ***In-Situ* Neutron Diffraction Measurement of Transient Temperature and Thermal/Elastic Stresses during a Severe Thermal-Mechanical Process**

W. Woo (University of Tennessee), Z. Feng, X. L. Wang (Oak Ridge National Laboratory), K. An (University of Tennessee), D. W. Brown, B. Clausen (Los Alamos Neutron Science Center, Los Alamos National Laboratory), H. Choo (University of Tennessee), C. R. Hubbard, S. A. David (Oak Ridge National Laboratory)

Rapidly changed material states (e.g., temperature and stress) are one of the issues in the severe thermal-mechanical process such as welding, forming, and heat treatment. Deep penetration capability of neutrons can be used to simultaneously characterize the mechanical properties and structures of materials. However, separating the thermal and elastic strains under the rapidly changing transient temperature of the thermal-mechanical process has been a problem for *in-situ* neutron diffraction measurements. A novel experimental approach and results of direct measurements of the transient temperature and stress field was performed using *in-situ* neutron diffraction measurements inside of 6061-T6 aluminum plate during severe thermal-mechanical deformation process, called friction-stir welding

(FSW). This novel technique is based on the “quasi-steady state (QSS)” phenomenon induced by moving, localized thermal mechanical processing and the QSS allows circumventing the neutron flux limitation for studying the rapid transient material behavior. This poster will present (1) decomposition of the thermal and elastic stresses from the lattice spacing changes measured using the neutron diffraction revealed the stress state during the FSW and (2) profile of the transient temperature as a function of distance from the heat source using the de-convoluted thermal strain component coupled with the coefficient of the thermal expansion. Furthermore, the feasibility of the *in-situ* neutron-diffraction measurement for microstructure variations during the severe thermo-mechanical processing will be discussed.

*Acknowledgement* – This research is sponsored by the Laboratory Directed Research and Development program of Oak Ridge National Laboratory (ORNL), managed by UT-Battelle, LLC for the U. S. Department of Energy under Contract No. DE-AC05-00OR22725.

#### MP22

### **Study of the Liquid-Liquid Transition in Confined Supercooled Water by Small Angle Neutron Diffraction**

D. Liu, Y. Zhang (Massachusetts Institute of Technology), P. Thiyagarajan, D. Wozniak (Intense Pulsed Neutron Source, Argonne National Laboratory), S. Chen (Massachusetts Institute of Technology)

Water is essential for existence of life. Its properties impact our lives directly. Hence the unusual behavior in its supercooled state stimulates enormous interests in scientific communities. Our work involves small angle neutron diffraction (SAND) experiments on confined water in nano-pores of mesoporous silica, which allows us to access the hitherto unreachable range of supercooled temperatures. Our recent SAND experiments show that water density changes along with the temperature changing. It indicates a phase transition from low density water to high density water at the supercooled region. What we observed coincides with the first-order liquid-liquid thermodynamic transition predicted by MD simulation.

MP23

**Emergence of Magnetism in  $\text{La}_{1-x}\text{Sr}_x\text{CoO}_3$** 

D. P. Phelan, D. Louca (University of Virginia), S. Rosenkranz (Argonne National Laboratory, Material Science Division), S. H. Lee (University of Virginia), J. F. Mitchell (Argonne National Laboratory, Material Science Division), Y. Motome (Riken), Y. Moritomo (Nagoya University), S. Klausen, R. Osborn (Argonne National Laboratory, Material Science Division), K. Kamazawa (University of Virginia)

Orbital, spin, and charge degrees of freedom play a central role in the physics of CMR-type transition metal perovskite oxides.  $\text{La}_{1-x}\text{Sr}_x\text{CoO}_3$  is a perovskite series in which the parent compound has a non-magnetic, Mott-insulating ground state because the  $\text{Co}^{3+}$  ions have a  $S=0$  ground spin configuration. The energy splitting between the  $S=0$  configuration and either the  $S=1$  or  $S=2$  configuration is small (whether  $S=1$  or  $S=2$  is lower in energy is being debated), and a broad paramagnetic transition occurs between 35K and 100K, while a ferromagnetic, metallic ground state emerges upon hole doping ( $\text{Sr}^{2+}$  substitution). We have used neutron scattering methods to study these magnetic transitions. We find that both ferromagnetic and antiferromagnetic spin correlations develop in the thermally excited paramagnetic phase of the parent, and we interpret these correlations as resulting from a short-ranged dynamic orbital ordering associated with the  $S=1$  state. As holes are doped into the system, the condensation of static ferromagnetic droplets is observed. These droplets consist of short-ranged, isotropic regions, within which spins are ferromagnetically aligned and the double exchange interaction is dominant. The percolation of droplets forms the ferromagnetic, metallic state. Below the droplet condensation temperature, a second magnetic transition is observed, indicating a local spin ordering. The wave-vector associated with this second magnetic transition is incommensurate, and possible scenarios leading to this transition are considered.

MP24

**Designing Balanced Surfactants for Immiscible Polymers by Tuning Attractive and Repulsive Interactions**

M. L. Ruegg, B. J. Reynolds (University of California, Berkeley), D. J. Lohse, M. Y. Lin (ExxonMobil Research and Engineering), N. P. Balsara (University of California, Berkeley)

The phase behavior of A/B/A-C polymer blends with attractive and repulsive interactions was analyzed with neutron scattering experiments and mean field theories. Transitions between lamellar phases, microemulsions, homogeneous phases and macrophase separated states are easily accessed in A/B/A-C blends simply by adjusting the temperature. A microemulsion phase was observed in a blend with only 1 % of the diblock copolymer in the blend. To our knowledge, this is the lowest amount of polymeric surfactant to organize two immiscible homopolymers. The domain spacing was predicted utilizing the Random Phase Approximation (RPA) and Self-Consistent Field Theory (SCFT) in the homogeneous and organized states, respectively, with no adjustable parameters. The only inputs into the calculations were the binary Flory-Huggins interaction parameters and statistical segment lengths. The domain spacing determined from theory was often within 10 percent of the experimental values. The transition temperature from single-phase systems to a macrophase separated state determined from theory was in good agreement with experimental values. The theoretical results further confirm the existence of an organized phase with a minimal concentration of diblock copolymer surfactant.

MP25

**Inelastic Neutron Scattering Study of  $\text{La}_{1/3}\text{Sr}_{2/3}\text{FeO}_{3-\delta}$  Perovskite**

J. Ma (Iowa State University), J. Yan, S. Chang (Ames Laboratory), F. R. Trouw, M. P. Hehlen (Los Alamos National Laboratory), W. Beyermann (University of California, Riverside), R. J. McQueeney (Iowa State University)

$\text{La}_{1/3}\text{Sr}_{2/3}\text{FeO}_{3-\delta}$  has an unusual magneto-structural transition around 210K, below which charge disproportionation occurs according to  $2\text{Fe}^{4+} \rightarrow \text{Fe}^{3+} + \text{Fe}^{5+}$ . Consequently, the different iron valences order along the body diagonal  $[111]_c$ , resulting in a change in crystal structure and antiferromagnetic ordering. Inelastic neutron scattering was used to determine the effect of

simultaneous charge and magnetic ordering on the phonon and spin wave excitations. The results are compared to those for the parent compound  $\text{LaFeO}_3$ .

MP26

### **Self-assembly models for binary phospholipid mixtures: Understanding Bicelle Formation**

D. Singh (Johns Hopkins University), L. Porcar, P. D. Butler (National Institute of Standards and Technology), U. Perez-Salas (University of California, Irvine), W. A. Hamilton, G. Lynn (Oak Ridge National Laboratory)

Systems consisting of mixtures of a long and a short-tail lipid have recently shown promise in membrane protein crystallization and have been used for some time as an alignable media for protein structure determination using NMR. However, the phase diagram of these phospholipid mixtures remains poorly understood. In particular, much of the literature posits the existence of bicelles, or discotic micelles, as the agents of the useful properties. Recent work however suggests that such structure only exist below the melting transition temperature of the long tail lipid, with a transition to a lamellar phase at higher temperature. A detailed understanding of the phase behavior is crucial to adapting these systems for more general applications. In this work, we report on a systematic study at the lowest temperature isotropic fluid like phase in DMPC and DHPC mixtures. Using a series of small angle neutron scattering (SANS) experiments with hydrogenated and deuterated lipids, we show direct evidence of the discoidal morphology with the two lipids being segregated in different parts of the disk. Using a model which properly accounts for the geometric packing as well as the thermodynamic nature of the system, we show how radius of the planar domain of the disks is governed by the effective molar ratio  $q_{\text{eff}}$  of lipids in aggregate and not the molar ratio  $q$  ( $q = [\text{DMPC}]/[\text{DHPC}]$ ) as has been understood previously. We propose a new quantitative (packing) model and show that in this self assembly scheme,  $q_{\text{eff}}$  is the real determinant of disk sizes. Based on  $q_{\text{eff}}$  a master equation can then scale the radii of disks from mixtures with varying  $q$  and total lipid concentration. At higher temperature, but still well below the chain melting temperature, the system clearly becomes much more complicated and we see evidence of mixing of the two lipids.

MP27

### **Misfit Evolution in a Single Crystal Superalloy at High Temperatures using Pulsed Neutron Diffraction Measurements**

Y. Lu, B. S. Majumdar (New Mexico Tech)

*In situ* pulsed neutron diffraction measurements were conducted on a [001] oriented Ni-based superalloy PWA 1484 single crystal to determine the evolution of elastic strains in the constituent gamma and gamma-prime phases during high temperature creep. These are coherent phases, and the constraint imposed by the strong gamma-prime phase on the weaker 50-80 nm wide gamma channels, has a strong influence on overall the creep deformation behavior. Currently, there is debate regarding the mechanisms leading to tertiary creep and failure in such single crystal alloys and it was felt that *in situ* monitoring of elastic microstrains would shed insight on local mechanisms. In our experiments, we had to overcome problems associated with diffraction experiments with single crystals, as well as the need to deconvolute lattice parameters in phases of very low elastic misfit. The experimental and analysis methodologies will be discussed. Experiments were conducted at temperatures ranging between 760 C and 1092 C, and stresses from 120 MPa to 825 MPa. The misfit strains were determined both before loading, and during the creep and tensile tests. Finite element modeling was conducted using ABAQUS to shed insight on the measured elastic strain evolution behavior.

*The project is funded by NSF DMR 0413852, and we thank LANSCE, Los Alamos National Laboratory for the neutron diffraction experiments.*

MP28

### **Presence of nano-scale $\alpha$ -structural domains in the phonon-glass thermoelectric material $\beta\text{-Zn}_4\text{Sb}_3$ from atomic pair distribution function (PDF) analysis**

H. Kim, E. S. Bozin (Michigan State University), S. Haile, G. J. Snyder (California Institute of Technology), S. Billinge (Michigan State University)

The promisingly high thermoelectric figure of merit (ZT) of  $\beta\text{-Zn}_4\text{Sb}_3$  between 450 K and 670 K is known to be due to its exceptionally low thermal conductivity which is comparable to that of a glass. The discovery of significant Zn interstitial disorder in  $\beta\text{-Zn}_4\text{Sb}_3$  provides foundation for better understanding of the origin of its low thermal conductivity [1]. Furthermore, it has been reported



that Zn interstitial atoms become ordered in the  $\alpha$ -phase [2]. We report on the local structural study of  $\text{Zn}_4\text{Sb}_3$  in both the  $\alpha$  and  $\beta$ -phases using the atomic pair distribution function (PDF) technique, which has been successfully applied to solve the structures of crystallographically challenged materials [3,4]. Neutron powder diffraction measurements were carried out on the NPDF diffractometer at the Lujan Center at Los Alamos National Laboratory which provides high resolution. Data were collected at 15 K ( $\alpha$ -phase) and 300 K ( $\beta$ -phase). The PDF analysis shows that despite the higher average symmetry of the  $\beta$ -phase, the low  $r$ -region of the PDF of  $\beta$ - $\text{Zn}_4\text{Sb}_3$  is best explained by a structural model that retains features of the  $\alpha$ -phase, suggesting the formation of nano-scale domains.

[1] G. J. Snyder et al. *Nat. Mater.* **3**, 458 (2004)

[2] J. Nylén et al. *J. Am. Chem. Soc.* **126**, 16306 (2004)

[3] T. Egami and S. J. L. Billinge, *Underneath the Bragg peaks*, Pergamon Press, Elsevier, Oxford, England, 2003

[4] S. J. L. Billinge and M. G. Kanatzidis, *Chem. Commun.*, **749** (2004)

#### MP29

##### Neutron and thermodynamic study of small hydrocarbons adsorbed on metal oxides

R. E. Cook (University of Tennessee), T. Arnold (Oak Ridge National Laboratory), A. M. Barbour, S. Z. Chanaa, M. J. Farinelli, L. Frazier, P. N. Yaron (University of Tennessee), S. Clarke (Bp Institute and Cambridge University), J. Z. Larese (University of Tennessee and Oak Ridge National Laboratory)

We present our recent investigations of the structure, dynamics and adsorption properties of small hydrocarbons adsorbed on the  $\text{MgO}(100)$  and  $\text{ZnO}$  surfaces. Using high-resolution adsorption isotherms, elastic and inelastic neutron scattering techniques and some molecular modeling we have systematically explored the first six members of the normal alkane family, ethylene, cyclo-hexane and pentane, and pyridine sorption properties. While the thermodynamical data is nearly complete, our structural information is limited to methane, ethane, propane, butane, hexane and ethylene. Vibrational and rotational spectra are also available for some of the alkane family. We will present our findings in light of the information they provide for development of accurate potential energy surfaces.

*This work is supported by the Division of Materials Science, Office of Science, Basic Energy Sciences under contract DE-AC05-00OR22725 and the NSF under DMR-0412231. JZL is also a joint faculty member at ORNL.*

#### MP30

##### Study of water intercalation in superconducting sodium cobalte

C. Metallo, T. Egami (University of Tennessee), T. Proffen (Los Alamos National Laboratory), D. Mandrus, B. Sales (Oak Ridge National Laboratory)

Superconductivity appears in the hydrated sodium cobalt oxide  $\text{Na}_x\text{CoO}_2\cdot y\text{H}_2\text{O}$  near the composition  $x=0.3$  and  $y=1.4$  with  $T_c=4.5\text{K}$ . As of yet, the role of water is still unknown. Here we present the results of our neutron diffraction measurements on the deuterated cobaltate superconductor  $\text{Na}_{0.35}\text{CoO}_2\cdot 1.4\text{D}_2\text{O}$  at two different temperatures  $T=15\text{K}$  and  $T=100\text{K}$ . The neutron diffraction data were analyzed using the Pair Density Function (PDF) method, which provides information about local ordering. The PDF of  $\text{Na}_{0.35}\text{CoO}_2\cdot 1.4\text{D}_2\text{O}$  was compared with the PDF of  $\text{D}_2\text{O}$  and the PDF of the non-deuterated sodium cobalt oxide  $\text{Na}_{0.7}\text{CoO}_2$ . At both temperatures, our results suggest that the geometry of the water molecules inserted in the parent compound  $\text{Na}_{0.7}\text{CoO}_2$  is strongly modified. The D-D distance drastically changes and two coexisting distributions of the D-O-D angle are found. We discuss the possible implications in terms of electron conduction and superconductivity.

#### MP31

##### Virtual experiments for data analysis using interface to the control program at RITA-II, PSI

J. Hjøllum (Riso National Laboratory, Denmark), M. Könnecke (Paul Scherrer Institute), L. Udby (Riso National Laboratory, Denmark), U. Filges, C. Niedermayer (Paul Scherrer Institute), P. K. Willendrup, P. Christiansen, K. Lefmann (Riso National Laboratory, Denmark)

Recently the control software for the RITA-II triple-axis-spectrometer at the Paul Scherrer Institute (PSI), has been updated to run the control software SICS. As a part of the reimplementation of the control software, an interface was created for running virtual experiments, using the McStas [1] simulation package. This should enable the user to predefine and tune their scans, before running the actual experiments. Furthermore it will be helpful in data analysis, since it is possible to simulate properties of the instrument to high precision. This is desirable since the RITA-II is a very complex spectrometer, using 7 (9) analyzer blades, and is capable of running in several different modes. A

similar setup for performing virtual experiments has been set up for the DMC, PSI[2].

We present a full virtual experiment on RITA-II using the McStas package with the SICS control software. Furthermore we present comparisons of scans made at the actual RITA-II instrument and scans made using the SICS/McStas package.

[1] K. Lefmann and K. Nielsen, "McStas, a General Software Package for Neutron Ray-tracing Simulations", *Neutron News* 10, **20**, (1999).

[2] P. Willendrup, U. Filges, L. Keller, E. Farhi, K. Lefmann, "Validation of a realistic powder sample using data from DMC at PSI", *in press* (2006)

MP32

### Neutron and X-ray powder diffraction study of magnetism and phase separation in $\text{Ca}_{2-x}\text{La}_x\text{FeReO}_6$ ( $x=0, 0.2, 0.4$ ) double perovskites

S. Avci (Northern Illinois University), L. Suescun (Argonne National Laboratory, Material Science Division), S. Kolesnik (Northern Illinois University), O. Chmaissem (Northern Illinois University & Argonne National Laboratory), B. Dabrowski (Northern Illinois University & Argonne National Laboratory), J. D. Jorgensen (Argonne National Laboratory, Material Science Division)

The ferrimagnetic double perovskite  $\text{Ca}_2\text{FeReO}_6$  ( $T_c \sim 540\text{K}$ ) has been found to display giant magnetostriction properties [1]. These phenomena have been associated with a phase separation process in the ferrimagnetic state [2]. Magnetization curves for this compound show the existence of two transition temperatures ( $T_c \sim 540\text{K}$  and  $T_c' \sim 150\text{K}$ ) where a change in the ratio of both magnetic phases was observed. We have observed that La-doping of  $\text{Ca}_2\text{FeReO}_6$  produces structural changes that are reflected in the magnetic behavior of the system. Similar to  $x=0$ , the  $x=0.2$  sample also displays two transition temperatures ( $T_c \sim 500\text{K}$ ,  $T_c' \sim 120\text{K}$ ), while the  $x=0.4$  sample shows only the high temperature transition ( $T_c \sim 520\text{K}$ ). The low-temperature magnetic transitions can be removed with external magnetic field for both compositions  $x=0$  and  $0.2$ . Using high-resolution neutron powder diffraction (Argonne's IPNS-SEPD instrument) and high-resolution high-energy x-ray diffraction (Argonne's APS-11IDC station) in combined Rietveld refinements we have determined the amounts of separated phases, the Fe/Re mixing ratio, and the magnetic structure of  $x=0$  and  $0.4$  phases at RT. Furthermore, using NPD we have studied evolution of the amounts of various monoclinic phases with temperature for both samples. We have been able

to assign unique magnetic arrangement of ordered Fe and Re magnetic moments to each of the phases using  $P21'/n'$  and  $P21/n$  Shubnikov symmetries for the majority and minority phases, respectively. The phase ratio in  $\text{Ca}_2\text{FeReO}_6$  shows a clear change from  $\sim 80/20$  to  $\sim 60/40$  near  $150\text{K}$  where the low temperature magnetic transition occurs, while such change is not observed for the  $\text{Ca}_{1.6}\text{La}_{0.4}\text{FeReO}_6$  sample with an approximately constant  $80/20$  phase ratio. The coexistence of phases over a wide temperature range implies their very similar energies. The stabilization of one of the magnetic ordering arrangement without applied field could be the cause of the low temperature transition.

[1] Serrate et al, *JMMM* 290-291 (2005) 843-845. [2] Granado et al, *PRB* 66 (2002) 64409. Supported by the NSF-DMR-0302617 and by the US Department of Transportation

MP33

### Observation of Fragile-to-Strong Dynamic Crossover in DNA Hydration Water

S. Chen, L. Liu, X. Chu (Massachusetts Institute of Technology), E. Fratini, P. Baglioni (University of Florence, Italy), A. Faraone, E. Mamontov (National Institute of Standards and Technology)

We used high-resolution quasielastic neutron scattering technique to study the single-particle dynamics of water molecules on the surface of hydrated DNA powder samples. The DNA powder was hydrated at the level of about 15 water molecules per base pair. Both  $\text{H}_2\text{O}$  and  $\text{D}_2\text{O}$  hydrated samples are measured. The contribution of scattering from DNA is subtracted off by taking the difference of the signals between the two samples. The measurement was made at a series of temperatures from  $270\text{K}$  down to  $185\text{K}$ . We used the Relaxing Cage Model to analyze the quasielastic spectra and were able to extract the average translation relaxation time  $\langle\tau_T\rangle$  as a function of temperature. We observe a clear evidence of the fragile-to-strong dynamic crossover at  $220\text{K}$  by plotting  $\log\langle\tau_T\rangle$  vs  $1/T$ . The detailed analyses of the quasielastic spectra are described. We discuss the consequence of the observed crossover in triggering the so-called glass transition in DNA molecule is inferred from the results.

MP34

**Neutron diffraction study of average and local structure in  $\text{La}_{0.5}\text{Ca}_{0.5}\text{MnO}_3$** 

E. E. Rodriguez (University of California, Santa Barbara), A. Llobet, T. Proffen, J. J. Rhyne (Los Alamos Neutron Science Center, Los Alamos National Laboratory), J. F. Mitchell (Argonne National Laboratory)

We used neutron powder diffraction to obtain the local and long-range structure of  $\text{La}_{0.5}\text{Ca}_{0.5}\text{MnO}_3$  at room temperature and 20 K. By combining Rietveld and pair distribution function analysis of the total neutron scattering data, we have analyzed the structure of the compound using two competing models describing the low temperature phase: first the charge-ordered-orbital-ordered model and second the Mn-Mn dimer model. These structural models fit the 20 K neutron powder diffraction pattern equally well using a Rietveld analysis. Therefore, pair distribution function analysis is used to probe the local and medium-range structure revealing a system with two distinctly distorted Mn octahedra and Mn ions with nonintegral valence states. The distorted octahedra differ with the structural model for the Zener polaron-type Mn-Mn dimer picture proposed for  $\text{Pr}_{0.60}\text{Ca}_{0.40}\text{MnO}_3$  and order in a similar checkerboard configuration associated with the CE-type antiferromagnetic structure. Therefore, locally the charge difference and structural ordering between the two Mn is appreciable enough to describe the system at 20 K as “partially charge ordered”.

MP35

**Crystallographic and Magnetic Structural Investigations on Ternary  $\text{Ga}_2\text{CrFe}$  Compound: a Gamma-Brass Related Structure Isoelectronic with  $\text{GaMn}$  Binary Intermetallic Compound**

H. Ko, G. J. Miller (Ames Laboratory), O. A. Gourdon (Los Alamos Neutron Science Center, Los Alamos National Laboratory)

Shifted phase line is observed for  $\text{Ga}_x\text{Mn}_{1-x}$  binary compounds in the range of  $0.36 \leq x \leq 0.375$ . The structure is refined by single crystal x-ray diffraction analysis ( $\text{Mn}_{98}\text{Ga}_{57}$ ;  $a = 12.7082 \text{ \AA}$ ,  $c = 15.6105 \text{ \AA}$ ) and a trigonal distortion from known  $\gamma$ -brass structure is observed by the powder x-ray diffraction analysis. Also, an isoelectronic ternary compound ( $\text{Ga-Cr-Fe}$ ) is prepared and the single crystal x-ray diffraction refinement adopts trigonal structure for  $\text{Ga}_{13}\text{Fe}_6\text{Cr}_7$  with lattice parameters of  $a = 12.5504 \text{ \AA}$ ,  $c = 7.8637 \text{ \AA}$ . However, due to the small

differences in the x-ray scattering factors between Cr and Fe metals, different model structures are constructed and investigated theoretically using self-consistent, spin polarized TB-LMTO method to further study their electronic structure and magnetic properties which yields the most suitable crystalline structure. Both Extended Huckel calculation and LSDA-TB-LMTO calculation results are consistent to have lower total energy on the experimentally refined structure. In order to have a conclusion about the Ga-Cr-Fe compound's crystallographic and magnetic structures, bulk samples are being prepared for neutron diffraction experiments and for other physical property measurements. Neutron diffraction study results are also in agreement with theoretical results showing slightly higher Cr content in the system. It is clear that all the structures show antiferromagnetically coupled interactions between the face sharing site (occupied by one metal type) of the icosahedrons and the other icosahedrons site (occupied by the other metal type) which has been validated by magnetic property measurements, neutron diffraction studies, as well as theoretical investigations.

MP36

**Total neutron scattering: the key to the local and medium range structure of complex materials**

T. Proffen (Los Alamos Neutron Science Center, Los Alamos National Laboratory)

Structural characterization is mainly based on the measurement of Bragg intensities and yields the average structure of the crystalline material. However, this approach ignores any defects or local structural deviations that manifest themselves as diffuse scattering. It also fails in case of disordered materials, badly crystalline such as many nano-materials, or not crystalline at all, such as glasses. In some cases crystalline and amorphous phases coexist making the traditional crystallographic structure refinement difficult or incomplete. The total scattering pattern, however, contains structural information over all length scales [1] and can be used to obtain a complete structural picture of complex materials.

Here we present different applications of this technique including data taken on the new high resolution neutron powder diffractometer NPDF located at the Lujan Neutron Scattering Center at

Los Alamos National Laboratory. This instrument is design for total scattering studies using the Pair Distribution Function (PDF) approach. We hope to attract many new users to use total scattering as a tool to fully characterize their materials structurally.

[1] Th. Proffen, S.J.L. Billinge, T. Egami and D. Louca, Z. Krist. **218**, 132-143 (2003).

MP37

### Coexistence of ferro- and antiferromagnetic spin correlations in $\text{La}_{1.2}\text{Sr}_{1.8}\text{Mn}_2\text{O}_7$

T. Chatterji, M. M. Koza (Institut Laue-Langevin, France), F. Demmel (ISIS, CCLRC)

We have investigated the antiferromagnetic (AF) fluctuations in quasi-2D ferromagnetic  $\text{La}_{1.2}\text{Sr}_{1.8}\text{Mn}_2\text{O}_7$  that shows colossal magnetoresistive (CMR) behaviour by inelastic neutron scattering both on a cold triple-axis and a time-of-flight neutron spectrometer. The AF fluctuations, which appear at temperatures above about 120 K, increase in intensity with increasing temperature, show a peak at  $T_C = 128$  K and then decrease very slowly with temperature. The scattered neutron intensity due to the AF fluctuations is much weaker compared to that due to ferromagnetic fluctuations and coexist with the latter. The half-width at half-maximum (HWHM) of the AF fluctuations is about 1.86 meV at  $T = 200$  K. This corresponds to a decay time of about 0.35 pico second. The temperature and magnetic field dependence of the AF fluctuations suggest that they are intrinsic and are not due to any AF impurity phase. In addition the magnetic field dependence of the antiferromagnetic intensity correlate strongly with the field dependence of resistivity suggesting that the AF fluctuations are related to the CMR effect.

MP38

### Bose-Einstein Condensation in liquid $^4\text{He}$ films

S. Diallo, J. V. Pearce (University of Delaware), R. T. Azuah (NIST Center for Neutron Research), H. R. Glyde (University of Delaware)

Neutron scattering measurements of Bose-Einstein condensation in liquid  $^4\text{He}$  films will be presented. The measurements were carried out on the MARI time-of-flight spectrometer at the CCLRC ISIS Facility, Rutherford Appleton Laboratory, UK. The goal is to determine whether the condensate fraction,  $n_0$ , is enhanced above the bulk liquid value

at a liquid  $^4\text{He}$  surface. It is also to determine  $n_0$  in 2D thin films and, by varying the film thickness, observe a 2D to 3D cross-over. Data for films on carbon-black will be presented.

MP40

### Breakdown of magnon quasiparticles in quantum magnets

I. Zaliznyak (Brookhaven National Laboratory), M. Stone (Oak Ridge National Laboratory), T. Hong, C. Broholm, D. Reich (Johns Hopkins University), S. H. Lee (University of Virginia), S. Petrov (P. Kapitza Institute for Physical Problems)

Recent neutron scattering experiments indicate that failure of the quasi-particle construct, which is the basis of the standard description of condensed matter where the quasi-particles are the fundamental carriers of energy and momentum quanta, is a common feature of quantum magnets with non-magnetic ground state that can be identified as quantum spin liquids [1,2]. Coherent magnon excitations in such systems exist above an energy gap and dramatically disappear when their dispersion enters the two-particle continuum, which opens a decay channel. In fact, this type of spectral instability is a generic feature of quantum Bose fluids with a gap and was originally predicted and studied in the superfluid helium-4. Here we present experimental evidence for its existence in spin-1 Haldane chains [1] and quantum dimer systems [2].

[1] I. A. Zaliznyak, S.-H. Lee and S. V. Petrov, *Phys. Rev. Lett.* **87**, 017202 (2001).

[2] M. B. Stone, I. A. Zaliznyak, T. Hong, C. L. Broholm, and D. H. Reich, *Nature* **440**, 189 (2006).

MP41

### Neutron deflection by a perfect crystal prism

S. Abbas, A. G. Wagh (Bhabha Atomic Research Centre, Mumbai, India), M. Strobl, W. Treimer (Hahn-Meitner Institut)

For neutron incidence near a Bragg reflection of a single crystal prism, the deflection  $\delta_{cr}$  of the transmitted neutron beam differs from its off-reflection value  $\delta_{am}$ , the difference increasing monotonically in magnitude as the Bragg reflection is approached from either side. Near a Bragg reflection, the sensitivity of  $\delta_{cr}$  to the angle of incidence gets enhanced by nearly 3 orders of magnitude over that of  $\delta_{am}$ . The prism deflection attains extrema at either extreme of the total reflectivity range. Using the narrow ( $\sim 2$  arcsec wide) virgin peak of  $5.24 \text{ \AA}$  neutrons at the USANS



(Ultra-Small Angle Neutron Scattering) facility in HMI, we have observed the variation of  $\delta_{cr}$  and transmitted intensity with angle of incidence for single crystal silicon prisms in several symmetric and asymmetric {111} Bragg configurations and different apex angles. The neutron deflection and transmittivity data agree well with predictions of two dynamical diffraction theory. These observations can be used to reduce the widths of USANS spectra still further.

MP42

### **Defects, Hydrogen Bonding, and Superconductivity in $\text{Na}_x\text{CoO}_2 \cdot 4x\text{H}_2\text{O}$ ( $x=1/3$ )**

J. D. Jorgensen, D. G. Hinks, M. Avdeev, P. W. Barnes, S. Short (Argonne National Laboratory)

We have used neutron powder diffraction to explore the relationships among oxygen vacancy defects, hydrogen bonding, and superconductivity in  $\text{Na}_x\text{CoO}_2 \cdot 4x\text{H}_2\text{O}$  ( $x=1/3$ ). Oxygen vacancy defects form on the  $\text{CoO}_2$  sublattice in response to the high oxidation state of Co. In metastable samples, we have monitored the formation of these vacancies, and the evolution of  $T_c$ , vs time and used this information to learn the dependence of  $T_c$  on Co oxidation state to high precision. Using neutron powder diffraction at high pressure we have selectively compressed the hydrogen bonds and observed the resulting charge transfer to the  $\text{CoO}_2$  layers as measured by the layer thickness (which increases with pressure). This demonstrates that hydrogen bond ordering could also affect  $T_c$ .

*This work was supported by the U.S. Dept. of Energy, Basic Energy Sciences.*

MP43

### **Single Crystal Diffraction with Elastic Discrimination**

S. Rosenkranz, R. Osborn (Argonne National Laboratory)

Single crystal diffuse neutron scattering is a powerful technique for probing complex disorder in crystalline materials. It provides a determination of not only of the local distortions around a point defect but also the morphology and length scale of nanoscale correlations. Accurate modeling of complex disorder requires measurements over a large volume of three-dimensional reciprocal space, which can be performed efficiently at a pulsed neutron source by time-of-flight Laue diffraction. However, conventional time-of-flight diffractometers cannot separate quasi-static diffuse scattering from vibrational and other inelastic

scattering. We propose to use a statistical chopper, with a pseudo-random sequence of apertures, to provide elastic discrimination using the cross-correlation method. The effectiveness and limitations of this method for single crystal diffuse scattering will be discussed based on the results of our Monte Carlo simulations.

MP44

### **Charge transfer and phonon thermodynamics in vanadium alloys**

O. Delaire, M. Kresch, B. Fultz (California Institute of Technology)

We investigated the effects of dilute alloying on the lattice dynamics and electronic structure of bcc vanadium. Using inelastic neutron scattering, we measured the phonon density of states (DOS) and vibrational entropy of random solid solutions of vanadium with transition metal impurities. A clear trend is observed for all solutes. Elements to the left of V in the periodic table cause a softening of the V phonons, while elements to the right of V induce a gradually increasing stiffening. This stiffening correlates well with the electronegativity difference between impurity and host. The restructuring of the phonon DOS is large and the corresponding change in vibrational entropy is comparable to the configurational entropy of mixing.

Using density functional theory (DFT), we calculated the relaxation and electronic structure for all alloys. The experimental trends in the phonons are reproduced by DFT. The charge transfer calculated from these first-principles simulations is in good agreement with the electronegativity trend and provides insight into the bonding between impurities and host atoms in transition metals.

MP45

### **Temperature dependent bilayer ferromagnetism in $\text{Sr}_3\text{Ru}_2\text{O}_7$**

M. B. Stone, M. D. Lumsden, R. Jin, B. C. Sales, D. G. Mandrus, S. E. Nagler (Oak Ridge National Laboratory)

The Ruthenium based perovskites exhibit a wide range of interesting physical behaviors, including exotic superconductivity, metal insulator transitions, and strong quantum fluctuations. Exciting magnetic phenomena have been identified in several ruthenates, but a clear understanding of the underlying magnetic excitation spectrum

in these layered perovskites is far from complete. We present results of detailed inelastic neutron scattering measurements of  $\text{Sr}_3\text{Ru}_2\text{O}_7$ . Measurements were performed to probe the ferromagnetic fluctuations of the bilayer structure. A magnetic response is clearly visible for a range of temperatures,  $T = 3.8$  K up to  $T = 100$  K, and for energy transfers between  $\hbar\omega = 2$  and 14 meV. These measurements indicate that the ferromagnetic fluctuations explicitly shown in the bilayer magnetic form-factor persist to temperatures large compared to the energy-scales of the fluctuations. This high temperature behavior is proposed as a manifestation of the proximity of the system in zero magnetic field to the metamagnetic/ferromagnetic transition.

*Research sponsored by the U.S. Department of Energy, under contract DE-AC05-00OR22725 with Oak Ridge National Laboratory, managed and operated by UT-Battelle, LLC.*

MP46

#### **Slow spin-glass and fast spin-liquid components in quasi-two-dimensional $\text{La}_2(\text{Cu,Li})\text{O}_4$**

Y. Chen (NIST Center for Neutron Research and University of Maryland), W. Bao (Los Alamos National Laboratory), Y. Qiu (NIST Center for Neutron Research and University of Maryland), J. E. Lorenzo (CNRS, France), J. L. Sarrao (Los Alamos National Laboratory), D. L. Ho (NIST Center for Neutron Research and University of Maryland), M. Y. Lin (ExxonMobil Research and Engineering Company and NIST Center for Neutron Research)

In conventional spin glasses, magnetic interaction is not strongly anisotropic and the entire spin system is believed to be frozen below the spin-glass transition temperature. In  $\text{La}_2\text{Cu}_{0.94}\text{Li}_{0.06}\text{O}_4$ , for which the in-plane exchange interaction dominates the interplane one, only a fraction of spins with antiferromagnetic correlations extending to neighboring planes become spin glass. The remaining spins with only in-plane antiferromagnetic correlations remain spin liquid at low temperature. Such a partial spin freezing out of a two-dimensional spin liquid observed in this cold neutron scattering study is likely due to a delicate balance between disorder and quantum fluctuations in the quasi-two-dimensional  $S=1/2$  Heisenberg system.

MP47

#### **Spin correlations in a spin-1 triangular lattice antiferromagnet**

S. Jonas, C. Stock, C. Broholm (Johns Hopkins University), S. Nakatsuji, Y. Nambu, H. Tonomura, O. Sakai, Y. Maeno (Kyoto University), J. Gardner (NIST Center for Neutron Research), A. Faraone (NIST Center for Neutron Research and University of Maryland)

Spin correlations in the triangular lattice antiferromagnet  $\text{NiGa}_2\text{S}_4$  were investigated as a function of temperature and magnetic field through neutron scattering. At  $T = 1.5$  K the in plane correlations are incommensurate with a wave vector  $(1/6-\delta, 1/6-\delta, 0)$  where  $\delta = 0.0086(6)$ . The in-plane correlation length is  $6.9(8)$  lattice spacings while inter-plane correlations cannot be detected beyond the second nearest plane. These correlations persist on a time scale that exceeds 0.3 ns. Application of an in-plane magnetic field of 10 Tesla only slightly reduces the inter-plane correlations with no appreciable effect on intra-plane correlations, while heating reduces the frozen moment, the in-plane correlation length, and the correlation time. We shall discuss what can be inferred about the spin Hamiltonian for  $\text{NiGa}_2\text{S}_4$  as well as the spin-1 triangular lattice antiferromagnet from these data.

MP48

#### **Cold Neutron Scattering by Ultrasound in Silicon. Suppression Ultrasound Contribution to the Debye-Waller Factor Effect**

E. Iolin, L. Rusevich (Institute of Physical Energetic, Riga, Latvia), M. Strobl, W. Treimer, F. Mezei (Hahn-Meitner Institut)

It is well known that thermal motion decreases intensity  $I_h$  of the elastic kinematic scattering in the mosaic crystal. This decrease is described by the DW factor,  $I_h \sim \exp(-2M)$ ,  $2M = \langle (HU)^2 \rangle$ ,  $H$  – vector of scattering,  $U$  – nuclear thermal displacement from the equilibrium crystal position. For the case of perfect single crystal, the thermal motion changes the value of gap between Dispersion Surface branches, so that intensity of scattering becomes  $I_h \sim \exp(-1 * M)$ , (Batterman, 1962). We studied how ultrasound affects dynamic scattering. We excited high-frequency 70 – 210 MHz LAW and TAW ultrasonic waves in perfect Si(111) s.c. and studied the energy spectrum of the Bragg diffracted neutrons ( $\lambda = 0.52 - 0.54$  nm). We used Neutron Spin Echo technique with moderate momentum

resolution and triple bounces Bonse – Hart channel cut Si(111) analyzer with excellent momentum resolution. We easily observed up to  $\pm 4$  ultrasonic satellites, so that the contribution of ultrasound to the value of  $M$  was significant. However, the observed intensity of the elastic scattering  $I_h(0)$  was almost independent on the value of ultrasonic wave amplitude  $W$ ! We interpreted that as follows. The local amplitude of the elastic scattering is defined by the value of  $f = \text{BesselJ}(0, H \cdot W \cos(K_s \cdot z))$ .  $K_s$  is the momentum of the standing LAW. Ultrasonic displacement is significant at the inlet surface of silicon. Therefore neutron corresponding to the external sides of the Darwin plateau penetrates inside of crystal. The gap between DS branches is spreading to the bottom  $\sim \pi/(2 K_s)$  inside of crystal, so that the neutron bounces and flies out from sample. This picture is applicable to the case of cold, slow neutrons with small extinction length. The similar approach – cold neutron reflection from regions with small ultrasonic displacements – is applicable also to the case of TAW. Therefore, h.f. ultrasonic effect at the elastic scattering is qualitatively different from that of factor  $\exp(-1 \cdot M)$ .

MP49

#### Time-of-flight studies of magnetic excitations in $\text{La}_{2-x}(\text{Ba,Sr})_x\text{CuO}_4$

J. M. Tranquada, G. D. Gu (Brookhaven National Laboratory), S. Wakimoto (Japan Atomic Energy Agency), M. Fujita, K. Yamada (IMR, Tohoku University), C. D. Frost, T. G. Perring (ISIS, CCLRC)

We have used the MAPS spectrometer at ISIS to study magnetic excitations up to  $\sim 100$  meV as a function of temperature in  $\text{La}_{1.875}\text{Ba}_{0.125}\text{CuO}_4$  (LBCO) and as a function of doping in  $\text{La}_{2-x}\text{Sr}_x\text{CuO}_4$  (LSCO) with  $x = 0.25$  and  $0.30$ . The compound LBCO exhibits static stripe order for  $T < 50$  K. We find that, for energies greater than about 10 meV, there is little change in the excitation spectrum on going from the ordered state at 12 K, to the disordered state at 65 K. On warming up to 300 K, there is some broadening of the spectra in  $Q$ , but little change in the distribution of spectral weight versus energy. These results are consistent with the presence of a charge-stripe liquid in the disordered phase. In contrast, measurements on the overdoped LSCO samples indicate that there is negligible magnetic scattering between 10 and 100 meV in comparison with LBCO. This is consistent with disappearance of the stripe-liquid phase in overdoped cuprates.

Work at Brookhaven is supported by the Office of Science, U.S. Dept. of Energy, under Contract No. DE-AC02-98CH10886.

MP50

#### Excitations in MCCL from FM-AFM Alternating-sign Chains

W. Tian (University of Tennessee), M. B. Stone, M. D. Lumsden (Oak Ridge National Laboratory), G. E. Granroth (Spallation Neutron Source, Oak Ridge National Laboratory), D. G. Mandrus (Oak Ridge National Laboratory), J. H. Chung (NIST Center for Neutron Research, Gaithersburg, MD), F. Fernandez-Alonso (ISIS Pulsed Neutron Facility), N. Harrison (Los Alamos National Laboratory), S. E. Nagler (Oak Ridge National Laboratory)

We report neutron scattering investigations of excitations in single crystals of the spin  $1/2$  quantum magnet dimethylammonium trichlorocuprate ( $\text{DMACuCl}_3$  or MCCL). MCCL had been understood as consisting of alternating ferromagnetic-antiferromagnetic chains running along the crystalline  $a$ -axis, however until now there have been no measurements of the magnetic excitations. The new results clearly indicate that the direction of strong magnetic couplings in MCCL is along the crystalline  $b$ -axis, not the  $a$ -axis. The measured spectrum is consistent with the expectations for an alternating sign-chain with a gap of  $D = 0.98$  meV and an approximate bandwidth of 0.67 meV. Fitting the spectrum with first order perturbation theory yields a ratio of  $J_{AF}/J_F = -0.5$ , but a more exact calculation shows that  $J_{AF}/J_F = -0.9$ , placing the system in the very interesting physical regime where the behavior is a crossover from Haldane-like to dimer like. In light of this description, we make comparisons to previously measured specific heat and magnetization measurements. We also place a limit on inter-dimer interactions perpendicular to the chain axis and propose a potential multi-chain model for MCCL.

MP51

#### Features of NRSF2, the New Neutron Residual Stress Mapping Facility at HFIR

C. R. Hubbard, W. B. Bailey, F. Tang, K. An, A. D. Stoica, M. C. Wright, H. Choo (Oak Ridge National Laboratory)

The installation and testing of the new, second generation neutron residual stress mapping facility at HFIR is over 90% complete and productive user and laboratory studies are being conducted. The facility at beam line HB-2B of HFIR consists of the following major components: (1) twin silicon multi-wafer, doubly focusing "Missouri" monochromator

which provides six different wavelengths; (2) large capacity sample XY and rotation stage with two optionally mounted Z-stages; (3) a seven position sensitive detector array; and (4) precision interchangeable incident and diffracted beam slits for definition of the gage volume. Accessories include a uniaxial tension/compression mechanical properties load frame and a Huber phi-chi sample orienter. LabView software packages NRSF2-MAP, NRSF2-LOAD and NRSF2-VIEW work together and provide robust, easily learned, real-time data collection, calibration and analysis tools.

To date, research projects conducted on NRSF2 during the commissioning and testing phase fall into the following three classifications:

- (1) Mapping of residual strains in welds, compact tension fatigue specimens, quenched rods, cast and machined cylinder liners, nuclear reactor tubes, and cylinders deformed in tension and torsion.
- (2) Materials deformation behavior under applied load in aluminum metal matrix composites, aluminum alloys, porous ceramic filter materials, and of compaction of granular quartz particles
- (3) Phase and hydrogen content mapping in Zircalloy using both Bragg peak and incoherent background intensity
- (4) Dynamic real time experiments such as real-time mechanical property loading and a moving hot spot simulating the heat input from friction stir welding.

*The NRSF2 facility is sponsored by the DOE-EERE Office of FreedomCAR and Vehicle Technologies via the High Temperature Materials Laboratory User Program. Industry, university and other laboratory engineers and scientists can gain access via the HTML user program ([www.html.ornl.gov](http://www.html.ornl.gov)).*

MP52

### **Magnetic and charge/orbital ordering in the half-doped layered manganite $\text{Pr}_{0.5}\text{Ca}_{1.5}\text{MnO}_4$**

F. Ye, J. A. Fernandez-Baca (Oak Ridge National Laboratory), S. Chi, P. Dai (University of Tennessee), R. Mathieu, Y. Tokura (University of Tokyo, Japan)

We use elastic and inelastic neutron scattering to study magnetic and charge/orbital ordering (CO-OO) in the half doped single layer manganite  $\text{Pr}_{0.5}\text{Ca}_{1.5}\text{MnO}_4$ . This system enters CO-OO at around 325K and forms a checker-board like CE-type antiferromagnetic (AF) structure below 125K. There is a strong magneto-elastic effect close to the Neel temperature, causing the suppression

of a lattice distortion. The low-T spin-wave dispersion is highly anisotropic, revealing that the ferromagnetic interactions within the zigzag chain are considerably stronger than the AF coupling between the chains. Such observation is consistent with recent theoretical models where the quasi-1D FM zigzag chains are the building blocks of the CE-type CO-OO.

*This work was supported by the DOE No.DE-AC05-00OR22725 with UT/Battelle, LLC and U. S. NSF DMR-0139882.*

MP53

### **Wavelength-Shifting Fiber Scintillation Neutron Detectors for POWGEN3 & VULCAN at SNS**

L. Crow, J. Hodges, L. Heroux, B. Hannan (Spallation Neutron Source, Oak Ridge National Laboratory)

We have constructed and tested the initial production wavelength-shifting fiber scintillation neutron detector module for the POWGEN3 powder diffractometer the Spallation Neutron Source (at Oak Ridge National Laboratory). The design is based on a successful prototype [1]. POWGEN3 and the VULCAN engineering diffractometer require neutron detector systems with large, narrow pixels (about 5mm x 50 mm), good efficiency at up to about 0.5 eV, and areas of several square meters. The detector uses a  $^6\text{LiF}/\text{ZnS:Ag}$  scintillation screen for neutron conversion. The light is collected using a two-layer grid of wavelength-shifting plastic optical fibers with 1 mm diameter. 308 vertical fibers are spaced 2.5 mm apart, and 152 horizontal fibers are also spaced 2.5 mm apart. The detector has an area of 780 mm  $\times$  400 mm with an active area of nearly 95%. The vertical fiber ends are mapped to an array of 20 photomultiplier tubes (PMTs) in a 2Cn coincidence pattern. This pattern encodes the 5 mm wide horizontal pixels. Each horizontal fiber is mirrored at one end, and the other end conducts light to a PMT; bundling of these fibers defines the vertical pixels. The detector operates in coded coincidence, requiring signals from one PMT corresponding to a vertical pixel and two PMTs corresponding to a horizontal pixel. The PMT output is converted to digital signals using fast comparators, and the neutron identification and position encoding are processed digitally. The  $\sim 0.3 \text{ m}^2$  module is an integrated unit, with scintillator, grid, PMTs, and digital processors mounted in a single frame. The detector module has been successfully tested at the High Flux Isotope Reactor. Production is beginning on additional



modules which will form the initial detector complement for POWGEN3 and VULCAN.

[1] M. L. Crow, J. P. Hodges, and R. G. Cooper, *Nucl. Instr. Meth. A* **529** (2004) 287.

MP54

### **IINS/QC studies of $(C_3N_2H_5)_5Bi_2Cl_{11}$**

K. Z. Holderna-Natkaniec (Institute of Physics A.Mickiewicz University, Poznan, Poland), I. Natkaniec (H.Niewodniczanski Institute of Nuclear Physics Polish Academy of Sciences Krakow, Poland), R. Jakubas (Department of Chemistry Wrocław University, Wrocław, Poland), D. Nowak (Joint Institute for Nuclear Research)

Imidazolium undecachlorodibismuthate (III)  $(C_3N_2H_5)_5Bi_2Cl_{11}$  has been studied by means of inelastic incoherent scattering methods over a temperature range 20 K, 290 K. The IINS spectra were recorded using the inverted geometry time-of-flight spectrometer NERA-PR working at the pulsed reactor IBR-2 in Dubna (Russia). The experimental spectra were converted in the approximation of the one-phonon scattering approximation into generalized function of phonon density of state. They were interpreted against the results of the calculation performed by density functional theory method using Gaussian 03 program taking into account the X-Ray diffraction data. The  $(C_3N_2H_5)_5Bi_2Cl_{11}$  salt appear to be a ferroelectric compound below 166 K. The calculation were performed using the harmonic force field. The assignment of low temperature normal modes was proposed. The low temperature spectra show the ordering of imidazolium cation.

*Financial support under the grant of the Polish Plenipotentiary at JINR is gratefully acknowledgment by authors. The QC computations were performed at PSCS in Poznan.*

*Present affiliation: I. Natkaniec, Frank Laboratory of Neutron Physics, JINR, 141980 Dubna,*

MP55

### **Proton Dynamics of Bulk Ammonia Borane and Ammonia Borane Confined in Mesoporous Silica by Quasielastic Neutron Scattering**

N. J. Hess, A. S. Stowe (Pacific Northwest National Laboratory), C. M. Brown, E. Mamontov (NIST Center for Neutron Research and University of Maryland), L. L. Daemen (Los Alamos Neutron Science Center, Los Alamos National Laboratory), T. Autrey (Pacific Northwest National Laboratory)

We have studied the proton dynamics in bulk ammonia borane,  $NH_3BH_3$ , in both the low temperature orthorhombic phase and the room temperature tetragonal phase following the

increasingly rapid proton motions over wide range of time scales using both the HFBS and DCS spectrometers at NIST. The proton residence times and rotational energy barriers for the amine ( $-NH_3$ ) and the borane ( $-BH_3$ ) protons change dramatically across the phase transition boundary. The rotational energy barrier for either amine or borane protons in the tetragonal phase is lower than it is in gas phase. This is surprising given the strong intermolecular dihydrogen bonding interactions in solid state ammonia borane. We have also studied the proton dynamics in ammonia borane adsorbed into mesoporous silica substrates. Our QENS results indicate that the deposition of ammonia borane on a mesoporous silicate results in longer proton residence times and lower energy barriers for proton motion compared to bulk ammonia borane. Our initial results can be interpreted by a model that includes at least two proton populations, one that is stationary on the time frame of the QENS measurement and one that is rapidly rotating. This model is also consistent with our recent deuterium NMR results.

MP56

### **Neutron Spin Echo Results from Frustrated Magnets**

J. S. Gardner (National Institute of Standards and Technology), G. Ehlers (Spallation Neutron Source, Oak Ridge National Laboratory)

Neutron Spin Echo (NSE) on spin ice and related compounds will be discussed.  $Ho_2Ti_2O_7$  was the first of these to be measured. The intermediate scattering function was measured as a function of temperature and Q. Recently two related compounds, namely  $(Ho,Y)_2Ti_2O_7$  and  $Ho_2Ru_2O_7$  were measured. One has a diluted spin ice lattice while the other has a second magnetic sublattice. Although the spin dynamics are similar in both, subtle differences provide unique information on the spin dynamics in the system.

MP57

### **Spin excitations in $La_{1.5}Sr_{0.5}CoO_4$**

A. T. Savici, I. A. Zaliznyak, G. D. Gu (Brookhaven National Laboratory)

Spin excitations in the Co-based layered perovskite  $La_{1.5}Sr_{0.5}CoO_4$ , a structural relative of the high-temperature superconducting cuprates, were studied by inelastic neutron scattering. At room temperature the excitation spectrum is dominated by phonons, with strong diffuse scattering at low



energies that have a characteristic wave vector dependence. At low temperatures we observe a mix of lattice vibrations and spin excitation modes. By subtracting phonon contributions we are able to identify two distinct excitations of purely magnetic origin. Around 27 meV there is a broad resonance-like mode whose intensity follows the momentum dependence of the magnetic form factor of cobalt ions. At low energies we find a band of gapless magnons with unusual dispersion, which is indicative of the proximity to a spin-liquid ground state.

MP58

### Compositional changes of the first sharp diffraction peak in binary selenide glasses

C. J. Benmore (Argonne National Laboratory, Intense Pulsed Neutron Source), E. Bychkov (University of Littoral, France), D. L. Price (CNRS, France)

Compositional changes of the first sharp diffraction peak (FSDP) in the measured structure factor have been studied for several binary selenide glasses using pulsed neutron and high-energy x-ray diffraction techniques. The observed variations in the FSDP (factor of 10 in the amplitude and  $\approx 0.5 \text{ \AA}^{-1}$  in the peak position) reflect multiple aspects in the glass network on both the short- and intermediate-range scale and are also correlated with macroscopic properties. An empirical relation has been discovered relating the compositional dependence of the FSDP position to the local coordination number of the guest atom.

MP59

### Magnetic Excitation Spectrum of $\text{Ca}_{2-x}\text{Sr}_x\text{RuO}_4$

M. D. Lumsden, S. E. Nagler (Oak Ridge National Laboratory), S. Wilson, P. Dai (University of Tennessee), R. Jin, D. Mandrus (Oak Ridge National Laboratory)

We have performed inelastic neutron scattering studies of the magnetic excitation spectrum for several concentrations of the layered perovskite ruthenate,  $\text{Ca}_{2-x}\text{Sr}_x\text{RuO}_4$ . Samples with concentrations near that of pure  $\text{Sr}_2\text{RuO}_4$  exhibit incommensurate excitations sharply peaked in  $Q$  at  $(\pm 0.3, \pm 0.3, q_z)$  as in the parent compound. The excitation spectrum evolves with Ca doping into a broad distribution of inelastic intensity centered around the 2d ferromagnetic zone center. We have carefully studied this distribution in single crystal samples with  $x=1$  and  $x=0.6$ . Previous

measurements on an  $x=0.62$  sample [1] were interpreted as broad inelastic peaks centered at  $(\pm 0.22, 0, 0)$  and  $(0, \pm 0.22, 0)$ . We see clear evidence of more structure in this distribution with several components coexisting. This includes significant spectral weight at the same wavevector as pure  $\text{Sr}_2\text{RuO}_4$ ,  $(\pm 0.3, \pm 0.3, 0)$ , together with components at  $(\pm 0.3, 0, 0)$  and  $(0, \pm 0.3, 0)$  and a central component at the ferromagnetic zone center. One possible interpretation is the coexistence of a central ferromagnetic component together with an incommensurate “ridge” of scattering at  $\pm 0.3$  in  $h$  and  $k$  as was predicted theoretically for pure  $\text{Sr}_2\text{RuO}_4$  [2].

[1] O. Friedt et al., *Phys. Rev. Lett.* **93**, 147404 (2004).

[2] I. I. Mazin and David J. Singh, *Phys. Rev. Lett.*, **82**, 4324 (1999).

Work supported by the U.S. DOE, under contract DE-AC05-00OR22725, ORNL, managed and operated by UT-Battelle, LLC.

MP60

### Quantum Critical Point in Itinerant Antiferromagnet CrV

D. Sokolov (University of Michigan)

We report results of neutron scattering experiments on  $\text{Cr}_{0.965}\text{V}_{0.035}$ . We have found temperature dependent elastic scattering at the incommensurate satellites of  $q=2\pi/a$   $(0,0,1)$ . Width of the elastic scattering is almost resolution limited, which correspond to scattering from regions, which are at least 500 Å long. The intensity of elastic scattering is comparable to scattering intensity of pure Cr. We suggest the electronic phase separation scenario to account for observed elastic scattering. Inelastic scattering at  $q=2\pi/a$   $(0,0,1)$  is temperature independent between 2 and 250 K and has a characteristic energy scale of  $\sim 18$  meV typical for a Fermi liquid. We found that the intensity of inelastic scattering at the incommensurate wavevector increases relative to commensurate scattering on cooling to 2 K at energies between 5 and 25 meV. The width of the inelastic incommensurate scattering becomes more narrow at the lowest energy transfers and temperatures, which is consistent with a susceptibility of a system approaching magnetic order. The remarkable temperature independence of the intensity of the incommensurate scattering indicates a possibility of a marginal Fermi liquid state at the incommensurate wavevector, previously found in heavy fermion quantum critical antiferromagnets.

MP61

**Incommensurate spin order of a geometrically frustrated spinel  $\text{CdCr}_2\text{O}_4$** 

J. Chung (National Institute of Standards and Technology), M. Matsuda (Japan Atomic Energy Agency), S. Lee (University of Virginia), K. Kakurai (Japan Atomic Energy Agency), H. Ueda (University of Tokyo, Japan), T. Sato, H. Takagi (National Institute of Standards and Technology)

The antiferromagnetic spins in the cubic pyrochlore lattices are known to be one of the most strongly frustrated magnetic systems. In such systems, magnetic orders are established often via coupling to lattice degrees of freedom. The B-site chromium spinels exhibit particularly large frustration parameters due to its absence of orbital degeneracy. For instance,  $\text{ZnCr}_2\text{O}_4$  develops multiple-k commensurate magnetic order via cubic-to-tetragonal transition ( $c < a$ ) at  $T_N \sim -\Theta_{\text{CW}}/33$ . In this talk, we report our studies on a closely related compound, namely  $^{114}\text{CdCr}_2\text{O}_4$  using elastic and inelastic neutron scattering techniques. Although it had been regarded similar to  $\text{ZnCr}_2\text{O}_4$ , the magnetic order and the associated lattice distortion were found to be strikingly different. The magnetic order at  $T_N = -\Theta_{\text{CW}}/11.4$  could be described by a single incommensurate propagation vector,  $(0 \delta 1)$ . Simultaneously, the spin-Peierls-like cubic-to-tetragonal transition occurred with  $c$ -axis becoming longer than  $a$ . By the combination of the field dependence of the magnetic Bragg peaks and the spin wave dispersions, we found that the spins form helices along diagonal chains with the helical axes along  $b$ . This incommensurate spin structure cannot be understood via next-nearest neighbor interactions, and strongly suggests possible involvement of an antisymmetric exchange.

MP62

**Magnetic neutron scattering studies of the high-Tc superconductors  $\text{Nd}_{2-x}\text{Ce}_x(\text{Cu,Ni,Zn})\text{O}_4$  and  $\text{HgBa}_2\text{CuO}_{4+\delta}$** 

G. Yu, I. Vishik, E. Motoyama (Stanford university), O. Vajk (NIST Center for Neutron Research, Gaithersburg, MD), X. Zhao, Y. Cho (Stanford university), P. Bourges (Laboratoire Léon Brillouin (UMR 12 CNRS/CEA) CEA-Saclay 91191 Gif sur Yvette France), M. Greven (Stanford university)

In order to arrive at a deeper understanding of the interplay between superconductivity and magnetism in the high-temperature superconductors, it is of interest to study the effects of impurity-doping on the copper site. A

large body of work along these lines exists for hole-doped materials, yet relatively little is known about the effects of such impurities on the prototypical electron-doped material  $(\text{Nd,Ce})_2\text{CuO}_4$  (NCCO). We grew large Zn and Ni doped NCCO single crystals using the traveling-solvent floating-zone technique, and report here on our neutron scattering results for the antiferromagnetic spin correlations as a function of impurity concentration. A second study focused on the hole-doped model superconductor  $\text{HgBa}_2\text{CuO}_{4+\delta}$  (Hg1201), which exhibits a simple tetragonal crystal structure and possesses the highest  $T_c$  (97 K at optimal doping) among all the single-layer cuprates. In a significant breakthrough, we were able to grow large Hg1201 crystals using flux growth techniques. We will present here our preliminary inelastic magnetic neutron scattering results in this system.

MP63

**Neutron Spectroscopic studies of amorphous beryllium hydride and lithium beryllium hydride**

S. Sampath (Arizona State University), A. I. Kolesnikov (Argonne National Laboratory, Intense Pulsed Neutron Source), K. M. Lantzky (3Department of Chemistry, St. John Fisher College, Rochester, New York), J. L. Yarger (Arizona State University)

Metal hydrides are of great scientific and technological interest in view of their potential applications for hydrogen storage in fuel cells, as electrodes for rechargeable batteries, in energy-conversion devices, and in nuclear science. Metal hydrides are also of fundamental importance because of their intriguing electronic, structural, and dynamical properties associated with the hydrogen atoms. In particular, low-Z compounds such as hydrogen-dominant metallic alloys,<sup>1</sup> lithium beryllium hydride,<sup>2</sup> alkali hydrides,<sup>3</sup> and beryllium hydride<sup>4</sup> have been of interest.  $\text{BeH}_2$  with its low mass and high hydrogen content, is a very interesting metal hydride for both theoretical calculations and its potential for hydrogen storage. Neutron diffraction measurements<sup>5</sup> indicate that structure of amorphous  $\text{BeH}_2$  is composed of network of corner-sharing tetrahedra, analogous with classic network-forming glasses such as amorphous  $\text{H}_2\text{O}$ ,  $\text{BeF}_2$ ,  $\text{SiO}_2$ , and  $\text{GeO}_2$ .

We report the first study of vibrational spectra of solid-amorphous  $\text{BeH}_2$  and amorphous  $\text{LiBeH}_3$  using inelastic neutron scattering (INS) measurements. The experiments were done at 5K on the HRMECS

instrument at IPNS-ANL. The positions of the symmetrical and antisymmetrical stretching modes and that of the bending mode in  $\alpha$ -BeH<sub>2</sub> is in good agreement with recent theoretical calculations<sup>6</sup>. Addition of lithium to the BeH<sub>2</sub> network, has resulted in softening of the modes, indicating a less rigid structure. IR measurements done on these materials provides complimentary support of the INS data.

- [1] N. W. Ashcroft, *Phys. Rev. Lett.* **92**, 187002, 2004.
- [2] M. Seel, A. B. Kunz, and S. Hill, *Phys. Rev. B* **39**, 7949, 1989.
- [3] T. Ogitsu, E. Schwegler, F. Gygi, and G. Galli, *Phys. Rev. Lett.* **91**, 175502, 2003.
- [4] P. Vajeeston, P. Ravindran, A. Kjekshus, and H. Fjellvag, *Appl. Phys. Lett.* **84**, 34, 2004
- [5] S. Sampath, K. M. Lantzky, C. J. Benmore, J. Neufeld, J. E. Siewenie, P. A. Egelstaff, and J. L. Yarger, *J. Chem. Phys.* **119**, 1, 2003.
- [6] X. Wang, L. Andrews, *Inorg. Chem.* **44**, 610-614, 2005.

#### MP64

### **Magnetism and hybridization in U(Cu, Pd)S**

S. T. El-Khatib, A. Llobet (Los Alamos Neutron Science Center, Los Alamos National Laboratory), A. Purwanto (Neutron Scattering Laboratory, BATAN, Serpong, Tangerang 15314, Indonesia), H. Nakotte (New Mexico State University)

UCuSn crystallizes in an orthorhombically-distorted structure that is closely related to the hexagonal GaGeLi structure. Bulk studies reveal that UCuSn undergoes two magnetic transitions at about 60 and 25 K. Here, we present more detailed neutron-diffraction studies that performed on the High-Intensity Powder Diffractometer (HIPD) at the Manuel Lujan, Jr. Neutron Scattering Center at Los Alamos. Neutron-diffraction studies provide clear evidence for a non-collinear configuration of the magnetic moments in both magnetic phases. We propose a simultaneous existence of two magnetic allowed-symmetry structures as one possible explanation to fit the observed magnetic intensities below 25 K. We will discuss the relationship between magnetic and structural properties in UCuSn. We observe regular thermal contraction with decreasing temperature down to 60 K, below which we observe discontinuities for the interatomic spacing,  $d_{U-U}$ ,  $d_{U-Cu}$  and the cell parameters, which provides a measure of the hybridization effects in UCuSn. We were able to correlate the structural changes with the magnetism in UCuSn. UPdSn will be discussed and compared with UCuSn in term of hybridization point of view.

#### MP65

### **Measurement of the 3-D Born-Oppenheimer Potential of a Proton in a Superprotonic Conductor Using Neutron Compton Scattering**

D. Homouz, G. Reiter (Physics Department, University of Houston), J. Eckert (Los Alamos National Laboratory), J. Mayers (ISIS, Rutherford Appleton Laboratory), R. Blinc (Stefan Josef Institute, Ljubljana, Slovenia)

We report the first model free direct measurement of the proton 3-D Born-Oppenheimer potential in any material. The proton potential surfaces in the superprotonic conductor Rb<sub>3</sub>H(SO<sub>4</sub>)<sub>2</sub> are extracted from the momentum distribution measured using Neutron Compton Scattering. The results are sufficiently accurate to easily see structural changes in going from 10K to 70K in this material, despite the absence of a phase transition.

#### MP66

### **The new wide angle polarization analyzer installed at POSY1**

S. Park (Intense Pulsed Neutron Source, Argonne National Laboratory), S. G. E. te Velthuis (Argonne National Laboratory), T. Krist (Hahn-Meitner Institut)

In grazing incidence scattering experiments, the off-specular scattering is determined by lateral variations in the magnetic and structural properties of the thin film. In order to fully understand magnetic domain behavior or lateral nanostructured magnetic films, it is essential to be able to perform polarization analysis on both the off-specular scattering, as well as on the specularly reflected beam. In the past, POSY1 at IPNS was equipped with a mirror analyzer which was capable of analyzing the polarization of a beam reflected over a very limited solid angle. Typically this was used to analyze only the specularly reflected beam. Recently a new analyzer was installed on POSY1, which allows the simultaneous analysis of both the specular and off specular scattering. The horizontal dimensions of the analyzer are matched to the dimensions of the position sensitive detector, and covers a solid angle of about 2 degrees. The analyzer consists of numerous polarizing channels. The channel walls consist of Ni coated absorbing plates. Inside each channel a Si wafer coated with polarizing supermirror is inserted diagonally making the channel optically closed and thereby allowing only one spin state to be transmitted through the analyzer. In order

to be able to analyze all the scattered intensity with the same efficiency, the channels are oriented such that they lie within the horizontal scattering plane of the sample, i.e. the surface of the channel walls are oriented perpendicular to the vertically oriented surface of the sample. Any variation of the polarization efficiency is perpendicular to the scattering plane of the sample. Details of the analyzer as well as the results of measurements of the polarizing and transmission properties will be reported.

MP67

### **Magnetic Properties of Coupled Ni/Gd/Ni Films**

I. Zoto, G. J. Mankey (University of Alabama)

The magnetic recording industry badly needs higher magnetization materials in order to write high anisotropy media which is required for thermal stability at small bit sizes. It is conceivable that transition metal-rare earth bilayers might allow magnetizations higher than that available from transition metal alloys if the strong exchange interactions of the transition metal layer could be used to raise the Curie temperature of an adjacent, high moment rare earth layer. Gd is particularly attractive because it has an intrinsically low anisotropy. Literature suggested for a ferromagnetic interaction in the Ni-Gd bulk film (ref. 1), and preliminary reports indicate an increased moment at room temperature when Gd layer is deposited onto thin Co and permalloy films (ref. 2). Here, a study of a Ni/Gd/Ni trilayers is presented. The hysteresis loops were measured with VSM in the temperature range 5-250K. We find that Ni and Gd have a negative interfacial exchange interaction, so they align antiferromagnetically at zero applied field. A Stoner-Wolfarth model is used to simulate the hysteresis loops, which are in good agreement with the experimental results and confirm the antiferromagnetic coupling of Ni and Gd. Polarized neutron reflectivity also confirms the antiferromagnetic coupling of Ni and Gd in the remnant state and indicates that the magnetic moment of both Ni layers and Gd are aligned parallel to the field as the applied field is increased to 0.8 T.

[1] T. Hatano, et al., *J. Electron Spectrosc. Relat. Phenom.* **78**, 217 (1996)

[2] A. Pogorily, E. Shypil and C. Alexander, *J. Magn. Magn. Mater.* **286**, 493 (2005)

## Tuesday, June 20

T1-A (8:30 – 10:00 am)

### Neutron Facilities – Worldwide Status

Chair: R. Teller (New Orleans Ballroom)

T1-A1 (8:35 am)

### Neutron Scattering Developments and Initiatives in Asia and Australia (Plenary)

M. Arai (J-PARC)

T1-A2 (8:55 am)

### Neutron Scattering Developments and Initiatives in Europe (Plenary)

A. Taylor (Rutherford Appleton Laboratory)

T1-A3 (9:15 am)

### Neutron Scattering Developments and Initiatives in North America (Plenary)

R. Pynn (Indiana University)

T1-A4 (9:35 am)

### First Neutrons at the Spallation Neutron Source (Plenary)

T. E. Mason (Oak Ridge National Laboratory)

The wavelengths and energies of thermal and cold neutrons are ideally matched to the length and energy scales in the materials that underpin technologies of the present and future: ranging from semiconductors to magnetic devices, composites to biomaterials and polymers. The Spallation Neutron Source will use an accelerator to produce the most intense beams of neutrons. The project is being built by a collaboration of six U.S. Department of Energy laboratories. It will serve a diverse community of users drawn from academia, industry, and government labs with interests in condensed matter physics, chemistry, engineering materials, biology, and beyond. Results from the initial commissioning runs will be presented together with an overview of the instruments that will become available in the next few years.

TP (10:30 am – 12:15 pm)

### Poster session (St. Charles Ballroom)

TP01

**SANS method study mixture system of surfactant solutions: C14E7+CTACl without and with add of salt**  
A. G. Rajewska (Institute of Atomic Energy, 05-400 Swierk-Otwock, Poland)

Aqueous mixtures of oppositely charged or non-ionic/ionic surfactants exhibit interesting phase behaviour and properties. The mixing of amphiphiles in water may lead to the formation of mixed micelles which often present new properties with respect to the pure component solutions [1, 2]. The mixture system of classic non-ionic surfactant C14E7 (heptaethylene glycol monotetradecyl ether) and cationic CTACl (cetyltrimethyl ammonium chloride) in heavy water solutions for concentrations: 0.25g/l, 0.5g/l, 1g/l, 2g/l, 3g/l, 5g/l, 7g/l, 10g/l, 15g/l without and with add of salt KCl were investigated at temperature 25°C on the time-of-flight small-angle neutron scattering (TOF SANS) spectrometer ("YuMO") of the IBR-2 on pulsed neutron source [3] at FLNP, JINR in Dubna (Russia). Measurements have covered Q range from  $8 \times 10^{-3}$  to  $0.4 \text{ \AA}^{-1}$ .

[1] McDonald J. A., Rennie A. R., *Langmuir*, **11** (1995) 1493  
Garamus V. M., *Langmuir*, **13** (1997) 6388 Rosen Milton et al.,  
*J. Colloid. Interface Sci.*, **110** (1986) 224

[2] Bulavin L.A. et al., *Colloids and Surfaces*, **131** (1998) 137  
Pils H., et al., *J. Phys. Chem.*, **97** (1993) 2745 Hassan P.A.,  
Bhagwat S.S., Manohar C., **11** (1995) 470

[3] Kuklin A. I. et al., *Neutron News*, **16**, no3 (2005) 16-18

TP02

### LANSCE Single Crystal Diffractometer (SCD): Present Status and Future Goals

A. I. Acatrinei, L. L. Daemen, M. A. Hartl (Los Alamos National Laboratory), D. Mikkelsen, R. Mikkelsen (University of Wisconsin-Stout), L. Falvello (Universidad de Zaragoza, Spain), L. J. Banuelos, J. Urquidi (New Mexico State University)

The Single Crystal Diffractometer (SCD) at LANSCE, Los Alamos National Laboratory, represents a powerful tool for many crystallographic and magnetic structure determinations. The instrument is located at the Manuel Lujan, Jr. Neutron Scattering Center and utilizes the time-of-flight (TOF) Laue technique for neutron scattering data collection. This technique, combined with a 25 cm × 25 cm multi-wire <sup>3</sup>He position-sensitive detector and the possibility of two axis



of rotation for sample orientation provides up to 80% hemisphere coverage in reciprocal space. The redesign and status of the Single Crystal Diffractometer at LANSCE are reported. The Integrated Spectral Analysis Workbench software (ISAW) is used to read data from (NeXus) data files, and then to reduce and analyze the data. Instrument control and automation programs are written in Perl and LabVIEW. We give an overview of the instrument characteristics and of the calibration and data evaluation activities (higher intensity, lower background, better profile shape, improved resolution). The applications to date are many (single crystal and texture analysis, incommensurate structures, magnetic scattering, hydrogen bonding, diffuse scattering, temperature/pressure dependent measurements) and we will present several examples illustrating the performance of the instrument.

#### TP03

### Development of the South African Small Angle Neutron Scattering Facility

T. Tjebane, C. B. Franklyn (South African Nuclear Energy Corporation)

As part of an IAEA sponsored initiative, the SAFARI-1 research reactor based at the Necsa near Pretoria, South Africa, has re-established a small angle neutron scattering (SANS) capability using a radial beam port. Construction of this facility has been undertaken in two phases. Phase I of the facility development consists of a beam line with three main elements; 1) a cooled Be filter, 2) a MEET neutron velocity filter for selecting sub-thermal neutrons between 3 and 10 Angstroms, 3) a bank of one-dimensional position-sensitive neutron detectors (60 cm. active length) stacked in a short 5m vacuum chamber. This facility is already producing a huge scope for training and development of the South African scientific community in the use of SANS as analytical tool in selected applications, namely nanosciences and polymer science. Aspects of the present facility including the measured energy spectrum, background characteristics and first results of SANS measurements performed, will be presented. Details of the expected enhancements in resolution and sensitivity of the facility after implementation of Phase II - installation of a curved neutron guide and large scattering chamber (10 metres), will also be presented.

#### TP04

### Investigation of modulated structures in g-brass systems using PDF from neutron diffraction

D. Gout, T. Proffen, O. Gourdon (Los Alamos Neutron Science Center, Los Alamos National Laboratory)

The real-space atomic pair distribution function ( $G(r)$ ; PDF) complements conventional crystal structure analysis since it takes into account non-crystallographic features of solids as intrinsic atomic disorders or aperiodic order. Recently, PDF successfully gave structural information on quasicrystal in Mg-Zn-RE (RE = Ho, Y) icosahedral systems [1]. Thus, PDF has allowed a new approach on aperiodic structures, which were exclusively treated by the way of high-dimensional unit cells (4, 5 or 6 dimensions). The recent investigation of the g-brass structure in the Zn-Pd system revealed a new way to further understand the structure relationships between intergrowth compounds and quasicrystals (two of three classes of aperiodic structures known) [2,3]. Based on this major discovery we pursued the study of other g-brass systems such as Cu-Zn and Ga-Zn systems using neutron powder diffraction. Indeed, since the scattering factors for Cu, Ga and Zn may not permit to discern these atoms by X-ray powder diffraction (just one electron apart), neutron powder diffraction was more suitable. Time-of-flight (TOF) neutron diffraction data were collected at various temperatures on the high resolution Neutron Powder Diffractometer (NPDF) [4] at the Manuel Lujan Neutron Scattering Center of Los Alamos National Laboratory. The PDF analyses of these data show that this technique is not only adapted to understand and refine quasicrystal structures but also to determine the modulated waves at the origin of these intergrowth compounds.

[1] *PDF from X-Ray powder diffraction for nanometer-scale atomic structure analysis of quasicrystalline alloys.* Bruhne S., Uhrig E., Luther K.-D., Assmus W., Brunelli M., Masadeh A. S. and Billinge S. J. L. *Z. Kristallogr.* (2005), **220**, 962-967.

[2]  $Zn_{1-x}Pd_x$  ( $x=0.14$  to  $0.24$ ): A missing link between intergrowth compounds and quasicrystal approximants. Gourdon O. and Miller G. J. (2006) *Philos. Mag.* **86** (3-5), 419-425.

[3] *Intergrowth Compounds in the Zn-rich Zn-Pd System: Towards 1D Quasicrystal Approximants.* Gourdon O. and Miller G. J. (2006) *Chem. Mat.* In Press.

[4] Th. Proffen, T. Egami, S.J.L. Billinge, A.K. Cheetham, D. Louca and J.B. Parise, *Appl. Phys. A* **74**, S163-S165 (2002).

TPO5

### Neutron holography

V. K. Ignatovich (Joint Institute for Nuclear Research), R. Gahler (Institut Laue-Langevin, France), R. Golub (North Carolina State University)

Precession of polarization of moving neutrons and periodic change of the neutron intensity can be considered as wave phenomena. We show how to use them to get a holographic image of structure of nontransparent magnetic and nonmagnetic objects.

TPO6

### Optimization of Magnetic Polarization and Guide Field Assemblies

B. L. Winn (Brookhaven National Laboratory)

The magnetic polarization and guide field assemblies for a neutron triple axis spectrometer are modeled using the 3D magnetostatics computation software Radia, to determine the field distribution in the neutron path. The development of the thermal neutron (20 meV) precession angle is traced in this field for various neutron flight paths, assuming neutron polarization is initially vertical. The design was adjusted to minimize the final angle between neutron moments and magnetic field.

TPO7

### Scientific Achievements and Technological Advances of High P-T Neutron Diffraction at LANSCE

Y. Zhao, L. Daemen, J. Zhang, D. He (Los Alamos Neutron Science Center, Los Alamos National Laboratory), K. Lokshin (University of Tennessee), J. Qian, C. Pantea, K. Tait, H. Xu, D. Williams (Los Alamos Neutron Science Center, Los Alamos National Laboratory)

We have successfully conducted high P-T neutron diffraction experiments at LANSCE. To date, we have achieved pressures up to 30 GPa, and simultaneous high pressure and temperature of 10 GPa and 1800 K. With an average 3-6 hours of data collection, the diffraction data are of sufficiently high quality for the determination of structural and thermal parameters. We have studied the hydrous mineral  $\text{Mg}(\text{OD})_2$ , perovskite  $(\text{K},\text{Na})\text{MgF}_3$ , clathrate hydrates ( $\text{CH}_4$ ,  $\text{CO}_2$ , and  $\text{H}_2$ ), metals (Mo, Al, Zr), and amorphous materials (carbon black, BMG). Our research aims at accurately determining crystal structure, local atomic environment, and phase stability in P-T-X space. High-pressure neutron diffraction is a multidisciplinary endeavor and we welcome researchers from all fields of science to come use and develop this advanced technique.

Several high pressure devices are available for neutron diffraction at high pressure. We have developed a 500-ton toroidal press, TAP-98, to conduct simultaneous high P-T (10 GPa, 1800 K) neutron diffraction experiments with HIPPO (High-Pressure and Preferred-Orientation diffractometer). Hydrostatic pressure cells made of Al-7075 allow users to perform experiments at high pressures (up to 200 MPa) and low temperatures (down to 20 K). We have also developed a large gem-crystal anvil cell -the ZAP cell- to conduct neutron diffraction experiments at high-P and low-T. The ZAP cell can be used for integrated experimental techniques of neutron diffraction, laser spectroscopy, and ultrasonic interferometry. Pressures up to 10 GPa are attainable. We are pursuing further developments of high P-T technology with a new 2000-ton press, TAPLUS-2000, and a cubic anvil package to reach a pressure of 20 GPa and temperature of 2000 K. The new design of a dedicated high pressure neutron beamline, LAPTRON, is also underway for simultaneous high P-T neutron diffraction, radiography, and tomography. We seek strong community support for this new development.

TPO8

### The U.S.-Japan Cold Neutron Triple-Axis Spectrometer at the High Flux Isotope Reactor Cold Guide Hall

B. L. Winn, S. M. Shapiro, J. Tranquada (Brookhaven National Laboratory), K. Hirota, N. Aso, H. Yoshizawa (University of Tokyo, Japan), S. Nagler, L. Robertson, S. Moore, R. Maples (Oak Ridge National Laboratory)

The U.S.-Japan Cold Neutron Triple-Axis Spectrometer will be an important component of Oak Ridge National Laboratory's High Flux Isotope Reactor (HFIR) User Program, the U.S.-Japan Cooperative Research Program on Neutron Scattering, and Brookhaven National Laboratory's Neutron Scattering Group. This spectrometer is finding new life at HFIR's new Cold Guide Hall. In addition to describing the expected performance and anticipated scientific impact, we present the current status of this relocation, especially recent progress on the new monochromator shield.

## TP09

**Neutron Powder Diffraction Study of  $\text{MmFe}_{4-x}\text{Co}_x\text{Sb}_{12}$  Thermoelectric Materials**

C. J. Rawn (Oak Ridge National Laboratory), J. Yang (Materials and Processes Laboratory, GM R&D Center, Warren, MI 48090 USA), H. Wang (Oak Ridge National Laboratory), B. L. Pedersen (Department of Chemistry, Aarhus University, Aarhus, Denmark), B. C. Chakoumakos (Oak Ridge National Laboratory), J. K. Stalick (NIST Center for Neutron Research)

Filled skutterudites,  $\text{A}_{1-x}\text{M}_4\text{Pn}_{12}$ , where A can be a lanthanide, actinide, alkaline earth, alkali, or thallium atom, M is a Group VIII transition metal, and Pn a pnictogen, are of interest due to their high electrical conductivity, relatively high Seebeck coefficient, and low thermal conductivity making them viable components for use in thermoelectric devices. By using a misch metal (Mm) that is an alloy of Ce, La, Nd, and Pr, the materials costs are greatly reduced, while not compromising the physical properties. Neutron powder diffraction has been used to study  $\text{MmFe}_4\text{Sb}_{12}$  and  $\text{MmFe}_{3.5}\text{Co}_{0.5}\text{Sb}_{12}$  in the temperature range from 10 to 300 K. The data have been analyzed using the Rietveld method and refined structural parameters including the unit cell length, atomic displacement parameters, and positional parameter for the Sb have been determined. These parameters are compared with those reported for other filled skutterudites to further elucidate the relationships between the atomic structure and the physical properties key to optimizing thermoelectric performance. At 300 K the refined lattice parameter for the composition with Co is  $a = 9.1294(2)$  Å and the refined lattice parameter for the composition without Co is  $a = 9.1436(2)$  Å. For both compositions the atomic displacement parameter of the Mm site showed more positional disorder than for the Sb and Fe or Fe/Co sites.

*This research was supported by the Assistant Secretary for Energy Efficiency and Renewable Energy, Office of Transportation Technologies as part of the High Temperature Materials Laboratory User Program and by the Waste Heat Recovery Program via a GM and DOE corporate agreement DE-FC26-04NT42278 at Oak Ridge National Laboratory managed by the UT-Battelle LLC, for the Department of Energy under contract DE-AC05000OR22725.*

## TP10

**ARCS in Motion: a status report on the wide Angular-Range Chopper Spectrometer at the SNS**

D. L. Abernathy, M. J. Loguillo, K. M. Shaw (Spallation Neutron Source, Oak Ridge National Laboratory), B. Fultz (California Institute of Technology)

ARCS, a wide Angular-Range Chopper Spectrometer, is under construction on beamline 18 at the Spallation Neutron Source. ARCS is optimized to provide a high neutron flux at the sample and a large solid angle of detector coverage. The spectrometer will be capable of selecting from the full energy spectrum of neutrons provided by an ambient water moderator, making it useful for studies of excitations from a few meV to several hundred meV. An elliptically-shaped supermirror guide in the incident flight path will boost the performance at the lower end of this range. The sample and detector vacuum chambers provide a window-free final flightpath, and incorporate a large gate valve to allow rapid sample changeout. A new T-zero neutron chopper is being developed to block not only the prompt radiation from the source, but also eliminate unwanted neutrons from the incident beamline. The instrument layout accommodates a user control cabin, sample storage and setup areas, with special access for large sample equipment. Installation of major components is well underway, and ARCS is on-track for commissioning in 2007.

## TP11

**Load-frame and high temperature furnaces for in-situ neutron scattering at VULCAN**

S. Cheng, J. J. wall, P. K. Liaw, H. Choo (University of Tennessee), X. L. Wang (Spallation Neutron Source, Oak Ridge National Laboratory), C. R. Hubbard (Oak Ridge National Laboratory), H. Li, C. Xu (University of Tennessee), G. Q. Rennich (Spallation Neutron Source, Oak Ridge National Laboratory)

A state-of-art servohydraulic mechanical testing facility (load-frame) with high temperature furnace attachment will be built as a part of the sample environment suite for the VULCAN diffractometer at Spallation Neutron Source (SNS), Oak Ridge National Laboratory. Specification for the load-frame and furnaces are currently in final review. The load-frame will aim to run both standard-size samples and miniature samples, with a maximum load capacity of approximately 100 kN. The load-frame will have the capability of conducting in-situ

uni-axial tensile/compressive tests and high/low frequency cyclic loading both at ambient and elevated temperatures up to 1,500°C. Vacuum/inert gas/air furnaces will be designed to meet a variety of thermal and environmental studies. In addition to improve control of the gauge volume contributing to diffraction, this load frame will automatically keep the sample centered during testing. Data acquisition for stress/strain/temperature will be interfaced with diffraction data. A state-of-the-art and user-friendly software for the control and analysis will be implemented. A full function of this testing system is expected by the mid of year 2008.

*The authors are very grateful to the National Science Foundation Major Research Instrumentation (MRI) Program (DMR-0421219) for the financial support with Dr. C. Bouldin as the Program Director.*

#### TP12

### Phase Transitions in the Organic-Inorganic Perovskites

I. P. Swainson (National Research Council Canada)

The organic-inorganic perovskites are perovskites in which the A-cations are molecular cations, typically amines. Very short-chained amines can be encapsulated into a true  $ABX_3$  perovskite framework structure: these include the monoamine methylammonium and the diamine formamidinium, as well as tetramethylammonium. The  $BX_3$  anions are often halides of e.g.,  $Pb^{2+}$ ,  $Sn^{2+}$ ,  $Ge^{2+}$ . Longer-chained cations cannot be accommodated in this 3d-framework and often crystallize in the layer perovskite structure  $A_2BX_4$ . The inorganic octahedra undergo transitions that are related to classical tilt transitions as well as to stereochemical activity of the outer shell  $s^2$ -lone pair of  $Sn^{2+}$ ,  $Ge^{2+}$  and  $Pb^{2+}$  ions. These changes in the inorganic component are coupled to order-disorder phenomena of the A-cations. On cooling, neutron and synchrotron diffraction show there is a remarkable variation of structures with composition. These structures are typically superlattices of tilt modes, associated with lone pair activity and orientational ordering of the cations. The competition between order parameters associated with the octahedra and with the amines often leads to incommensurate structures. Examination of the many modulated structures of the famous propylammonium (PA) tetrachlorometallates  $PA_2BCl_4$  show that all correspond to rigid unit buckling instabilities of the layers. However, the incommensurate

structures of the  $ABX_3$ -types all require distortion of the octahedra. This is due to (i) greater degrees of constraint in the  $ABX_3$  structure-type and (ii) the fact that the organic cations are more rigid than the octahedra. DFT-calculations of the effect of hydrogen-bonding on lone pair distortions in  $Sn^{2+}$  salts, and the on the effects of pressure will be reported in comparison to diffraction measurements.

#### TP13

### The use of ISAW on the SCD at the Lujan Neutron Scattering Center

J. Urquidi (New Mexico State University), D. Mikkelsen, R. Mikkelsen (University of Wisconsin-Stout), L. R. Falvello (Universidad de Zaragoza, Spain), A. I. Acatreñi (Los Alamos National Laboratory)

The integrated spectral analysis workbench (ISAW) project was begun through the collaboration of the Intense Pulsed Neutron Source (IPNS) at Argonne National Labs and Dennis and Ruth Mikkelsen of the University of Wisconsin Stout in an effort to create an effective platform for the visualization and reduction of neutron data. The use of JAVA makes ISAW portable and platform independent. It has been adopted and is in current use on several instruments at the IPNS. Amongst these are the Single Crystal Diffractometer (SCD) and, most recently, the Glass, Liquid, and Amorphous Diffractometer (GLAD). At the Lujan Neutron Scattering Center at Los Alamos National Labs the SCD has recently been refurbished and brought on-line. The software procedures for data reduction and visualization make extensive use of ISAW. A discussion of recent measurements, how ISAW is employed on the SCD at the Lujan Neutron Scattering Center and how it compares with the procedures used at the IPNS will be presented. Also, an update on the use of ISAW in the reduction and visualization of amorphous materials on the High Pressure, Preferred Orientation (HIPPO) Diffractometer at the Lujan Neutron Scattering Center will be given.



TP14

### The effect of Hoffmeister Salts on the Structure of Water

J. Urquidi (New Mexico State University), J. Neufeind (Spallation Neutron Source, Oak Ridge National Laboratory), C. J. Benmore (Intense Pulsed Neutron Source), J. L. Banuelos (New Mexico State University)

The effect of specific ions on the solubility of proteins was first reported by Franz Hofmeister over a century ago. Since then, many properties of aqueous systems have been found to follow the same ranking of ions in solution. The series today is catalogued so as to measure whether a specific ion binds water strongly (structure breaking) or whether it binds water weakly (structure making). While anions hydrate more strongly than cations of similar ionic radius due to the closer approach of the hydrogen atoms it is generally believed that Hofmeister ions induce their influence by affecting the hydrogen bonding in water. This is of considerable interest as different structure breaking anions tend to stabilize macromolecular structures. The current work introduces a series of structure breaking and structure making ions into aqueous solution and measures their effects on the local water structure. The measurements employ the use of null-scattering water to study the changes in the O-O correlation function with changes in ion and ion concentration.

TP15

### Neutron and X-ray Reflectivity Studies of Enhanced DNA Adsorption by DC-Cholesterol Monolayer with Ions

T. Lin, J. Wu (National Tsing Hua University, Hsinchu, Taiwan), U. Jeng, H. Lee (National Synchrotron Radiation Research Center, Hsinchu, Taiwan), N. Torikai (High Energy Accelerator Research Organization), T. Gutberlet (Paul Scherrer Institute)

We conducted in-situ neutron reflectivity measurements of DNA adsorption by the DC-Cholesterol monolayer at the air-liquid interface and X-ray reflectivity measurements on the LB films prepared on silicon wafers to investigate the effects of cations on the DNA adsorption. Anionic DNA can bind electrostatically with cationic lipids to form a complex and it is widely used in gene delivery researches. It was found that divalent ions could condense DNA molecules confined to two-dimensional cationic surfaces such as in cationic liposomes. It is less known

about the effects of divalent ions on the DNA adsorption by cationic lipid monolayers at the air-liquid interface. In our previous studies we found that a dense DNA layer was adsorbed to the DC-Cholesterol monolayer at the air-liquid interface. In this study, using the in-situ neutron reflectivity and X-ray reflectivity, we found that the presence of divalent ions can enhance the DNA adsorption to the DC-Cholesterol monolayer. By increasing the calcium ion concentration from 0, 1, 5, 10, to 30 mM, the DC-Cholesterol/DNA LB film thickness was found to increase from 3.1, 4.4, 5.8, 6.8, to 10 nm, respectively. The increase in film thickness indicates there are more adsorbed DNA molecules. The depth profile obtained by fitting the in-situ neutron reflectivity data showed that in the presence of divalent ions there is a dense DNA layer of about 2 nm thickness formed right beneath the DC-Cholesterol monolayer and followed by a loose DNA layer. The thickness of the loose DNA layer increases with increasing calcium ion concentrations. The enhanced DNA adsorption could be attributed to the bridging effect of the divalent ions between the adjacent adsorbed DNA molecules. We also report the results of comparing conducted experiments. The existence of the well ordered and compact first adsorbed DNA layer could also be critical to the enhanced DNA adsorption. We will also report the studies of the ion size effect on the enhanced DNA adsorption.

TP16

### Conformational Changes in Guanylate Kinase Studied by Osmotic Stress and SANS

C. Stanley, S. Krueger (NIST Center for Neutron Research), V. A. Parsegian, D. C. Rau (National Institutes of Health)

Protein conformational changes induced by ligand binding are accompanied by a change in the number of water molecules sequestered in pockets, cavities, and grooves. The significance of hydration to protein-ligand interactions has been illustrated using the osmotic stress technique. We are using small-angle neutron scattering (SANS) coupled with the osmotic stress technique to directly probe the connection between protein structural change and thermodynamics for guanylate kinase. We chose this enzyme because it is known to undergo large conformational changes upon GMP and ATP ligand binding. We are able to follow this conformational change using SANS to determine the radius of gyration,  $R_g$ , and the pair-distribution



function,  $P(R)$ , and now we are investigating protein mechanics by using osmotic stress to induce the conformational change in the absence of ligand. This should offer new opportunities for protein structure research by allowing the energetics of the conformational change to be measured apart from the ligand binding energy.

TP17

**The 40m and 35m Small-angle Neutron Scattering Instruments at Oak Ridge National Laboratory**

G. D. Wignall, W. T. Heller, G. W. Lynn, D. A. Myles (Oak Ridge National Laboratory), L. J. Magid (University of Tennessee), Y. B. Melnichenko, V. S. Urban (Oak Ridge National Laboratory)

A series of upgrades have been undertaken at the High Flux Isotope Reactor (HFIR), including the installation of a supercritical hydrogen moderator ( $T \sim 20^\circ\text{K}$ ), which feeds four cold neutron guides with new instrumentation, funded by the Office of Basic Energy Sciences, including a 40m small angle neutron scattering (SANS) facility whose construction is partially funded by the University of Tennessee, Knoxville. In addition, a 35m SANS instrument is being funded by the Office of Biological and Environmental Research, and is optimized for the study of biological systems as part of the Center for Structural Molecular Biology. Both SANS facilities utilize mechanical velocity selectors, pinhole collimation and high count-rate ( $> 10^5$  Hz), large-area ( $1\text{m}^2$ ) two-dimensional position-sensitive detectors. The incident wavelength ( $\lambda$ ), resolution ( $\Delta\lambda/\lambda$ ), incident collimation and sample-detector distance are independently variable under computer control. The detectors can translate 45cm off axis to increase the overall Q-range ( $< 0.001 < Q = 4\pi\lambda^{-1}\sin\theta < 1 \text{ \AA}^{-1}$ ), where  $2\theta$  is the angle of scatter. As the HFIR is one of only two reactors with a core flux  $> 10^{15}$  neutrons/sec/cm<sup>2</sup>, the beam intensities (up to  $10^7$ /sec/cm<sup>2</sup>) are comparable to the best facilities worldwide and were designed to expedite data collection from biological macromolecules, to study smaller sample quantities and to permit kinetic (time-resolved) experiments.

*Supported by the U.S. Department of Energy under contract DE-AC05-00OR22725 with the Oak Ridge National Laboratory, managed by UT-Battelle, LLC.*

TP18

**Density profiles of “looped” polymer brushes at the liquid-solid interfaces by neutron reflectivity measurements**

Z. Huang (University of Tennessee), J. Alonzo (Clemson University), M. Lay, M. Liu, H. Ji (University of Tennessee), Y. Zhang (University of Utah), J. W. Mays (University of Tennessee), G. Smith (University of Utah), S. M. Kilbey (Clemson University), M. D. Dadmun (University of Tennessee)

Preferential assembly of poly(2-vinyl pyridine)-d-polystyrene-poly(2-vinyl pyridine) (P2VP-dPS-P2VP) triblock copolymers from toluene, which is a selective solvent for polystyrene, on silicon leads to the formation of the dPS loops tethered by the P2VP end blocks. We have measured, using neutron reflectometry, the segment density profiles of these “looped” brushes in toluene, a good solvent for dPS block, and in cyclohexane at  $20^\circ\text{C}$  (poor solvent),  $32^\circ\text{C}$ , (near-theta solvent), and  $50^\circ\text{C}$  (marginal solvent). Some unusual features were revealed by the density profiles obtained while the swelling behavior still qualitatively agrees with what was observed for singly-grafted brushes. In good solvent, the density profiles were composed of a parabolic part and a long extended tail. In cyclohexane with various qualities, we observed an exponential decay behavior. It was also found that the change of degree of swelling with solvent quality can be correlated with the surface density of chains.

TP19

**Polyaromatic Fuel Cell Membranes, Morphology Characterization and Performance Evaluation**

M. Yoonessi, M. F. Durstock, R. A. Vaia (Air Force Research Laboratory)

While polymer electrolyte fuel cells have shown promising potential as a pollution-free energy source and an alternative for oil-based fuels, they have operational limitations at elevated temperatures. Membrane is a vital component of a fuel cell which separates hydrogen and oxygen while providing a path for proton transport. In order to develop high performance membranes for operation at elevated temperatures ( $>120^\circ\text{C}$ ), highly sulfonated endcapped polyarylenethioethersulfone polymers were synthesized. These polymers show excellent thermal ( $T_g \sim 200^\circ\text{C}$ ) and mechanical properties (up to three times higher than Nafion).

They form tough films while maintaining a high degree of flexibility. Highly sulfonated endcapped polyarylenethioethersulfone copolymers (SPTES 80, SPTES 70, SPTES 60, SPTES 50) have shown superior proton conductivity compared to Nafion. The activation energies of the SPTES copolymers indicate a different hydronium ion transport mechanism (vehicular hydronium ion transport and structural diffusion) compared to Nafion or different contribution of the two mechanisms in the SPTES copolymers. SPTES 50 membrane electrode assemblies (MEA) have shown comparable performance with Nafion and improved performance at elevated temperatures. Small angle neutron scattering studies have shown the presence of nanoscale water domains (nanoclusters) on the order of 4-5nm. It was found that the presence of ionic aggregates is an interfacially driven phenomenon. The sharp interfaces between the water domains and polymer medium were quantified in terms of surface to volume ratio, number of sulfonic groups per aggregate and area per polar head. The scattering data were fitted to a scattering model from which information about the domain sizes were obtained. The size of ionic aggregates strongly depends on the type and the size of the exchanged counterion. HR-TEM revealed the presence of nanometer domains when the sulfonic sites were exchanged with silver. Extensive scanning electron microscopy examinations were performed on the cryofractured swollen membranes, cryofractured dry membranes and Ag exchanged membranes. A series of AFM studies showed a change in the surface features with a change in the relative humidity.

TP20

### **Neutron Powder Diffraction of radioactive irradiated low enrichment Uranium-Molybdenum nuclear reactor fuel**

I. P. Swainson (National Research Council Canada), K. T. Conlon (Atomic Energy of Canada Ltd.), L. M. Cranswick, R. L. Donabarger, J. Fox, L. McEwan, R. Rogge (National Research Council Canada), D. Sears (Atomic Energy of Canada Ltd.), D. Sediako, T. Whan (National Research Council Canada)

Chalk River staff have significant experience at performing measurements on radioactive samples. Some samples only require shielded transport, proper handling procedures, remote instrument control, and appropriate barriers to reduce risk to levels that duly respect the As Low As Reasonably

Achievable, ALARA, principle. For other, more active samples, ALARA also requires sufficient sample shielding during the diffraction experiment. We have previously reported<sup>(1)</sup> on a shielded cell that permitted examination on samples with calculated activities as high as 20,000 REM/hr (200 Sievert/hr) on contact. Recently, a new shielded-cell was constructed at Chalk River, to examine irradiated Uranium-Molybdenum fuel samples (20% burnup) with on-contact activities of 60 to 80 REM/hr (0.6 to 0.8 Sievert/hr) by constant wavelength neutron powder diffraction. The primary aim was to determine the structure and composition of reaction products in the fuel core. This is part of an international initiative to help develop low-enriched fuel for research-reactor applications. There has been limited published work on the crystallography of irradiated nuclear fuels because of the challenges associated with safely handling radioactive materials. Work reported in the literature is primarily on Uranium Silicide fuels<sup>(2,3)</sup>. However, to accurately determine what is occurring to the fuel in the reactor, post-irradiation studies on the spent fuel can be more appropriate than studies on non-irradiated fuel. While this is a high-risk diffraction experiment, high-risk does not mean unsafe<sup>(4,5,6)</sup>. High-risk means that, compared to the consequences of success, the consequences of being unsafe are very severe<sup>(7,8,9)</sup>. Thus decisions must err on the side of being safety-conservative to the point that if anything feels unsafe, the procedure must stop until safety can be assured. The main emphasis of the presentation is to describe the experimental hardware, and elaborate on the methods to ensure a safe, unrushed procedure. As well as a written procedure developed for the experiment, and the use of multiple dummy-runs to test the procedure in advance, an easy and effective passive safe-stand-down procedure (by the use of Do-Not-Operate tags placed on the initially unloaded shielded cell) was also included. If any experimentalist or technician feels the experiment is becoming unsafe in any form during the setup, the experiment can be immediately halted in a safe condition. Preliminary diffraction patterns taken at 1.33010Å and 2.37115Å (20 to 100° 2-theta) will be shown with some initial analysis. The ability to routinely perform neutron diffraction on very active materials not only benefits crystallographic analysis of spent reactor fuel, but has potential applications such as the

study of stored radioactive waste and studies of other in-core materials.

- [1] K.T. Conlon, D. Dye, R.B. Rogge and J.H. Root, "Application of Neutron Diffraction in Materials Science and Engineering", *Neutron News*, (2003) **14** (4), pp. 14-19.
- [2] J.W. Richardson, R.C. Birtcher and S-K. Chan, "Neutron Irradiation Induced Amorphization of Uranium Silicides", *Physica B*, vol. **241-243** (1998), pp. 390-92.
- [3] J.W. Richardson, R.C. Birtcher and M.H. Mueller, "Neutron Diffraction Study of Highly Radioactive U<sub>3</sub>Si<sub>2</sub> Reactor Fuel", in: *Microstructure of Irradiated Materials* (I.M. Robertson et al. eds.) *MRS Symposium Proceedings*, v. **373** (1995), p. 233-36.
- [4] T.R. Laporte, G.I. Rochlin, and K.H. Roberts. "The Self-Designing High-Reliability Organization: Aircraft Carrier Flight Operations at Sea", *Naval War College Review*, Autumn 1987:76-90; repr. Summer 1998:97-113
- [5] "High Reliability Theory", *The Columbia Accident Investigation Board (CAIB) Report Volume I, Chapter 7, sections 7.2 to 7.3*, August 2003, pp180-184, <http://caib.nasa.gov/>
- [6] "NASA/Navy Benchmarking Exchange (NNBE)", NNBE Benchmarking Team, NASA Office of Safety & Mission Assurance, NAVSEA 08 Naval Reactors and NAVSEA 07Q Submarine Safety & Quality Assurance Division, *Progress Report*, (July 15 2003).
- [7] Trevor A. Kletz, "What Went Wrong?, Fourth Edition: Case Studies of Process Plant Disasters", Gulf Professional Publishing; (1998), ISBN: 0884159205.
- [8] Trevor A. Kletz, "Still Going Wrong!, First Edition: Case Histories of Process Plant Disasters and How They Could Have Been Avoided", (2003), Gulf Professional Publishing, ISBN: 0750677090
- [9] Trevor A. Kletz, "Lessons from Disaster - How Organisations have No Memory and Accidents Recur", (1993), IChem, ISBN: 0852953070.

#### TP21

### **VULCAN – The Engineering Diffractometer at the SNS**

X. Wang (Spallation Neutron Source, Oak Ridge National Laboratory), T. M. Holden (Northern Stress Technology, Canada), A. D. Stoica, G. Q. Rennich (Spallation Neutron Source, Oak Ridge National Laboratory), P. K. Liaw, H. Choo (University of Tennessee), C. R. Hubbard (Oak Ridge National Laboratory)

The VULCAN diffractometer at the SNS is designed for materials science and engineering studies. Examples include high-speed and high-resolution spatial mapping of residual stress distribution in components, deformation behaviors under static and cyclic loading over a wide range of temperatures, and time-dependent phase transformation phenomena. The instrument was first conceptualized in June 2000. The optics design features a focusing neutron guide system, wide-angular detector coverage, and a small-angle area detector. By employing an interchangeable neutron guide-collimator system, the instrument can be optimally configured for individual experiments. In the high-resolution mode, the instrument

resolution is 0.2%, with an incident beam flux of  $2.5 \times 10^7$  n/cm<sup>2</sup>/s (over a bandwidth of 1.3 Å). In the high-intensity mode, the incident beam flux reaches  $1.5 \times 10^8$  n/cm<sup>2</sup>/s while the resolution remains better than 0.6%. With such a high flux, the count rate in detector is estimated to reach a few thousand counts per pulse. Experiments have been carried out to validate the design concepts developed for VULCAN. It was shown, for example, that the wide-angular detector coverage greatly facilitated the determination of the grain-orientation-dependent intergranular stress due to cyclic loading. *In-situ*, simultaneous measurements of diffraction and small angle scattering data was essential for elucidating the multi-length scale nature of nanocrystallization in bulk metallic glass. To be ready for exploiting the high-flux that will be realized with VULCAN, tests are also underway to measure the dynamic response during a welding transient. The construction of VULCAN is supported by the Canada Foundation for Innovation.

*In addition, the US National Science Foundation funded the sample environment suite for VULCAN, which includes load-frames, furnaces, and electro-chemical cells. The US Department of Energy, Office of Energy Efficiency and Renewable Energy, provides additional funding for completing the instrument. VULCAN is on schedule to be commissioned in the spring of 2008.*

#### TP22

### **A DVD on Basic Neutron Activation and Radioactive Decay Experiments for High Schools and Introductory Physics Courses**

S. C. Sahyun (University of Wisconsin-Whitewater)

Due to the increasing difficulty and cost of obtaining, storing, and using radioactive material at the high school and introductory level, this video was created to provide demonstrations and substitute laboratory experiences that would be otherwise unavailable to teachers and instructors. This poster will showcase an instructional DVD video that contains an introduction to the neutron activation process, video clips of a source, the neutron activation of five different materials, and video of the recording of the decay data collection for those materials. The DVD also contains a table of data from the experiments and suggested exercises so that students can analyze the data to determine the half-lives of the elements displayed in the video.

## TP23

**Controlled Atmospheres at High Temperatures for Neutron Scattering Experiments**

K. J. Volin, E. R. Maxey (Intense Pulsed Neutron Source, Argonne National Laboratory)

Increased scientific and engineering interest in the characterization of materials in extreme environments has led to the development of high temperature, controlled atmosphere sample environments for neutron scattering experiments. In the case of high temperature studies, furnaces operating up to  $\sim 2000^\circ\text{C}$  are widely used at neutron scattering facilities. However, they are predominately used in a vacuum environment for diffraction experiments. Consequently, high-temperature properties, particularly atomic dynamics of ceramics under ambient or oxidizing atmospheres, cannot be properly characterized. In-situ investigations of chemical reactions, corrosive behavior or densification processes further demand accurate control and monitoring of molecular streams or application of pressure in conjunction with very high temperature. Sample environment equipment at the Intense Pulsed Neutron Source (IPNS) has matured to meet these needs. The structure of materials can be studied in a controlled oxidizing, reducing, or inert atmosphere, or under vacuum at temperatures up to  $1450^\circ\text{C}$ . Using the Experimental Physics and Industrial Control System (EPICS) to monitor and control both the temperature and atmosphere through a graphical user interface (GUI) helps tie the sample environment control to the execution of a particular experiment data set.

## TP24

**Inelastic Neutron Scattering and Periodic DFT Studies of Aromatic Hydrocarbons: Structure Determinations beyond Diffraction**

N. Verdal, D. G. Allis, S. Rivera (Syracuse University), P. M. Kozlowski (University of Louisville), B. S. Hudson (Syracuse University)

The standard method for determination of molecular structure is x-ray or neutron diffraction. There are limits to the level of detail of structure that can be obtained by analysis of diffraction data. An example that is relevant to the present work is the case discussed by Burgi and co-workers [Chemistry-A European Journal 8 (15): 3512-352, 2002] in which the issue of whether or not benzene has 6-fold symmetry on the basis of its diffraction pattern. This is certainly true for the average

position of the atoms but a 3-fold symmetric structure with bond alternation in a disordered crystal would give rise to the same diffraction pattern. Here we discuss an approach to such subtle problems based on the determination of the INS spectrum of several aromatic hydrocarbons that might exhibit bond alternation due to electronic structure effects or that might exhibit deformations in the crystal due to intermolecular forces. The emphasis is on the molecular structure as reflected in its vibrational spectrum rather than in the analysis of diffraction data. The approach is to compute the INS spectra using two or more different methods that differ in their description of the extent of bond alternation and then compare the results with the INS experiments. The underlying argument is that vibrational spectra are very sensitive to small changes in structure and are not influenced by crystal disorder. This method is here applied to the cases of azulene, corannulene, triphenylene and biphenylene.

## TP25

**Molecular Structures in Solids without Diffraction: INS as a method for conformational analysis**

N. Verdal, B. S. Hudson (Syracuse University)

The internal vibrations of a molecule are sensitive to the molecular conformation. Thus, measurement of a vibrational spectrum and comparison of the experimental result with the predictions of reliable calculations for several possible conformations of the isolated molecule can be used to determine which conformation exists in its crystalline state. INS spectroscopy is the preferred spectroscopic method in this case since the spectral intensities are easily computed. In a study of the cycloalkanes [J. Phys. Chem. A (2006), 110(8), 2639-2646.] it was shown that in those cases where the molecular structure is known from diffraction studies, this method was able to determine the correct structure and eliminate alternative conformations with reasonable statistical confidence. New conformational determinations are obtained for those cases where molecular structure determination on the basis of analysis of diffraction data has not proven possible. In the present study this method is applied to cases of cycloalkenes, cyclic ethers, biphenyl and cis- and trans-stilbene. This method may prove to be useful in the analysis of powder diffraction data especially for molecules that have multiple single bond rotations.



TP26

### **The Spallation Neutron Source Extended Q-range Small Angle Neutron Scattering Diffractometer**

H. Z. Bilheux, J. K. Zhao, P. R. Summers, S. M. Rodgers, S. H. McCall (Spallation Neutron Source, Oak Ridge National Laboratory)

The construction of the Extended Q-range Small Angle Neutron Scattering (EQ-SANS) diffractometer is currently on tract to meet the SNS baseline requirement. Commissioning of the instrument is expected in 2007 and user-mode operation should start in 2008 when the Spallation Neutron Source (SNS) reaches its full power. The EQ-SANS will be a high intensity, high precision diffractometer with an unprecedented Q-range. Details of the instrument layout and specifications will be presented.

TP27

### **SALSA – SpICE à la Small Angle**

W. A. Hamilton, W. T. Heller, S. J. Kulan, B. K. Larkins, D. L. Maierhafer, M. D. Lumsden, J. L. Robertson, M. Yethiraj (Oak Ridge National Laboratory)

SpICE is a LabVIEW-based data acquisition system whose core is composed of a command line processor and a modular hardware interface layer. Commands are added to an execution stack through either a simple command line, the included graphical user interface, or from a web browser using a CGI interface. The code has a modular structure allowing for relatively easy extension to a wide range of scattering instruments. The first instruments to use this software were the triple-axis spectrometers at the High Flux Isotope Reactor (HFIR) and they have been running successfully for more than 3 years. We have recently extended SpICE, to the specific case of the two new small-angle neutron scattering instruments at HFIR. We have developed LabVIEW drivers for all the hardware components including, most notably, the ORDELA 21000N 2d position sensitive neutron detector with full timing capabilities. A graphical user interface (GUI) has been developed whose appearance can be tailored to the experience level of the experimenter where all the advanced features of SpICE such as the use of aliases, execution of macros, and full scripting via an interface with Python are available to the experienced user. The GUI incorporates a configuration builder allowing users to easily configure, save, and restore custom instrumental settings for each measurement, easy to use tools

for instrument alignment, and on-the-fly 2d and 1d data reduction and plotting including azimuthal, radial, and sector averaging.

*Work supported by the U.S. DOE, under contract DE-AC05-00OR22725, ORNL, managed and operated by UT-Battelle, LLC. We would like to acknowledge P.D. Butler for his acronymic contribution.*

TP28

### **Portable, Customizable Software for Single Crystal Neutron Scattering Data Visualization and Reduction in ISAW**

D. J. Mikkelsen, R. L. Mikkelsen (University of Wisconsin-Stout), A. J. Schultz, P. M. Piccoli (Argonne National Laboratory, Intense Pulsed Neutron Source), J. Urquidi (New Mexico State University), L. R. Falvello (Universidad de Zaragoza, Spain), T. G. Worlton, J. P. Hammonds (Argonne National Laboratory, Intense Pulsed Neutron Source)

A portable set of software tools for single crystal time-of-flight neutron scattering experiments has recently been implemented using capabilities from the Integrated Spectral Analysis Workbench, ISAW. Instrument calibration software, an interactive 3D visualization of the reciprocal lattice, and software “wizards” that step the user through the data reduction process are included. The software has been used with data from the SCD instruments at IPNS and LANSCE, and with data from the SXD at ISIS. The portability of the software is facilitated by using appropriate abstractions for detectors and sample orientations. The data reduction “wizards” are basically GUIs wrapped around scripts and can be easily customized by modifying the scripts.

TP29

### **Neutron Diffraction Studies of the Bilayer Structure of Lipopolysaccharide from *Pseudomonas aeruginosa***

T. Abraham (National Research Council Canada), S. Schooling (University of Guelph), T. Harroun, M. Nieh, J. Pencer (National Research Council Canada), T. Beveridge (University of Guelph), J. Katsaras (National Research Council Canada)

Lipopolysaccharides are the major macromolecular component of the cell envelope of Gram-negative bacteria. These macromolecular layers essentially control surface properties of these microorganisms and play crucial role in the permeability and the barrier function of the outer membrane. The elucidation of the molecular architecture and the structure of this highly complex macromolecule is of great scientific interest because of its role in the host-parasite interactions, and the



bacterial resistance to hydrophobic antibiotics and the antimicrobial peptides. We report here neutron diffraction studies performed on the lipopolysaccharide molecules isolated from *Pseudomonas aeruginosa*. In this study, we used oriented multiple bilayers of lipopolysaccharide and examined the physical state of the bilayers by neutron diffraction method. The temperature scans have been conducted at various hydration levels and the phase state and the transition temperature have been identified. We found that the phase state, the phase transition and the d-spacing are influenced by the factors such as temperature and the hydration level. In order to specifically address the issue of phase state and the permeability of LPS bilayers, the higher order Bragg peaks have been measured in gel, liquid crystalline as well as in the phase transition regime, where the gel and the liquid crystalline phases coexist. The scattering length density profiles of the lipopolysaccharide bilayers have been constructed and the structural details based on the available molecular information have been presented. The central finding here is that we have found that the water molecules penetrate into the hydrocarbon region of the lipopolysaccharide bilayers irrespective of the phase state. We have also found significant penetration of water molecules in the outer region of the lipopolysaccharide bilayers irrespective of the phase state.

TP30

### Commissioning Status of the SNS Liquids Reflectometer

J. F. Ankner, T. A. McHargue, R. J. Goyette, T. Chae, P. M. Rosenblad (Oak Ridge National Laboratory)

By the time of this conference, a liquids reflectometer will have been installed as one of the first instruments at the Spallation Neutron Source. This instrument is designed to view liquid and solid surfaces in specular, off specular, and near-surface small angle scattering geometries. The guide system supplies 2.5-16.5 Å neutrons at vertical incident angles ranging from 0- 5.5° for free liquid surfaces and up to 45° for solid surfaces. Three bandwidth choppers, synchronized with the spallation source and operating at 15, 20, 30, or 60 Hz, provide neutrons in bandwidths ranging from 3.5-14 Å at a fixed incident angle onto a sample. The sample stage enables all of the motions necessary for positioning liquid and solid surfaces, while

the detector arm allows position-sensitive or  $^3\text{He}$  detectors to view the sample at specular or off specular angles up to 90° and can scan out of the specular plane by up to 30°. We will report on our progress commissioning the liquids reflectometer, which essentially involves making the vast parameter space accessible to the instrument accessible to expert and novice users in a coherent and reliable fashion. We will also provide a date for first availability of the instrument to users, currently estimated to be at the end of this year.

TP31

### Multi-scale Microstructural Characterization of Ferritic-Martensitic Steels using Combined SANS and USANS Techniques

G. Muralidharan, M. Agamalian, R. L. Klueh, W. Ren, J. P. Shingledecker, M. L. Santella (Oak Ridge National Laboratory), M. H. Kim (NIST Center for Neutron Research)

Ferritic/martensitic steels are candidate structural materials for use at elevated temperatures in various energy systems, including the Generation IV fission reactor concepts, Ultrasupercritical (USC) boilers, heat recovery steam generators, turbines, and fuel cells. For example, steel grades such as modified 9Cr-1Mo (Grade P91), and HCM12A (Grade P122) consist of about 9 and 12% Cr, respectively, with about 0.1 wt. % C along with varying levels of Mo, V, Nb, and W. These steels are typically used in the normalized-and-tempered or quenched-and-tempered condition. In this condition, their microstructure consists of a martensitic lath structure with a relatively high density of dislocations along with  $\text{M}_{23}\text{C}_6$  precipitates (60-150 nm in size) on the lath boundaries and prior austenite grain boundaries. With the addition of V and Nb, small (20-80 nm sized) MX carbides, nitrides, or carbonitrides are also present within the matrix. MX retards recovery and stabilizes the microstructure at high temperatures by pinning dislocations and lath boundaries, thus retaining strength. In other steels such as 2.25Cr-1Mo (Grade 22) which do not contain V or Nb, the microstructure consists mainly of large  $\text{M}_{23}\text{C}_6$  and  $\text{M}_7\text{C}_3$ -type carbides and is devoid of MX carbides. There is a need to understand the precipitation and growth of various types of carbides and relate the microstructural evolution to the creep properties of these steels. Small-angle neutron scattering (SANS) is sensitive to the variation of the neutron coherent scattering length density and thus can be

used in the study of internal inhomogeneities with the dimensions of  $\sim 1 - 100$  nm corresponding to a  $q$ -range,  $\sim 10^{-2} < q < 1$  nm $^{-1}$ . Ultra-small-angle neutron scattering (USANS), a relatively new technique, extends this range to lower  $q$  values,  $\sim 10^{-4} < q < 10^{-2}$  nm $^{-1}$  enabling the study of micro-structural features with sizes upto  $\sim 10$  nm. The world's best BT-5 USANS instrument at NIST covers a dynamical  $q$ -range of  $3 \times 10^{-4} < q < 2 \times 10^{-1}$  nm $^{-1}$ , which overlaps with that for the conventional pin-hole NG-3 NIST SANS facility, thus permitting combined USANS/SANS experiments even in cases of weakly scattering samples. We present the results of our preliminary SANS/USANS studies of precipitation in advanced steels carried out at BT-5 and NG-3 facilities at NIST.

*Research sponsored by the Laboratory Directed Research and Development Program of Oak Ridge National Laboratory (ORNL), managed by UT-Battelle, LLC for the U. S. Department of Energy under Contract No. DE-AC05-00OR22725.*

#### TP32

### **A Neutron Reflectivity Study of Thin ErT<sub>2</sub> Films as a Function of <sup>3</sup>He Concentration**

J. F. Browning (Sandia National Laboratories), G. S. Smith (Oak Ridge National Laboratory), G. M. Bond (New Mexico Tech), E. B. Watkins (Los Alamos Neutron Science Center, Los Alamos National Laboratory)

Metal hydride systems containing tritium, the radioactive isotope of hydrogen, are of interest to the fusion community. Rare earth (RE) tritides have been shown to exhibit favorable properties in regard to the reversible cycling of tritium gas stored in such systems. A common observation in RE tritides is that, initially, most of the <sup>3</sup>He produced via tritium decay is retained within the tritide lattice. In addition, the release of <sup>3</sup>He during this initial period has been shown to remain constant until some critical concentration of helium has been achieved within the lattice. Once this critical concentration has been achieved helium evolves from the tritide at a rate equal to or greater than its generation rate. These observed characteristics are believed to be governed by near surface conditions within the material. In order to gain a better understanding of <sup>3</sup>He behavior in metal tritides we have used neutron reflectometry to study thin films of ErT<sub>2</sub> over a time period sufficient to observe the transition from low, constant fraction emission to rapid <sup>3</sup>He emission from the films. In this study we identify a near surface region of higher scattering length density than that of the tritide. We also find that the tritide

layer thickness increases in an approximately linear fashion as a function of helium concentration within the lattice. These experiments were carried out on the Surface Profile Analysis Reflectometer (SPEAR) at the Los Alamos Neutron Science Center (LANSCE).

*Sandia is a multiprogram laboratory operated by Sandia Corporation, a Lockheed Martin Company, for the United States Department of Energy under contract DE-AC04-94AL85000.*

#### TP33

### **Neutron Diffraction Study of Cyanate Ligand Order/Disorder in AgNCO at 50-300 K**

D. J. Williams, S. Vogel, L. L. Daemen (Los Alamos Neutron Science Center, Los Alamos National Laboratory)

The study of ordered/disordered cyanate ligands in AgNCO was carried out using the neutron powder diffractometers HIPPO (High Pressure Preferred Orientation Powder) and HIPD (High Intensity Powder Diffractometer). Structural analysis was performed on AgNCO at five different temperatures (300 K, 200 K, 150 K, 100 K and 50 K). AgNCO (No. 11, P2<sub>1</sub>/m,  $a=5.4742(3)$  Å,  $b=6.3784(2)$  Å,  $c=3.4170(1)$  Å,  $\beta=90.931(5)^\circ$ , Vol.=119.298(8), density=4.173 g/cm<sup>3</sup>, and  $Z=2$ ) Å was found to have ordered OCN ligand from 300 K to 50 K. The bond lengths results from the analysis yielded Ag-N=2.1483(14) Å and C-N=1.1708(33) Å and C-O=1.1829(35) Å.

#### TP34

### **Structural and Hydriding Behaviors Neutron Studies on Li-Based Hydrogen Storage Materials**

W. Chien, D. Chandra (University of Nevada, Reno), A. Huq, J. W. Richardson, Jr, E. Maxey (Argonne National Laboratory, Intense Pulsed Neutron Source), S. Fakra, M. Kunz (Lawrence Berkeley National Laboratory)

Recent researches in the Li-based complex hydrides show the great potential for hydrogen storage in fuel cell, on-board vehicular and other applications. The lithium nitride (Li<sub>3</sub>N) can store up to 11 wt.% hydrogen, and lithium aluminum hydride (LiAlH<sub>4</sub>) can store (theoretically) up to 7.9 wt.% hydrogen below 250°C. In this study, low temperature neutron powder diffraction studies have been performed to understand the structural behaviors of both Li<sub>3</sub>N and LiAlD<sub>4</sub> samples from 10 K to 300 K. Neutron and synchrotron studies on the commercial Li<sub>3</sub>N sample shows that Li<sub>3</sub>N contains a two-phase (alpha + beta) mixture at room temperature. Crystal structures of both alpha and beta phases of Li<sub>3</sub>N are hexagonal, and LiAlD<sub>4</sub>

is monoclinic. Volume expansions of  $\text{Li}_3\text{N}$  alpha and beta phases are 0.56% and 1.1%, respectively, and for  $\text{LiAlD}_4$  is 0.88% from 10 K to 300 K.  $\text{Li}_3\text{N}$  hydriding experiment by the in-situ neutron diffraction with the deuterium gases flowing are performed at different temperatures. Time resolved hydriding results show  $\text{Li}_2\text{ND}$  and  $\text{LiD}$  phases appearing at 200°C.  $\text{Li}_2\text{ND}$  phase is transferred to  $\text{LiND}_2$  at 250°C. Detail lattice and volume expansions, and weight percent change of different lithium hydride phases will be presented.

#### TP35

### A High Performance Diffractometer at a Low Intensity Source

R. Berliner, A. I. Hawari (North Carolina State University)

The PULSTAR Neutron Powder Diffractometer (PNPD) is currently in the final stages of installation at the 1-MW PULSTAR reactor at North Carolina State University. The instrument is located on a 6" diameter radial beamport with a nominal neutron flux of  $10^{10}$  n/cm<sup>2</sup>.s at its exit. The PNPD uses a 9-bladed double focusing bent perfect crystal Si monochromator designed by Popovici and a 90° take-off angle to obtain a 1.478 Å monochromatic beam. The monochromator has an almost unobstructed view of the source with a 3" thick 5.25" diameter sapphire filter placed at the source end of the primary collimator to reduce fast neutron background. The instrument detector is a 15 element linear position sensitive proportional counter array that is 31 cm high x 61 cm wide and spans 20° two-theta at 1.6 m from the specimen position. A complete 125° two-theta diffraction pattern is obtained by indexing the detector assembly about the sample position in 20° steps. The detector position resolution is nominally 2.5 ~ 3 mm which supports an angular resolution of slightly less than 0.1°. The detector array is enclosed in a high-density PE/Borated-PE Cd enclosed shield supported by 3 air pads on a laminate covered aluminum slab. The detector can be placed at two different positions within the shield: 1.6 m from the sample position for high resolution ( $\delta d/d \sim 1.0 \times 10^{-3}$ ) or 1.1 m from the source for x6 higher throughput at slightly lower resolution ( $\delta d/d = 1.5 \times 10^{-3}$ ). Instrument performance data will be presented. The PNPD will be employed as a platform for the education of students and for preliminary and speculative experiments.

#### TP36

### Functional toxin pores in tethered bilayers: Membrane association of $\alpha$ -hemolysin

D. J. McGilivray, F. Heinrich (Carnegie Mellon University and CNBT at the NIST Center for Neutron Research), I. Ignatjev, G. Valincius (Institute of Biochemistry, Vilnius, Lithuania), D. J. Vanderah, J. J. Kasianowicz (National Institute of Standards and Technology), M. Loesche (Carnegie Mellon University and CNBT at the NIST Center for Neutron Research)

The toxin  $\alpha$ -hemolysin ( $\alpha$ HL) from *Staphylococcus aureus* is a paradigm of a pore-former in biomembranes. The protein has been extensively investigated in single-molecule electrophysiologic studies of free-standing membranes, its atomic-scale structure has been solved by X-ray crystallography, and the suggestion to use the molecular pores in DNA-sequencing devices has received considerable attention. Aiming at both structural studies of its membrane incorporation, and the incorporation of the protein into a sensor format with long-term stability, we demonstrate the reconstitution of these toxin pores in a biomimetic tethered bilayer membrane (tBLM) on a solid substrate. The electrical characteristics of the pore, determined from electrical impedance spectroscopy, are consistent with measurements of functional proteins in free-standing lipid membranes while being stable over long periods of time (days). Neutron reflectometry shows the protein's cap domain outside the bilayer membrane, and significant impact of the protein on the head group region of the outer membrane leaflet. A more sophisticated analysis of the neutron data using the known X-ray structure of the protein is targeted at obtaining more detailed structural information about the interaction of the protein with the membrane.

#### TP37

### Double bond effect on the bending elasticity of lipid membranes studied by Neutron Spin Echo technique

Z. Yi, D. P. Bossev (Indiana University, Bloomington, IN)

We have used neutron spin echo (NSE) spectroscopy to study the effect of the unsaturated double bond on the bending elasticity of lipid membranes made of 1,2-Dioleoyl-sn-Glycero-3-phosphocholine (DOPC) as a function of temperature in D<sub>2</sub>O. The double bond causes a kink of the lipid hydrocarbon chain wherever it occurs. That has a profound effect on the

collective behavior of the lipid molecules and results in a looser packing and lower melting points. This feature plays an important role in the relationship between temperature and the fluidity of the cell membrane. NSE is the most direct method to monitor the thermal undulations of the lipid bilayers in solution because it is a unique scattering technique that covers the time scale of 0.01 – 100 ns, characteristic of these motions. In this work, we take advantage of the NSE technique to determine the bending elasticity of lipid membranes through Zilman-Granek theory for thermal undulations. Vesicles made of a lipid with two double bonds, DOPC, were studied and the results compared to those for a saturated lipid, DMPC, studied previously. We have found that the bending modulus of DOPC in lipid bilayers is higher than that of DMPC. These results are interpreted in terms of hydrocarbon chain length and lipid ordering.

TP38

### Neutron Bragg Fabry - Perot Resonator. Existence of the Quasi Stationary States

E. Iolin (Institute of Physical Energetic, Riga, Latvia)

During the recent years, there has been increased interest in the research on devices which utilize multiple Bragg diffraction in perfect single crystals (neutron confinement, Spin-Pendellozung resonance and so on). Dombeck et al [1] proposed to use multiple Bragg Scattering (BS) from the slot in the perfect single crystal placed in the magnetic field for the Neutron Electric Dipole Moment (EDM) search. The neutron spin is disturbed by EDM or Schwinger interactions in the slot wall and rotates at the angle  $\pi$  during the transit from one slot side to another. The effect of perturbation is accumulated during multiple,  $\sim 10^4$  reflections from slot walls. Authors [1] used simple geometrical approach for necessary estimates. Recently we fulfilled [2] dynamical theory analysis of this device – Bragg Fabry - Perot Resonator (BFPR). The calculated neutron modes have a discrete spectrum (DS) of a momentum along the slot axis. An external magnetic field causes some modes with opposite spin orientation to become degenerate and therefore sensitive to a very weak Schwinger or even EDM interaction. Here we continue calculations. We used Laplace transformation and found not only poles corresponding to DS, but also additional poles at the unphysical complex

momentum plane. These additional poles are corresponded to the neutron quasi stationary states (QSS) in BFPR. We calculated amplitude of the exciting BFPR modes when reactor core neutrons are reflected by triple bounces Bonse – Hart perfect silicon monochromator. Intensity  $I_{0,h}$  neutrons reflected as discrete DS BFPR modes  $I_{0,h} = 0.5(1 - \text{abs}(\delta\theta_m/\delta\theta_0)) * \text{Heaviside}(1 - \text{abs}(\delta\theta_m/\delta\theta_0))\delta\theta_0$ ,  $\delta\theta_m$  – Darwin plateau half width and deviation of monochromator from the exact anti parallel position. Therefore almost all neutrons are spreading in discrete BFPR resonance mode regime inside of a thick,  $\sim 1\text{mm}$ , slot when  $\delta\theta_m = 0$ . Deviation from the exact anti parallel position decreases  $I_{0,h}$ . What is happened with remained incident neutrons? These neutrons fly away from BFPR. We found that angular distribution of these flying off neutrons contains strong peaks created by the decay of the quasi stationary neutron states. Probably, these QSS peaks could be observed due to a small neutron absorption in silicon. At our knowledge, the existence of these neutron QSS was not known before. Calculated amplitudes of discrete modes could be used for the analysis of BFPR experiments.

[1] T.Dombeck, et al. "A Bragg scattering method to search for the neutron electric dipole moment", Phy-9814-TH-2001, Argonne National Laboratory, March 2001.

[2] E.Iolin, et al. "Propagation of neutron de Broglie waves inside the slot cut in a single Si crystal", Proceedings of SPIE, vol. 4509, p.33-43 (2001)

TP39

### <sup>3</sup>He neutron spin filters for the thermal triple axis spectrometry and diffuse reflectometry

W. C. Chen (NIST Center for Neutron Research and Indiana University), R. W. Erwin, J. A. Borchers (NIST Center for Neutron Research, Gaithersburg, MD), Y. Chen (NIST Center for Neutron Research and University of Maryland), K. V. O'Donovan, S. McKenney, C. F. Majkrzak, J. W. Lynn, T. R. Gentile (NIST Center for Neutron Research, Gaithersburg, MD)

Polarized <sup>3</sup>He neutron spin filters (NSF) are of great interest in the neutron scattering community due to recent significant improvements in their performance. Here I will discuss their successful application to a polarized neutron reflectometer (PNR) and a thermal triple-axis spectrometer (TAS). In PNR, the conventionally used supermirrors have limited angular acceptance and hence are impractical for polarization analysis of off-specular scattering. A polarized <sup>3</sup>He analyzer in conjunction with a position-sensitive detector allows for much



more efficient collection of off-specular scattering with polarization analysis over a broad range of reciprocal space. The results from artificially patterned thin films measured at NG1 and AND/R reflectometers using a  $^3\text{He}$  analyzer at the NCNR will be presented. For thermal TAS, Heusler crystals have commonly been used to polarize and/or analyze the neutron beam. However, they typically have low reflectivity and exhibit 1/2 contamination. A  $^3\text{He}$  NSF decouples the polarization and energy selection and thus provides greater versatility and higher intensity compared to a Heusler polarizer. At the NCNR, we have applied  $^3\text{He}$  NSFs to polarize and analyze a 10-cm tall neutron beam on the BT-7 thermal TAS. In combination with a double focusing pyrolytic graphite monochromator, the intensity in the polarized mode is at least an order of magnitude higher than the previous BT-2 instrument. For these experiments,  $^3\text{He}$  gas is polarized offline by the spin-exchange optical pumping method and delivered to the neutron beam and stored in a uniform magnetic field provided by a magnetically shielded solenoid. Using 52 W of spectrally narrowed 795 nm diode laser arrays we have routinely achieved  $^3\text{He}$  polarization of 75% in cell volumes up to 1 L.

#### TP40

### Self-assembled nanostructures in copolymer blends

S. Malkova (Argonne National Laboratory, Intense Pulsed Neutron Source), J. Holoubek, J. Baldrian (Institute of Macromolecular Chemistry, Academy of Sciences of the Czech Republic, Prague, Czech Republic), J. Lal (Argonne National Laboratory, Intense Pulsed Neutron Source)

“Bottom-up” nanofabrication uses guided assembling of molecular-scale entities to create larger ones for possible engineering usage. Self assembly of block copolymers or functionalized nanostructures can generate a rich variety of nanomorphologies (such as lamellar, cylindrical, gyroid, various cubic).

Phenomena associated with the order-disorder transition (ODT), microdomain morphology and phase behavior of two block copolymer systems have been studied by small-angle X-ray scattering (SAXS), small-angle neutron scattering (SANS), scanning and transmission electron microscopy (SEM, TEM).

The microdomain morphology and phase behavior in copolymer blends of A-*b*-B/A-*b*-C i.e. with one

common block (deuterated PS-*b*-PMMA / deuterated PS-*b*-PI) were investigated by SAXS, SANS and TEM. The studied (almost symmetric) copolymers differ essentially in microdomain morphology. One of them is in disordered microdomain state, while the other one displays lamellar morphology at usual temperatures. Self-assembled structures in blends were investigated as a function of concentration of the added microphase-separated copolymer and of temperature.

Self-assembled structures in binary mixtures of A-*b*-B/A (deuterated PS-*b*-PMMA/PS homopolymer) were studied as a function of molecular weight and concentration of the added polymer. Changes in microdomain morphology are interpreted using concept of “wet and dry brush” based on solubilization of the homopolymer in microdomain morphology.

#### TP41

### Nuclear and Magnetic Structure of Biosynthesized Magnetic $(\text{Zn}_x\text{Fe}_{1-x})\text{Fe}_2\text{O}_4$ Nanoparticles

L. Yeary, C. J. Rawn, J. W. Moon, B. C. Chakoumakos, M. E. Madden, T. J. Phelps, L. J. Love (Oak Ridge National Laboratory)

Nuclear and Magnetic Structure of Biosynthesized Magnetic  $(\text{Zn}_x\text{Fe}_{1-x})\text{Fe}_2\text{O}_4$  Nanoparticles L.W. Yeary<sup>1</sup>, C.J. Rawn<sup>2</sup>, J.-W. Moon<sup>3</sup>, B.C. Chakoumakos<sup>2</sup>, M.E. Madden<sup>3</sup>, T.J. Phelps<sup>3</sup>, and L.J. Love<sup>1</sup>, <sup>1</sup>Engineering Science and Technology Division, <sup>2</sup>Materials Science and Technology Division, <sup>3</sup>Environmental Sciences Division, Oak Ridge National Laboratory, Oak Ridge, TN 37831

Mixed iron oxides in nano-size are attracting increasing interest in both scientific and technological research because of their potential applications and for use as an instrument by which we study nanoscale phenomena. In particular, zinc ferrite has generated a large research effort since it offers a simpler magnetic system to study than other metal oxides because of the preference of the zinc ion to the tetrahedral site in the spinel structure. The biomineralization process used for this study is of interest due to the environmentally favorable synthesis at relatively low temperatures that produces nanoparticles without a costly milling process and is promising for its sizeability and reproducibility followed by scalability. Nanoparticle magnetite with Zn substituting for some of the Fe has been synthesized at 60°C by a biologically induced mineralization using the thermophilic bacteria strain, *Thermoanaerobacter ethanolicus*, TOR-39. Both pure magnetite and



substituted-magnetite with increasing amounts of Zn have been produced. Particle size and morphology were verified using TEM, X-ray powder diffraction, and time-of-flight (TOF) powder neutron diffraction. Crystallite size, according to the Scherrer method, began at 38 nm for the pure magnetite and reduced to 14 and 9 nm for samples with the nominal compositions of  $\text{Zn}_{0.6}\text{Fe}_{2.4}\text{O}_4$  and  $\text{Zn}_{0.9}\text{Fe}_{2.1}\text{O}_4$ . The addition of Zn increases the lattice parameter, the background, and the peak width. The latter two results suggest an increase in disorder, a decrease in crystallinity, and/or a decrease in crystallite size. Rietveld refinements using the TOF data show that the Zn prefers the tetrahedral site in the structure and the refined site occupancies for the samples with Zn are  $x = 0.629(7)$  and  $x = 0.804(7)$  atom per formula unit in  $\text{Zn}_x\text{Fe}_{3-x}\text{O}_4$  with corresponding lattice parameters of  $a = 8.4040(1)$  and  $a = 8.4253(1)$  Å compared to the sample without Zn that has a lattice parameter of  $a = 8.36965(6)$  Å. The magnetic properties were characterized by using a superconducting quantum interference device (SQUID) magnetometer. Pure magnetite showed a saturation magnetization of 82.4 emu/g. Increasing the amount of zinc increased this to a value of 85.8 emu/g, however, with further substitution a reduction of magnetization was observed and the sample with the most amount of zinc recorded a value of 64.4 emu/g.

*This work was supported by the Defense Advanced Research Projects Agency (DARPA) Biomagnetics Program under Contract 1868-HH43-X1. Oak Ridge National Laboratory is managed by UT-Battelle, LLC, for the U.S. Department of Energy under Contract DE-AC05-00OR22725.*

#### TP42

### VISION, A Neutron Vibrational Spectrometer for SNS: Status Report

J. Z. Larese (University of Tennessee), U. Wildgruber (Spallation Neutron Source, Oak Ridge National Laboratory), L. L. Daemen, P. A. Seeger (Los Alamos Neutron Science Center, Los Alamos National Laboratory)

We will describe the current status of VISION, a neutron scattering instrument for vibrational spectroscopy with capability for simultaneous diffraction to be constructed at the SNS. The use of neutron vibrational spectroscopy is growing at a significant rate in Europe thanks to the recent improvements in TOSCA II at ISIS, the spallation neutron facility at the Rutherford-Appleton Laboratory in England. VISION will substantially expand the range and flexibility of neutron

investigations in the United States where the main objective is to characterize molecular motions in areas such as nanoscience, hydrogen storage and catalysis.

#### TP43

### Toward User Friendly and Easily Supportable Sample Environment Control Software

R. R. Porter (Argonne National Laboratory, Intense Pulsed Neutron Source)

Sample environment monitoring and control is an integral part of many neutron scattering experiments. This includes sample position and orientation, temperature, pressure or vacuum, and magnetic field. Software has been written to remotely monitor and/or control these variables using the Experimental Physics and Industrial Control System (EPICS). This software is standardized across the upgraded instruments at the Argonne National Laboratory, Intense Pulsed Neutron Source (IPNS). This software is continually updated to provide more functionality and greater reliability. The use of EPICS also allows for the sharing of code with the IPNS accelerator, the Argonne National Laboratory, Advanced Photon Source, and the wider EPICS collaboration.

#### TP44

### Magnetic Properties of the $\text{La}_{1.4}(\text{Sr}_{1-y}\text{Ca}_y)_{1.6}\text{Mn}_2\text{O}_7$ solid solution ( $y=0, 0.25$ and $0.50$ )

L. Malavasi, M. C. Mozzati (University of Pavia, Italy), V. Pomjakushin (Paul Scherrer Institute), C. Ritter (Institut Laue-Langevin, France), C. Tealdi, C. B. Azzoni, G. Flor (University of Pavia, Italy)

There is an increasing interest in materials that show magnetoresistance, because of their use in magnetic information storage or as magnetic field sensors. Most of the available theoretical and experimental work has, until now, been focused on the 3D perovskite structures, “infinite” end-member of the that is the  $n = A_{n+1}B_nO_{3n+1}$  Ruddlesden-Popper family, in which  $n$  2D layers of  $\text{BO}_6$  corner-sharing octahedra are joined along the stacking direction and separated by rock-salt AO layers. The optimally-doped  $n = 2$  members of this family ( $\text{La}_{2-2x}\text{B}_{1+2x}\text{Mn}_2\text{O}_7$  where  $B = \text{Ca}$  or  $\text{Sr}$ ) behave analogously to the perovskite manganites in the sense that they undergo an insulating- to metallic-like state transition together with a ferromagnetic transition at temperatures around 120-140 K; moreover they present a large magnetoresistance

in this temperature range. However, the change in dimensionality and resulting pronounced cation dependence of the electronic properties can produce physical properties which contrast strongly with the perovskite systems.

In this work we have studied the role of cation size on the magnetic structure and properties of the  $\text{La}_{1.4}(\text{Sr}_{1-y};\text{Ca}_y)_{1.6}\text{Mn}_2\text{O}_{7+\delta}$  solid solution for different Ca/Sr ratios ( $y=0, 0.25$  and  $0.5$ ). Samples have been characterized by means of x-ray diffraction, magnetometry, magnetoresistance measurements and x-ray absorption spectroscopy at the Mn-K edge. Neutron diffraction was employed to study the magnetic structure of the samples. Data show that considerable effect is produced by the cation replacement, with the progressive evolution of the system from a ferromagnetic-metal ( $y=0$ ) to a short-range ordered material with metallic behaviour ( $y=0.50$ ) [1].

[1] L. Malavasi, M.C. Mozzati, C. Ritter, C.B. Azzoni, e G. Flor, *Solid State Comm.* **137** (2006) 350-353.

#### TP45

### **Small Angle Neutron Scattering (SANS) study of nitrogen doped ultrananocrystalline diamond (UNCD) film: morphology and electronic film structure**

P. Bruno, M. Bleuel, J. Lal, D. Gruen (Argonne National Laboratory)

Ultrananocrystalline diamond (UNCD) film consists of 2-5 nm grains of pure  $\text{sp}^3$ -bonded carbon and 0.5 nm wide grain boundaries (GB), consisting of  $\text{sp}^2$ ,  $\text{sp}^{2-x}$  and  $\text{sp}^3$  bonded carbon. Many UNCD film properties are closely connected to their unique nanoscale morphology and electronic structure. It has recently been reported that the incorporation of nitrogen into the grain boundaries of UNCD films has a profound impact on the film electrical conductivity up to several hundreds S/cm at ambient temperatures. Hall measurements at the higher nitrogen concentrations indicate that the carrier concentration increases dramatically, resulting in the highest known ambient temperature n-type conductivity of any diamond thin film. The conductivity mechanism in UNCD appears to involve both the grain boundaries and the grains; however the effective modifications caused by the nitrogen on the film bonding structure and morphology as well as on the electronic structure are among the important open questions for ultrananocrystalline diamond films. SANS measurements carried out for the first time on

a set of UNCD films grown at different nitrogen concentrations show in detail the effect of nitrogen on the film nanostructure. Ordering of the UNCD structures as well as changes in shape and size have been observed by SANS measurements. The results of these investigations have been correlated with SEM and electrical conductivity data. Summarizing, the investigations carried out in the present work help to give a consistent idea of the morphological and structural modifications in the UNCD films resulting from nitrogen additions to the plasma phase. Correlation with the electrical film properties can better elucidate the mechanism of conduction in UNCD films.

*This work is supported by the U.S. Department of Energy, Basic Energy Sciences, Materials Sciences, under Contract W-31-109-ENG-38.*

#### TP46

### **Dynamic Responses in Nanocomposite Hydrogels**

G. Schmidt, E. Loizou (Louisiana State University), P. D. Butler, L. Porcar (NIST Center for Neutron Research)

The shear response of a series of polymer-clay gels has been investigated by means of rheology and small angle neutron scattering (SANS). The gels have the same composition by mass but different polymer molecular weights (Mw). While long polymer chains can interconnect several platelets, which act as multifunctional cross-links, very short polymer chains should not be able to do so, allowing us to explore the effects of bridging on structure and dynamical responses. Increasing the polymer Mw in the gels leads to increasingly strong anisotropy in the SANS data indicating a larger and larger degree of shear-orientation. This relative increase in orientation however is accompanied by a relatively lower amount of shear thinning. Simple solutions of anisotropic particles usually shear thin by alignment of the particles with the flow, allowing them for example to slide past each other more easily. In a connected gel, breaking of the connectivity should also lead to shear thinning. Thus the inverse relationship between shear orientation and shear thinning, combined with the fact that the lowest Mw, which exhibits the highest shear thinning, does not orient at all, supports our earlier hypothesis that the alignment mechanism in these systems stems from the coupling between the clay and the polymer mediated by the shear flow and nicely demonstrates the effect of bridging on the strength and dynamics of these gels.

TP47

# **The “coloring problem” in the Cu-Zn g-brass structure**

O. Gourdon, D. Gout (Los Alamos Neutron Science Center, Los Alamos National Laboratory), G. J. Miller (Iowa State University), T. Proffen (Los Alamos Neutron Science Center, Los Alamos National Laboratory)

The reinvestigation of the Cu-Zn binary system in the g-brass region is based on our recent exploration of new approximants to quasicrystals. Numerous observations confirmed some structural and electronic relations between quasicrystals and their approximants and cubic g-brass [1,2,3,4,5]: for example, the [110] direction of the cubic g-brass structure is parallel to the ten-fold axis of decagonal phases or the five-fold axis of icosahedral phases [4]. The cubic g-brass phase is preferred for a valence electron concentration (vec = valence s, p electrons/ atom ratio) of 1.61 (~21/13) valence s and p electrons/atom, which lead to the “ideal” composition of “Cu<sub>5</sub>Zn<sub>8</sub>” [3]. However, a wide range of composition has been observed from both side of this concentration. Here, we report the crystal structure of three different Cu<sub>5-x</sub>Zn<sub>8+x</sub> samples for x= -1.31, 0 and 0.79 with the g-brass structure. These structures have been both refined by neutron and X-ray powder diffraction. Our crystallographic studies emphasize two major information: (1) a wider range of stability for the g-brass phase toward the Cu rich side and (2) a specific site substitution on both side of the ideal composition of “Cu<sub>5</sub>Zn<sub>8</sub>”. The first aspect suggests a modification of the boundaries between the b-brass phase and the g-brass phase especially in the vicinity of 55 atomic percentages Cu where both phases are supposed to coexist according to literature [6]. The second characteristic of our crystallographic work focus on what is called in the field of the solid state chemistry as the “coloring problem”. The “coloring problem” addresses the issues of the structural preference as well as the distribution of the different elements within a given structure. The reasons of such atomic arrangements in a solid-state structure are usually defined by some energetic contributions that influence how elements are order in a structure: the site energy and the bond energy. To analyze such contributions and to explore the chemical parameters consistent with the specific ordering, TB-LMTO-ASA band structure calculations have been carried out on the series Cu<sub>4.21</sub>Zn<sub>8.79</sub>, Cu<sub>5</sub>Zn<sub>8</sub> and Cu<sub>6.31</sub>Zn<sub>6.69</sub>.

[1] V. Demange, J. Ghanbaja, F. Machizaud, J. M. Dubois, *Philos. Mag.*, (2005), **85**, 1261.

[2] V. Demange, A. Milandri, M. C. de Weerd, F. Machizaud, G. Jeandel, J. M. Dubois, *Phys. Rev. B*, (2002), **B65**, 144205.

[3] S. Ebalard & F. Spaepen, *J. Mater. Res.*, (1991), **6**, 1641.

[4] C. Dong, *Philos. Mag. A*, (1996), **A73**, 1519.

[5] M. Boström & S. J. Houmøller, *Solid St. Chem.* (2000), **153**, 398.

[6] Brandon J. K., Brizard R. Y., Chieh P. C., MnMillan R. K. and Pearson W. B. *Acta Cryst.* (1974), **B30**, 1412.

TP48

# **Alignment Techniques for Installing Neutron Scattering Instruments**

S. A. Moore, J. L. Robertson, G. B. Taylor, M. W. Humphreys, E. R. Blackburn (Oak Ridge National Laboratory)

We describe the technical concepts incorporating the latest Laser Interferometry technology as applied to the installation and alignment of modern neutron scattering instruments. We are able to mechanically install our new neutron scattering instruments to a previously unattainable degree of accuracy when given engineering data locating the instrument in its theoretical operational location. Using this technology we develop a three dimensional coordinate system in the general area of the instrument and install the permanent positioning equipment (i.e. high precision rails or mounting plates) prior to delivery of the instrument. Upon delivery, the instrument is pre-aligned when installed. This methodology was previously not feasible due to combinations in limits in theodolite technology and time to perform the lengthy geometric calculations between measurements. We have had successful installations incorporating these techniques with accuracies of less than 0.08 mm in each of the x, y, and z axis of our neutron scattering instruments as compared to +/- 0.30 mm using previous alignment techniques. We will discuss the schedule and economic benefits from these techniques as well as our mechanical installations and alignments.

TP49

# **Dynamics of water in low-hydrated clays by quasi-elastic neutron scattering and microscopic simulation**

N. Malikova (Argonne National Laboratory), A. Cadene, V. Marry, E. Dubois, P. Turq (Laboratoire Liquides Ioniques et Interfaces Chargees, Univeristy Pierre et Marie Curie, Paris, France)

The dynamics of water in montmorillonite clays with Na<sup>+</sup> and Cs<sup>+</sup> counterions in monolayer and bilayer states was investigated on the microscopic

scale by neutron spin echo (NSE), time-of-flight (TOF) and classical molecular dynamics simulations (MD) [1,2]. These low-hydration states of clays correspond to only a few H<sub>2</sub>O molecules per ion (order of 10). Motion of water is studied here experimentally exploiting the incoherent scattering signal from powder clay samples.

Intermediate scattering functions from NSE and MD are compared directly, and all three sets of data are then analysed, in their respective domains, applying the model of continuous isotropic translation. This yields diffusion coefficients of water in the range of  $0.5 - 1.5 \times 10^{-10} \text{ m}^2\text{s}^{-1}$ , thus not reaching above 2/3 of the value for bulk water. However, data from all three techniques suggest significant departure from “mono-modal” situation, e.g. mono-exponential behaviour in the  $Q, t$  domain. Possible reasons are discussed.

In the low  $Q$  range, NSE data feature consistently slower dynamics (higher average relaxation times) than TOF. This is rationalised by the lower cut-off of accessible correlation times (TOF: 70-100ps, NSE: 1ns), limited by the resolution of the TOF set-up. For MD and NSE, the ranges of accessible correlation times coincide, very good agreement is found for the monohydrated systems, while they differ by a factor of 2-3 in the Na-bilayer. Complexity of the real clay system, including its hydration pattern, not represented in the model clay is in part seen as responsible for this.

In the present TOF and NSE experiments, the interpretation of the Elastic Incoherent Structure Factor (EISF) in terms of geometry of confining media is rendered very difficult due to the use of powder samples and limited resolution. MD has been used to decouple the particle motion in the two principal directions (parallel and perpendicular to clay layers) and show clearly the signs of ‘true’ and ‘apparent’ confinement, the latter being linked to the limited range of correlation times probed.

[1] N. Malikova, A. Cadene, V. Marry, E. Dubois, P. Turq, J.-M. Zanotti and S. Longeville, *Chem. Phys.* **317** (2005), pp. 226-235.

[2] N. Malikova, A. Cadene, V. Marry, E. Dubois, P. Turq, *J. Phys. Chem. B* **110** (2006), pp. 3206-3214.

#### TP50

### **<sup>3</sup>He neutron polarization analyzer for the SNS Magnetism Reflectometer**

W. T. Lee (Oak Ridge National Laboratory), T. R. Gentile, W. C. Chen (National Institute of Standards and Technology), G. L. Jones (Hamilton College)

We report progress on the construction of a polarized <sup>3</sup>He based neutron polarization analyzer for use at the Magnetism Reflectometer at the Spallation Neutron Source. The analyzer uses the Spin Exchange Optical Pumping (SEOP) method to polarize the <sup>3</sup>He gas. The <sup>3</sup>He cells have 11 cm inner diameter, which will allow off-specular scattering measurements to be carried out on the reflectometer. Continuous online optical pumping will be used to maintain the maximum <sup>3</sup>He polarization during an experiment. In order to analyze both neutron spin states, adiabatic-fast-passage technique nuclear magnetic resonance will be employed to invert the <sup>3</sup>He polarization.

#### TP51

### **Neutron scattering investigations and DFT modeling of molecular structure and dynamics of neohexane and diisopropyl**

I. Natkaniec (Joint Institute for Nuclear Research), K. Holderna-Natkaniec, D. Nowak (Institute of Physics, Adam Mickiewicz University, 61-614 Poznan, Poland)

Hexane isomers, C<sub>6</sub>H<sub>14</sub>, are components of solvents used in petrochemical industry and can be also found in gasoline. The low temperature thermal data indicate phase transitions in some of these isomers, however, the structure and dynamics of solids are not yet well investigated. The aim of these studies was to get insight into the influence of molecular structure on the vibrational spectra and solid state polymorphism of the neohexane (2,2-dimethylbutane), 2,2-DMB, and diisopropyl (2,3-dimethylbutane), 2,3-DMB, isomers. Simultaneous, neutron powder diffraction (NPD) and incoherent inelastic neutron scattering (IINS) investigations of these substances show, that both solidify into a so-called plastic crystal or orientationally disordered (ODIC) phase. At cooling down neohexane shows a structural phase transition to the ordered crystal phase at about 126K, while diisopropyl remains within the ODIC phase structure down to 20K. Molecular reorientations at this temperature are hindered and vibrational density of states for both substances can be well determined from their IINS



spectra. The structure and dynamics of the 2,2-DMB and 3,3-DMB molecules have been calculated by DFT computational methods using the Gaussian03 codes. The dependence of potential energy on rotation of molecular subunits around C2 - C3 bond gives rotational barriers, which determine rotamer conformations of the investigated substances. The 2,2-DMB molecule has only one conformation, while the 2,3-DMB molecule can have two rotamer conformations with a slightly different potential energy. Twisting of molecular subunits around the C2 - C3 aliphatic bond has become the lowest frequency internal mode of the calculated molecules. For 2,3-DMB rotamers this mode is calculated at about 60 cm<sup>-1</sup>. In the experimental spectrum of diisopropyl this mode is mixed with the lattice modes, which form a broad band with maximum at 60 cm<sup>-1</sup> and cut-off frequency at about 120 cm<sup>-1</sup>. In neohexane this mode is calculated at 95 cm<sup>-1</sup>, and in the ordered crystal phase at 20K is observed as a narrow band at 112 cm<sup>-1</sup>, just above the lattice modes, which cut off at about 90 cm<sup>-1</sup>. Other internal modes of the investigated molecules are observed above 200 cm<sup>-1</sup>, and they are quite well reproduced by the calculated vibrational spectra of free molecules.

#### TP52

##### **A-site size effects and suppression of orbital ordering in Ba-substituted manganites**

O. Chmaissem, B. Dabrowski, S. Kolesnik, J. Mais, D. E. Brown, Y. Ren (Northern Illinois University & Argonne National Laboratory), J. D. Jorgensen (Argonne National Laboratory)

The effects of A-site ordering and disordering on the structural, magnetic and transport properties of La<sub>1-x</sub>Ba<sub>x</sub>MnO<sub>3</sub> (x = 0.48, 0.5, & 0.52) and Ba-substituted La<sub>0.5</sub>Sr<sub>0.5</sub>MnO<sub>3</sub> materials have been fully investigated. Using neutron and synchrotron powder diffraction, we will demonstrate the existence of low temperature phase separation, A-type antiferromagnetism and complex charge ordering in A-site ordered La<sub>1-x</sub>Ba<sub>x</sub>MnO<sub>3</sub> compositions with x ~ 0.5. Synchrotron powder diffraction experiments successfully demonstrate the melting and suppression of the low temperature charge and/or orbital ordered separated phases by the application of external magnetic fields up to ~ 6T. A-site disordered La<sub>1-x</sub>Ba<sub>x</sub>MnO<sub>3</sub> materials, on the other hand, only exhibit ferromagnetic properties and crystallize in pseudocubic structures. In La<sub>0.5</sub>Sr<sub>0.5</sub>MnO<sub>3</sub>, we show that the previously

observed low temperature orbital-ordered and A-type antiferromagnetic phase may be suppressed by the isovalent substitution of Ba for Sr at the A-sites. Details of the nuclear and magnetic structures and phase diagrams will be presented.

*This work was supported by NSF-DMR-0302617 (NIU) and the U.S. Department of Energy, BES – Materials Sciences (W-31-109-ENG-38) (ANL).*

#### TP53

##### **Neutron Diffraction Residual Stress Study of Intensive Quenching Steel Parts**

F. Tang, C. R. Hubbard, T. R. Watkins (Oak Ridge National Laboratory), M. A. Aronov, N. I. Kobasko, J. A. Powell (IQ Technologies Inc.), B. L. Ferguson, Z. Li (Deformation Control Technology, Inc.)

The effect of two quenching processes on residual stress in cylindrical rods was studied using neutron diffraction residual stress mapping facility (NRSF2) at ORNL's High Flux Isotope Reactor. The test specimens were AISI 5160 steel rods 25 mm in diameter and 127 mm in length. Three different samples were evaluated. Two samples were intensively quenched in highly agitated water by the intensive quench process and were tempered at two different temperatures. One specimen was conventionally quenched in oil and then tempered. The surface and through thickness residual stresses in the three sets of test specimens were measured by the X-ray diffraction and neutron diffraction methods, respectively. The residual stress distribution for each quench process was also calculated using the DANTE computer program for modeling quench processes. The results of the study demonstrate that the intensive water quenching process significantly changes the through thickness residual stress distribution compared to the standard oil quench process

*Research sponsored by the Assistant Secretary for Energy Efficiency and Renewable Energy, Office of FreedomCAR and Vehicle Technologies, as part of the High Temperature Materials Laboratory User Program, Oak Ridge National Laboratory, managed by UT-Battelle, LLC, for the U.S. Department of Energy under contract number DEAC05-00OR22725.*

#### TP54

##### **Dynamics of Random Copolymers in a Homopolymer Matrix**

S. Y. Kamath, M. D. Dadmun (University of Tennessee)

Copolymers can be used as interfacial modifiers in phase separated polymer blends and selective surface segregation. Important parameters in



this process include the amount of copolymer that migrates to the surface and the rate of this process, both of which are altered by changing the copolymer composition. The dynamics of random copolymers in a homopolymer matrix are studied using Neutron Reflectivity (NR), Quasi-Elastic Neutron Scattering (QENS) and Lattice Monte Carlo simulations. We have carried out NR and QENS measurements on blends containing 10% Poly(S-ran-MMA) random copolymers with 3 different copolymer compositions dispersed in a PMMA matrix. We have also carried out lattice Monte-Carlo simulations on blends of A-B random copolymers containing 33%, 50% and 66% A in a matrix of a homopolymer melt containing only A monomers using the bond-fluctuation model for polymer melts. Our results indicate that the copolymer composition has a significant impact on the dynamics of the copolymer. Our simulation results also indicate that copolymer composition has a significant impact on the structure which in turn has an impact on the system dynamics.

## TP55

#### Neutron Diffraction study of Ru doping in charge ordered $\text{Pr}_{0.5}\text{Ca}_{0.5}\text{MnO}_3$

K. Ramesha, A. Llobet, T. Proffen (Los Alamos Neutron Science Center, Los Alamos National Laboratory)

Small amount of Ru substitution (<10 %) for Mn in charge-ordered manganites destroys charge-ordering (CO) and induces ferromagnetic metallic state. To probe the dramatic role played by Ru in preventing the CO state, we have carried out neutron diffraction studies of  $\text{Pr}_{0.5}\text{Ca}_{0.5}\text{Mn}_{1-x}\text{Ru}_x\text{O}_3$  compounds ( $x = 0.0, 0.05$  and  $0.10$ ) in the temperature range 300-10 K. Evolution of lattice parameters with temperature points out that lattice distortion which accompanies charge ordering disappears on Ru doping. Also Ru doping alters the  $\text{MnO}_6$  octahedron shape from 4-long/2-short type to 2-long/4-short type that suppresses the antiferromagnetic ordering and hence induces ferromagnetism through double exchange interactions. The local structure of  $x = 0, 0.05$  and  $0.10$  compositions were analyzed using Pair Distribution Function (PDF) at 295 K and 15 K.

## TP56

#### Retroaction and Shielding Properties of the Magnetic Enclosure for the Neutron Spin Echo Spectrometer at the Spallation Neutron Source in Oak Ridge

H. P. Soltnner, U. Pabst, M. Monkenbusch, M. Ohl, M. Butzek (Forschungszentrum Jülich GmbH)

A computational lay out of a magnetically shielded room (MSR) was carried out in order to reduce the detrimental influence of inhomogeneous magnetic fields on the future Neutron Spin Echo (NSE) spectrometer at the Spallation Neutron Source (SNS) in Oak Ridge, Tennessee. Two generic sources of magnetic field were investigated. First, magnetic fringe fields from high-field magnets operated at neighboring beamlines; second, the retroactive magnetic fields on the high-permeable walls of the MSR generated by the well compensated but still not magnetically silent coils of the NSE spectrometer itself. Design criteria for the MSR evolving from field homogeneity requirements along the neutron trajectories are suggested, based both on finite element and boundary element calculations.

## TP57

#### Polarized $^3\text{He}$ neutron spin filter program at the NCNR

W. C. Chen (NIST Center for Neutron Research and Indiana University), R. W. Erwin, J. A. Borchers, S. McKenney (NIST Center for Neutron Research), Y. Chen (NIST Center for Neutron Research and University of Maryland), K. V. O'Donovan, T. R. Gentile, C. F. Majkrzak, J. W. Lynn, D. A. Neumann (NIST Center for Neutron Research)

Polarized  $^3\text{He}$  gas, produced by optical pumping, can be used to polarize or analyze neutron beams because of the strong spin dependence of the neutron absorption cross section for  $^3\text{He}$ . Polarized  $^3\text{He}$  neutron spin filters (NSF) have been of great interest in the neutron scattering community due to recent significant improvements of their performance during the last several years. Compared to the most commonly used polarizers, such as Supermirrors and Heusler crystals, a NSF has two main advantages, (1) it is broadband and can polarize thermal or hot neutrons effectively and (2) it can polarize angularly divergent neutron beams. The polarized  $^3\text{He}$  neutron spin filter program has been initiated to enhance or add the capability of polarizing incident beams and/or analyzing scattered beams for different types

of neutron scattering instruments at the NCNR. Our short-term goal is to develop (1) a  $^3\text{He}$  NSF based polarizer and analyzer for the BT-7 thermal triple axis spectrometer and (2) a  $^3\text{He}$  analyzer for polarization analysis in diffuse reflectometry. Our long-term goal is to apply these  $^3\text{He}$  NSF devices to as many instruments at the NCNR as possible, including small-angle neutron scattering, spin-echo spectrometer, high resolution powder diffractometer, disk chopper spectrometer, filter analyzer neutron spectrometer, and multi-axis crystal spectrometer. To meet our short-term goal, we are designing and building two spin exchange optical pumping stations which are capable of providing 75% polarized  $^3\text{He}$  gas at an overall rate of 4 bar-liters per day. The preliminary results for the diffuse reflectometry (NG-1 and AND/R) and the triple axis spectrometry (BT-7) using these  $^3\text{He}$  neutron spin filter devices will be discussed.

TP58

#### **Application of ultrasound to multi crystal neutron diffractometer**

E. Iolin, L. Rusevich (Institute of Physical Energetic, Riga, Latvia), M. Strobl, W. Treimer (Hahn-Meitner Institut), P. Mikula (Nuclear Physics Institute, Rez near Prague)

It is known that high frequency ultrasound increases the intensity by quasi elastic scattering in single crystals accompanied by a loss of the impulse resolution. It was supposed (E.I., 1989) that resolution losses could be avoided by exciting ultrasound with the same frequency in single crystal monochromator and analyzer of a diffractometer. We realized such experiment with a double crystal diffractometer with Si(111) crystals ( $l=0.523\text{nm}$ ) and observed ~ 60% intensity increase in the peak of the instrumental curve. Simultaneously a strong improvement of the ultrasonic phonon satellite contrast could be registered. A coherent (one-mode) ultrasonic field was not necessary for these results. Applying ultrasound to a triple bounce analyzer by means of several LiNbO<sub>3</sub> transducers ( $f= 70.3\text{ MHz}$ ) enabled the observation of separated ultrasonic phonon satellites ( $\pm 1$ ) for the first time. Furthermore we investigated back-face diffraction (Agamalian, M. et al, Phys. Rev. Lett., 81, 602, 1998) in order to examine possible deformations created by the coupling between transducer and perfect Si crystal. We found that this deformation is moderate and

observed ultrasonic satellites in the back-face regime as well. Dynamical theory calculations were complicated due to the multi phonon scattering (we observed up to  $\pm 4$  ultrasonic satellites) and instability of standard numerical procedures for the case of large, ~8 mm, crystal thickness. Our theoretical results are in a good agreement with experiment.

TP59

#### **Neutron Scattering And thermodynamic Investigations of Hydrogen Adsorbed on or within Nanomaterials**

J. Z. Larese, L. Frazier, R. Cook, R. J. Hinde (University of Tennessee), T. Arnold (Oak Ridge National Laboratory), A. Cuesta-Ramirez (ISIS Pulsed Neutron Facility)

Nanometer scale materials offer neutron scatters significant opportunities to investigate the adsorption or entrainment properties of hydrogen bearing molecular gases and liquids. We report our latest investigations of combined thermodynamic, computation, neutron diffraction and inelastic scattering (INS) studies of the structure and dynamics of H<sub>2</sub> films adsorbed on MgO (100) surfaces and entrained within an oriented, ordered-hexagonal array of cylindrical tunnels within an amorphous carbon material. Our INS studies indicated when H<sub>2</sub> is adsorbed on MgO at low coverage, a prominent peak, is observed at ~11.2meV. For film thicknesses between 0.8 and ~3 layers this peak becomes asymmetric with additional scattering on the high-energy transfer side of the peak. As H<sub>2</sub> is added to the third layer a concomitant growth of a peak at 14.7 meV (i.e. where the para-ortho transition is expected in bulk H<sub>2</sub>) is observed. Recent results for H<sub>2</sub> deposited within the open carbon cylindrical pore network suggest a different behavior. Even at low doses of gas, INS signals are observed in the neighborhood of 14.7 meV. As the gas loading increases a distinct, yet small peak appears at ~13 meV. By combining the INS data with our neutron diffraction results using D<sub>2</sub> on the same materials and with computational efforts we propose adsorption behavior that accounts for our findings. Finally, we indicate what other opportunities exist for future experiments in these areas.

*This work is supported by the Division of Materials Science, Office of Science, Basic Energy Sciences under contract DE-AC05-00OR22725 and the NSF under DMR-0412231. JZL is also a joint faculty member at ORNL.*

TP60

**A GEM of a Neutron Detector**

R. Berliner (Instrumentation Associates), D. DiJulio, A. I. Hawari (North Carolina State University)

A Gd-CsI neutron converter, Gaseous Electron Multiplier (GEM) amplifier, position sensitive neutron detector is currently under development as a candidate system for SNS applications. The detector will be composed of multiple modules, each module consisting of the neutron converter, several cascaded GEMs and an anode pickup plate on both sides of the neutron converter. A CsI-Gd-Kapton-Gd-CsI sandwich converts incoming neutrons to a detectable electronic signal. Kapton forms the mechanical support for the much thinner Gd and CsI layers. Low energy electrons emitted from CsI drift through the cascade of GEM foils and are amplified. The position sensitive anodes and localization electronics are then used to detect, timestamp, and record the resulting signal. It is possible to show that a high efficiency detector can be assembled from multiple modules where each module absorbs only a fraction of the incident neutron beam. The TOF separation for each of the modules is fixed and can be easily offset in hardware or software.

Extensive simulations using Penelope, a Monte-Carlo electron transport code, have been used to optimize the secondary electron emission and therefore the detector performance of the individual modules.[i] These simulations show the relative contribution of the various components of the Gd capture electron spectra and the effect of the thickness of the different elements of the neutron converter itself. The results of the secondary electron simulations will be presented.

Early experiments using the prototype detector at IPNS were only partially successful, stimulating a study of alternative position sensitive anode plate designs. Three position sensitive anode designs have been under consideration. The first is an X-Y pickup anode where the X- and Y-pickup conductors weave from side to side of a simple printed circuit board. This is the "dog-bone" pickup plate. The second is an X-Y anode composed of orthogonal X-Y conductors on opposite sides of a printed circuit board with small holes drilled through where the X- and Y-layer conductors cross. Finally, we have fabricated a 2-D resistive plate

anode. Circuit simulations have been useful in predicting the performance of the anode designs and will be compared to experimental results obtained at the North Carolina State University PULSTAR reactor.

*Work supported under the DOE SBIR Phase-II grant: "A GEM of a neutron Detector", DE-FG02-03ER83685.*

*Salvat, F., Fernandex-Varea, J.M., Acosta, E., and J. Sempau. "PENELOPE-A Code System for Monte Carlo Simulation of Electron and Photon Transport," Workshop Proceedings ,Issyles-Moulineaux, France, ISBN: 92-64-1874-9 (2001).*

TP61

**Conceptual Design of a Time-of-flight Laue Macromolecular Neutron Diffractometer (MaNDi) for the Spallation Neutron Source (SNS)**

P. Thiyagarajan, A. J. Schultz (Argonne National Laboratory, Intense Pulsed Neutron Source), J. P. Hodges (Spallation Neutron Source, Oak Ridge National Laboratory), D. A. Myles (Oak Ridge National Laboratory, Center for Structural Molecular Biology), C. Rehm (American Scientific Instrumentation, Oak Ridge), P. Langan (Los Alamos National Laboratory), A. D. Mesecar (University of Illinois at Chicago, Dept of Medicinal Chemistry and Pharmacognosy)

We have designed a time-of-flight Laue neutron macromolecular diffractometer (MaNDi) for the Spallation Neutron Source (SNS) that is under construction at Oak Ridge National Laboratory. MaNDi is optimized to achieve 1.5 Å resolution from crystals of 0.1 to 1 mm<sup>3</sup> with lattice repeats in the range of 150 Å. We determined that locating MaNDi on a decoupled hydrogen moderator beam line with a curved guide will provide data of higher resolution and higher signal-to-noise than a coupled hydrogen moderator at the SNS. In addition, for an instrument with an initial flight path of 24 m at the 60 Hz source and a wavelength bandwidth of  $\Delta\lambda \sim 2.7$  Å, bandwidth selection disk choppers can shift the wavelength range higher or lower for different experiments. With a wavelength range of 1.5–4.2 Å and  $d_{\min} = 2.0$  Å, simulations predict experiment duration times of 1 to 7 days which is expected to revolutionize neutron macromolecular crystallography (NMC) for applications in the fields of structural biology, enzymology and computational chemistry.

*The US Department of Energy, Basic Energy Sciences–Materials Sciences, supported this work under contract W-31-109-ENG-38 at IPNS, and under contract DE-AC05-00OR22725UT-Battelle at SNS.*

TP62

### **Repetition Rate Multiplication: A New Standard in Inelastic Scattering at Pulsed Sources**

F. Mezei (Los Alamos National Laboratory), M. Russina (Hahn-Meitner Institut)

In order to fully use the available data collection time-of-flight (TOF) neutron spectrometers need to work with typically 50 – 1000 Hz pulse rate on the sample, depending on the incoming neutron wavelength and the distance between sample and detectors. This range of frequencies is most often poorly matched by the pulse source repetition rates. The principle Repetition Rate Multiplication (RRM), i.e. extracting several monochromatic pulses of different neutron wavelengths from a single source pulse, allows us to remedy or reduce this mismatch. A prototype RRM chopper system is being commissioned at LANSCE Lujan Center and the method has been extensively studied by analytic and simulation calculations. These show that, on the one hand side, the optimization of the instrument configuration leads to different results for conventional mode of operation with a single incoming wavelength and for RRM. On the other hand, the use of RRM also substantially enhances the data collection efficiency in instruments configuration optimized for conventional use. The RRM gain  $N$  in data collection rate primarily depends on the source repetition rate, the incoming neutron wavelength range of interest and the moderator to sample distance. This number tends to increase with this distance and, it will already reach substantial values ( $>5$ ) over most of the incoming neutron energy range for relatively short instruments, such as LET planned at the 10 Hz Target Station 2 at ISIS with the moderator to sample distance fixed at 25 m. RRM has by now been adopted both for LET and for several TOF instruments being designed at J-PARC. We will also report on the first neutron beam experiments with the first RRM prototype IN500 at Lujan Center.

TP63

### **User Science Opportunities at the Lujan Neutron Scattering Center at LANSCE**

A. J. Hurd (Los Alamos Neutron Science Center, Los Alamos National Laboratory)

The Lujan Center has a new set of tools for users in neutron scattering and nuclear physics research. These tools further the Center's unique position

for performing user-driven research including national security science. Since 2000, four new scattering instruments have been commissioned and three scattering instruments were substantially upgraded. For nuclear physics and nuclear chemistry, two new instruments have been built; these complement the Isotope Production Facility at LANSCE commissioned in 2004. This new suite of tools, along with user-support facilities in chemistry, x-ray scattering, and Raman scattering, plus new sample-environments in extreme pressure, magnetic fields, and temperature, provide the research community a superb environment to address academic, industrial, and national security issues. The ability to perform research requiring special security is a key unique factor at the Lujan Center. Alliances with Theory Division, the Center for Integrated Nanotechnologies (LANL and SNL), the National High Magnetic Field Laboratory (LANL), and the Molecular Foundry (LBNL) expand the possibilities for applying unique tools to the most challenging problems.

*The Lujan Neutron Scattering Center at LANSCE is funded by the Department of Energy's Office of Basic Energy Sciences and Los Alamos National Laboratory, operated by the University of California under DOE Contract W-7405-ENG-36.*

TP64

### **Competitive solvation of lithium ion in (deuterium oxide + perdeuterated poly(ethylene oxide)) from neutron diffraction with isotopic substitution**

J. M. Simonson, B. K. Annis, Y. S. Badyal (Oak Ridge National Laboratory)

Lithium ion interactions with polymeric solvents are significant in assessing ion transport in polymer-electrolyte electrochemical applications. Due to their small size and high solubility, the solvation environment of lithium ion in aqueous solution is also important as a model system for ion-solvent interactions over wide ranges of solution concentration. To address questions of competitive solvation between aqueous ( $D_2O$ ) and polymeric oxide (poly(ethylene oxide)) environments, we have studied local structure in ternary electrolyte solutions including lithium salt, deuterium oxide, and poly(ethylene oxide), varying the  $Li/D_2O/PEO$  atom ratios to accent specific solvation interactions. Using an annular cylindrical cell geometry to minimize absorption and multiple scattering, isotopic difference experiments with selectively enriched ( $^6Li^+$ ,  $^7Li^+$ ) salts in mixed



solvent. Where sufficient water ( $D_2O$ ) is available to fully hydrate the lithium ion, the resulting local partial structure factor is typical of those observed for aqueous solution. Under water-poor conditions, the local structure factor near lithium ion is more complex and difficult to resolve fully, indicating a mixed solvation environment including both water and polymer sites as first or second neighbors. These results coupled with known salt solubilities in the respective solvents give further insight into the relative solvation interactions of lithium ion with water and polymeric oxides.

#### TP65

### The SNS Magnetism Reflectometer

F. R. Klose, T. Chae, A. Parizzi, H. Lee, R. J. Goyette (Oak Ridge National Laboratory)

The Spallation Neutron Source recently reached an important milestone when, on Friday, April 26, 2006 at 2:04 P.M., the SNS officially became a neutron facility by producing neutrons for the first time.

Among the first three instruments in the user program is the Magnetism Reflectometer. With the official installation completion of the Magnetism Reflectometer in May, 2006, low power commissioning and testing will begin in July, 2006, with initial scientific users expected later this year.

The magnetism reflectometer is designed for polarized neutron reflectometry and high-angle diffraction studies of magnetic thin films, superlattices, and surfaces. The combination of the high-power SNS neutron source and the use of advanced neutron optics will also allow off-specular diffraction and diffuse scattering studies of in-plane structures. Today, even at the world's most advanced neutron sources, such experiments are extremely difficult to perform. Our presentation will give an overview of the major instrument components such as neutron transport system, choppers, polarization circuit, shielding, mechanical design of the spectrometer etc. We will also review scientific opportunities for this next-generation reflectometer that will provide users with up to two orders of magnitude more usable neutron flux than today's best instruments.

#### TP66

### The Denaturation Transition of DNA in Mixed Solvents

B. Hammouda (NIST Center for Neutron Research), D. Worcester (University of Missouri Biological Sciences)

The helix-to-coil denaturation transition in DNA has been investigated in mixed solvents at high concentration using ultra-violet (UV) light absorption spectroscopy and small-angle neutron scattering (SANS). Two solvents have been used: water and ethylene glycol. The "melting" transition temperature was found to be 94°C for 4 % mass fraction DNA/d-water and 38°C for 4 % mass fraction DNA/d-ethylene glycol. Deuterated solvents (d-water and d-ethylene glycol) were used to enhance the SANS signal and 0.1 M NaCl salt concentration was added to screen charge interactions in all cases. The DNA melting transition temperature was found to vary linearly with the solvent fraction in the mixed solvents case. DNA structural information was obtained by SANS including a correlation length characteristic of the inter-distance between the hydrogen-containing (desoxyribose sugar-amine base) groups. This correlation length was found to increase from 8.5 Å to 12.3 Å across the melting transition. Ethylene glycol and water mixed solvents were found to mix randomly inside the solvation region in the helix phase, but non-ideal solvent mixing was found in the melted coil phase. In the coil phase, solvent mixtures are more effective solvating agents than either of the individual solvents. Once melted, DNA coils behave like swollen water-soluble synthetic polymer chains.



T2-A (10:30 am – 12:15 pm)

## Heavy Fermions

Chair: R. Osborn (Turquoise A-B Room)

T2-A (10:30 am)

### Studies on Ferromagnetism in Kondo lattice systems CeNiSb<sub>3</sub> and CeZnSb<sub>2</sub> (Invited)

H. Lee (University of California, Davis), S. Nakatsuji (University of Tokyo, Japan), R. T. Macaluso (Argonne National Laboratory), J. Y. Chan (Louisiana State University), Y. Chen (National Institute of Standards and Technology), W. Bao (Los Alamos National Laboratory), Z. Lynn (National Institute of Standards and Technology), T. Park, E. Bauer (Los Alamos National Laboratory), Z. Fisk (University of California, Irvine)

Ferromagnetic Kondo lattice compounds have got growing interest in regard to their properties compared to the corresponding intensively studied antiferromagnetic materials to broaden current knowledge on heavy fermion system. Unlike the antiferromagnetic cases, where the quantum critical behavior or superconductivity near its quantum critical point appears at certain conditions, ferromagnetic systems studied so far show different behaviors with rather complicated phase diagram. In this talk, I will introduce two ferromagnetic Kondo lattice systems, a canonical type Kondo lattice CeNiSb<sub>3</sub> ( $T_K=6K$ ) and unusual ferromagnetic system CeZnSb<sub>2</sub> ( $T_C\sim 2.3K$ ), presenting magnetic, thermal, transport properties, transport under pressure, and magnetic spin structure of f-electron sites.

T2-A2 (11:00 am)

### Localized magnetic excitation in YbAl<sub>3</sub> (Invited)

J. M. Lawrence, A. D. Christianson, V. R. Fanelli (University of California, Irvine), E. A. Goremychkin, R. Osborn (Argonne National Laboratory), E. D. Bauer, J. L. Sarrao, J. D. Thompson (Los Alamos National Laboratory), C. D. Frost (ISIS, CCLRC), J. L. Zarestky (Iowa State University)

YbAl<sub>3</sub> is an intermediate valence compound with a Kondo temperature  $T_K \sim 600$  K and with a hybridization gap of order  $E_g \sim 30$  meV. We report inelastic neutron scattering results for a single crystal sample performed on both time-of-flight and triple-axis spectrometers. A broad magnetic excitation is observed near  $E_1 = 50$  meV ( $\sim k_B T_K$ ) which at low temperatures qualitatively has the momentum ( $Q$ ) dependence expected for interband scattering across the indirect gap. In the Fermi

liquid state ( $T < T_{coh} \sim 40$  K) a new peak in the scattering occurs at  $E_2 = 33$  meV ( $\sim E_g$ ), which is a weak function of  $2Q$  over a large fraction of the Brillouin zone and is smallest near  $(1/2, 1/2, 1/2)$ . This is *opposite* to what is observed in the Kondo insulators for similar low temperature peaks. We argue that the peak at  $E_2$  arises from a spatially-localized magnetic excitation in the hybridization gap.

T2-A3 (11:30 am)

### Spin Fluctuations in the CeCoIn<sub>5</sub> superconductor

J. Hudis, C. Broholm, C. Stock (Johns Hopkins University)

CeCoIn<sub>5</sub> has the highest superconducting temperature of 2.3 K of any known heavy fermion material [1]. The pairing mechanism is not well understood and studying its magnetic fluctuations is of interest. Through the use of cold neutron inelastic scattering, we find the spin fluctuations are well described by weakly correlated planes of Cerium spins, with the Cerium moment preferentially aligned along [001] direction. The scattering is commensurate and dominated by low energy fluctuations similar to that found in insulating CeIn<sub>3</sub> [2]. These results are different from other CeXIn<sub>5</sub> materials (X=Rh and Ir) where the scattering is incommensurate along [001] presumably due to strong Fermi surface nesting [3]. Comparisons to other Ce systems and transport properties will be made.

[1] C. Petrovic et al. J. Phys. Condens Matter **13**, L337 (2001).

[2] W. Khafo et al. J. Phys. Condens Matter **15**, 3741 (2003).

[3] W. Bao et al. Phys. Rev. B **65**, 100505 (2002).

T2-A4 (11:45 am)

### Composition Dependence of Non-Fermi Liquid Scaling in URu<sub>2-x</sub>Re<sub>x</sub>Si<sub>2</sub> ( $x\sim 0.2-0.35$ )

V. V. Krishnamurthy (Oak Ridge National Laboratory), D. T. Adroja (ISIS Pulsed Neutron Facility), N. P. Butch (University of California, San Diego), R. Osborn (Argonne National Laboratory), S. K. Sinha (University of California, San Diego), J. L. Robertson (Oak Ridge National Laboratory), M. C. Aronson (University of Michigan), M. B. Maple (University of California, San Diego)

Non-Fermi liquid (NFL) scaling in the bulk magnetic, transport, and thermal properties of several f electron systems has been observed at a critical alloy composition, which is known as a quantum critical point. Novel features of NFL behavior have been recently discovered in magnetic, thermal and transport properties of URu<sub>2-x</sub>Re<sub>x</sub>Si<sub>2</sub> [1] whose

magnetic phase diagram shows that hidden order and superconducting transitions are rapidly suppressed with the doping of Re for Ru. NFL behavior, characterized by logarithmic temperature dependence of the electronic specific heat  $C = T$ , and power laws in the temperature dependence of electrical resistivity, appear over a wide range of Re concentrations  $x$  from 0.15 to 0.6 [1]. Because  $\text{URu}_{2-x}\text{Re}_x\text{Si}_2$  has different electronic ground states at different  $x$ , and the NFL scaling has been found over a wide Re doping composition range, it is desirable to know the underlying mechanism for the quantum critical properties. We have investigated the spin dynamics of uranium in  $\text{URu}_{2-x}\text{Re}_x\text{Si}_2$  for the Re composition range  $x = 0.2$  to 0.6 using inelastic neutron scattering. The measurements were performed in the range of 5-300 K using the HET spectrometer at ISIS with an incident energy of 23 meV. We find that the inelastic magnetic scattering from uranium has a strong composition dependence. At  $x=0.2$ , the magnetic scattering is strong, localized in  $q$  and follows  $w/T$  scaling below 100 K. The magnetic scattering is found to be almost uniformly extended in  $q$  for higher Re doping  $x=0.25$  and 0.35. We suggest that short range antiferromagnetic correlations play a role in the onset of a quantum phase transition at about  $x=0.2$  and that their competition with ferromagnetic interactions gives rise to glassy correlations and scaling behaviors in the higher Re doping regime.

[1] E. D. Bauer et al., *Phys. Rev. Lett.* **94** 46401 (2005).

This work was supported by the Oak Ridge National Laboratory, managed by UT-Battelle, LLC, for the US Department of Energy under the Contract No. DE-AC05-00OR22725. Research at UCSD was sponsored by the U.S. Department of Energy under Research Grant No. DE-FG02-04ER46105 and the National Science Foundation under Research Grant No. DMR 0335173 (M.B.M.). This work was supported in part by the Office of Basic Energy Sciences, U.S. Department of Energy Grant No. DE-FG02-03ER46084 (S.K.S.). Research at Argonne National Laboratory was sponsored by the US Department of Energy, Office of Sciences under the Contract No. W-31-109-ENG-38. Work at the University of Michigan is supported under the grant NSF-DMR-0405961.

T2-A5 (12:00 pm)

### Neutron diffraction studies of the complex magnetic phase diagram of single-crystal $\text{Ce}_2\text{Fe}_{17}$

Y. Janssen, A. Kreyssig\*, S. Chang, R. J. McQueeney, V. O. Garlea, J. Zarestky, S. Nandi, A. I. Goldman (Ames Laboratory)

$\text{Ce}_2\text{Fe}_{17}$  shows antiferromagnetic behavior below  $T_N \approx 208$  K [1], which is unlike other, ferro- or ferrimagnetic,  $\text{R}_2\text{Fe}_{17}$  ( $R$  = rare earth) compounds. Magnetization experiments on polycrystalline samples hinted at a rich magnetic ( $H$ - $T$ ) phase

diagram, in which at  $\sim 125$  K a second magnetic-order transition occurs in zero applied fields [2]. Recently, we succeeded to prepare high-quality single crystals. Extensive studies of specific heat, magnetization, electrical resistivity, and x-ray diffraction have revealed a complex and anisotropic magnetic phase diagram.

Here, we report on neutron-diffraction experiments on a  $\text{Ce}_2\text{Fe}_{17}$  single crystal in applied magnetic fields up to 4.5 T applied along the  $a$  axis (hexagonal notation) and for temperatures between 4 K and 300 K. The magnetic structures are characterized by propagation vectors  $(0\ 0\ q)$ , with  $0.5 \leq q < 0.57$ . Just below 125 K, there is a jump in  $q$  along with the appearance of new nuclear reflections indicating a doubling of the crystallographic unit cell in the  $c$  direction, as well as new, corresponding, magnetic satellites. In applied fields, the metamagnetic phase transitions are characterized by shifts in  $q$  and changes in the intensities of all satellite reflections.

Ames Laboratory is operated for the US Department of Energy by Iowa State University under contract number W-7405-ENG-82. The authors thank P. C. Canfield for the thought provoking discussions.

\*Presenting author.

[1] R. Plumier and M. Sougi, *Proceedings of ICM 1973 Moscow* (1973) 487.

[2] Y. Janssen et al., *Phys. Rev. B* **56** (1997) 13716.

T3-A (1:45 - 3:30 pm)

### Biomembranes, Membrane Proteins and Functional Complexes

Chair: D. McGillivray (New Orleans Ballroom)

T3-A1 (1:45 pm)

### Neutron Diffraction from Phospholipid Multilayers, including Crystalline Dimyristoyl-Phosphatidylcholine (Invited)

D. Worcester (University of Missouri Biological Sciences), E. Oldfield, C. Lee (University of Illinois), E. Mihailescu (University of California, Irvine), C. Majkrzak (NIST Center for Neutron Research, Gaithersburg, MD)

Structure and dynamics of phospholipids in membrane multilayer samples are studied using specific covalent deuterium labeling and neutron diffraction. Difference analysis of data from labeled and unlabeled samples provides the positions and Debye-Waller factors for labeled groups even when the Debye-Waller factors are quite large, as in fluid-disordered multilayers. These data allow detailed

and quantitative comparisons with molecular dynamics simulations.

In several multilayer samples prepared for this work, crystallization of the phospholipids after prolonged storage at low temperature has been discovered. Sharp in-plane diffraction to about 3Å resolution was found for samples of dimyristoyl-, dipalmitoyl- and dilauryl-phosphatidylcholine and was also found for samples containing cholesterol, in which separation into cholesterol-free crystals of phospholipids and cholesterol-rich phospholipid multilayers occurred. Lamellar diffraction extends to 1.5Å resolution. Constant Q scans for samples of dimyristoyl-phosphatidylcholine using AND/R at NIST show that the samples are 3D crystals, rather than (2+1)D crystals of the subgel phase. The crystals are stable at room temperature and relative humidity in the range 40 to 86%, but at high humidity, they revert to multilayers with 1D periodicity and if then returned to lower humidity and stored at low temperature, 3D crystals form once again. The long (lamellar) repeat spacing of the crystals is constant for relative humidity from 50 to 86%.

The crystal domains have the long axis oriented normal to the thin glass substrates with mosaic spreads of 1.5° to 5°, much as the original multilayer samples were oriented. The domains have full rotational disorder about the long axis (2D powder). The crystals are monoclinic, space group P2<sub>1</sub>, a=9.35Å, b=8.72Å, c=54.7Å, beta=90°±1°. The thin glass substrates allowed measurements in transmission by X-ray and neutron diffraction and Fourier Transform Infra-red Spectroscopy (FTIR). This has helped clarify some previous discrepancies between diffraction studies and FTIR studies. Deuterium labeled samples allowed direct structural analysis by neutron diffraction. Debye-Waller factors, determined by deuterium label difference methods and least squares fitting in reciprocal space, were found to be similar to values for single crystal phospholipid structures solved by X-ray diffraction. Some aspects of the structure are similar to the previous single crystal structure for dimyristoyl-phosphatidylcholine (Pearson and Pascher, 1979) but there are also surprising differences. Because the new crystals are formed from multilayers of bilayers, rather than organic solvents, relating the crystal structure to bilayer structure should be reliable.

*This work was done as part of the CNBT project, supported by the National Institutes of Health under grant no. 1 R01 RR14812 and the Regents of the University of California. DW was supported by UC-Irvine while on research leave.*

T3-A2 (2:15 pm)

**pH-dependent conformational changes and insertion of diphtheria toxin adsorbed to lipid membranes by neutron and X-ray reflection (Invited)**

M. S. Kent, Y. Yim, J. K. Murton (Sandia National Laboratories), S. Satija, D. McGillivray, C. F. Majkrzak (NIST Center for Neutron Research), M. Loesche (Johns Hopkins University), I. Kuzmenko (Argonne National Laboratory), J. Majewski (Los Alamos Neutron Science Center, Los Alamos National Laboratory)

The bacterial toxins botulinum, tetanus, and diphtheria are among the most poisonous biological substances known. They each contain separate domains for receptor-specific binding, translocation, and enzymatic activity. All three toxins are taken up into endosome-like acidic compartments, where the translocation domains insert into the endosomal membranes and release the catalytic domains into the cytosol of the respective target cells. It has been shown that each of these toxins accomplishes translocation of the enzyme without the aid of other cellular proteins. This raises the interesting question as to how these biochemically distinct toxins accomplish this same challenging goal. The processes by which the enzymes are translocated across the endosomal membrane are known to involve pH-induced conformational changes within (at least) the translocation (T) domain. While some important information has been discovered about this process, it is not known how the relatively large enzymes are able to pass through the endosomal membrane. It is not known whether the enzymes unfold or whether they refold in an altered configuration that facilitates translocation. Neutron and X-ray reflectivity (NR and XR) can supply direct structural information on the toxins as they adsorb and subsequently undergo pH-dependent conformational changes to insert and translocate their enzymes. In this study we examined the binding, conformational changes, and insertion of DT (CRM197) interacting with Langmuir monolayers of DPPG as a function of pH at a constant pressure of 30 mN/m. This mutant form of DT results from a single base change in the structural gene resulting in the substitution of glutamic acid for glycine in the C-domain, rendering

the protein nontoxic. The data provide intriguing details of the conformational changes with pH, but represent just the beginning of the insights that will come with further measurements. The present data clearly show several stages of conformational change as a function of pH (including increase and subsequent decrease in the thickness of the outer layer and collapse and insertion of the inner layer), and pH ranges over which little conformational change occurs.

*T3-A3 (2:45 pm)*

### **Reflectometry Studies of Membrane Protein Arrays at the Liquid Solid Interface**

S. A. Holt (ISIS, CCLRC), J. H. Lakey (School of Cell and Molecular Biosciences, The Medical School, The University of Newcastle-upon-Tyne, United Kingdom), D. J. McGillivray, C. F. Majkrzak (National Institute of Standards and Technology)

We have been studying the nanoscale structure of an outer membrane protein (OmpF) from *E. coli*, embedded within a lipid matrix at the solid liquid interface. [1,2] This project relies upon the directed self assembly of the OmpF into trimers on a gold surface. The OmpF has been engineered so that a single cysteine residue is inserted into one of the periplasmic loops enabling a chemical binding to the gold substrate. The aim is to use the protein's voltage gated channels to connect to the conductive gold surface in the development of medical sensing devices. As the maximum measured surface coverage is circa 55 % [3] the space between the OMPF trimers must be 'filled in' with insulator. This is done by the insertion of a thiolipid which attaches to the gold surface via sulfur chemistry resulting in a densely packed surface where the impedance across the layer is determined by the state of the OMPF channels. [1]

A key aspect of this work is that the protein assembly is directed and that the tertiary conformation and orientation relative to the substrate is controlled. Given the nature of the structures formed and the orientational control Neutron Reflectometry (NR) presents and excellent method to study in situ the structure of these assemblies. The precision of our previous measurements had been limited primarily by substrate preparation. This issue has been addressed in the current work, in addition we have collected data using magnetic reference layers which will enable direct inversion of the

datasets. The initial analysis of these datasets, via simultaneous fitting with box models, has demonstrated excellent quality substrates with an increased surface coverage of protein compared to our previous series of experiments.

The iron/gold coated silicon is first coated with a layer of  $\beta$ -mercaptoethanol (BME), rendering the surface hydrophilic. The sensitivity of the magnetic reference layer approach is such that a BME layer is required to be included in the fit for the substrate prior to OMPF adsorption. This layer is also required after protein adsorption with a reduced volume fraction to account for protein adsorption. This is direct evidence that the protein adsorption does not completely remove the BME. This presentation will describe the work and the progress that has been made with the direct inversion approach

[1] S. Terrettaz, W.-P. Ulrich, H. Vogel, Q. Hong, L. G. Dover, J. H. Lakey, *Protein Science* 2002, **11**, 1917.

[2] S.A. Holt, J.H. Lakey, S.M. Daud, N. Keegan, *Aus J. Chem.* 2005, **58**, 674.

[3] F. A. Schabert, C. Henn, A. Engel, *Science* 1995, **268**, 92.

*T3-A4 (3:00 pm)*

### **Amyloid $\beta$ Peptide - Mechanisms of Alzheimer's Toxicity**

F. Heinrich, D. J. McGillivray (Carnegie Mellon University and CNBT at the NIST Center for Neutron Research), J. E. Hall (University of California, Irvine), M. Loesche (Carnegie Mellon University and CNBT at the NIST Center for Neutron Research)

Amyloid plaques associated with dead or damaged neurons are a characteristic property of neuronal cells suffering from Alzheimer's disease. A major component of these plaques is the  $\beta$ -amyloid peptide (1-42), which is widely accepted to play a key role in the progress of Alzheimer's disease. It has recently been shown that soluble oligomers are the primary toxic species of amyloid, although the actual mechanism of cell toxicity remains unclear [1]. Generally, two contrary hypotheses exist: either  $\beta$ A forms ion channels in the membrane [2] or  $\beta$ A leads to membrane thinning and disruption [3]. Neutron reflectivity is able to test both hypotheses by measuring bilayer thickness and completeness in presence of  $\beta$ A oligomers. The neutron experiments presented here reveal interactions of  $\beta$ A with artificial cell membranes using a well-characterized tethered lipid bilayer system which show thinning of the membrane, and



at high  $\beta$ A oligomer activity destruction of the outer lipid leaflet, without evidence of pore formation.

[1] R. Kaye *et al.*, *Science* 300:486 (2003)

[2] S. Micelli *et al.*, *Biophys. J.* 86:2231 (2004)

[3] R. Kaye *et al.*, *J. Biol. Chem.* 279:46363 (2004)

T3-A5 (3:15 pm)

### Neutron Diffraction Studies of Fluid Bilayers with Transmembrane Proteins: Structural Consequences of a Pathogenic Amino Acid Mutation

K. Hristova, X. Han (Johns Hopkins University)

We have used neutron diffraction to determine the disposition of transmembrane proteins in fluid lipid bilayers. In particular, we have investigated whether the Gly380Arg mutation in the fibroblast growth factor receptor 3 (FGFR3) transmembrane (TM) domain, a mutation known as the cause for human dwarfism, affects protein topology by introducing a shift in the TM segment. To do so, we have selectively deuterated two consecutive amino acids, Phe384/Leu385, in both wild-type and mutant FGFR3 TM domains and we have determined their depths of penetration in 1-Palmitoyl-2-Oleoyl-sn-Glycero-3-Phosphocoline (POPC) bilayers along the bilayer normal using neutron diffraction. Furthermore, the depth of penetration of Leu388/Val389/Val390 of the mutant TM domain was also determined to unambiguously position the mutant TM domain with respect to the bilayer center. Our results demonstrate that, at 76% relative humidity, the Arg380 mutation induces a slight shift of the TM domain by about 2 amino acids. The center of the TM segment is close to the mid-point between Arg380 and Arg397, in agreement with measurements of Arg insertion energetics into the ER.

Supported by NIH GM 068619

T3-B (1:45 – 3:30 pm)

### Structure and Dynamics of Hydrogen Bonded Systems

Chair: S.-H. Chen (Amphitheater)

T3-B1 (1:45 pm)

#### The relationship between intermediate and short range order in amorphous ice, silicon and germanium (Invited)

C. J. Benmore, R. T. Hart (Argonne National Laboratory, Intense Pulsed Neutron Source), C. A. Tulk (Spallation Neutron Source, Oak Ridge National Laboratory), D. D. Klug (NRC, Ottawa, Canada)

Pulsed neutron and high energy x-ray diffraction have been employed to investigate the relationship between local structure and network formation in amorphous ice as a function of density. An analogy is made with the structures of liquid and amorphous Silicon and Germanium. The role of interstitial molecules (or atoms) between the first and second shells is shown to greatly affect the extent of intermediate range order.

T3-B2 (2:15 pm)

#### Quasielastic and inelastic neutron scattering investigation of fragile-to-strong crossover in deeply supercooled water confined in nanoporous silica matrices (Invited)

L. Liu, S. Chen (Massachusetts Institute of Technology), A. Faraone (NIST Center for Neutron Research), C. Yen, C. Mou (National Taiwan University), A. Kolesnikov (Intense Pulsed Neutron Source, Argonne National Laboratory), J. Leao (NIST Center for Neutron Research)

It has been predicted by Molecular Dynamics simulations of various phenomenological water models that there is a liquid-liquid transition between two structurally distinct states of water at low temperature: the high-density liquid (HDL) and the low-density liquid (LDL). The end point of this first-order liquid-liquid coexistence line is the proposed second low-temperature critical point of water as opposed to the well-known high temperature gas-liquid critical point. Up to now, the proposed second critical point was never found experimentally because it lies in the inaccessible supercooled temperature range of water. By confining water in nano-pores of silica glass MCM-41, we succeeded in bypassing the crystallization process and were able to study the dynamics of water in this inaccessible range of temperatures.

The behavior of shear viscosity or equivalently the



structural relaxation time of a supercooled liquid as it approaches the glass transition temperature is called 'fragile' if it exhibits non-Arrhenius temperature dependence; on the other hand, if shear viscosity or the structural relaxation time obeys Arrhenius law, the behavior is called 'strong'. The fragile behavior is typical to systems with ionic and van der Waals type interactions. In contrast, a liquid characterized by strong behavior has its structural makeup controlled by a strong covalent bond, or by a directional hydrogen bond, which results in an open tetrahedral structure.

We investigated, using quasi-elastic and inelastic neutron scattering, the slow single-particle dynamics of water confined in lab synthesized nanoporous silica matrices, MCM-41-S, with pore diameters ranging from 10 Å to 18 Å. Inside the pores of these matrices, the freezing process of water is strongly inhibited down to 160 K. We analyzed the quasi-elastic part of the neutron scattering spectra with a relaxing-cage model and determined the temperature and pressure dependence of the Q - dependent translational relaxation time and its stretch exponent for the time dependence of the self intermediate scattering function. The calculated Q-independent average translational relaxation time shows a fragile-to-strong (FS) dynamic crossover for pressures lower than 1600 bar [1, 2]. Above this pressure, it is no longer possible to discern the characteristic feature of the FS crossover. Identification of this end point with the predicted second low-temperature critical point of water is discussed [2]. A subsequent inelastic neutron scattering investigation of the librational band of water indicates that this FS dynamic crossover is associated with a structural change of the hydrogen-bond cage surrounding a typical water molecule from a denser liquid-like configuration to a less-dense ice-like open structure.

*This subject will be presented in a student poster as well.*

[1] A. Faraone, L. Liu, C. Y. Mou, C.-W. Yen, and S.-H. Chen, *J. Chem. Phys. Rapid Comm.* **121**, 10843 (2004).

[2] L. Liu, S.-H. Chen, A. Faraone, C.-W. Yen, and C.-Y. Mou, *Phys. Rev. Lett.* **95**, 117802 (2005).

T3-B3 (2:45 pm)

### **Water in carbon nanotubes, new results and anomalies**

A. I. Kolesnikov, C. K. Loong, N. R. de Souza (Argonne National Laboratory, Intense Pulsed Neutron Source), C. J. Burnham, G. Reiter (The University of Houston), E. Mamontov (National Institute of Standards and Technology), J. Mayers, M. A. Adams (ISIS Pulsed Neutron Facility)

The incorporation of water into carbon nanotubes provides a simple analogue of biologically important trans-membrane channels and so is of large interdisciplinary scientific interest. Recently [1] we have studied quasi-1D water inside single-walled carbon nanotubes (SWNT) of 14 Å diameter, here referred to as nanotube-water, by means of neutron scattering and MD simulations (performed using the TTM2-F polarizable flexible water model with smeared charges and dipoles). The observed extremely soft dynamics of nanotube-water at low temperatures were consistent with the MD model that includes shell water molecules near the inner wall of the nanotubes plus a central water-chain structure. It was found that these chain water molecules are responsible for the observed large mean-square displacements which are a result of their low coordination and weak bonding to the outer shell.

Here we extend this research to water confined in SWNT of different diameters, at different pressures (P) and temperatures (T). Using a 'parallel tempering' MD algorithm, we calculated the structural and dynamical properties of nanotube-water from low to high temperatures, which clearly showed a phase transition from high to low density liquid at  $T_c \approx 200$  K, and that above  $T_c$  the structure becomes a disordered H-bonded network similar to the bulk liquid.

The T dependence of the relaxation time for water in the 14 Å SWNT measured with backscattering spectrometer exhibits a crossover at 218 K from a Vogel-Fulcher-Tamman (VFT) law to an Arrhenius law, indicating a fragile-to-strong liquid transition. On the other hand, water in the 16 Å nanotubes obeyed a VFT law at least down to 195 K.

The measured vibrational spectra of nanotube-water at  $P=3.7$  kbar and 40 K show features similar to high-density amorphous ice. MD simulations under pressure reproduce well the observed phenomena and show large change in nanotube-water structure: it becomes more dense (by ~30%) like bulk ice.

Deep inelastic neutron scattering (DINS) shows that at low T the momentum distribution for nanotube-water protons is much narrower compared to other forms of bulk water/ice, reflecting their large spatial delocalization. Furthermore, the kinetic energy of ground-state water protons at 5 K is about 30% smaller than in other ice forms. Thus, DINS showed that the quantum state of the nanotube-water is qualitatively different from that of any phase of water seen so far, and a possible explanation is discussed.

[1] A.I. Kolesnikov et al., *Phys. Rev. Lett.* **93**, 035503 (2004).

T3-B4 (3:00 pm)

### Structural phase transitions and hydrogen bonding in hexaquoazinc(II) hexafluorosilicate

A. I. Acatrinei, M. A. Hartl, L. L. Daemen, J. Qian, J. Zhang (Los Alamos National Laboratory)

In Si chemistry, the octahedral coordination is fairly unusual. Although it has been postulated that Si coordinates to O octahedrally at extremely high pressures deep in the Earth mantle, no known Si compound exists at ambient conditions in this state. Hexafluorosilicates, such as zinc hexafluorosilicate  $[\text{Zn}(\text{H}_2\text{O})_6][\text{SiF}_6]$  could act as surrogate materials to study Si in this six-fold coordination state in hydrated materials.

Hexafluorosilicates crystallize in a distorted CsCl-type structure at room temperature, consisting of  $\text{M}(\text{H}_2\text{O})_6^{2+}$  and  $\text{SiF}_6^{2-}$  octahedra coupled by hydrogen bonds [1]. The relative arrangement of the octahedra with respect to each other determines the space group the respective hexafluorosilicate crystallizes in. The hydrogen bonding network plays an important role in determining the arrangement of octahedra and therefore helps explaining the structural phase transitions in hexafluorosilicates with changing temperature and pressure.

We observed the behavior of  $[\text{Zn}(\text{H}_2\text{O})_6][\text{SiF}_6]$  as a function of temperature by collecting incoherent inelastic neutron scattering spectra at the Filter Difference Spectrometer FDS in the temperature range from 10 K to 270 K. The changes in the hydrogen bonding network due to the second order phase transition at 170 K can be observed in the vibrational spectra.

Diffraction patterns of  $[\text{Zn}(\text{D}_2\text{O})_6][\text{SiF}_6]$  at two different temperatures (one above and one below the phase transition) were collected on the Neutron

Powder Diffractometer, NPDF at LANSCE. Although the crystal structure of  $[\text{Zn}(\text{H}_2\text{O})_6][\text{SiF}_6]$  [2] and the phase transition from alpha-R-3 to beta-R-3 [1] has been determined by X-ray diffraction before, neutron diffraction allowed us to determine the exact hydrogen positions in the structure. The pair distribution function (PDF) was extracted and gives further information on the hydrogen bonding in our compound.

Additionally, X-ray diffraction data collection was done at the high-pressure beamline X17B2 at NSLS. We measured the sample at temperatures between r.t. and 700°C and pressures up to 8.7 GPa. temperature from to and could observe changes in the structure.

[1] Kamenev et al., *J. of Phys.: Condens. Matter*, **13**, 2001, 3709-3716

[2] Ray et al., *Acta Cryst. B* **29** (1973) 2741.

T3-B5 (3:15 pm)

### Translational dynamics of surface water in oxides: A quasielastic neutron scattering study

E. Mamontov (Spallation Neutron Source, Oak Ridge National Laboratory)

While neutrons is traditionally considered a bulk probe, we demonstrate that the mobility of surface water on oxide nano-powders can be investigated using quasielastic neutron scattering. We discuss how the reduced number of hydrogen bonds per water molecule associated with surface confinement leads to a qualitative modification of single-particle translational dynamics compared to bulk water. The mobility of surface water in zirconium oxide with two hydration layers present is discussed in detail. The outer hydration layer exhibits translational dynamics on the time scale of tens of picoseconds, and thus can be studied using time-of-flight neutron spectrometry. The translational dynamics of the inner hydration layer in the range of hundreds of picoseconds can be assessed with backscattering neutron spectrometry. Interestingly, despite being slower by two orders of magnitude, the translational motion of the molecules of the inner hydration layer may share more common traits with bulk water compared to the motion of the outer hydration layer, the dynamics of which is slower than that of bulk water by just one order of magnitude. Similar to bulk water, the temperature dependence of the residence time for the water molecules of the inner hydration layer is non-Arrhenius, and

can be described by a Vogel-Fulcher-Tammann (VFT) law. On the other hand, the molecules of the outer hydration layer demonstrate Arrhenius-type temperature dependence indicative of thermally activated surface jump diffusion. Our recent study of surface water on cerium oxide, which exhibits faster dynamics compared to water on zirconium oxide, has ventured into the low-temperature region (down to 200 K). Below 215 K, we have found a deviation from the VFT temperature dependence for the residence time indicative of a surprise “fragile”-to-“strong” transition in the surface water. While “fragile”-to-“strong” transition has been predicted and observed in supercooled bulk water, there has been no prediction of such a transition in surface water. We discuss the links between our results and recent work on hydration water in carbon nanotubes and proteins.

*T3-C (1:45 – 3:15 pm)*

### **Thin Film Magnetism**

*Chair: J. Borchers (Ruby Room)*

*T3-C1 (1:45 pm)*

### **Neutron reflectivity studies of magnetic semiconductor superlattices (Invited)**

T. M. Giebultowicz (Oregon State University), H. Kepa (Warsaw University, Poland)

Magnetic semiconductors (MSCs) – and, especially, thin film and multilayered forms made of MSCs – currently receive much attention because such systems are expected to play a crucial role in future spin electronics (spintronics). There are several possible ways in which neutron scattering tools may be employed for investigating these thin film forms. For instance, neutron reflectometry may be used for studying interlayer magnetic coupling effect, and reveal details about the magnetic domain structure that forms in the ultrathin MSC layers. We will present the results of such studies we have carried out on the NG-1 reflectometer at NIST, with particular emphasis on EuS-based superlattices (SLs). We have investigated SL specimens in which the ferromagnetic EuS layers were separated by two different non-magnetic semiconducting spacer materials – PbS (narrow-gap) or YbSe (wide gap). In both these systems the measurements revealed pronounced antiferromagnetic coupling between

the EuS layers. Since the concentration of carriers in the systems is very low, the coupling cannot be caused by RKKY interactions, as is the case in magnetic/nonmagnetic metallic SLs. Taking advantage of the fact that the electronic band structure of the constituent materials is quite well known, our collaborators performed theoretical calculations which led to the conclusion that the coupling is maintained by valence electrons. The model results have been found to be in good qualitative agreement with the experimental data. The in-plane magnetic anisotropy and the population of the magnetic domains in the EuS/PbS and EuS/YbSe systems was studied by polarized neutron reflectivity. We will also briefly discuss the results of similar studies on another ferromagnetic/nonmagnetic all-semiconductor SL system, Ga(Mn)As/GaAs. Finally, we will present a brief overview of some recent developments in the synthesis of new ferromagnetic semiconductor thin film forms, and we will discuss the possibilities of employing neutron scattering tools in studies of such systems.

*T3-C2 (2:15 pm)*

### **Inhomogeneous Magnetization Profiles in $\text{La}_{0.7}\text{Ca}_{0.3}\text{MnO}_3/\text{YBa}_2\text{Cu}_3\text{O}_{7-\delta}$ Superlattices (Invited)**

S. G. E. te Velthuis, A. Hoffmann (Argonne National Laboratory), V. Peña, D. Arias, C. Leon, Z. Sefrioui, J. Santamaria (Universidad Complutense de Madrid), N. M. Nemes, M. García Hernández, J. L. Martínez (Instituto de Ciencia de Materiales de Madrid (ICMM-CSIC)), M. R. Fitzsimmons (Los Alamos National Laboratory), S. Park, B. Kirby (Los Alamos Neutron Science Center, Los Alamos National Laboratory), M. Varela (Oak Ridge National Laboratory)

The interplay between ferromagnetism and superconductivity has been of longstanding research interest, since the competition between these generally mutually exclusive types of long-range order gives rise to a rich variety of phenomena. In particular, layered systems enable a straight-forward combination of the two types of long-range order. There is interest in studying these effects in superlattices of high  $T_c$  superconductors and colossal magnetoresistance oxides, where the superconducting and ferromagnetic properties depend strongly on the charge carrier density and thus charge transfer across the interface may be important. Recent studies of  $\text{La}_{0.7}\text{Ca}_{0.3}\text{MnO}_3$  (LCMO) manganite and high  $T_c$  superconducting  $\text{YBa}_2\text{Cu}_3\text{O}_{7-\delta}$  (YBCO) superlattices have found evidence of this interplay. Insight into these phenomena is

obtained by polarized neutron reflectivity (PNR) experiments, from which the depth dependent magnetization profiles of the superlattices are determined. In epitaxial tri-layers an unexpected magnetoresistance in excess of 1000%, was found below the superconducting transition. With PNR, differences in the magnetization profiles of the two LCMO layers is observed, as well as antiferromagnetic alignment during the magnetization reversal process, which correlates with the large magnetoresistance. Furthermore, PNR determined an inhomogeneous magnetization profile within the LCMO layers. Specifically, the magnetization in each LCMO layer is suppressed close to the interfaces with the YBCO, which can be correlated to charge transfer across the interface.

*Work supported by MCYT MAT 2005-6024, CAM GR- MAT-0771/2004, UCM PR3/04-12399 and by the U.S. Department of Energy, Basic Energy Sciences under contracts W-31-109-ENG-38, W-7405-ENG-36, and DE-AC05-00OR22725.*

T3-C3 (2:45 pm)

### **Polarized Neutron Reflectometry Analysis of Spin Valves with Ultra Thin Antiferromagnetic Layers**

S. M. Watson (NIST Center for Neutron Research), S. M. Moyerman (Harvey Mudd College), J. A. Borchers, M. Doucet (NIST Center for Neutron Research), W. Gannett (Harvey Mudd College), M. J. Carey (Hitachi Global Storage Technologies), P. D. Sparks, J. C. Eckert (Harvey Mudd College)

We have investigated exchange-biased spin valves (EBSV) with ultra thin antiferromagnetic (AF) layers using Polarized Neutron Reflectivity (PNR). A simple spin valve consists of a free ferromagnetic (FM) layer, a non-magnetic spacer layer, and a pinned ferromagnetic layer adjacent to an AF layer. As a result of coupling between the pinned FM and AF layers, the magnetic hysteresis loop of the pinned layer is shifted by a value known as the exchange-bias field, causing it to be asymmetrical about zero field. Magnetoresistance studies at 5 K have verified the presence of exchange bias in spin valves with AF layers as thin as 0.4 nm at 5 K [1], suggesting that exchange biasing is an interfacial effect. To probe the nature of the interfacial coupling and domain wall formation, we have studied the field-dependent magnetic structure of EBSV samples using PNR, which is sensitive to the depth-dependent vector magnetizations of individual FM layers on sub-nanometer length scales. Our previous PNR studies of a spin valve with a 1.6 nm antiferromagnetic IrMn layer [2]

reveal that a vertical domain wall develops in the pinned  $\text{Co}_{86}\text{Fe}_{14}$  layer near the FM/AF interface after magnetic training (i.e., field cycling). We have extended our PNR investigations to an EBSV with an ultra thin AF layer (0.6 nm) and an overall structure of Si/5 nm Ta/3 nm  $\text{Ni}_{80}\text{Fe}_{20}$ /1 nm  $\text{Co}_{60}\text{Fe}_{40}$ /3 nm Cu/3 nm  $\text{Co}_{60}\text{Fe}_{40}$ /0.6 nm IrMn/1 nm Cu/5 nm Ta deposited by DC magnetron sputtering. Measurements were performed at 5K for several points along the magnetic hysteresis loop after field cooling in -4.2 kG. Analysis of the PNR data reveals parallel alignment of the ferromagnetic CoFe layers in saturating fields, as expected. Upon increasing the field to 165 G, the pinned and free FM layers align antiparallel, giving rise to an increased magnetoresistance. The antiparallel alignment and magnetoresistance maximum persist in fields larger than 400 G. During a second field sweep, significant spin-flip scattering signals the development of a spiral domain wall. The resultant magnetic structure differs noticeably from the simple antiparallel alignment of the FM layers during the first sweep, and this change correlates with a reduced maximum of the magnetoresistance. High-field saturation clearly has a significant effect on the pinning of the CoFe layer by the neighboring IrMn. The pitch and span of the spiral domain wall will be compared to that of a similar spin structure that develops in an spin valve with a 0.4 nm IrMn layer which does not exhibit exchange biasing.

[1] K. L. Purdue, M. J. Carey, P. D. Sparks, and J. C. Eckert, *IEEE Trans. On Magnetics* **41**, 2706 (2005)

[2] S. Moyerman, J.C. Eckert, J.A. Borchers, K.L. Purdue, M. Doucet, P.D. Sparks, M.J. Carey, *J. Appl. Phys.* (in press).

T3-C4 (3:00 pm)

### **High pressure neutron inelastic scattering investigations of exchange interactions in diluted semimagnetic semiconductors Zn(Mn)Te, Zn(Mn)S, and Zn(Mn)O**

Z. Wiren (Oregon State University), H. Kepa (Warsaw University, Poland), C. M. Brown, J. Leao (NIST Center for Neutron Research), S. Kolesnik, B. Dabrowski (Northern Illinois University), J. K. Furdyna (University of Notre Dame), T. M. Giebultowicz (Oregon State University)

The intrinsic antiferromagnetic (AFM) interactions between nearest-neighbor Mn ions in Zn(Mn)O, Zn(Mn)S and Zn(Mn)Te have been studied by inelastic neutron scattering at ambient pressure and at 4 kbar.

Because of the emergence of spintronics technology there is a renaissance of interest in



studying the exchange interactions in magnetic semiconductors. Material technologists in many labs are attempting to “make semiconductor ferromagnetic” (FM) by substituting some part of their non-magnetic atoms by magnetic ions, and to introduce high concentration of carriers into their lattices that would give rise to RKKY-type FM interactions between these ions. However, in addition to the carrier-induced FM exchange, in such alloys there are always intrinsic exchange interactions that exist even in the insulating state, and are virtually insensitive to the presence of carriers. They are produced by a superexchange mechanism mediated by intervening anions, and are almost always AFM. In order to obtain a material that is ferromagnetic, the carrier-induced FM component has to overcome that intrinsic antiferromagnetism. Hence, the characterization of the AFM intrinsic exchange, as well as good understanding of the physical mechanisms underlying this interaction, are certainly of considerable current importance. In a recent paper [1], Szuszkiewicz et al. have presented a thorough analysis of the existing Mn-Mn AFM exchange interactions data from the family of diluted magnetic semiconductors based on the II-V compounds. The analysis revealed one intriguing fact - namely, when the  $J$  values from sulfides, selenides and tellurides are plotted vs. spin-spin distance  $R$  in the same figure in log-log scale, all points fall practically on the same line - in other words, all those superexchange interactions somehow “ignore” the fact that they are mediated by three different anions. In order to obtain more experimental insight into this issue, and, in particular, to find how the  $J$  values in a single alloy change when the Mn-Mn distance  $R$  decreases, we have launched systematic measurements of the nearest-neighbor exchange constants  $J_1$  in these alloys using inelastic neutron scattering spectrometry. This technique (described in detail in Ref. [2]) enables one to directly determine the  $J_1$  value with an excellent accuracy. We present the  $J_1$  data so far obtained at 4 kbar for the three aforementioned systems, as well as the result of measurements of the pressure dependence of the Mn-Mn distance. We discuss the findings from our experiments in the context of the analysis presented in the paper by Szuszkiewicz et al. [1].

- [1] W. Szuszkiewicz, E. Dynowska, B. Witkowska, B. Hennion, *Spin-wave measurements on hexagonal MnTe of NiAs type by inelastic neutron scattering*, *Phys. Rev. B* (in print).
- [2] H. Kępa, Le Van Khoi, C. M. Brown, M. Sawicki, J. K. Furdyna, T. M. Giebultowicz, T. Dietl, *Probing hole-induced ferromagnetic exchange by inelastic neutron scattering*, *Phys. Rev. Lett.* **91** (2003) 0807205.

T3-D (1:45 – 3:15 pm)

## Modeling and Simulation of Nanostructured Materials

Chair: N. Balsara (Turquoise A-B Room)

T3-D1 (1:45 pm)

### Multiscale Simulations of Block Copolymer Micelles (Invited)

G. D. Smith (University of Utah)

Poly(ethylene oxide)/poly(propylene oxide)/poly(ethylene oxide) triblock copolymers (Pluronic) form micelles in aqueous solution. Self-assembly of Pluronic unimers into (usually) spherical micelles occurs with increasing temperature and Pluronic concentration and is driven by the decreasing quality of water as a solvent for poly(ethylene oxide) and poly(propylene oxide) with increasing temperature. Further increase in temperature results in significant intermicellar attraction that leads to gelation and ultimately to the formation of micellar crystals. Numerous neutron scattering studies have been performed on Pluronic/water solutions in order to better understand the structure of Pluronic micelles and the hierarchical self-assembly exhibited by these fascinating and important materials. Interpretation of the neutron structure factor is greatly complicated by the need to assume models for both the micelle form factor and the intermicellar structure factor. We have carried out multiscale simulations of Pluronic micelles and micellar assemblies using coarse-grained models that were systematically parameterized to reproduce the structure of fully atomistic molecular dynamics simulations of Pluronic solutions. The structure factors obtained from our multiscale simulations are in good agreement with those obtained from neutron scattering and can be interpreted without resorting to arbitrary structural models, yielding new insight into the structure of Pluronic micelles and the nature of intermicellar interactions.



T3-D2 (2:15 pm)

**Nanoscale magnetic order in perovskite cobaltites**  
(Invited)

D. Louca (University of Virginia)

The class of perovskite oxides that display high magnetoresistance (MR) in the presence of an applied external field is governed by phenomena such as phase separation, charge/spin stripe formation and competing interactions between tendencies for strong localization via polaron formation and metallic itineracy. In one class of perovskites, the cobaltites, the colossal MR (CMR) response remains mysteriously suppressed. We examine the possibility of the reduced CMR effect relating to an ordering phenomenon of spins and possibly charge carriers, and show evidence for nanoscale magnetic superstructures. Cold inelastic magnetic neutron scattering results will be presented to show a novel and peculiar effect in  $\text{La}_{1-x}\text{Sr}_x\text{CoO}_3$  that appears below the magnetic ordering temperature.

T3-D3 (2:45 pm)

**Inter-droplet potential in a microemulsion evaluated by the relative form factor method**

M. Nagao (University of Tokyo, Japan), H. Seto (Kyoto University), N. L. Yamada (High Energy Accelerator Research Organization)

The “relative form factor” is a new method proposed by the authors in order to analyze small-angle scattering data without assuming any structure factors. In cases of monodisperse systems, the relative form factor can be obtained by the ratio of two scattering intensities obtained by different scattering contrasts. The relative form factor does not include the information of the structure factor since the structure factor does not depend on the contrast. Usually, the form factor can be modeled easier than the structure factor, and the form factor for each scattering contrast can be extracted from the relative form factor. Once the form factor is determined, the structure factor can be calculated. Thus, it is possible to deduce the interaction potential between scatterers by this method. In order to demonstrate the possibilities of this method, the droplet density dependence of the structure of AOT/water/decane microemulsion is investigated. The droplet concentration,  $C$ , dependence of the form factor and structure factor is discussed at  $0.05 < C < 0.75$ . The result implies that the inter-droplet interaction can be explained by the model with sticky soft core potential.

T3-D4 (3:00 pm)

**Quasielastic neutron scattering study of the dynamics of 1,3-diphenylpropane grafted to the pore surface of MCM-41**

E. J. Kintzel, K. W. Herwig (Spallation Neutron Source, Oak Ridge National Laboratory), M. K. Kidder, A. C. Buchanan III, P. F. Britt (Oak Ridge National Laboratory), A. Chaffee (University of Monash)

An initial study of the dynamics of 1,3-diphenylpropane (DPP,  $\text{Si-O-C}_6\text{H}_4(\text{CH}_2)_3\text{C}_6\text{H}_5$ ) attached to the surface of the mesoporous silica MCM-41 has been carried out using quasielastic neutron scattering. Measurements of the elastic intensity were carried out in the temperature range 50-380 K and indicate a trend in DPP dynamics with changing grafting density and pore size. Full quasielastic scans over an energy range of  $\pm 17$   $\mu\text{eV}$  were carried out at temperatures of 240 K, 280 K, and 320 K. Initial analysis employed a stretched exponential to model the Fourier transformed data in the time domain. An average relaxation time, defined as  $\langle \tau \rangle = (\tau/\beta)\Gamma(1/\beta)$  shows a dependence on temperature, pore size, and DPP grafting density. Molecular dynamics simulations using a model for DPP grafted onto the surface of MCM-41 was compared with the experimental results.

---

T4-A (4:00 – 5:45 pm)

**Protein Structures, Mechanisms and Functional Complexes**

Chair: D. Worcester (Amphitheater)

T4-A1 (4:00 pm)

**Locating Active-site Hydrogen Atoms in D-Xylose Isomerase: Time-of-Flight Neutron Diffraction** (Invited)

G. J. Bunick (University of Tennessee), A. K. Katz (Fox Chase Cancer Center), X. Li (University of Tennessee), H. L. Carrell (Fox Chase Cancer Center), B. L. Hanson (University of Toledo), P. Langan, L. Coates, B. P. Schoenborn (Los Alamos National Laboratory), J. P. Glusker (Fox Chase Cancer Center)

Time-of-flight neutron diffraction has been used to locate hydrogen atoms that define the ionization states of amino acids in crystals of D-xylose isomerase. This enzyme, from *Streptomyces rubiginosus*, is one of the largest enzymes studied to date at high resolution (1.8 Å) by this method. We have determined the position and orientation of a metal ion-bound water molecule that is located in the active site of the enzyme; this water has

been thought to be involved in the isomerization step in which D-xylose is converted to D-xylulose or D-glucose to D-fructose. It is shown to be water (rather than a hydroxyl group) under the conditions of measurement (pH 8.0) near maximal enzyme activity. Our analyses also reveal that one lysine probably has an  $\text{-NH}_2$  terminal group (rather than  $\text{NH}_3^+$ ). The ionization state of each histidine residue was also determined. High-resolution X-ray studies (at 0.94 Å) indicate disorder in some active-site side chains when a truncated substrate is bound. This suggests how they might move during catalysis. The combination of time-of-flight neutron diffraction and X-ray diffraction can contribute greatly to the elucidation of enzyme mechanisms.

*T4-A2 (4:30 pm)*

#### **Neutron diffraction studies of the enzyme dihydrofolate reductase (Invited)**

C. Dealwis, B. Bennett (University of Tennessee, Knoxville), P. Langan, L. Coates, M. Mustyakimov, B. Schoenborn (Los Alamos National Laboratory), E. Howell (University of Tennessee, Knoxville)

The role hydrogen atoms play in biochemical processes cannot be overstated, yet they are difficult to visualize by X-ray crystallography. Neutron crystallography has a proven track record in locating hydrogen, but limited neutron fluxes and accessibility to reactor sources have made it impractical. Spallation neutron sources provide a new arena for protein crystallography, as higher fluxes and time-of-flight measurements enhance data collection efficiency. Here we report a 2.2 Å resolution neutron structure and a 1.0 Å ultrahigh resolution X-ray (UHRX) structure of *E. coli* Dihydrofolate Reductase (DHFR) in complex with methotrexate (MTX), a chemotherapeutic agent. Neutron data were collected on a 0.25 mm<sup>3</sup> D<sub>2</sub>O-soaked crystal at the Protein Crystallography Station (PCS) at the spallation source operated by Los Alamos Neutron Scattering Center (LANSCE). This study provides an example of using spallation neutrons to identify protonation states *directly* in macromolecules from nuclear density maps. In particular, the neutron structure reveals the N1 atom of MTX is protonated, and thus charged, when MTX is bound to DHFR. In contrast, the UHRX structure does not directly identify the protonation state of either MTX or the active site Asp27 residue. However, results from full matrix refinement of this structure show that the Asp27 carboxylate

bond lengths are equivalent, indicating the Asp27 is charged when MTX is bound. Taken together, these results clarify a long-standing controversy, revealing that the Asp27 MTX interaction is ionic in nature. Additionally, the neutron maps show that nearly 2/3 of amide backbone hydrogens in DHFR have been exchanged for deuterium.

*T4-A3 (5:00 pm)*

#### **Neutron Protein Crystallography at the PCS**

L. Coates, P. Langan, M. Mustyakimov, B. Schoenborn (Los Alamos National Laboratory)

The PCS (Protein Crystallography Station) at Los Alamos Neutron Science Center, is a high performance neutron protein crystallography beam line funded by the Office of Biological and Environmental Research of the U.S. Department of Energy. Beam-time is free to expert and non-expert users and is allocated twice a year through a call for proposals and a peer review process.

Although most protein structures are determined using X-rays, the position of hydrogen atoms and the coordination, sometimes even the position of water molecules, cannot be directly determined at resolutions typical for most protein crystals. Hydrogen atoms are the primary motive force in most enzymatic processes. Neutron diffraction is a powerful technique for locating hydrogen atoms even at resolutions of 2-2.5 Å and can therefore provide unique information about enzyme mechanism, protein hydrogen and hydrogen bonding.

For an experiment on the PCS, protein crystals have to be 1 mm in volume. Crystals of perdeuterated protein can be significantly smaller. The co-development of a Biological Deuteration Laboratory for efficient molecular labeling allows users to make best use of the PCS. Deuteration services are free to users and are again allocated through a peer review process. Users of the PCS have access to neutron beam-time, perdeuteration facilities and also support for data reduction and structure analysis.

T4-A4 (5:15 pm)

### **The Center for Structural Molecular Biology (CSMB) at Oak Ridge National Laboratory (ORNL)**

W. T. Heller, G. W. Lynn, A. N. Raghavan, V. S. Urban, G. D. Wignall, K. L. Weiss, D. A. Myles (Oak Ridge National Laboratory)

The CSMB at ORNL is developing facilities and techniques for the characterization and analysis of biological systems at the High Flux Isotope Reactor (HFIR) and the Spallation Neutron Source (SNS). The cornerstone of the effort is a small angle neutron scattering instrument (Bio-SANS) currently under construction at HFIR that will be dedicated to the analysis of the structure, function and dynamics of complex biological systems. In support of this program, we are developing advanced computational tools for neutron analysis and modeling, alongside a supporting biophysical characterization and X-ray scattering infrastructure. Specifically, we established a Bio-Deuteration Laboratory for in vivo production of H/D labeled macromolecules that will permit selected parts of macromolecular structures to be highlighted and analyzed in situ using neutron scattering. These new facilities will make ORNL a world-leading scientific center and user facility for neutron-based studies of bio-molecular structure and function.

*This work was supported by the Office of Biological and Environmental Research of the U. S. Department of Energy project KP1101010, under contract No. DE-AC05-00OR22725 with Oak Ridge National Laboratory, managed and operated by UT-Batelle, LLC. The submitted manuscript has been authored by a contractor of the U.S. Government under Contract DE-AC05-00OR22725. Accordingly, the U.S. Government retains a nonexclusive royalty-free license to publish or reproduce the published form of this contribution, or allow others to do so, for U.S. Government purposes.*

T4-A5 (5:30 pm)

### **Scattered intensity and the composition and phase morphology of bacterial PHA inclusion bodies by contrast variation SANS**

C. J. Garvey, R. A. Russell, P. J. Holden, K. L. Wilde, K. M. Hammerton (Australian Nuclear Science and Technology Organisation), L. J. Foster (University of New South Wales)

Often small angle neutron scattering (SANS) data from biological systems may be of insufficient information content to make meaningful interpretation of the scattering from quite heterogeneous systems. Here we make use of the ability of bacteria to metabolise deuterated substrates into their structure and we examine the

interpretation of scattered intensity of contrast variation SANS from aqueous suspensions of intracellular inclusion bodies produced by the bacteria, *Pseudomonas oleovorans*. Under growth-limiting conditions, these bacteria are able to metabolise excess organic acids into polyhydroxyalkanoates (PHA) and store these polymers as intracellular inclusions until the return of favorable conditions. While the inclusion bodies are quite chemically heterogeneous the low-resolution nature of the SANS experiment allows us to express the composition of the inclusion bodies in terms of the volume fraction lipid and protein phases. The data is interpreted under the assumption that the sample may be approximated by a three-phase system where the scattering length density (SLD) of two of these phases may be varied. The contrast of the aqueous phase may be varied by changing the H<sub>2</sub>O to D<sub>2</sub>O ratio of the solution phase. However, by providing substrates of varying H/D ratio during the bacterial production of the polymer, we were also able to modulate the SLD of the polymer phase and examine structural models of the inclusion body.

---

T4-B (4:00 – 5:45 pm)

### **Low-D Magnetism**

*Chair: I. Zaliznyak (Ruby Room)*

T4-B1 (4:00 pm)

### **Quantum phase transitions and spin dynamics in S=1 chains in strong magnetic fields (Invited)**

A. Zheludev (Oak Ridge National Laboratory)

A comparison of inelastic neutron spectra measured for the S=1 quasi-1D bond-alternating antiferromagnet NTENP, the uniform anisotropic S=1-chain Haldane-gap compound NDMAP and the uniform isotropic “composite” Haldane spin chain IPA-CuCl<sub>3</sub> reveals key differences in the spin dynamics of these distinct types of quantum spin liquids. In modest applied fields the spectra of NDMAP [A. Zheludev *et al.*, Phys. Rev. Lett. **88**, 077206 (2002)] and IPA-CuCl<sub>3</sub> features three sharp gap excitations. In contrast, in NTENP, the highest-energy mode is broadened and anomalously weak at H=0, and rapidly vanishes when the field is turned on. A unique feature of IPA-CuCl<sub>3</sub> is an abrupt truncation of all three excitation branches at

a certain critical wave vector [Masuda *et al.*, Phys. Rev. Lett. **96**, 047210 (2006)]. Above the critical field of magnon condensation, the spectral differences become even more pronounced. NDMAP retains a triplet of massive long-lived excitations [A. Zheludev *et al.*, Phys. Rev. B **68**, 134438 (2003)]. In IPA-CuCl<sub>3</sub> there are also three sharp modes, but one is actually gapless. In NTENP only one sharp excitation branch is observed in this regime [Hagiwara *et al.*, Phys. Rev. Lett. **94**, 177202 (2005)], but there is new evidence of additional low-lying excitation continua [Regnault *et al.*, cond-mat/0602357].

T4-B2 (4:30 pm)

### **Frustration in magnetic spinels (Invited)**

S. Lee (University of Virginia)

Competing interactions are a common feature in physical and biological systems. Novel and complex phenomena emerge as systems attempt to resolve the frustration by reorganizing the underlying degrees of freedom. An extreme situation can be found in magnetic systems with triangular spin arrangements where all magnetic interactions cannot be satisfied due to the topology of the lattice, possibly leading to an infinite zero-point entropy. The important issues in this field are (1) what the nature of the spin liquid phase is and (2) how the system responds to the ground state degeneracy. I will address these issues with neutron scattering results obtained from some spinel antiferromagnets AM<sub>2</sub>O<sub>4</sub> where the transition metal M ions form a network of corner-sharing tetrahedrons.

T4-B3 (5:00 pm)

### **Possible Cluster Orbitons in the S = 1 Trimer LiVO<sub>2</sub>**

S. E. Nagler (Oak Ridge National Laboratory), W. Tian (University of Tennessee), M. B. Stone, D. G. Mandrus, B. C. Sales, R. Jin (Oak Ridge National Laboratory), D. T. Adroja, T. Perring (ISIS, CCLRC)

The magnetic properties of LiVO<sub>2</sub> arise from S=1 V<sup>3+</sup> ions forming a two dimensional triangular lattice. At T<sub>i</sub> ≈ 500 K [1] a first-order structural phase transition is accompanied by an orbital ordering involving the threefold degenerate t<sub>2g</sub> orbitals. At temperatures above the phase transition the magnetic susceptibility is Curie-Weiss like as expected for a paramagnet. The susceptibility is quenched below the phase transition with no indication of long-range magnetic order [2]. It has

been proposed that the phase transition is driven by spin-orbit coupling, with the directional ordering of the t<sub>2g</sub> orbital resolving the magnetic frustration present in the system, leading to the formation of V<sup>3+</sup> trimers in a spin-singlet ground state. We have performed a series of powder and single-crystal inelastic neutron scattering measurements investigating this scenario in LiVO<sub>2</sub>. We observe an excitation at 58 meV for temperatures below T<sub>i</sub> that we identify as the principal excitation associated with the magnetic trimer. We also observe excitations for T < T<sub>i</sub> at much higher energy transfers that should not appear in neutron scattering measurements from simple spin only trimers. A model that explicitly accounts for the orbital order predicts the presence of such excitations, visible in neutron scattering via both spin and orbital matrix elements. These excitations can be described as cluster orbitons associated with the trimers in LiVO<sub>2</sub>.

[1] H. F. Pen, van den Brink, D. I. Khomskii, G. A. Sawatzky, Phys. Rev. Lett. **78**, 1323 (1997).

[2] J. B. Goodenough, Magnetism and the Chemical bond, Interscience, New York, (1963).

T4-B4 (5:15 pm)

### **The low-dimensional magnet, ZnMn<sub>2</sub>O<sub>4</sub>**

W. D. Ratcliff, Y. Chen, Y. Qiu, J. Lynn (National Institute of Standards and Technology), S. W. Cheong, V. Kiryukhin, S. Park, S. Yeo (Rutgers University), A. Schultz, P. Piccoli (Intense Pulsed Neutron Source, Argonne National Laboratory)

ZnMn<sub>2</sub>O<sub>4</sub> crystallizes at high temperatures in the spinel structure. At lower temperatures, it undergoes a Jahn Teller distortion which lowers its symmetry to tetragonal. At lower temperatures (T<sub>N</sub>~60 K), the system orders magnetically. Fits to the order parameter, line shape of powder diffraction peaks, and the direct observation of rods of scattering in single crystal diffraction experiments show the system to be two dimensional. This is likely due to an interplay of orbital ordering and frustration. In this talk, I present the results of recent neutron diffraction experiments performed on this compound and discuss the nature of the magnetism.



T4-B5 (5:30 pm)

**Neutron scattering study of a strong-rail spin ladder**

T. Hong, C. Stock (Johns Hopkins University), G. Tremelling, M. M. Turnbull, C. P. Landee (Clark University), C. Broholm (Johns Hopkins University)

Charge and spin dynamics in Heisenberg spin-1/2 ladders have attracted much attention because of their possible relevance to High- $T_c$  superconductivity. Coordination polymer magnets are excellent systems in which to explore quantum magnetism. Here we investigate a possible spin ladder system  $(2,3\text{-dimethylpyridinium})_2\text{CuBr}_4$  by inelastic neutron scattering from a powder and a single crystalline sample. Conclusive evidence will be presented that  $\text{Cu}^{2+}$  ions in this material form two-leg spin ladders that extend along the monoclinic  $a$ -axis. As opposed to most spin ladders known so far the rail exchange exceeds the rung exchange in this material.

---

T4-C (4:00 – 5:45 pm)

**In situ Experiments: Emerging Applications**

*Chair: R. Rogge (Turquoise A-B Room)*

T4-C1 (4:00 pm)

**From stainless steel to nanocrystalline nickel: deformation micromechanics studies** *(Invited)*

H. Choo (University of Tennessee)

In situ neutron diffraction with a combination of applied stress and temperature for the studies of mechanical behavior of structural materials is a well-established technique. For example, the understanding of intergranular strains and texture evolution in polycrystalline structural materials during elastic and plastic deformations has been of fundamental interest for many years. This talk will illustrate recent research examples of deformation micromechanics studies of various structural alloys, ranging from conventional stainless steels and nanocrystalline nickel alloys to advanced ultrafine-grained TRIP (transformation-induced plasticity) steels. In particular, the focus will be on the strain hardening mechanism during plastic deformation of these alloys and its implications to the macro- and meso-scopic deformation behavior.

T4-C2 (4:30 pm)

**In-situ observation of textural and microstructural changes with neutron diffraction** *(Invited)*

R. Wenk (University of California, Berkeley)

Systematic relationships in texture patterns during phase transformations in metals as well as rocks have been of longstanding interest. Examples are the bcc-fcc-bcc transformation in iron, the hcp-bcc-hcp transformation in zirconium and titanium and the trigonal-hexagonal-trigonal transformation in quartz ( $\text{SiO}_2$ ). One problem in understanding the observed patterns and developing a comprehensive theory was that high temperature phases could not be observed in situ and the high temperature texture had to be inferred indirectly with much uncertainty. With new TOF neutron diffractometers HIPPO and SMARTS at LANSCE textural and structural changes in polycrystalline aggregates can be observed in situ at high temperature as well as under stress. In all systems definite orientation relationships were observed that are related to structural correspondences between low and high temperature phases (such as Kurdjumov-Sachs and Burgers relationships). In addition selection rules among the symmetrically equivalent structural possibilities apply and are expressed in a “texture memory”. As yet there is no general model to explain the results but it appears that apart from microstructural features, stresses imposed by neighbors are significant. One of the most interesting systems is quartz that transforms from trigonal to hexagonal at 573C by a displacive mechanism with only two variants. The two variants are related by mechanical Dauphiné twinning. An almost perfect memory has been observed when a textured naturally deformed textured quartz aggregate returns to trigonal. But memory is lost if the texture was initially random and then experimentally induced. With strain diffractometers such as SMARTS at LANSCE or ENGINX at ISIS activation of mechanical twinning during straining at temperature reveals the influence of elastic anisotropy. In situ experiments with the new neutron facilities enable us to investigate dynamic changes in bulk polycrystalline materials that occur during phase transformations as well as recrystallization and provide information about the kinetics of such processes.



T4-C3 (5:00 pm)

**In situ Fuel Cell tomography at the new NIST Neutron Imaging Facility**

D. S. Hussey, D. L. Jacobson, M. Arif (National Institute of Standards and Technology), J. P. Owejan, T. A. Trabold, J. Gagliardo (General Motors)

The polymer electrolyte fuel cell (PEFC) is a promising, low emission replacement for the internal combustion engine. Water plays a crucial role in the electrochemistry and the heat and mass transport of the PEFC, but the three-dimensional water distribution is not well understood in current PEFC models. Because of the neutron's strong interaction with hydrogen, as compared to common PEFC materials such as Aluminum and Carbon, neutron radiography has made significant contributions to engineering issues such as water management in the flow channels. Despite these major steps forward, there have been no measurements of the three-dimensional water profile in an operating PEFC with neutron tomography, mainly due to the time required to collect a tomographic image set. A new neutron imaging facility has been built and commissioned at the National Institute of Standards and Technology Center for Neutron Research, and some of its new features will be briefly discussed. Making use of this new facility's fuel cell test and control infrastructure, as well as the high quality neutron imaging beam, a set of tomographic images of an operating PEFC has been taken. Using thick (about 1 mm) gas diffusion media (GDM) the reconstructed voxel size of  $(0.127 \text{ mm})^3$ , gives sufficient resolution to distinguish the water distribution in the anode GDM versus cathode GDM as well as water gradients within the GDM themselves. We show that there is water accumulation in both the anode and cathode and that the liquid water concentration increases near the membrane electrode assembly.

T4-C4 (5:15 pm)

**In-situ Neutron Diffraction Study of Gas Tungsten Arc Welding of 1018 Plain Carbon Steel**

M. A. Gharghouri (Canadian Neutron Beam Centre, National Research Council Canada), D. Dye (Imperial College London), K. T. Conlon (Atomic Energy of Canada Ltd.), M. J. Watson, I. Moner (Canadian Neutron Beam Centre, National Research Council Canada)

Welding is the dominant method of joining in manufacturing. The rapid heating and cooling

cycles that occur in fusion welding result in stress distributions, temperature distributions, and metallurgical changes that must be understood in order to develop improved methods and models for welding. In-situ neutron diffraction studies of welding require that a quasi-steady state be established to allow data collection under constant conditions. At the Canadian Neutron Beam Centre, a rig for Gas Tungsten Arc Welding (GTAW) has been constructed which develops constant conditions by rotating and translating a tube specimen such that the beam samples material at a fixed position relative to the head of the welding torch. The sampling volume can be moved relative to the torch head in order to generate stress, temperature, and phase maps. The tube geometry allows long welds without the need for excessive linear travel. In this work, the state of stress, the phase composition, and the temperature around a moving weld bead in a 1018 plain carbon steel are examined.

T4-C5 (5:30 pm)

**Residual strain evolution in 3-D stress conditions with torsion and tension for steel using a spallation neutron source**

D. Penumadu, X. Luo (University of Tennessee), D. W. Brown (Los Alamos Neutron Science Center, Los Alamos National Laboratory)

Determining residual stress state under one-dimensional loading conditions has been well studied in the past using tensile testing. However, evaluation of residual strain or stress state under pure torsion or generalized 3-D loading conditions has not been done to date. Torsion provides unique opportunity to probe mechanical behavior of materials under pure shear stress, and in combination with axial load, provides a mechanism to rotate principal stresses in a controlled fashion so that complete three-dimensional mechanical behavior can be investigated and anisotropic materials can be characterized. This study is part of a research work aimed to evaluate the role of torsion in residual strain evolution for specimens having the geometry of hollow cylinder made of 12L14 steel. The cylindrical specimens were first subjected to either pure torsion or simple tension that corresponds to a target magnitude of equivalent octahedral shear strain, and were studied ex-situ using the pulsed neutron source corresponding to Spectrometer for Materials Research at Temperature and Stress (SMARTS)

at Los Alamos Neutron Science Center (LANSCE), Los Alamos National Laboratory (LANL). Residual strains in terms of changes in the lattice spacing were measured in radial and circumferential direction using a gage volume of  $1 \times 1 \times 5 \text{ mm}^3$ , and along axial direction using a gage volume of  $1 \times 1 \times 1 \text{ mm}^3$ . The residual strain results based on typical lattice planes which have been reported to be weakly or strongly affected by intergranular strain for tension stress path from prior literature were discussed. The results indicate considerable difference in the measured residual strain variation between the steel specimens subjected to torsion versus tension. This study is first of its kind for evaluating residual strains in generalized loading conditions and also helped to demonstrate the need for having a multi-axial loading system (axial and torsional) for the anticipated residual stress testing facility at VULCAN for the Spallation Neutron Source (SNS) users.

*T4-D (4:00 – 5:45 pm)*

### **Instrumentation, Optics and Special Environments**

*Chair: K. Herwig (New Orleans Ballroom)*

*T4-D1 (4:00 pm)*

#### **Recent experience with neutron microfocusing using K-B super-mirror pairs (Invited)**

C. A. Tulk, G. E. Ice (Oak Ridge National Laboratory), D. Locke (Stony Brook University), I. Swainson, L. Cranswick, R. Rogge (NRC Chalk River Laboratories, Canada), J. B. Parise (Stony Brook University), J. Xu (Carnegie Institution of Washington)

Neutron diffraction has historically required large sample volumes on the order of  $10 \text{ mm}^3$ , these are orders of magnitude larger than that required for complimentary x-ray diffraction. This has been problematic for sample synthesis and particularly for high-pressure neutron techniques. Modern x-ray sources are capable of pushing pressure into the multi-mega bar range, an order of magnitude higher than that routinely achievable with neutron techniques. Recent progress in micro-focused neutron beams demonstrates that neutron diffraction from sub 100 micron samples held within 'more standard' opposed gem anvil cells (e.g. DACS) might be feasible. A prototype set of neutron Kirkpatrick-Baez (K-B) mirror pairs

fitted to the L3 beam at the NRU reactor at Chalk River Labs has demonstrated beams focused to  $100 \times 100$  microns to produce at least an order of magnitude increase in flux at the focal spot. White Beam Laue diffraction patterns have been collected from samples of Forsterite ( $\text{Mg}_2\text{SiO}_4$ ) mounted on silica glass capillaries. Data was collected using a MAR 345 Image plate detector. Scattering volumes have been estimated to be as small as  $100 \times 300$  microns (cylindrical). These patterns are sufficient for indexing and extracting crystallographic information. Additionally, preliminary in-situ high pressure diffraction experiments with a  $200 \times 500$  micron cylindrical single crystal of FeO in a MAC cell have been performed. These experiments indicate the effectiveness of neutron focusing by K-B mirrors for diffraction studies of small single crystals either as static mounts or in-situ with high-pressure apparatus.

*T4-D2 (4:30 pm)*

#### **Spin echo resolved grazing incidence scattering (Invited)**

G. P. Felcher, P. Falus, S. G. E. te Velthuis (Argonne National Laboratory), A. Vorobiev, J. Major, H. Dosch (Max-Planck-Institut für Metallforschung)

The encoding of neutron momentum transfer by spin-echo makes possible the detection of objects of lateral dimensions ranging from a few nanometers to some microns, either in the bulk or at interfaces, with features that are novel and distinct from those of conventional scattering. Spin-echo directly provides the correlation of the scattering objects in real space, without operating a mathematical Fourier transform on the recorded intensities. Secondly, spin-echo resolves the scattering vector  $\kappa = \kappa_{\text{in}} - \kappa_{\text{sc}}$  without the need of defining separately the wave vector of the incoming ( $\kappa_{\text{in}}$ ) or of the scattered ( $\kappa_{\text{sc}}$ ) beam. The combined effect of these properties was evident in a recent experiment on anodic porous alumina, for which an exceptionally clean pair-density function of the 2-dimensional pore assembly was obtained, with details unsmeared by the divergence of the incident beam. By lifting the requirement of a tight collimation a higher effective neutron flux becomes available. This is particularly important when the scattering objects are confined to the surface or to an interface (rather than filling an entire volume): since the number of objects is small, the total scattering from the assembly is weak. This point was proven in a grazing incidence scattering

experiment aimed at finding the average distance between polymer droplets dewetted on top of a silicon surface. The type and number of scientific problems that can profitably be addressed with this technique is still being explored, but includes the study of surface and interface landscapes such as islands, facets and capillary waves in inorganic and biological membranes.

*T4-D3 (5:00pm)*

### **The Neutron Spin Echo Spectrometer at the NIST Center for Neutron Research: Characteristics and Scientific Highlights**

A. Faraone (NIST Center for Neutron Research and University of Maryland)

The neutron spin echo (NSE) spectrometer at the National Institute of Standards and Technology (NIST) Center of Neutron Research is the only NSE spectrometer currently operating in North America. It is accessible to researchers through reviewed proposals up to ~65% of its beam time (~175 days a year). The spectrometer can measure wave-vector transfers from 0.02 to 1.6 Å<sup>-1</sup>. The accessible time range extends to nearly 10<sup>-7</sup> s at the longest accessible wavelength. These characteristics make the NSE spectrometer valuable for the investigation of soft condensed matter systems, such as polymers, glass formers, complex fluids, proteins... On the other hand, by using polarized neutrons, it provides an intrinsic separation of magnetic and nuclear scattering, making data analysis easy and the interpretation unambiguous for this kind of experiments. In this contribution, we present the principles, characteristics, and specificity of the spectrometer. Moreover, we will also report a few examples of the research carried on with the instrument.

*T4-D4 (5:15 pm)*

### **Developments in neutron optics**

T. Krist (Hahn-Meitner Institut)

In the last years two-dimensional polarisation analysers and solid state neutron optical devices like polarisers and collimators have been developed at HMI. We show results of solid state polarising benders, solid state collimators with absorbing and also with reflecting walls and a solid state radial bender for the polarisation analysis of neutrons over an angular range of 3.8 deg. In another set up neutrons were polarised by the use of a solid state polarising bender used

in transmission together with a collimator which has the advantage that the polarised neutrons are not deflected. Results from two-dimensional polarisation analysers for an angular range of 5 degrees in both directions are presented. In all cases polarisations above 95% were realised. First results from a focusing lens will be shown.

*T4-D5 (5:30 pm)*

### **MISANS (modulated intensity small angle neutron scattering)- a quasielastic SANS experiment**

M. Bleuel (Argonne National Laboratory), R. Gahler (Institut Laue-Langevin, France), J. Lal (Argonne National Laboratory)

The setup of the small angle neutron scattering (SANS) instrument SASI at the IPNS in Argonne was changed in order to transform the small angle beamline into a MIEZE (modulation of intensity by zero effort)-type instrument [1]. Due to that changes SASI became the first polarized SANS beamline on a pulsed source. The new focusing solid state collimators are significantly shorter than the older Mylar collimators and give room to install the additional components upstream the collimators without changing the moderator-sample distance, which would change the accessible neutron wavelength bandwidth due to frame overlap. The MIEZE spin echo method was chosen because with that the SANS characteristics of the beamline remain unchanged and this spin echo option is relatively easy to install and remove. It is also very easily adapted to time structure of the pulsed neutron beam and can use the whole neutron bandwidth of every pulse, while a huge area detector is used. Furthermore the analyzer is installed before the sample so the signal is not affected by spin flip scattering in the sample. That is how a huge gain of the performance can be achieved compared to a standard spin echo instrument, which uses a smaller detector, a limited neutron wavelength band and suffer intensity loss due to spin flip scattering in the sample. Last year the functionality of this principle on a pulsed source was demonstrated in a low resolution experiment [2]. In 2006 the resolution is increased to a maximum of about 1ns with the existing wire chamber detector, which limits the MIEZE frequency to 100kHz. Much higher resolution could be reached with faster scintillation detectors and longer neutron wavelengths.

[1] P. Hank, et al., *Physica B* **234** (1997) 431.

[2] M. Bleuel, et al., *Physica B*, in press (2006).

---

TB (7:30 pm)

**Banquet at the Morton Arboretum**

TB1 (8:30 pm)

**From the Italian Navigator to SNS – the Saga of Neutrons in the US: a Personal View (Plenary)**

G. Lander

---

**Wednesday, June 21**

---

W1-A (8:30 – 10:00am)

**Plenary Session**

*Chair: R. Pynn (New Orleans Ballroom)*

---

**NSSA 2006 Sustained Research Prize Lecture**

W1-A1 (8:30 am)

**Twenty Years of Chasing Zurich Oxide (Plenary)**

J. M. Tranquada (Brookhaven National Laboratory)

It is now two decades since Bednorz and Müller discovered high-temperature superconductivity in  $(\text{La,Ba})_2\text{CuO}_4$  (Zurich oxide or LBCO), setting off an explosion of research. The subsequent prediction by Anderson that the parent compound should be an antiferromagnetic insulator, and its confirmation by neutron diffraction, set a research course that many of us have followed since. Numerous experiments have shown that magnetic correlations similar to those of the parent insulator survive in the superconducting state. But how could the characters of a correlated insulator and a superconductor coexist? Somewhat ironically, an important clue comes from the original LBCO system. As a function of doping, there is a sharp dip in the curve of superconducting transition temperature at a hole concentration of 1/8 per Cu. Neutron scattering experiments have shown that the dip correlates with the appearance of an ordered state in which the holes segregate into stripes that separate antiferromagnetic domains. Current experiments are probing whether a dynamic stripe phase might underlie the superconductivity. I will review the development of this story, and mention some of the current questions.

## NSSA 2006 Science Prize Lecture

W1-A2 (9:00 am)

### Unravelling secrets of complex materials through first-principles computation, theory and neutron scattering (Plenary)

T. Yildirim (NIST Center for Neutron Research)

In this talk, we will give a sneak preview of several projects that exemplify the power of combined first-principles and neutron scattering studies to characterize and understand properties of a wide range of materials classes. In particular we will consider systems that are of great fundamental and practical interest. Systems will include unusual superconductors, novel hydrogen storage materials, frustrated quantum magnets such as (Kagome-Antiferromagnet Fe-jarosite), structure and spin-waves in complex magnetoelectric systems including TbMnO<sub>3</sub>, and buckled Kagome systems (M<sub>3</sub>V<sub>2</sub>O<sub>8</sub> M=Co, Ni, etc), which show very complex magnetic phase diagram with incommensurate spin structures and magnetoelectric effects.

W1-A3 (9:30 am)

TBA

WP (10:30 am – 12:00 pm)

### Poster Session (St. Charles Ballroom)

WP01

#### SANS with Contrast Variation Enables the Visualization of Biomacromolecular Assemblies

W. T. Heller (Oak Ridge National Laboratory)

Small-angle neutron scattering is poised to play an important role in the post-genomics era as the focus of study shifts to the interactions that exist among the systems of proteins and nucleic acids that are responsible for higher-order biological processes. Advances in structural modeling from solution small-angle scattering data have made it possible to visualize the solution structures of protein-protein and protein-nucleic acid complexes. The combination of small-angle neutron scattering, selective deuteration, contrast variation and modeling make it possible to develop an understanding of the assembly of complex biological systems. Structural characterization of subunits as they exist within

the complex is possible, thereby providing insight into conformational changes that may take place upon complex formation. Additionally, this approach allows for the study of local and global conformational changes that occur as a result of external stimuli, which can alter the interactions between the subunits in multiple-component complexes. A brief overview of the efforts in the Center for Structural Molecular Biology at Oak Ridge National Laboratory will be presented with examples of the application of these methods to the study of protein-protein and protein-nucleic acid interactions.

*This work was supported by the Office of Biological and Environmental Research of the U. S. Department of Energy project KP1101010, under contract No. DE-AC05-00OR22725 with Oak Ridge National Laboratory, managed and operated by UT-Batelle, LLC. The submitted manuscript has been authored by a contractor of the U.S. Government under Contract DE-AC05-00OR22725. Accordingly, the U.S. Government retains a nonexclusive royalty-free license to publish or reproduce the published form of this contribution, or allow others to do so, for U.S. Government purposes.*

WP02

#### Double-focusing Thermal Triple Axis Spectrometers at the NCNR

Y. Chen, J. W. Lynn (NIST Center for Neutron Research), M. Murbach, C. Wrenn (University of Maryland), C. Brocker, N. Maliszewskyj (NIST Center for Neutron Research)

A major milestone was achieved in the modernization of the NCNR's thermal neutron instruments with the installation and commissioning of the first two stages of the new thermal triple-axis spectrometer at the BT-7 beam port. The new instrument features a choice of either a Cu(220) or PG(002) doubly-focusing monochromator, providing a continuous incident neutron energy range from 5 to 500 meV. The 400 cm<sup>2</sup> reflecting area for each monochromator yields as much as an order-of-magnitude gain of neutrons onto the sample compared with the old thermal triple-axis spectrometers. The reactor beam and post monochromatic beam elements offer a wide range of choices to optimize the resolution and intensity of the instrument, with available fluxes well into the 10<sup>8</sup> n/cm<sup>2</sup>/s range. The sample stage of the instrument includes two coaxial rotary tables, one for sample rotation and one for the independent rotation of magnetic field coils, and a computer controlled sample goniometer and elevator. He<sup>3</sup> cells have been tested and provide full polarization capability with both



monochromators and any of the standard analyzer crystals. The interchangeable analyzer/detection systems are supported on air pads, and the first new analyzer system will be installed soon. It will have a multi-strip PG(002) analyzer array that can be used in a horizontally focused mode, or in a flat configuration either with a linear position-sensitive detector or with conventional Söller collimators. All options will be under computer control and can be selected and interchanged by the experimenter without requiring any mechanical changes or user intervention. A separate diffraction detector is provided in front of the analyzer for Bragg peak measurements, and a series of 13 detectors imbedded in the shielding behind the analyzer to continuously monitor the neutron flux entering the analyzer system. These detectors can also be used for measurements of the instantaneous correlation function, for example, or with a radial collimator to determine a diffraction pattern over a limited angular range.

A similar spectrometer is being developed for the BT-9 beam port.

WP03

### **Coupled protein domain motion in Taq polymerase revealed by neutron spin echo spectroscopy**

Z. Bu (Fox Chase Cancer Center), R. Biehl, D. Richter (Institut fuer Festkoerperforschung), D. J. Callaway (Fox Chase Cancer Center)

Long-range conformational changes in proteins are ubiquitous in biology for the transmission and amplification of signals; such conformational changes can be triggered by small amplitude, nanosecond protein domain motion. Understanding how conformational changes are initiated requires the characterization of protein domain motion on these timescales, and on length-scales comparable to protein dimensions. Using neutron spin-echo (NSE) spectroscopy, normal mode analysis, and a statistical-mechanical framework, we reveal overdamped coupled domain motion within DNA polymerase I from *Thermus aquaticus* (Taq polymerase). This protein utilizes correlated domain dynamics over 70 Å to coordinate nucleotide synthesis and cleavage during DNA synthesis and repair. We show that NSE spectroscopy can determine the domain mobility tensor, which determines the degree of dynamical coupling between domains. The mobility tensor defines the domain velocity response to a force

applied to it or to another domain, as the sails of a sailboat determine its velocity given the applied wind force. The NSE results provide insights into the nature of protein domain motion that are not appreciated by conventional biophysical techniques (PNAS 2005, 102(49):17646-17651).

WP04

### **In-situ neutron powder diffraction characterization of $\text{La}_{1-y}\text{Sr}_y\text{MnO}_{3-x}$ materials**

L. Suescun (Argonne National Laboratory, Material Science Division), B. Stillwell, J. Mais, S. Remsen (Northern Illinois University), B. Dabrowski (Northern Illinois University & Argonne National Laboratory), J. D. Jorgensen (Argonne National Laboratory, Material Science Division), E. R. Maxey, J. W. Richardson Jr. (Argonne National Laboratory, Intense Pulsed Neutron Source)

$\text{La}_{1-y}\text{Sr}_y\text{MnO}_{3-x}$  materials (LSM) have been extensively studied due to their interesting fast oxygen permeation and high electronic conductivity for a wide range of  $y$  values at high temperatures ( $T > 250^\circ\text{C}$ ). This high ionic and electronic conductivity combined with very good mechanical and chemical compatibility with Yttria Stabilized Zirconia ( $\text{Y}_2\text{O}_3/\text{ZrO}_2$ -YSZ), has made  $\text{La}_{0.8}\text{Sr}_{0.2}\text{MnO}_{3-x}$  one of the most important material for use as cathodes in Solid Oxide Fuel Cell devices. The combined ionic and electronic conductivity in these materials has been attributed to the oxygen vacancy disorder present in the materials with a small amount of oxygen deficiency. On the other hand, similar compounds showing ordered vacancies and orbital ordering of Mn cations have shown to be poor ionic and electronic conductors. Traditional synthetic routes for LSM's allowed the preparation of materials with  $y < 0.55$ , so a wide region of the phase diagram was unexplored until recent years [1] when a three-step synthetic procedure was devised to prepare LSM's in the  $0 < y < 1$  range. Electrochemical and chemical stability studies performed on LSM's with  $0.7 < y < 0.9$  have shown that  $\text{La}_{0.2}\text{Sr}_{0.8}\text{MnO}_{3-x}$  ( $y = 0.8$ ) could be a better cathode material for SOFC than the currently used ( $y = 0.2$ ). In-situ neutron diffraction experiments (at Argonne's IPNS-GPPD station) have been performed to characterize the vacancy ordering process in highly oxygen deficient LSM's ( $y = 0.8$  and 1) and the stability of these phases at different temperatures and oxygen partial pressures. New vacancy ordered phases displaying charge and oxygen ordering have been found in the experiments. The thermodynamic conditions where

these phases are formed and where they lose the long range vacancy ordering have been established and will be presented.

*This work has been supported by the Department of Transportation.*

#### WP05

### **Contributions of Neutron Scattering to the Chemistry of the Hydrogen Storage Material Ammonia-Borane**

A. C. Stowe (Pacific Northwest National Laboratory), M. Hartl, L. L. Daemen, T. Proffen (Los Alamos National Laboratory), C. Brown (National Institute of Standards and Technology), E. Mamontov (Oak Ridge National Laboratory), T. Udovic (National Institute of Standards and Technology), M. Gutowski, N. Hess, T. Autrey (Pacific Northwest National Laboratory)

Ammonia borane  $\text{NH}_3\text{BH}_3$  has received a great deal of interest recently as a solid state hydrogen storage material since it was discovered to release hydrogen under mild thermal conditions. The unique di-hydrogen bonding interactions between the adjacent protic NH and hydridic BH groups control the dynamics of hydrogen motion and formation. In order to understand the fundamental interactions of the hydrogens in ammonia borane, quasielastic and inelastic neutron scattering techniques have been used to study the structure, phase transitions, vibrational spectroscopy, and rotational dynamics. The low frequency region of the neutron vibrational spectrum has been probed to investigate the nature of dihydrogen bonding in the ammonia borane solid and assignments have been made based on isotopic labeling and theory. The structural phase transitions have been explored with powder samples to gain insight into proton disorder in the tetragonal phase. Further, the proton rotational dynamics have been probed throughout the temperature range 10-300K to determine the nature of the proton motion as well as the rotational energy barrier.

#### WP06

### **Spin relaxation in diluted spin ice $\text{Ho}_{2-x}\text{Y}_x\text{Ti}_2\text{O}_7$ and $\text{Ho}_{2-x}\text{La}_x\text{Ti}_2\text{O}_7$ studied by neutron spin echo spectroscopy**

G. Ehlers (Oak Ridge National Laboratory), J. S. Gardner (Brookhaven National Laboratory), A. L. Cornelius, D. Antonio (University of Nevada, Las Vegas), C. H. Booth, M. Daniel (Lawrence Berkeley National Laboratory), S. T. Bramwell, J. Lago (University College London), W. Haeussler (FRM II)

We have studied the spin relaxation in diluted spin ice  $\text{Ho}_{2-x}\text{Y}_x\text{Ti}_2\text{O}_7$  and  $\text{Ho}_{2-x}\text{La}_x\text{Ti}_2\text{O}_7$  by means of neutron spin echo spectroscopy, to study the extent to which magnetic voids assist in the spin relaxation of  $\text{Ho}_2\text{Ti}_2\text{O}_7$ . We show that doping with non-magnetic Y or La has different effects on the spin dynamics at low temperature,  $T < 50\text{K}$ , while at higher temperatures the thermally activated dynamics already found in the pure spin ice is unchanged and persists to low Ho concentration in the samples. In the Y-doped system, at high Y concentrations ( $x > 1.6$ ), a new relaxation process appears below  $T = 50\text{K}$  which is more than 10 times faster than the thermally activated main relaxation process, but which has only small spectral weight and does not seem to affect the quantum relaxation found in the pure spin ice  $\text{Ho}_2\text{Ti}_2\text{O}_7$ . In the La-doped system, residual dynamics persists down to very low temperatures which is able to completely relax all Ho spins, extinguishing the quantum relaxation. At all concentrations, in both systems all Ho spins participate in the dynamics. The results are compared to a.c. susceptibility measurements. X-ray absorption (EXAFS) spectra show that the samples are structurally well ordered. The differences between the Y and La-doped systems are attributed to the different sizes of the involved ions, and the strain introduced by the larger La ion.

#### WP07

### **High Resolution Neutron Diffraction Study of Gallium Nitride Bulk and Nanoparticles: Implications of the Particle Size on the Local Structural Distortions**

N. G. SUNDARAM (University of California Santa Cruz), T. Proffen (Los Alamos Neutron Science Center, Los Alamos National Laboratory)

Gallium Nitride nanoparticles display blue light photo-luminescence. It is important to understand the structural changes that contribute to these properties at the nano scale. It is known that the structural coherence in nanoparticles dies out on a nanometer length-scale. Hence in addition

to conventional Rietveld refinement, a Pair Distribution Function (PDF) analysis was attempted in order to obtain better insights on their local structure on an atomic scale. Fine nanopowders of Gallium Nitride were synthesized by the reaction of ammonia on the precursor Gallium isopropoxide at two different temperatures (800°C and 1100°C)[1]. TEM measurements showed that the particles grown at 800°C were in the size range 20-60nm. High resolution Neutron powder diffraction data were obtained ( $Q=30\text{\AA}^{-1}$ ) from the upgraded diffractometer (NPDF) in the Lujan center. Following routine Rietveld refinements, the atomic pair distribution function was extracted from these data using the software PDFgetN[2]. It was observed that the PDF rapidly drops off for the nano sample at 800°C than for the sample at 1100°C indicating that better structure coherence at 1100°C. The PDF of the nano particles is analyzed for different 'r' ranges with the program PDFFIT[2] using the parameters from the Rietveld refinement as the model. The PDF show local structural deviations from the bulk after  $r=5\text{\AA}$ . These deviations manifest themselves significantly in the bond lengths of the nanocrystalline material. The PDF of the bulk, also analyzed for comparison, fits well with the model. These measurements prove that PDF can be used to understand the extent to which the average structural model is dependent on the particle size. The results are discussed with respect to the Wurtzite-crystal structure type of the Ga-N sample.

WP08

**The effects of a cylindrical detector bank geometry on the analysis of single crystal data that will be collected on the SEQUOIA spectrometer at the SNS**  
G. E. Granroth (Spallation Neutron Source, Oak Ridge National Laboratory)

The SEQUOIA spectrometer is a fine resolution Fermi chopper spectrometer under construction at the SNS. It has an incident operating regime of  $E_i = 20 - 2000\text{meV}$  with  $\Delta E/E_i$  as low as  $\sim 1.5\%$ . It will have a large detector bank of 5 rows of  $\text{He}^3$  Linear Position Sensitive Detectors (LPSDs) that are 2.5 cm wide by 120 cm long. These rows can either be placed on a spherical or cylindrical surface. This contribution describes the implications, for the analysis of single crystal data, if a cylindrical geometry is chosen. Specifically all pixels in the

spherical configuration have the same path length to within 0.5%. Therefore signals from any two pixels can be compared directly without any transforms. However, the spherical design has triangle shaped gaps between detector packs and presents significant engineering and maintenance challenges. These challenges are eliminated if a cylindrical configuration is chosen. But the cylindrical design has a 14% flight path difference between an in plane pixel and the most extreme out of plane pixel. This difference means the data must at least be reduced to  $Q$  and  $\omega$  before pixel to pixel comparisons can be made. Therefore the engineering gains are only worthwhile if it can be shown that the added restrictions in analysis do not degrade the science performance of the instrument. Other studies have shown that the cylindrical detector configuration is fine for the case of powder and liquid samples [1]. This study extends the case to single crystal samples. Specifically it describes a Monte Carlo simulation study that shows the limits where the cylindrical configuration has a negligible effect. The full spectrometer, with a cylindrical detector configuration, was simulated using Mcstas. A sample that produces delta functions in  $Q$  and  $\omega$  space was used to measure the resolution function of SEQUOIA in the most extreme scattering angle in the vertical direction and at same angle in the horizontal direction. The results show that, for a broad energy range if the detectors are sufficiently pixilated in time and space, they can be converted to  $Q$  and  $\omega$  space and then summed or subtracted as is the traditional analysis method. However if the pixels are not sufficiently pixilated the change in their shape from the inplane to the extreme out of plane orientation severely complicates collective manipulation. SEQUOIA has a sufficiently pixilated detector bank in space. Furthermore the advanced detector electronics for  $\text{He}^3$  LPSDs at the SNS allows for the small time pixilation. Therefore the cylindrical detector geometry can be used on SEQUOIA.

[1] R. Lechner to be published in the J. Neu. Res.

## WP09

**Residual Strains Measurement in a Crimped Splice Connector of High-Temperature Low-Sag Conductors for High-Voltage Transmission Lines**

J. Wang, K. An, E. Lara-Curzio, C. R. Hubbard (Oak Ridge National Laboratory), J. Graziano (Tennessee Valley Authority), J. Chan (EPRI)

The majority of overhead high-voltage transmission lines currently are steel-reinforced aluminum conductors (ACSR), which consist of an array of steel wires that are surrounded by aluminum wires. Under normal operation conditions of a Drake conductor at 60°F, the steel wires are responsible for carrying 55~72% of the mechanical load, while the aluminum wires are responsible for carrying 90~95% of the electrical current. Segments of transmission lines are typically joined using crimped aluminum splice connectors. Recently, the state of residual strains in a crimped single stage ACSR splice connector assembly was determined at the neutron strain mapping instrument NRSF2 at HFIR. A finite-element stress analysis of the splice connector assembly was also performed and the model predictions have been compared with the experimental results. The results of these analyses will be presented and the implications of these results on the reliability of transmission lines will be discussed.

*Research sponsored by the Assistant Secretary for Energy Efficiency and Renewable Energy, Office of FreedomCAR and Vehicle Technologies, as part of the High Temperature Materials Laboratory User Program, Oak Ridge National Laboratory, managed by UT-Battelle, LLC, for the U.S. Department of Energy under contract number DEAC05-00OR22725.*

## WP10

**Magnetic and phonon spectra of a model spin-frustrated triangular copper lattice**

M. B. Stone (Oak Ridge National Laboratory), F. Fernandez-Alonso, D. T. Adroja (ISIS, CCLRC), N. Dalal (Florida State University), D. Villagran, F. A. Cotton (Texas A&amp;M University), S. E. Nagler (Oak Ridge National Laboratory)

We present an inelastic neutron scattering study of the low-energy excitation spectrum of the trimer single molecular magnet,  $\text{Cu}_3(\text{O}_2\text{C}_{16}\text{H}_{23})_61.2\text{C}_6\text{H}_{12}$ , and its benzoic acid derivative organic ligands. Prior structure measurements describe an equilateral triangle arrangement of coupled  $S=1/2$   $\text{Cu}^{2+}$  sites linked by triisopropyl-benzoic acid (HTiPB) carboxylate ligands. Individual trimers are well isolated from one another by the large ring structures of the HTiPB ligands. Prior bulk

magnetic susceptibility measurements describe a spin-gap which is consistent with the isolated trimer model. The inelastic neutron scattering measurements we present indicate that the lattice/molecular excitations are at frequencies similar to the predicted magnetic excitations. Investigating both magnetic samples and non-magnetic samples consisting of only the organic ligand portions of the molecule, HTiPB, reveals a series of excitations associated with this compound. Temperature dependent measurements of  $\text{Cu}_3(\text{O}_2\text{C}_{16}\text{H}_{23})_61.2\text{C}_6\text{H}_{12}$  are consistent with there being contributions from both magnetic scattering and lattice/vibrational excitations in the vicinity of the predicted spin-gap mode.

*Research sponsored by the U.S. Department of Energy, under contract DE-AC05-00OR22725 with Oak Ridge National Laboratory, managed by UT-Battelle, LLC.*

## WP11

**Evolution of the local Jahn-Teller distortion across the phase diagram of  $\text{La}_{1-x}\text{Ca}_x\text{MnO}_3$  ( $0 < x < 0.5$ )**

E. S. Bozin, X. Qiu, G. Paglia, A. DeConinck, S. Billinge (Michigan State University), M. Schmidt, P. G. Radaelli (ISIS, CCLRC), J. F. Mitchell (Argonne National Laboratory), T. Proffen (Los Alamos Neutron Science Center, Los Alamos National Laboratory)

We report on the most comprehensive study to date of the *local* Jahn-Teller (JT) distortion across the phase diagram of the colossal magnetoresistive (CMR)  $\text{La}_{1-x}\text{Ca}_x\text{MnO}_3$  ( $0 < x < 0.5$ ). The local structure has been measured, using the neutron powder diffraction based atomic pair distribution function (PDF) approach, over the wide temperature and Ca-doping range. These results are compared to the conventional crystallographic results obtained by Rietveld analysis. The magnitude of the *local* JT distortion is quantified over the entire phase diagram. The *local* JT distortion is not sensitive to the orthorhombic-to-pseudocubic structural phase transition. Furthermore, in the undoped endmember it even survives at temperatures corresponding to the rhombohedral phase where JT distortion is not allowed crystallographically. In agreement with earlier work, we see the *local* JT distortion disappear abruptly in the metallic phase. However, in contrast with some earlier studies, we show that in the insulating phases the magnitude of the JT distortion *decreases* with increasing doping. This new result should be incorporated in theoretical models of CMR manganites.



WP12

**IINS/QC studies of 4 aminopyridine cation with different acid radicals**

K. Z. Holderna-Natkaniec (Institute of Physics A.Mickiewicz University, Poznan, Poland), I. Natkaniec (Joint Institute for Nuclear Research), J. Swiergiel (Institute of Physics A.Mickiewicz University, Poznan, Poland), R. Jakubas (Wroclaw University, Poland), E. Grech (Szczecin University, Poland)

The subject of our studies were a few simple molecular-ionic crystals built of organic cation, with coplanar ring atoms within each pyridine moiety, and nearly spherical acid radicals. Heteroaromatic 4-aminopyridine cations (4-apy) with  $\text{BF}_4^-$ ,  $\text{SbCl}_4^-$ ,  $\text{SbCl}_6^-$ ,  $\text{HClO}_4^-$ , anions (type  $\text{XY}^-$ ) exhibit ferroelectric properties. The experimental inelastic incoherent neutron scattering spectra of 4-aminopyridine hemiperchlorate (4-apy  $\frac{1}{2} \text{HClO}_4$ ), tetrafluoroborate (4-apy  $\text{BF}_4$ ), chloroantimonate (Sb-III and Sb V) (4apy  $\text{SbCl}_4$  and 4apy  $\text{SbCl}_6$ ) are reported and compared with the results of quantum chemical calculations. The Gaussian 03 program package has been used for optimization of the molecular structure using the data available from the X-ray diffraction study by density functional theory method with different basis sets. The optimized geometries have been used in calculations of the harmonic force field. The calculated IINS spectra are compared with the experimental ones and the assignment of the normal vibration modes is proposed. The low frequency bands are shifted towards higher frequencies, as compared with the simple 4apy cation. This indicates strong coupling between pyridine rings. The lattice branch reveals some peculiarity that can be assigned as the out-of-plane torsional vibrations of the anion and also in-plane deformation of  $\text{d}[\text{NH}-\text{Y}]$  type. At the energy transfer close to 500 and 800  $\text{cm}^{-1}$ , there are also bands that can be explained as related to the presence of the hydrogen bond  $\text{NH}^+ \dots \text{Y}^-$ . The internal dynamics of 4-apy cation in these ferroic compounds is discussed taking into account the crystal structural data, i.e. the strength of  $\text{NH} \dots \text{N}$  hydrogen bond and results of the  $^1\text{H}$  NMR spin-lattice relaxation studies. Polar properties of these crystals are determined by introducing disordering of the hydrogen bond system.

*Financial support under the grant of the Polish Plenipotentiary at JINR is gratefully acknowledged by the authors. The QC computations were performed at PSCS in Poznan —  $^3\text{H}$ . Niewodniczański Institute of Nuclear Physics Polish Academy of Sciences, E. Radzikowskiego 152, 31-342 Kraków, Poland, .*

WP13

**Ti/Ni multilayer study using neutron reflectometer at HANARO**

J. Lee, C. Lee, B. Seong, K. Hong, S. Cho, H. Kim, K. Shin (Korea Atomic Energy Research Institute)

A new thermal neutron reflectometer has been installed at the HANARO, a research reactor in Korea. The scattering geometry is horizontal, thus the sample is placed vertically. The instrument operates in a monochromatic, angular dispersive mode for collecting the reflectivity data as a function of the angle. The wavelength of the incident neutron beam is 0.245 nm, and it is monochromated by a PG (002) crystal with a mosaicity of  $0.4^\circ$ . The maximum neutron momentum transfer,  $Q$  has been reached up to  $0.04 \text{ nm}^{-1}$  for the solid films. In addition, the allowable minimum reflectivity was  $10^{-6}$ . The Ti/Ni multilayer (10, 25 etc.), Ni mirror and supermirror were prepared. Those were all sputtered on a glass substrate by using sputtering chamber at KAERI. The reflectivity profiles of those were measured by HANARO neutron reflectometer. The profiles were refined by means of Parratt32 refinement program. As a result of the work, the characteristics of Ti/Ni multilayer as a monochromator were elucidated. Also, according to the Ni supermirror, characteristics like critical angle and reflectivity pattern below critical angle can be studied.

WP14

**Design and Development of the new SANS at LENS**

N. B. Remmes, N. L. Armstrong, H. Kaiser, D. V. Baxter, M. B. Leuschner, D. Bossev, P. E. Sokol (Indiana University, Bloomington, IN)

The new SANS instrument at LENS will be one of three instruments to be built at IUCF. It will utilize pinhole collimation and cover a  $Q$ -range of 0.005 -  $0.5 \text{ \AA}^{-1}$  with an expected integrated flux of  $>10^4 \text{ n/cm}^2/\text{sec}$  at the sample position. The instrument will be designed both for scientific studies and as a test bed for neutron optical devices. Conceptual design, simulations, and preliminary diffraction data taken with a temporary prototype instrument will be presented. Design criteria and instrument parameters as well as the status of the development and construction phase of the new instrument will be discussed.

*The LENS project is supported by the National Science Foundation (under grants DMR-0220560 and DMR-0320627).*



## WP15

**Examination of hydrogen clathrates vibrational spectra by inelastic neutron scattering**

T. A. Jenkins, R. J. Hemley, H. K. Mao (Carnegie Institution of Washington), W. Mao (Los Alamos Neutron Science Center, Los Alamos National Laboratory), V. Struzhkin, B. Militzer (Carnegie Institution of Washington), J. Leao (NIST Center for Neutron Research)

Hydrogen clathrate compounds provide a potential route for the storage of hydrogen. Structure II clathrates have been shown to allow hydrogen to pack in the  $5^{12}$  and  $6^4$  cages at 114 K and ambient pressure (1). With the addition of a tetrahydrofuran guest molecule the clathrate is stable at 270 K and ambient pressure with the additional disadvantage of decreased hydrogen concentration due to tetrahydrofuran occupation of the larger  $6^4$  cages. Inelastic neutron scattering provides an ideal way to investigate the vibrational structure of the clathrate compounds. We report the inelastic scattering spectra of tetrahydrofuran clathrate with hydrogen with comparison results using Raman scattering. Calculations on the vibrational spectra of the clathrate cage will also be examined.

[1] Wendy Mao, Ho-Kwang Mao (2004). *Hydrogen storage in molecular compounds. Proceedings of the National Academy of Sciences*, **101**(3), 708-710.

## WP16

**The nature of the disorder in the spin-glass pyrochlore,  $Y_2Mo_2O_7$ , by NPDF analysis**

J. E. Greedan, A. D. Lozano-Gorrin (McMaster University), T. Proffen (Los Alamos Neutron Science Center, Los Alamos National Laboratory), S. J. Billinge (Michigan State University)

Geometrically frustrated magnets have attracted much attention recently<sup>1</sup>.  $Y_2Mo_2O_7$ ,<sup>2,3</sup> is a key material in this field. It belongs to the family of pyrochlore oxides with the general formula  $A_2B_2O_7$ , crystallizing in space group  $Fd\bar{3}m$  with the  $Mo^{4+}$  ions ( $S = 1$ ) forming an infinite array of corner sharing tetrahedra<sup>3</sup>. This compound is characterized as a nearly canonical spin glass,  $T_f = 22.5$  K, from bulk magnetic susceptibility<sup>2</sup> measurements, non-linear DC magnetization<sup>4</sup> and specific heat data<sup>5</sup>. In spite of the fact that the average structure is apparently well ordered, crystallographically<sup>3</sup>, recent studies using local probes such as EXAFS<sup>6</sup> and NMR<sup>7</sup> show a type of short range disorder in  $Y_2Mo_2O_7$ , but it is still poorly characterized. In order to clarify and provide a more definitive picture of the type of

disorder present in this material with respect to all three sites, Y, Mo and O, simultaneously, and at the same time to establish a connection between that pair-distance disorder and the near classic spin-glass behavior, neutron diffraction data were collected on the NPDF diffractometer (LANSCE) at 9 temperatures between 15 K and 300 K. Pair-Distribution-Function Analysis (PDF) was carried out using the standard program PDFfit. As well, the parameters of the average structure were obtained by Rietveld analysis, including anisotropic displacement factors, and comparisons were made with various short range order models.

- [1] J.E. Greedan, *J. Mater. Chem.*, **11**, 37 (2001).
- [2] J.E. Greedan, M. Sato, Xu Yan, *Solid State Comm.*, **59**, 895 (1986).
- [3] J.N. Reimers, J.E. Greedan, M. Sato, *J. Solid State Chem.*, **72**, 390 (1988).
- [4] M.J.P. Gingras, C.V. Stager, N.P. Raju, B.D. Gaulin, J.E. Greedan, *Phys. Rev. Lett.*, **78**, 947 (1997).
- [5] N.P. Raju, E. Gmelin, R.K. Kremer, *Phys. Rev. B* **46**(9), 5405 (1992).
- [6] C.H. Booth, J.S. Gardner, G.H. Kwei, R.H. Heffner, F. Bridges, M.A. Subramanian, *Phys. Rev. B* **62**, R755 (2000).
- [7] A. Keren, J.S. Gardner, *Phys. Rev. Lett.*, **87**, 177201 (2001).

## WP17

**PDF Analysis of the new oxide fast-ion conductor  $La_2Mo_2O_9$  (LAMOX)**

L. Malavasi, C. Tealdi (University of Pavia, Italy), H. J. Kim, S. J. Billinge (University of Michigan), T. Proffen (Los Alamos Neutron Science Center, Los Alamos National Laboratory), G. Flor (University of Pavia, Italy)

Fast oxide-ion conductors, especially those based on oxygen ionic transport, are the subject of considerable interest, due to their relevant applications in solid oxides fuel cells, oxygen sensors and oxygen pumping devices. Recently, the discover of high ionic conductivity in a new family of oxides based on the parent compound lanthanum molybdate  $La_2Mo_2O_9$ , known as LAMOX [1], has given a new, important input to the research in this field. It has been reported that this compound undergoes a phase transition from a slightly monoclinic low temperature phase ( $\alpha$ ) to a cubic high temperature  $\beta$  form at about 580°C. At this transition temperature, the anionic conductivity abruptly increases by almost two orders of magnitude, reaching a value which is slightly higher than that of yttria-stabilized zirconia, the most widely used electrolyte.

Oxygen ions mobility is mediated by oxygen vacancies which are probably located on 2 of the three crystallographic independent sites. Indeed, Lacorre and co-workers have solved the high temperature structure of pure  $\text{La}_2\text{Mo}_2\text{O}_9$  by means of neutron diffraction [2]. They proposed a structural model in which two oxygen sites, called O2 and O3, are partially occupied. In particular, only 1/3 of the O3 sites are occupied whereas the occupancy on the O2 site is higher (about 80%). O1 is, instead, fully occupied. However, the structure of the cubic form determined does not look completely realistic, being the partially occupied O sites characterized by huge thermal factors. It seems that the description of the highly conductive phase of LAMOX by means of probe of the average structure such as the NPD is not effective. We could, at a first approximation, correlate these features to the presence of a sort of 'quasi-amorphous' oxygen sub-lattice.

In view of all these findings we tried to face the problem with a more local probe in order to be able to shed light on the actual structure of LAMOX. The power of the atomic Pair Distribution Function (PDF) analysis in obtaining information on the short range order in complex materials is well proved [3,4] The strength of the technique comes from the fact that it takes all components of the diffraction data (Bragg peaks and diffuse scattering) into account and thus reveals both the longer range atomic order and the local deviations from it.

In this work we were primarily interested in looking at the O-sublattice and as a consequence we carried out neutron diffraction experiments on the NPDF instrument (LANSCE Facility) up to a  $Q_{\text{max}}$  value of about  $30 \text{ \AA}^{-1}$ . We treated the data by extracting the PDF with the PDFgetN software and analysing the resulting PDF curves through PDFfit. Preliminary results show that the monoclinic structure of the non-conductive LAMOX polymorph can properly describe the local structure as well. On the opposite, the available average structure for the cubic phase, i.e. the highly-conductive one, totally fails in describing the local structure of the material. Interestingly, it looks that a good agreement can be obtained by describing the PDF of the cubic form by means of the monoclinic structure. Detailed description of the structural features obtained from the PDF analysis of both samples will be given considering also the variation with the temperature.

[1] P. Lacorre, F. Goutenoire, O. Bohnke, R. Retoux, *Nature*, **404** (2000) 856-858.

[2] F. Goutenoire, O. Isnard, E. Suard, O. Bohnke, Y. Laligant, R. Retoux, P. Lacorre, *J. Mater. Chem.*, **11** (2001) 119-124.

[3] S.J.L. Billinge, M.G. Kanatzidis, *Chem. Commun.* (2004) 749-760.

[4] Th. Proeffen, S.J.L. Billinge, T. Egami, and D. Louca, *Z. Kristallog.* **218** (2003) 132-143.

WP18

### Novel Approach to Penetration Depth Anisotropy Measurements in $\text{MgB}_2$ using Small-Angle Neutron Scattering

M. R. Eskildsen, D. Pal, L. DeBeer-Schmitt, T. Bera (University of Notre Dame), R. Cubitt, C. D. Dewhurst (Institut Laue-Langevin, France), N. D. Zhigadlo, J. Karpinski (ETH Zürich, Switzerland), V. G. Kogan (Ames Laboratory)

Traditionally the anisotropy of a type-II superconductor is described either by  $\gamma_\lambda = \lambda_c / \lambda_{ab}$  or  $\gamma_H = H_{ab} / H_c = \xi_{128ab} / \xi_{128c}$ , with the two considered to be identical. However, in materials with anisotropic gaps this is generally not the case. Magnesium Diboride ( $\text{MgB}_2$ ) represents an extreme case in which  $\gamma_\lambda$  differ from  $\gamma_H$ . While there is consensus on the value of  $\gamma_H(T)$ , measurements of  $\gamma_\lambda$  are still contradictory. Here we demonstrate a novel use of small-angle neutron scattering to determine  $\gamma_\lambda$  in  $\text{MgB}_2$ , by measuring the misalignment between the applied field and the direction of the flux-line lattice as the field is rotated between the *c*-axis and the basal plane. Using a two-band/two-gap model we can fit the angular dependence of the misalignment, yielding  $\gamma_\lambda = 1.1 \pm 0.2$  at 4.9 K and 0.4 T.

WP19

### Spin Dynamics and Anisotropic Exchange Interactions in the A-type Antiferromagnetic State of $\text{Pr}_{0.5}\text{Sr}_{0.5}\text{MnO}_3$

V. V. Krishnamurthy, J. L. Robertson, R. S. Fishman, M. D. Lumsden (Oak Ridge National Laboratory), J. F. Mitchell (Argonne National Laboratory)

Both the undoped and heavily hole doped manganites exhibit antiferromagnetic ordering, but only the later exhibits colossal magnetoresistance. In the half-doped manganites, a variety of antiferromagnetic phases compete for the ground state. Inelastic neutron scattering is used to investigate the spin dynamics in the layered A-type antiferromagnetic state of  $\text{Pr}_{0.5}\text{Sr}_{0.5}\text{MnO}_3$  at 20 K. Spin wave excitations from the manganese

sublattice and crystal field excitations of Pr are observed between 2 and 20 meV [1]. The spin wave dispersion for neutron momentum transfer,  $Q$ , parallel to the ferromagnetic planes is found to be much steeper than the dispersion when  $Q$  is perpendicular to the ferromagnetic planes, indicating strong anisotropy. We show that the 3D Heisenberg model with nearest neighbor exchange interactions, an interlayer antiferromagnetic coupling, and an intralayer ferromagnetic coupling and single ion anisotropy can account for these dispersions. A comparison of the ratio of exchange couplings in  $\text{Pr}_{0.5}\text{Sr}_{0.5}\text{MnO}_3$  and  $\text{LaMnO}_3$  shows that the magnitude and the anisotropy of exchange interactions strongly depend on the type of orbital ordering. These results enable us understand the role played by the orbital in the exchange interactions in the half-doped manganites.

[1] V. V. Krishnamurthy, J. L. Robertson, R. S. Fishman, M. D. Lumsden, and J. F. Mitchell, *Phys. Rev. B* **73**, 60404R (2006).

*This work was supported by the Oak Ridge National Laboratory, managed by UT-Battelle, LLC, for the US Department of Energy under the Contract No. DE-AC05-00OR22725. The work at Argonne National Laboratory was sponsored by the US Department of Energy, Office of Sciences under the Contract No. W-31-109-ENG-38.*

#### WP20

### **Performance and resolution results for the present SNS neutron Anger camera design for two diffractometers SNAP and TOPAZ**

J. D. Richards, R. G. Cooper, R. A. Riedel, T. Visscher (Oak Ridge National Laboratory)

An Anger camera for detecting thermal and epithermal neutrons has been designed for SNAP and TOPAZ diffractometers for the SNS. The design includes a type of photomultiplier tube, a Hamamatsu H8500, which has 64 anode detector segments with just 1.5 mm of inactive element area around each square tube. The thin region of inactive area allows these tubes to be tiled together to collectively form a large area Anger camera system. The scintillator is Li-6 doped glass from Applied Scintillator Technology, Ltd. and is chosen to be around 2mm thick. The prototype being constructed has 9 tubes in a close-packed configuration using one 158mm square Li-6 scintillator glass plate 2mm thick in front of the 9 tube configuration. Special electronics have also been designed and built for gain matching each anode segment of each tube. Initial test data has been taken with two tubes mounted in

the prototype situated with a 1 mm separation. This results in 4mm of inactive area between two regions of active detector area for each tube. This poster discusses resolution results for thermal neutrons detector across the whole field of view to include scintillation events over both active and inactive regions of the Anger camera prototype. Images taken in between two tubes in addition to on each tube are presented. It is shown that an optimum geometric and electronic configuration can be arrived at to image neutrons over a field of view tiled using these PMT elements. This achieves a new approach for constructing a large area Anger camera for neutrons achieving high resolution performance over a large area.

#### WP21

### **Structural Properties of Substituted $\text{SrRuO}_3$**

B. Dabrowski, O. Chmaissem, S. Kolesnik (Northern Illinois University & Argonne National Laboratory), P. W. Barnes, J. D. Jorgensen (Argonne National Laboratory)

$\text{SrRuO}_3$  is known as a unique among 4d perovskites metallic ferromagnet with a  $T_C$  of 160 K. Numerous band structure studies have shown that hybridization between the 4d orbitals of Ru and O 2p orbitals should lead to strong interplay between structural, magnetic, and electronic properties. In addition,  $\text{SrRuO}_3$  compound has been intensively studied for possible application as an electrode material in micro- and nano- electronic circuits. We have discovered that annealing of  $\text{SrRuO}_3$  in oxygen suppresses ordered moment per Ru from 1.6 to 0.8  $m_B$  and  $T_C$  to 45 K. Neutron powder diffraction revealed that annealing in oxygen produces compounds with vacancies on the Ru-sites (Phys. Rev. B 70, 014423 (2004)). Subtle structural changes that accompany creation of vacancies are different from the typical properties; the reduced charge screening caused by the Ru-vacancies offsets expected decrease of the average interatomic distance Ru - O and rotation of the  $\text{RuO}_6$  octahedra. Below  $T_C$  the unit cell volume is virtually temperature independent. We have identified that this unique in oxides invar-effect originates from freezing of the  $\text{RuO}_6$  octahedral tilting about the [001] axis (Phys. Rev. B 71, 104411 (2005)). We have established that Cr substitution for Ru increases  $T_C$  up to 188 K and identified from the bond lengths and magnetic moments dependence on doping the origin of enhancement from the minority band double-exchange interaction (Phys.

Rev. B 72, 054428 (2005)). We have discovered that similar substitution induces high-temperature ferromagnetism in  $\text{CaRu}_{1-x}\text{Cr}_x\text{O}_3$  making it a potential material for magnetic recording.

*This work was supported by NSF-DMR-0302617 (NIU) and the U.S. Department of Energy, BES – Materials Sciences (W-31-109-ENG-38) (ANL).*

WP22

### **Oriental correlations in the Glacial State of Triphenyl Phosphite**

Q. Mei, C. J. Benmore, J. Siewenie (Argonne National Laboratory, Intense Pulsed Neutron Source), P. Ghalsasi, J. L. Yarger (Arizona State University)

Spallation neutron and high-energy x-ray diffraction experiments have been performed to investigate the local structure of the glacial and supercooled liquid states in triphenyl phosphite. The observed diffraction patterns have been interpreted using a Reverse Monte Carlo modeling technique. The results show that the glacial state forms unusually weak intermolecular hydrogen bonds between an oxygen atom connected to a phenyl ring and an adjacent phenyl ring aligned in an approximately anti-parallel configuration. The structure is very different from the hexagonal crystal which is characterized by two weaker hydrogen bonds between linear arrays of molecules which are offset from each other and packed in a hexamer arrangement.

WP23

### **The Order Parameter Critical Exponent of the Chiral Phase Transition in $\text{VF}_2$**

Y. W. Rodriguez (University of California Santa Cruz), F. Ye (Oak Ridge National Laboratory), D. P. Belanger (University of California Santa Cruz), J. A. Fernandez-Baca (Oak Ridge National Laboratory)

The insulating, short-range interaction  $d=3$  magnet  $\text{VF}_2$  orders [1,2,3] with a chiral spin configuration below its transition temperature,  $T_c = 7.0\text{K}$ . The temperature dependence of the conventional order parameter below  $T_c$  is characterized using the neutron scattering intensity at the (0 0 0.53) and (0 0 1.47) magnetic Bragg points. Measurements were made using the HB1-A triple axis spectrometer at the High Flux Isotope Reactor (HFIR) at the Oak Ridge National Laboratory. The shape of the Bragg intensity versus  $T$  curves at the two magnetic points are the same, indicating that extinction effects are not significantly altering the apparent critical behavior. Power law fits were made to the

data to reduced temperatures  $t=1-T/T_c$  as small as  $10^{-3}$ . The order parameter exponent  $\beta=0.175 \pm 0.015$  was determined from fits to the data and is not significantly affected by the uncertainties in the background subtraction or in the subtraction of the critical scattering component. Kawamura [4] predicts  $\beta = 0.25 \pm 0.02$ . This short-range interaction system is a simpler example of chiral universality than Ho [5,7] which has RKKY interactions, making it difficult to reach asymptotic critical behavior, or  $\text{CsMnBr}_3$  [6,7], for which the transition is at a multicritical point.

[1] J. W. Stout, et al., *J. Appl. Phys.* **38** (1967) 1472; *J. Appl. Phys.* **37** (1966) 966.

[2] H. Y. Lau, et al., *J. Appl. Phys.* **40** (1969) 1136.

[3] A. Yoshimori, *J. Phys. Soc. Jpn.* **14** (1959) 807.

[4] H. Kawamura, *J. Phys. Cond. Matt.* **10** (1998) 4707; *J. Appl. Phys.* **63** (1988) 3086.

[5] V. P. Plakhty, et al., *Phys. Rev. B* **64** (2001) 100402.

[6] T. E. Mason, et al., *Phys. Rev. B* **39** (1989) 586.

[7] J. Wang, et al., *Phys. Rev. Lett.* **66** (1991) 3195.

WP24

### **Low temperature excitations in a dilute three-dimensional anisotropic antiferromagnet**

I. E. Anderson, Y. W. Rodriguez, D. P. Belanger (University of California Santa Cruz), H. Nojiri (IMR, Tohoku University), F. Yeng, J. A. Fernandez-Baca (Oak Ridge National Laboratory)

Measurements of the magnetic excitations in the dilute, anisotropic,  $d=3$  antiferromagnet,  $\text{Fe}_x\text{Zn}_{1-x}\text{F}_2$ , with magnetic concentration  $x=0.40$  were made using pulsed field spectroscopy and  $H=0$  inelastic neutron scattering techniques. The pulsed field data, with  $H$  up to 30 T, were collected at the Institute for Materials Research, Tohoku University. Four evenly-spaced peaks with the same field dependence were well resolved using several laser lines. Neutron scattering data were collected using the HB1-A triple-axis spectrometer at the High Flux Isotope Reactor (HFIR) at the Oak Ridge National Laboratory. The magnetic properties of  $\text{Fe}_x\text{Zn}_{1-x}\text{F}_2$  are very well known and it should be an excellent and simple model system for studying excitations in dilute magnetic materials. Constant  $q$  scans made well below the transition temperature provide the zero-field spectra. Five intensity peaks were resolved at the zone center ( $q=0$ ) four of which are consistent with the pulsed field measurements. Data at  $q \neq 0$  indicate nearly dispersionless excitations. Pulsed field data at other concentrations complement



earlier data obtained using Fourier-transform infrared spectroscopy [1] and inelastic neutron scattering [2]. The spectra of the higher magnetic concentration crystals at low temperature have been simulated [1,2] using a local mean field approximation for the exchange interactions of the dominant next-nearest neighbors of a single  $\text{Fe}^{2+}$  ion. This method does not adequately predict the number of excitations or the energies of resolved excitations, although it does give the general energy range and dispersion of them. Likewise, the spacing and field dependence of the seemingly fundamental magnetic excitations observed for  $x=0.40$  are not consistent with this simple model. As we will discuss, one must go beyond the local mean field approximation to describe the fundamental excitation in this very simple magnetic system.

[1] J. Satooka, *et al.*, *J. Appl. Phys.* **89** (2001) 7047.

[2] C. Paduani, *et al.*, *Phys. Rev. B* **50**, (1994) 193.

#### WP25

##### **Short, Strong Symmetric Hydrogen Bonds: The Zundel Cation in Perchloric Acid Dihydrate**

N. Verdal, D. G. Allis, B. S. Hudson (Syracuse University)

The Zundel cation,  $[\text{H}_2\text{O}-\text{H}-\text{OH}_2]^+$  is of interest because it exhibits a very short O-O distance for a hydrogen bond and because it is expected that the motion of the central proton in this cation is highly anharmonic. The material that is the best case for study of the dynamics of this central proton is that of the perchlorate salt,  $\text{H}_5\text{O}_2^+\text{ClO}_4^-$ , because of the centrosymmetric nature of the  $[\text{H}_2\text{O}-\text{H}-\text{OH}_2]^+$  cation in this crystal. In the present study we compare the INS spectra for this material in its fully protonated form with that for the tetra-deuterated material  $\text{HD}_4\text{O}_2^+\text{ClO}_4^-$  in which we expect the predominant form of the material to have the isotopic configuration with the proton in the central position,  $[\text{D}_2\text{O}-\text{H}-\text{OD}_2]^+$ . Predominance of this isotopic configuration is expected at low temperature due to the very much lower zero point energy: the H atom in central position has a very much lower vibrational energy than the peripheral positions. Whether this occurs in practice depends on the kinetics of isotopic exchange as the sample is cooled. The experimental results are compared to periodic DFT calculations for alternative isotopic configurations.

#### WP26

##### **Studying Intrinsically Disordered Proteins by Small-angle Neutron Scattering**

J. E. Curtis (NIST Center for Neutron Research), J. Zhou (University of Tennessee), W. Ratcliff II, N. F. Berk, S. Krueger (NIST Center for Neutron Research)

We are developing a suite of computational methods to aide in the design and analysis of small angle scattering data with applications to macromolecular systems. Specifically, we are merging methodologies developed to search conformational space of small molecular pharmaceuticals with the conformational search problem posed by intrinsically disordered proteins and nucleic acids. This is achieved by generating an ensemble of macromolecular structures by varying sets of backbone dihedral angles and using importance sampling and linear algebraic methods to rapidly determine structures that have small angle scattering spectra that are consistent with experiment. We have used these tools to predict a set of structures for the HIV-1 Gag protein under physiologically relevant conditions. These tools, once mature, may be useful in the study of intrinsically disordered proteins and the elucidation of macromolecular interactions in solution.

#### WP27

##### **A neutron scattering study on $\text{YMn}_2\text{O}_5$**

J. Kim (University of Virginia), J. Chung (NIST Center for Neutron Research and University of Maryland), S. Lee (University of Virginia), S. Park, S. Cheong (Rutgers University)

Multiferroics, such as  $\text{AMnO}_3$  and  $\text{AMn}_2\text{O}_5$  with rare-earth A ions, exhibit strong coupling between magnetic and electronic degrees of freedom, and they have generated lots of attention in regard to potential industrial applications. Here we report elastic and inelastic neutron scattering experiments on  $\text{YMn}_2\text{O}_5$ . Due to the lack of rare-earth ions, this system presents a good model system to investigate the correlations between magnetic Mn ions. We mapped out dispersion relations of spin waves along a few high symmetry directions at low temperatures, which provides important information to construct the effective spin Hamiltonians in  $\text{AMn}_2\text{O}_5$ .



WP28

### **An Investigation into the Dynamic Behavior of Coarse Grain Models for Lipid Bilayer Systems**

H. Nanda (NIST Center for Neutron Research), D. J. Tobias (University of California, Irvine), S. Krueger, J. E. Curtis (NIST Center for Neutron Research)

The limitations in time and length scales attainable with traditional all atom molecular dynamics simulations is a major motivation for the development of coarse grain (CG) molecular models. The application of these models for lipid systems is of particular interest because of long relaxation times of lipid molecules and proteins imbedded in the lipid matrix. Impressive efforts by several groups [J. Phys. Chem. B, 2001 (105) p.4464; J. Phys. Chem. B, 2004 (108) p.750] have developed CG models capable of reproducing many membrane structure and phase properties. We are interested in the use of coarse-grain simulations to study the dynamics of lipid membranes and their relation to membrane structural properties at the mesoscopic level. Our current work has focused on validating the semi-quantitative nature of the dynamics of DPPC and DOPC lipid membrane bilayers by comparison of coarse-grain simulations to previously validated all-atom simulations. From these simulations neutron scattering observables of specific molecular groups were calculated. We find that at least in one CG methodology that the relaxations of some groups do not match all atom simulations on the nanosecond time scale. From our work we hope to improve upon current coarse grain models as well as stimulate future neutron experiments.

WP29

### **An Investigation of the Hydrogen Storage Properties of a Copper Prussian Blue Analogue using Neutron Powder Diffraction and Neutron Vibrational Spectroscopy**

M. R. Hartman (NIST Center for Neutron Research), V. K. Petersen (University of Sydney, NSW), Y. Liu (NIST Center for Neutron Research and University of Maryland)

The adsorption of molecular hydrogen in the Prussian blue analogue  $\text{Cu}_3[\text{Co}(\text{CN})_6]_2$  was investigated using high resolution neutron powder diffraction and neutron vibrational spectroscopy. Rietveld structural refinement of the neutron data for hydrogen loadings of 1, 2, and  $\sim 2.3 \text{ H}_2/\text{Cu}$  showed that the hydrogen was adsorbed at two

sites within the structure. Hydrogen adsorption was observed at an interstitial site within the crystal structure as well as with exposed  $\text{Cu}^{2+}$  ion coordination sites. In addition, the rotational-vibrational density of states of the adsorbed hydrogen was probed using neutron vibrational spectroscopy and showed a range of local binding potentials.

WP30

### **Dispersive Crystal Field Excitation in $\text{Pr}_3\text{In}$**

A. D. Christianson, J. M. Lawrence (University of California, Irvine), R. Osborn, K. C. Littrell (Argonne National Laboratory), J. D. Thompson, J. L. Sarrao (Los Alamos National Laboratory), A. I. Kolesnikov (Argonne National Laboratory)

$\text{Pr}_3\text{In}$  appears to be a singlet-triplet system closely related to extensively studied  $\text{Pr}_3\text{Tl}$ . In contrast to ferromagnetic  $\text{Pr}_3\text{Tl}$ ,  $\text{Pr}_3\text{In}$  exhibits an antiferromagnetic phase transition. We have measured the inelastic neutron scattering spectrum for polycrystalline samples of  $\text{Pr}_3\text{In}$ . Working within the first Brillouin zone, we observe a remarkable dispersion of a crystal field excitation at 15 K. At 30 K the dispersion is unchanged while at 100 K the dispersion is much flatter. Interestingly, the static magnetic susceptibility indicates that the onset of ferromagnetic fluctuations occurs on the same temperature scale as the flattening of the dispersion of the crystal field excitation.

WP31

### **Neutron Science TeraGrid Gateway: A High Performance Computing Resource for Neutron Science**

J. W. Cobb, M. L. Chen (Oak Ridge National Laboratory), S. Lathrop (Argonne National Laboratory), V. E. Lynch (Oak Ridge National Laboratory), S. D. Miller (Spallation Neutron Source, Oak Ridge National Laboratory)

The TeraGrid ([www.teragrid.org](http://www.teragrid.org)) is a national scale distributed cyberinfrastructure created by the U.S. National Science Foundation. The TeraGrid combines leadership class computing, capacity computing, storage, and visualization resources all connected through a high bandwidth ( $\geq 10 \text{ Gbps}$ ) nationwide network. The TeraGrid has, in aggregate, over 100 TeraFlops of computing capacity, over 500 TeraBytes of online disk storage, and over five PetaBytes of archival storage. One of the eight TeraGrid resource providers is located at Oak Ridge National Laboratory. Its focus is on creating environments conducive to productive

HPC usage by the neutron science community. This is the so-called Neutron Science TeraGrid Gateway or NSTG. The NSTG's purpose is to provide the neutron scattering community resources, expertise, and assistance in applying advanced High Performance Computing (HPC) tools to key problems of interest in order to leverage the science capabilities of neutron scattering facilities. This poster will discuss the TeraGrid facilities, their availability to the Neutron Science community and their means of access. This will include portal and gateway access as well as traditional supercomputer center access and capabilities. Recent and ongoing collaborations in instrument simulation and experiment analysis will be discussed. Finally outreach opportunities for new and expanded collaborations will be described as well as discussed in person at the poster session.

#### WP32

### **An In Situ Neutron Reflectivity Study of Deuterium Uptake in Erbium Thin Films**

J. F. Browning (Sandia National Laboratories), E. B. Watkins (Los Alamos Neutron Science Center, Los Alamos National Laboratory), C. S. Snow (Sandia National Laboratories), G. S. Smith (Oak Ridge National Laboratory)

It is known that the surface condition of a metal will affect the rate at which it will adsorb hydrogen in the initial stage of a hydride forming reaction. In an effort to better understand the role of a surface oxide in the erbium-deuterium formation kinetics, we have performed in situ neutron reflectivity experiments to study the reaction as a function of equilibrium pressure. The experiments were carried out on the Surface Profile Analysis Reflectometer (SPEAR) at the Los Alamos Neutron Science Center (LANSCE) using thin films of erbium deposited onto silicon substrates. We report our findings as a function of deuterium pressure ranging from 4 Pa to  $1.1 \times 10^4$  Pa at a reaction temperature of 773 K.

*Sandia is a multiprogram laboratory operated by Sandia Corporation, a Lockheed Martin Company, for the United States Department of Energy under contract DE-AC04-94AL85000.*

#### WP33

### **In-situ Hot Plane Strain Compression Testing by Channel-Die Compression**

M. A. Gharghoury, M. J. Watson, D. Sediako (Canadian Neutron Beam Centre, National Research Council Canada)

Mechanical testing to large strains at elevated temperatures can be used to simulate forming operations under well-controlled conditions. Hot rolling, which is used at some stage for about one half of all manufactured metals, is particularly relevant. The state of stress encountered during rolling is one of compressive plane strain. A jig for high-temperature in-situ channel die compression has been fabricated to examine the evolution of texture and lattice strains under hot plane strain conditions. The jig is used with the Canadian Neutron Beam Centre high-temperature vacuum furnace, which is capable of sustained temperatures of up to 2000°C. The furnace can operate vertically or horizontally, allowing lattice strains parallel and normal to the applied load to be measured. The orientation of the scattering vector is continuously variable over a large range (60° with the scattering vector normal to the loading axis, 30° with the scattering vector in the plane of the loading axis), making the setup suitable for monitoring texture evolution. Typical specimen dimensions are 7mm (thickness) x 10-15 mm (width) x 10-20 mm (height). Temperature is controlled accurately via a thermocouple inserted into the specimen. Compressive strain is measured using a Linear Variable Differential Transformer (LVDT) transducer. Strains on the order of 50 – 75% are achievable. The jig has been used for temperatures up to 800°C, and loads up to 17 kN.

#### WP34

### **Options for wide angle TOF neutron polarization analysis with $^3\text{He}$**

L. Passell, L. D. Cooley (Brookhaven National Laboratory), T. R. Gentile (National Institute of Standards and Technology), V. Ghosh (Brookhaven National Laboratory), M. Hagen, W. T. Lee (Spallation Neutron Source, Oak Ridge National Laboratory), W. Leonhardt, S. M. Shapiro, I. Zaliznyak (Brookhaven National Laboratory)

Among the problems in which TOF neutron spectroscopy can be employed to advantage, there is a small but important sub-group that would benefit if both the energy and polarization of neutrons with energies  $10 < E_n < 100$  meV scattered

over a wide angular range could be simultaneously determined. In this energy range transmission through polarized  $^3\text{He}$  gas is the most effective neutron polarization analysis method currently available. Here we consider the requirements, practical problems and limitations involved in implementing  $^3\text{He}$  polarization analysis on TOF spectrometers with wide angular acceptance detector arrays. Three low temperature sample environments will be addressed: (i) a low field ( $<0.1\text{T}$ ) environment, (ii) a medium field ( $1\text{--}3\text{T}$ ) environment utilizing either a resistive or cryogen-free, compensated superconducting magnet and (iii) a high-field ( $10\text{--}15\text{T}$ ) environment produced by a compensated superconducting magnet. In case (i) an arrangement of coils generating a uniform field is a practical and convenient way to supply both the sample field and the holding field for the  $^3\text{He}$  cell. In case (ii) the fringing field of the sample magnet can be expected to perturb the cell holding field enough to impact significantly on the  $^3\text{He}$  polarization lifetime and the cell will need to be isolated in a separate, magnetically-shielded solenoid. In case (iii) the fringe field of the sample magnet escalates into an even more serious problem and it is unlikely that  $^3\text{He}$  polarization analysis will be possible unless the cell holding field solenoid is surrounded by a passive, persistent-mode, superconducting shield. Also addressed are constraints on the  $^3\text{He}$  cell geometry and possible ways to maintain the polarization of the gas by introducing continuous optical pumping.

#### WP35

### LENS: A New Low Energy Neutron Source Design for Research and Education

M. Leuschner, D. V. Baxter, H. Kaiser, C. M. LaVelle, W. R. Lozowski, N. B. Remmes, T. Rinckel, W. M. Snow, P. E. Sokol (Indiana University Cyclotron Facility)

The Low Energy Neutron Source (LENS) is currently under construction at the Indiana University Cyclotron Facility. LENS is a long pulse neutron source utilizing low-energy (p,xn) reactions on a beryllium target to produce neutrons. There are several unique features of the LENS facility. The low proton beam energy results in a low heat load on the moderator system, enabling the operation of the moderator at temperatures lower than  $10\text{ K}$ . The low beam energies also result in relatively low activation of the materials surrounding the target and moderator, thus enabling rapid prototyping

and turnaround times for a moderator studies program.

The LENS facility became operational when it produced its first neutrons in December 2004. Accelerator upgrades are in progress to increase the proton beam power. The design and optimization of the facility will be presented along with the construction status.

*The LENS project is supported by the National Science Foundation (under grants DMR-0220560 and DMR-0320627), the 21<sup>st</sup> Century Science and Technology fund of Indiana, Indiana University, and the Department of Defense.*

#### WP36

### Inelastic neutron scattering study of the Verwey transition in $\text{YBaFe}_2\text{O}_5$

S. Chang (Ames Laboratory), P. Karen (University of Oslo), M. P. Hehlen, F. R. Trouw (Los Alamos National Laboratory), R. J. McQueeney (Ames Laboratory)

$\text{YBaFe}_2\text{O}_5$  belongs to a new class of oxides with the chemical formula  $\text{RBaM}_2\text{O}_5$  (R=rare-earth, M=transition metal), based on the perovskite structure with a doubled unit cell and a layer of oxygen vacancies. The structure consists of pyramids of five-coordinated M-sites which are mixed valent in the stoichiometric formula unit (with an average valence of  $+2.5$ ). Therefore, charge and orbital ordering phenomena can exist on the M-site and be studied without introducing disorder. The charge ordered phase of  $\text{YBaFe}_2\text{O}_5$  is unusual, since it does not satisfy the Anderson criterion (i.e. it is not the lowest energy electrostatic arrangement of charges), but rather orders into alternating chains of  $2+/3+$  [1]. This indicates that other interactions, such as electron-phonon coupling, are necessary to arrive at the chain structure. Here, we present the results of an inelastic neutron scattering study of polycrystalline  $\text{YBaFe}_2\text{O}_5$ . We find the spectra of phonon and magnetic excitations are clearly modified at the charge- and magnetic ordering temperatures:  $T_{\text{CO}} = 308\text{ K}$  and  $T_{\text{N}} = 430\text{ K}$ , respectively.

[1] Woodward and Karen, *Inorg. Chem.* **42**, 1121 (2003)

#### WP37

### Electric Pulsed Heated Furnace for Neutron and Synchrotron Diffraction Experiments

V. A. Sarin, Y. A. Kareev, I. S. Glushkov (Troitsk Institute for Innovations and Fusion Research, TRINITI)

For characterization of titanium hydride materials at high temperatures and to study the time

resolved structural data on  $(\alpha + \gamma) \leftrightarrow \beta$  phase transition dynamics of the titanium hydride a new cell is proposed for neutron and synchrotron in situ diffraction experiments. Electric pulse heated furnace (EPHF) on the base of Electric Pulsed Hydride Injector (EPHI) for Tokamak fuelling will be described in our report. The EPHI was developed and used at carrying out experiments with thermonuclear plasma on tokamak T-11M at Troitsk Institute for Innovation and Fusion Research (TRINITI). The EPHI keeps the hydrogen isotopes in a chemically bound state on special absorbers – Ti foils. The dosed generation of gas occurs by heating selected absorbers with short, high electric current pulses. Speed of generation of deuterium at heating a foil by a direct current [1] up to temperature approximately 600°C equals 0.2 Pa·m<sup>3</sup> / (s·gTi). For filling the chamber of tokamak by deuterium for the characteristic time no more than for 0.01 s it is necessary with a speed approximately 105°C/s to raise the temperature of a titanium foil up to 900°C in the region of existence of  $\beta$ -phase. For pulse heating a foil the condenser battery is used. As the factor of diffusion of deuterium in  $\beta$ -titanium much higher, than in  $(\alpha + \gamma)$ -titanium, the speed of generation of gas will be appreciably increase. But it is still unknown with what a speed a lattice of  $(\alpha + \gamma)$ -titanium rebuilds in a lattice of  $\beta$ -titanium in dependence on a speed of a supply of energy into titanium foil and average quantity of deuterium atoms kept by one atom of titanium. The essence of investigation is the dynamics of phase transition of titanium chemically bound with deuterium from  $(\alpha + \gamma)$ -phase in  $\beta$ -phase. For this purpose the sample of a titanium foil with the known maintenance of deuterium placed in the container with atmospheric pressure no more than 0.001 Pa, is heated by a pulse of the current, received from the condenser battery, to the set value of energy with the help of specially developed device. Change of a current and a voltage is fixed by a scope and this allows knowing the brought capacity. Dynamics of phase transition in titanium chemically bound with deuterium is proposed to fix by means of a speed of rebuilding parameters of lattice parameters of  $(\alpha + \gamma)$ -titanium into a lattice parameters of  $\beta$ -titanium. For measurement of parameters of a lattice the time-of-flight neutron and energy dispersive synchrotron radiation diffraction technique

is proposed to use. Simultaneously recorded intensities of Bragg reflections will allow to calculate the crystal structure. The possibilities for such time resolved experiments are now presented by last generation high brightness synchrotron sources and high brilliance of spallation neutrons that will be produced at new SNS in USA [2].

[1] Yu. A. Kareev, U. Tamm, I. S. Glushkov, E. Hutter, Yu. G. Gendel, G. Mueller, R. -D. Penzhorn, V. P. Novikov, *Deuterium Generation Dynamics from Titanium Foils in an Electric Pulsed Hydride Injector. Hydrogen Materials Science and Chemistry of Metal Hydrides*, 159-169, 2002. Kluwer Academic Publishers. Printed in the Netherlands.

[2] J.M. Carpenter and J.W. Richardson. *Development of the Conceptual Design and the Science Case for a Long Wavelength Target Station for SNS. IPNS Progress Report Nineteen 96 – Twenty 01. Argonne National Laboratory*. P. 146 – 149.

### WP38

#### Spin-Waves in antiferromagnetic single-crystal LiFePO<sub>4</sub>

J. Li, V. O. Garlea, J. L. Zarestky, D. Vaknin (Ames Laboratory)

Spin-wave dispersions in the antiferromagnetic state of single-crystal LiFePO<sub>4</sub> were determined by inelastic neutron scattering measurements. The dispersion curves measured from the (0, 1, 0) reflection along both  $a^*$  and  $b^*$  reciprocal-space directions reflect the anisotropic coupling of the layered Fe<sup>2+</sup> ( $S = 2$ ) spin system. The spin-wave dispersion curves were theoretically modeled using linear spin-wave theory by including in the spin Hamiltonian in-plane nearest- and next-nearest-neighbor interactions ( $J_1$  and  $J_2$ ), inter-plane nearest-neighbor interactions ( $J_{\perp}$ ) and a single-ion anisotropy ( $D$ ). A weak (0, 1, 0) magnetic peak was observed in elastic neutron scattering studies of the same crystal indicating that the ground state of the staggered iron moments is not along the (0, 1, 0) direction, as previously reported from polycrystalline samples studies, but slightly rotated away from this axis.



WP39

### **Polarized neutron diffraction study of the ferromagnetic semiconductor $\text{Yb}_{14}\text{MnSb}_{11}$**

V. O. Garlea (Oak Ridge National Laboratory), . G.L. Jones, B. Collett (Hamilton College), T. R. Gentile (NIST Center for Neutron Research), W. C. Chen (NIST Center for Neutron Research and Indiana University), . P.M.B. Piccoli, M.E. Miller, A.J. Schultz (Intense Pulsed Neutron Source, Argonne National Laboratory), . H.Y. Yan, X. Tong, M. Snow (Indiana University, Bloomington, IN), . B.C. Sales, S.E. Nagler (Oak Ridge National Laboratory), . W.T. Lee, C. Hoffmann (Spallation Neutron Source, Oak Ridge National Laboratory)

Polarized neutron diffraction provides the spatial distributions of magnetization as well as the direction of the magnetization vector on an atomic scale in a wide range of materials of fundamental and technological importance. Recent advances in the development of  $^3\text{He}$  spin filters have made it possible to polarize neutrons efficiently at neutron spallation sources. We report the results of a test experiment carried out using a polarized  $^3\text{He}$  filter installed at the Single-Crystal Diffractometer (SCD) instrument at IPNS. The goal of the experiment was to determine the magnitude and direction of the magnetic moments for the elements in the Zintl semiconductor  $\text{Yb}_{14}\text{MnSb}_{11}$ . This compound is an unusual ferromagnet ( $T_c = 53\text{ K}$ ) in the sense that it is regarded as a rare example of an underscreened Kondo lattice. Of particular interest in our study is the distribution of the spin density in the  $\text{MnSb}_4$  tetrahedra, where a  $\text{Mn}^{2+}$  ( $d^5$ ) configuration with the moment compensated by the antialigned spin of an Sb  $5p$  hole is expected.

WP40

### **Better Neutron Science through Better Software: Powder Diffraction and Local Structure**

C. L. Farrow, S. Billinge, J. Bloch, E. Bozin, D. Bryndin, P. Juhas, J. Liu (Michigan State University)

We present details of the construction and use of PDFGui, a new software package for modeling pair distribution function (PDF) data. A live demo of PDFGui accompanies the presentation. The PDF method is a total scattering method that gives detailed local structure information about a material. PDFGui is built on top of the pdffft2 engine and is part of the DANSE project (Distributed Data Analysis for Neutron Scattering Experiments), which is to provide day-one instrument support for the Spallation Neutron Source at Oak Ridge National Laboratory. Among its many features,

PDFGui provides real-time plotting of model fits, multiple data set and phase refinement, and the option to run the cpu-intensive portion of a refinement on a remote computer. The program provides access to all model variables so that even the novice user can rigorously investigate the complex relationships between the physical and structural properties of real materials.

WP41

### **SANSPOL Experiments at a Pulsed Source**

E. A. Lang, M. Bleuel (Argonne National Laboratory, Intense Pulsed Neutron Source), T. Krist (Hahn-Meitner-Institut Berlin (HMI), Berlin, Germany), J. Lal (Argonne National Laboratory, Intense Pulsed Neutron Source)

The successful test experiments with a broad band solid state Polarizer in transmission at the Small Angle Neutron Scattering beamline SASI at the Intense Pulsed Neutron Source (IPNS) will be reported. A Polarizing solid state bender without adsorbing layers which works as a spin splitter was used. The bender transmits both spin components which are distinguished by different angles and one spin state is selected by a collimator in front of the bender (the bender matches the divergence of the collimators). The non-deflected transmitted component is chosen as the polarized beam. The other reflected spin state is not selected as it has an angle which is bigger than acceptable divergence of the collimator. The collimator used is made from silicon wafers 0.2 mm thick coated with Gd layer. An adiabatic spinflipper built in-house was used in order to flip a broad wavelength band of polarized neutrons from 3 to 14 angstroms for the SANSPOL technique to work.

WP42

### **Next Generation SANS Analysis Tools**

J. Zhou, P. D. Butler (National Institute of Standards and Technology)

SANS has attracted one of the largest and most diverse set of users in neutron scattering coming from industry, government and universities in fields ranging from physics, to chemistry, to engineering, to metallurgy, to biology. A major hurdle slowing development of small-angle scattering (SAS) applications to a broader user base in these communities and in the biological community in particular is data analysis and significant impact can be made by improving the basic analysis commonly done to SAS data. A strongly integrated, easy to use, and well documented and extensible



suite of tools would not only lower the barrier for the casual user to employ SAS without having to rely on an expert (or become one themselves), but significantly increase the amount of information extracted from the data.

We are developing a SANS data analysis libraries within the DANSE framework that will allow integration of various analysis and modeling methods with a GUI for general users, while also providing an extensible platform for scientific programmers who want to extend the functionality beyond the existing tools without writing everything from scratch. Specifically, this project will begin by incorporating existing SANS data reduction and analysis tools (e.g. IGOR Pro, CRYSON, LORES, etc) within the architecture of the DANSE framework. This will allow them to be independently combined with a variety of different standard optimization algorithms. Finally Novel modeling and analysis capabilities that will also be incorporated into this framework will be discussed. Input is welcome and solicited.

#### WP43

### **Common framework for performance characterization for short pulse, long pulse and continuous neutron sources**

F. Mezei (Los Alamos National Laboratory)

With the large variety of possible experimental conditions and requirements it is rather challenging to define a common meaningful metrics for the characterization of the efficiency of neutron sources and instruments. Background can for example be a decisive factor in many cases, but we do not really know by existing experience if one or the other type of source has an inherent advantage in this respect. For the case of comfortable signal to background ratio and sufficient resolution, the intensity of the signal can be considered as figure of merit. Thus for a given experiment in a first approximation (and assuming reasonable instrument design!!)  $F = F_{\min}(c, dl/l)$  can be considered as the figure of merit of the source, where  $F$  is the source peak flux and  $\min(c, dl/l)$  is the smaller of the source neutron duty factor  $c$  and the required wavelength resolution  $dl/l$ , and it is assumed, that the desired wavelength resolution is achieved in view of the source pulse length or chopper shaped pulse length. The validity of this rough estimate is benchmarked by simulated

medium resolution powder diffraction virtual experiments on a short pulse source and a 2 ms long pulse source. The results illustrate the high power of a 5 MW ESS type long pulse source even in this typically short pulse application.

#### WP44

### **Status of the ICE Control Software at the NCNR**

M. Doucet, R. Azuah, N. Maliszewskyj, S. Pheiffer (NIST Center for Neutron Research)

The recent commissioning of a state of the art thermal triple axis at the NCNR presented us with the opportunity to develop new software that addresses the needs of our local staff and outside users. An autonomous instrument control server mediates interactions of users with hardware, manages data acquisition, and sequences commands for batch execution. Client programs incorporating experiment planning tools are used to compose scans, issue instantaneous commands to be executed by the server, and provide the first layer of live status information. We will present an architectural overview of this suite and discuss the current state of the project.

#### WP45

### **Small Angle Neutron Scattering Studies on Blends of Poly (Styrene-ran-Vinyl Phenol) with Liquid Crystalline Polyurethane**

R. Mehta, M. Dadmun (University of Tennessee)

Molecular composites, composed of uniformly dispersed rigid-rod liquid crystalline polymer (LCP) molecules in a flexible amorphous polymer matrix, have remained hitherto elusive due to a scarcity of miscible systems containing a LCP and an amorphous polymer. The production of such a blend, with an experimentally accessible miscibility window, has become possible by modifying the architecture of the flexible polymer, so as to induce favorable intermolecular hydrogen bonding. Specifically, liquid crystalline polyurethanes (LCPU) are found to be miscible with a copolymer of styrene and vinyl phenol; with optimum hydrogen bonding between the carbonyl groups of the urethane linkages and the hydroxyl groups present in the styrenic matrix. Availability of a truly miscible molecular composite presents a unique opportunity of studying the conformation of polymer chains containing rigid-rods that are uniformly dispersed in a flexible coil matrix. A

system consisting of the LCPU and the deuterated styrenic copolymer containing 12% vinyl phenol is examined by Small Angle Neutron Scattering at the National Center for Neutron Research at Gaithersburg and Technology, and the Institute of Solid State Research (IFF) at Jülich. Scattering curves for neat dPS-VPh did not fit the Debye-Bueche model; indicating complex structure. The low-angle portion of the curve indicates presence of hydrogen bonded dynamic network, whose dimensions are determined by Debye-Bueche type analysis as well as modified Kratky and Zimm models. The rigidity of the LCP chain in the amorphous matrix was determined by Kratky analysis with fitting of the high-angle curve to Kratky Porod worm-like chain model.

*This work was possible due to the financial support of NSF (DMR 0241214) and The University of Tennessee's Neutron Science Scholar Program.*

WP46

#### **Evolution of the Elastic and Plastic Strains around a Fatigue Crack through the Retardation Period after an Overload**

Y. Sun (University of Tennessee), K. An, F. Tang, C. R. Hubbard (Oak Ridge National Laboratory), Y. L. Lu, H. Choo, P. K. Liaw (University of Tennessee)

An overload was applied during a fatigue crack-growth experiment, resulting in a temporary decrease in crack-growth rates, i.e., a retardation period. Neutron diffraction strain mapping at HFIR was used to investigate the retardation phenomenon by mapping the changes in the lattice strain around the fatigue-crack tip in a series of compact-tension (CT) specimens, which were fatigued to various stages through the retardation period after the overload. Following the overload, compressive-strain fields were observed along the loading direction close to the crack tip. As the crack grows out of the retardation period, the residual compressive strains decreased. The strain contours obtained from the two-dimensional mapping of the series of CT specimens show the evolution of the elastic and plastic strain fields during cyclic loading. The results provide a microscopic understanding of the overload effect during cyclic loading.

*We greatly appreciate the National Science Foundation for the financial supports of (1) the Integrative Graduate Education and Research Training (IGERT) Program (DGE-9987548), with Drs. C. J. Van Hardsveldt and D. Dutta as program directors; (2) the International Materials Institutes (IMI) Program (DMR-0231320),*

*with Dr. C. Huber as the program director; and (3) the Combined Research-Curriculum Development Program (EEC-9527527 and EEC-0202415), with Ms. M. Poats as the program director. Additional financial support was gratefully received from the Tennessee Advanced Materials Laboratory, with Dr. E. W. Plummer as the director. A portion of the research was sponsored by the Assistant Secretary for the Energy Efficiency and Renewable Energy, Office of FreedomCAR and Vehicle Technologies as part of the High Temperature Materials Laboratory User Program, Oak Ridge National Laboratory, managed by UT-Battelle, LLC, for the U.S. Department of Energy under the contract number of DE-AC05-00OR22725. Research at ORNL sponsored by the Assistant Secretary for Energy Efficiency and Renewable Energy, Office of FreedomCAR and Vehicle Technologies, as part of the High Temperature Materials Laboratory User Program, Oak Ridge National Laboratory, managed by UT-Battelle, LLC, for the U.S. Department of Energy under contract number DEAC05-00OR22725.*

WP47

#### **Temperature dependence of the phonon entropies of nickel and chromium**

M. Kresch, O. Delaire, R. Stevens, B. Fultz (California Institute of Technology)

The phonon densities-of-states of elemental nickel and chromium were measured on time-of-flight inelastic chopper spectrometers. In the same experiments, we also obtained neutron diffraction patterns. This allows us to compare the measured temperature dependence of the phonons to those predicted by classical thermodynamics. Additionally, we compare our data to previous results from triple axis spectrometers and to previous measurements of heat capacity. As an aside, we discuss differences between our measurements of scattering as a function of momentum and energy transfer,  $S(Q,E)$ , as measured on the Low Resolution Medium Energy Chopper Spectrometer at Argonne national laboratory, and on Pharos at the Los Alamos Neutron Science Center. In particular, we consider the resolution of coherent phonon scattering on the two instruments.

WP48

#### **The structure of liquid antimony pentafluoride**

C. J. Benmore (Argonne National Laboratory, Intense Pulsed Neutron Source), S. E. McLain, A. K. Soper (ISIS Pulsed Neutron Facility), J. L. Yarger (Arizona State University), J. J. Molaison, M. R. Dolgos, J. F. Turner (University of Tennessee)

The liquid structure of antimony pentafluoride at room temperature has been investigated using neutron and high energy X-ray diffraction and subsequently modelled using the disordered materials program Empirical Potential structure refinement. The neutron diffraction measurements

show that each antimony centre is surrounded by 6 fluorine atoms; four at a non-bridging distance of  $1.86 \pm 0.03$  Å and two bridging fluorines at a distance of  $2.03 \pm 0.06$  Å. The x-ray data show an additional peak at  $3.93 \pm 0.03$  Å attributed to fluorine-fluorine contacts. The diffraction data were fit to three models; cis-monomer, isolated tetramer and cis-linked chains. The x-ray data rule out the cis-monomer model but good fits are obtained for the isolated tetramer and cis-linked chain models. It is argued that the liquid is comprised of chains of cis-linked tetrameric building blocks.

WP49

### **Superconductivity and Cobalt Oxidation State in Sodium Cobaltate Hydrate**

P. W. Barnes, M. Avdeev, D. G. Hinks, J. D. Jorgensen, H. Claus, S. Short (Argonne National Laboratory)

We have extensively investigated how changing the average cobalt oxidation state ( $n$ ) affects superconductivity ( $T_c$ ) in sodium cobaltate hydrate,  $\text{Na}_{0.33}\text{CoO}_2 \cdot 1.3\text{D}_2\text{O}$ . Its structure contains two-dimensional  $\text{CoO}_2$  hexagonal planes formed from face-sharing  $\text{CoO}_6$  octahedra that are separated by layers of  $\text{Na}(\text{H}_2\text{O})_4$  units. The oxygen atoms in  $\text{D}_2\text{O}$  form a distorted tetrahedron around the sodium ions and each water molecule has one D atom hydrogen bonded to an oxygen atom in the  $\text{CoO}_2$  plane. Using neutron powder diffraction, we show that highly oxidized, metastable  $\text{Na}_{0.33}\text{CoO}_2 \cdot 1.3\text{D}_2\text{O}$  slowly forms oxygen vacancies, which directly affects the Co oxidation state and  $T_c$  of the material. By determining the superconducting transition temperature and oxygen site occupancy, we were able to map  $T_c$  as a function of cobalt oxidation state using a single  $\text{Na}_{0.33}\text{CoO}_2 \cdot 1.3\text{D}_2\text{O}$  sample.  $T_c$  (~2.2 K) was first observed when  $n \approx +3.6$  and reached a maximum value (4.5 K) when  $n \approx +3.5$ . Superconductivity then rapidly disappeared as the reduction of cobalt continued. We speculate that destruction of superconductivity in this metastable material is due to charge ordering when the average cobalt oxidation state is +3.5.

WP50

### **Studying the Structure of Bulk Amorphous Alloys by the Pair Distribution Function Method**

C. Fan (University of Tennessee), S. J. L. Billinge (Michigan State University), Th. Proffen (Los Alamos Neutron Science Center, Los Alamos National Laboratory), A. S. Masadeh (Michigan State University), J. W. Richardson, E. R. Maxey (Argonne National Laboratory, Intense Pulsed Neutron Source), H. Choo, P. K. Liaw, Y. Gao, C. T. Liu (University of Tennessee)

Forty years ago, the first amorphous metallic solid was only able to be produced by rapid quenching at  $\sim 10^6$  K/s. Since then, much progress has been made, and in the last ten years, bulk amorphous alloys (BAAs) can be formed by cooling at slow rates of about  $10^0$  to  $10^2$  K/s. Because of these slow cooling rates, instead of being “frozen” liquids, the solids should rather be thought of as “frozen supercooled liquids”. The synthesis and properties of amorphous alloys have been widely studied, but their structures on the atomic scale still remain a mystery. To further understand the structures of bulk amorphous alloys, a systematic study of pair distribution functions (PDFs) measured by neutron powder diffraction\* has been carried out at cryogenic and ambient temperatures and on samples in different structural states. We found that the atoms in BAAs are inhomogeneously distributed at the local atomic level. They exist as strong clusters with their bond lengths even shorter than their crystallized structures, and these structures exist stably in the amorphous state. In this study, an amorphous structural model is proposed, in which, strongly bonded clusters acting as units are randomly distributed and strongly connected to each other. Simulations, using the Reverse Monte Carlo (RMC) method in the DISCUS software package, were performed by combining icosahedral and cubic structures as the initial structures for  $\text{Zr}_{55}\text{Cu}_{35}\text{Al}_{10}$  bulk BAA, and the simulations show results consistent with our model. An attempt has been made successfully to correlate the amorphous structures and their mechanical properties. \*To characterize the local atomic structure of the as-cast and crystallized  $\text{Zr}_{55}\text{Cu}_{35}\text{Al}_{10}$ , structural studies were performed at low temperature of 15 K, using the time-of-flight neutron diffraction on the Neutron Powder diffractometer (NPDF), which is a high-resolution total-scattering powder diffractometer at the Lujan Neutron Scattering Center at the Los Alamos National Laboratory, USA.

*NPDF is funded by Department of Energy (DOE) under contract W-7405-ENG-36. Structural relaxation studies were performed using time-of-flight neutron diffraction on the General Purpose Powder Diffractometer (GPPD) at the Intense Pulsed Neutron Source (IPNS) at the Argonne National Laboratory, USA. IPNS is funded by the U.S. Department of Energy under Contract W-31-109-ENG-38. This work was supported by the NSF, the International Materials Institutes (IMI) Program under grant DMR-0231320.*

WP51

### **Structural Reorganization in Lithium Rich Lithium-Ion Battery Cathode Materials**

J. Vaughey (Argonne National Laboratory), A. R. Armstrong (University of St. Andrews), M. Holzapfel, P. Novak (Paul Scherrer Institute), C. S. Johnson, S. H. Kang, M. M. Thackeray (Argonne National Laboratory), P. G. Bruce (University of St. Andrews)

Rechargeable lithium ion batteries are one of the most important developments in portable power in the last 100 years. They play a vital role in a number of recent advances – including hybrid cars, implantable medical devices, and new consumer electronics. Further advances will require increases in energy density. The materials challenge lies in increasing the amount of lithium that can be inserted /removed in the cathode material. To date the most promising materials are based on lithium manganese nickel oxide, sometimes doped with cobalt. Crucially high capacities from such materials are only obtained, however, after an initial activation charge. This is believed to involve the simultaneous removal of Li and O at 4.5V (vs Li). Despite the vital role of this process, little is known on the exact mechanism. We have studied these materials by a combination of in-situ electrochemical mass spectroscopy and by powder neutron diffraction methods.

WP52

### **Rapid Approximations to the Scattering Form Factors for Orientationally Averaged Cylindrical Structures**

K. C. Littrell (Argonne National Laboratory, Intense Pulsed Neutron Source)

Many of the systems studied by small angle scattering contain structures that are cylindrical in form. These structures are typically fitted to either the scattering form factor of the cylindrical structure orientationally averaged by numerical integration or by approximate functions developed to describe the scattering from limiting-case structures where the length to radius aspect ratio is extremely asymmetric. Neither of these approaches is efficient for the routine fitting of

data. The calculation of the numerically-integrated form factor is very computationally intensive and is sensitive to the number of steps used in the integration; significant artefacts appear at large values of  $Q$  if the number of steps is insufficient; subtle problems may occur even at lower values. While the limiting-case approximations are rapid, they describe the data reasonably only for extremely asymmetric structures. We have recently developed an ad hoc approximation function to describe the scattering from a system of randomly-oriented solid circular cylinders. This function describes the data within a few percent both for highly asymmetric scatterers and those with an aspect ratio close to unity and is orders of magnitude faster than numerical integration and is better-behaved than even the high-resolution numerical integration at large  $Q$ . The faster calculation times make it practical to fit data using instrument resolution functions or numerically-integrated size distributions and make the real-time fitting of large numbers of data sets possible.

WP53

### **Parallel Instrument Simulations Using the TeraGrid**

J. W. Cobb, M. L. Chen (Oak Ridge National Laboratory), G. E. Granroth, M. E. Hagen (Spallation Neutron Source, Oak Ridge National Laboratory), J. A. Kohl (Oak Ridge National Laboratory), E. Mamontov, S. D. Miller (Spallation Neutron Source, Oak Ridge National Laboratory)

The Spallation Neutron Source (SNS) at Oak Ridge National Laboratory (ORNL), scheduled for completion in 2006, will provide the world's highest pulsed neutron flux. The SNS can support up to 24 neutron Beamlines, 18 of which are already under design and/or construction. Monte Carlo simulations have proven to be a powerful tool for instrument design optimizations (design, enhancement, upgrades.) Until now convenient access to High Performance Computing (HPC) has limited the usefulness of this technique for the design of specific beamline components. Full instrument simulation could not be performed at sufficient statistical levels rapidly enough to be effectively used in instrument design (although this has been done for moderator development.) This work describes a straightforward MPI parallelization of the standard Monte Carlo code McStas on HPC resources. Favorable speed-up and scaling will be reported. The high performance computing resources used in these investigations



were provided by the TeraGrid, a national scale distributed cyberinfrastructure created by the U.S. National Science Foundation. The TeraGrid combines leadership class computing, capacity computing, storage, and visualization resources through the TG backplane, a high bandwidth nationwide production network. One of the eight TeraGrid resource providers is located at ORNL. Its focus is on creating environments conducive to productive HPC usage by the neutron science community or the so-called Neutron Science TeraGrid Gateway or NSTG. Two software facilities have been designed and developed and deployed on the prototype NSTG to parallelize instrument simulations, requiring a little effort from the user side. They have been deployed on supercomputers across TeraGrid and available to SNS and other neutron scientists. This discussion will explore the design goals, software structure, and easy-of-use features of these software facilities. Furthermore it will describe the realized speed-up seen from MPI parallelized McStas running high resolution design simulations of the SEQUOIA and HYSPEC instruments at SNS. This capability creates not only the capability of full instrument simulation for design, but also simulation for testing proposal feasibility, pre-experiment planning, on-the-fly data comparison to resolution convolved models, and automated experiment adjustment. Advanced discussion topics will include; (1) simulations of neutron event data formats similar to the facility for neutron event data capture that will be provided by the SNS Data Acquisition System and (2) the increasing importance of incorporating accurate and detailed modeling of sample environment and scattering kernels to achieve realistic simulation results.

WP54

### **Structural Insights into Magneto-Elastic Coupling in $\text{CePd}_2\text{Ga}_2$**

R. Macaluso (Argonne National Laboratory), E. Goremychkin, L. C. Chapon (ISIS, CCLRC), R. Osborn (Argonne National Laboratory), B. D. Rainford (University of Southampton)

The 125 K structural phase transition of  $\text{CePd}_2\text{Ga}_2$  is accompanied by magnetic and resistivity transitions. The phase transition of the nonmagnetic analog,  $\text{LaPd}_2\text{Ga}_2$ , on the other hand, occurs at 62 K – a transition temperature only half that of  $\text{CePd}_2\text{Ga}_2$ . This suggests that the coupling between magnetic f-electron in  $\text{CePd}_2\text{Ga}_2$

and phonons and crystal field may contribute to destabilizing the crystal structure. We have combined powder diffraction and inelastic neutron scattering experiments performed on the HET beamline at ISIS to better understand the structural and dynamic behavior of these two compounds,  $\text{CePd}_2\text{Ga}_2$  and  $\text{LaPd}_2\text{Ga}_2$ . In this talk, we will discuss results from our diffraction experiments on the GEM beamline at ISIS to gain insight into the important role that magneto-elastic coupling plays on structural stability of materials. We also relate these results to structural instabilities found in isostructural compounds,  $\text{CePd}_2\text{Al}_2$  and  $\text{LaPd}_2\text{Al}_2$ .

WP55

### **Instrument simulation under DANSE**

J. Lin, B. Fultz, M. Aivazis, O. Delaire, M. McKerns (California Institute of Technology)

Instrument simulation could catch every detail of a neutron experiment. This kind of simulation will be helpful to both the design and the analysis of experiments.

For example, we can perform quantum chemistry computations to obtain phonon dispersions of a material. These dispersions can be converted to a scattering kernel, which, in turn, can be inserted to a Monte-Carlo simulation application to produce detector signals. Because in such a simulation instrument characteristics are considered quite comprehensively, the detector signal calculated can be directly compared to experimental detector data in order to test our physical models. Another example application would be, when researchers are preparing for an experiment, they can run simulations first to confirm if the proposed experiment will produce discernable signals.

In the last year, two python packages have been developed as a part of the DANSE project under pyre framework: “simulation” and “pyre-mcstas”. The simulation package provides a framework allowing flexible integration of virtual neutron instruments for simulation. A simulation application can be conveniently constructed as a python class for a neutron instrument. Currently most neutron components that can be used in such a simulation application are provided by package “pyre-mcstas”, which includes python components converted from McStas components. The “simulation” package, on the other hand, has a collection of generic components, which provide



a scheme for flexible and extensible simulation of samples and detectors.

WP56

### **Magnetic phase transitions and spin dynamics in $\text{LiNiPO}_4$**

J. Li, J. L. Zarestky (Ames Laboratory), T. B. Jensen, K. Lefmann, N. H. Andersen (Riso National Laboratory, Denmark), J. H. Chung (National Institute of Standards and Technology), M. Kenzelmann (Laboratory for Neutron Scattering, ETH Zurich and PSI Village, Switzerland), N. B. Christensen (Riso National Laboratory, Denmark), H. Roennow, C. Niedermayer (Laboratory for Neutron Scattering, ETH Zurich and PSI Village, Switzerland), D. Vaknin (Ames Laboratory)

Elastic and inelastic neutron scattering techniques were used to study the magnetic phase transition and spin dynamics in pure and Fe substituted  $\text{LiNiPO}_4$  single crystals. Pure  $\text{LiNiPO}_4$  undergoes a first-order magnetic phase transition from a long-range ordered incommensurate phase to an antiferromagnetic ground state at  $T_N = 20.8$  K. With the substitution of Fe for Ni, the magnetic phase transition changes from first-order to second-order, and moreover, the long-range ordered incommensurate phase of pure  $\text{LiNiPO}_4$  between 20.8 K to 21.5 K is suppressed in the  $\text{Li}(\text{Ni}_{0.8}\text{Fe}_{0.2})\text{PO}_4$  sample. Inelastic neutron scattering revealed a  $\sim 2$  meV energy gap and an anomalous "soft mode" in the spin wave dispersion curve along the [010] direction for pure  $\text{LiNiPO}_4$ . For  $\text{Li}(\text{Ni}_{0.8}\text{Fe}_{0.2})\text{PO}_4$ , however, the energy gap is reduced to 0.9 meV and the anomaly along the [010] direction is less pronounced.

WP57

### **Ab initio structure determination from pair distribution function**

P. Juhas, P. M. Duxbury, S. J. Billinge (Michigan State University)

Recent developments of synchrotron x-ray and neutron instruments and acquisition techniques allowed fast and precise measurements of experimental Pair Distribution Functions (PDFs) from molecules, crystals and disordered materials. However, it is not simple to extract the structure information from PDF data, and the PDF analysis typically consists of time consuming trial-and-error tests of different structure models. Our recent work<sup>1</sup> presents another way of obtaining structure from PDF data and it demonstrates a complete ab-initio structure solution of a single-component molecule from PDF data alone. We will describe the

extension of ab-initio PDF method to general, multi-component molecules and to periodic systems with large supercells. The application of chemical information, such as bond angle restraints or known structure fragments will also be discussed.

[1] P. Juhas, D. M. Cherba, P. M. Duxbury, W. F. Punch, S. J. L. Billinge, *Ab initio determination of solid-state nanostructure*, *Nature* (to be published in 2006).

WP59

### **Non-reentrant charge/orbital order in the 50% hole-doped bilayer manganites**

S. Nyborg Ancona, S. Rosenkranz, R. Osborn (Argonne National Laboratory, Material Science Division), Q. Li (Chinese Academy of Sciences, Beijing, CHINA and Argonne National Laboratory, Materials Sciences Division), K. Gray, J. Mitchell (Argonne National Laboratory, Material Science Division)

Previous neutron and x-ray scattering data from the 50% hole-doped bilayer manganite,  $\text{La}_{2-2x}\text{Sr}_{1+2x}\text{Mn}_2\text{O}_7$  ( $x=0.5$ ), has indicated that the CE phase, which involves charge/orbital ordering of the square planar Mn sublattice, is only stable between  $\sim 100$  and 200K. Below 170 K, an A-type antiferromagnetic phase was observed to compete with the CE state and destroy it below 100K (reentrant behavior). By studying a range of samples with nominal compositions close to  $x=0.5$  performing both conductivity and x-ray scattering measurements, we show that the CE phase is the low-temperature ground state (non-reentrant behavior), but only in a very narrow composition range, which we believe represents the true 50% material. This has been confirmed by neutron scattering measurements using some of the same samples, which provide evidence of the persistence of the antiferromagnetic order associated with the CE phase down to 10K in a non-reentrant sample, but its destruction below 70K in a reentrant sample. Our results highlight how sensitive the delicate balance between CE charge/orbital order and A-type antiferromagnetism is to sample quality.

WP60

### **Stripe Order in Single-layer Perovskite Cobaltites**

I. Zaliznyak (Brookhaven National Laboratory), N. Sakiyama (Institute for Solid State Physics, The University of Tokyo), S. H. Lee (University of Virginia), Y. Mitsui, H. Yoshizawa (Institute for Solid State Physics, The University of Tokyo)

Charge and spin order in cobalt-based relatives of high- $T_c$  cuprates,  $\text{Pr}_{2-x}\text{Ca}_x\text{CoO}_4$  ( $0.39 < x < 0.73$ ) and  $\text{La}_{2-x}\text{Sr}_x\text{CoO}_4$  ( $x=0.5, 0.61$ ), was investigated

by elastic neutron scattering. For  $x > 0.5$  we find a robust stripe-like charge order (SCO) existing up to temperatures  $T_{CO}$  of few hundred Kelvins. It is similar to the SCO in the structural-relative cuprates and nickelates, but has a characteristic doping dependence of the propagation vector which is governed by the number of  $e_g$  electrons remaining in the system,  $\sim 1-x$ , and not of the doped holes. For  $x < 0.5$  there is a large region of stability of the checkerboard charge order (CCO), which can be understood as the electronic-charge-stripe superstructure observed for  $x > 0.5$  where the smallest possible spacing has been achieved at half-doping. For all  $x$  we also find a static spin order with roughly twice the period of the SCO. However, in cobaltites spins only order at temperatures more than an order-of-magnitude smaller than  $T_{CO}$ , therefore playing no significant role in the mechanism(s) that drive the charge ordering.

WP61

### Pressure Independent Tolerance Factor of $\text{Sr}_{0.7}\text{Ca}_{0.3}\text{MnO}_3$

R. Kiyanagi (Argonne National Laboratory, Intense Pulsed Neutron Source), O. Chmaissem, B. Dabrowski (Northern Illinois University & Argonne National Laboratory), J. D. Jorgensen (Argonne National Laboratory, Material Science Division), J. W. Richardson, J. Fieramosca (Argonne National Laboratory, Intense Pulsed Neutron Source)

Manganese oxides have been investigated intensively because of its intriguing characters.  $\text{Sr}_{1-x}\text{Ca}_x\text{MnO}_3$  is a member of these materials and has a series of structural phase transitions as a function of  $x$  and a magnetic phase transition at between 100 K and 200 K depending on the  $x$  value. The transitions were understood to be describable in terms of a tolerance factor which is a function of Sr/Ca-O and Mn-O bond length. Thus this factor is considered to be very important to understand the phase transitions of these types of materials. Additionally pressure dependence of the tolerance factor is also important due to the fact that the tolerance factor is actually controlled by pressure when synthesizing a material which has an unfavorable tolerance factor under ambient pressure. In order to study the pressure dependence of the tolerance factor of  $\text{Sr}_{0.7}\text{Ca}_{0.3}\text{MnO}_3$  neutron powder diffractions were carried out under high pressure. From the observed variation of Sr/Ca-O and Mn-O bond lengths at room temperature it was found that the responses to pressure of

these bonds differ from their responses to variation in temperature. That is, the magnitude of the change in Sr/Ca-O bond length against pressure corresponds to a change in temperature of 70 K while the change of Mn-O bond length corresponds to 110 K. Consequently the tolerance factor was found unchanged within this pressure range. In this presentation the result of a low temperature experiment will be described as well.

WP62

### Growth and superconductivity of single crystals

$\text{La}_{1.875}\text{Ba}_{0.125}\text{CuO}_4$

G. D. Gu, G. Xu, J. M. Tranquada, Q. Li, A. R. Moodenbaugh (Brookhaven National Laboratory), H. Goka, K. Yamada (IMR, Tohoku University)

The origin of high temperature superconductivity in cuprate materials is one of the biggest puzzles in material science. Since the discovery of the significant anomalous suppression of superconductivity in high temperature superconducting oxide  $\text{La}_{2-x}\text{Ba}_x\text{CuO}_4$  ( $x=1/8$ )<sup>[1]</sup>, the so-called 1/8 anomaly has been a subject of considerable research attention. Many attempts to grow the single crystals have been made, but no single crystal  $\text{La}_{2-x}\text{Ba}_x\text{CuO}_4$  ( $x=1/8$ ) has been successfully grown. In this work, the effects of the growth condition and the compositions of a feed rod on the crystal growth of  $\text{La}_{2-x}\text{Ba}_x\text{CuO}_4$  has been studied by an infrared image floating zone method. The experimental result shows that a planar solid-liquid growing interface tends to break down into a cellular interface when the growth velocity is more than 1 mm/h. When the planar solid-liquid growing interface break down into a cellular interface, the single crystal size decreases abruptly and the as-grown rod is not single phase. The large single crystals of  $\text{La}_{2-x}\text{Ba}_x\text{CuO}_4$  ( $x=1/8$ ) has been successfully grown. The single crystals of  $\text{La}_{2-x}\text{Ba}_x\text{CuO}_4$  ( $x=1/8$ ) up to 8 mm diameter and 55 mm length have been cut from the as-grown bars. The superconductivity transition temperature  $T_c$  of as-grown single crystals is 2.5 K. The static stripe order in the large single crystals has been studied by neutron scattering method<sup>[2]</sup>.

[1] A. R. Moodenbaugh et al, *Phys. Rev. B*, **38** (1988)4596

[2] J. M. Tranquada et al, *Nature*, **429** (2004)534.

WP63

### Jahn-Teller distorted manganite frameworks: geometric modeling and interpretation of experimental results

A. Saribaeva, S. A. Wells (Arizona State University), S. J. Billinge (Michigan State University)

The manganese-based perovskite compounds have recently received considerable interest because of the discovery of their colossal magnetoresistance. The interpretation of experimental data on these materials is often difficult – with disagreement, for example, between determination of average and local structure [1]. A new method of Monte-Carlo with geometric constraints [2] with inclusion of JT-distortion is presented. It allows rapid simulations of large cells containing thousands of polyhedra, allowing us to simulate different patterns of local order for comparison with the experimental data.

- [1] X. Qiu, Th. Proffen, J.F. Mitchell and S.J.L. Billinge, "Orbital correlation in the pseudocubic (O) and rhombohedral (R) phases of  $\text{LaMnO}_3$ ". *PRL*, **94**, 177203, 2005.
- [2] A. Saribaeva, S.A. Wells and S.A.T. Redfern, "Li<sup>+</sup> ion motion in quartz and beta-eucryptite studied by dielectric spectroscopy and atomistic simulations". *JPCM*, **16**, 8173, 2004; Gatta D. and Wells S.A. "Rigid unit modes at high pressure: an explorative study of a fibrous zeolite-like framework with EDI topology", *PCM*, **31**, **1**, 2004.
- [3] J. Loudon, S. Cox, A.J. Williams, J.P. Attfield, P.B. Littlewood, P.A. Midgley and N.D. Mathur "Weak charge-lattice coupling requires reinterpretation of stripes of charge order in  $\text{La}_{1-x}\text{Ca}_x\text{MnO}_3$ ". *PRL*, **94**, 097202, 2005

WP64

### Commissioning Measurements for the Spallation Neutron Source, ORNL

E. B. Iverson, T. J. Shea, W. Blokland, D. W. Freeman, P. D. Ferguson, F. X. Gallmeier, W. Lu, J. D. Purcell (Spallation Neutron Source, Oak Ridge National Laboratory)

We present the results of characterization measurements performed as part of the commissioning activities at the Spallation Neutron Source at Oak Ridge National Laboratory. These activities include the storage of protons in the accumulator ring and their delivery to the target, the production of spallation neutrons and their moderation within a water moderator, and the extraction of a neutron beam from that water moderator to a characterization station on a neutron beam line. During commissioning operations, we accumulated in the ring and delivered to the target as much as up to  $1.75 \times 10^{13}$  protons in a single pulse, and measured a

neutron conversion efficiency resulting in a 1-eV moderator coupling of  $2.2 \times 10^{-3}$  n/ster/eV/p. Both measurements were significantly greater than formal requirements for Critical Decision 4 (representing the end of the construction project), and were reasonably close to predicted values. Finally, we provided our commissioning measurements via a live video feed and live website to the project staff as a whole and the larger community, respectively.

WP65

### SANS study on structures and counterion binding in anionic perfluorinated surfactant systems

G. T. Warren, D. P. Bossev (Indiana University, Bloomington, IN)

Tetraethylammonium ( $\text{TEA}^+$ ) counterions, in contrast to lithium ( $\text{Li}^+$ ) counterions, induce high viscosity in aqueous solutions of perfluorooctylsulfonate (FOS<sup>-</sup>) surfactant ions. This phenomenon was attributed to the degree and mechanism of counterion binding. The  $\text{TEA}^+$  counterion was found by using NMR to be preferentially bound to the micellar surface in mixtures of TEAFOS/LiFOS. In this work we have chosen small angle neutron scattering technique (SANS) to investigate the structures formed by the anionic perfluorooctylsulfonate surfactant ion in combination with various counterions. SANS is an ideal method to characterize the morphology of the micellar aggregation phase behavior, in providing answers to questions regarding structure, counterion binding, formation of Stern layer, and effective range of the diffuse double-layer with respect to the two counterion species of our perfluorinated surfactant system. We have taken advantage of the contrast variation techniques to obtain separate scattering curves from the micellar core and the counterion atmosphere. Based on the SANS data we determined the structures and the mechanism of the spherical to threadlike micellar transition in the presence of two different counterions at different ratios.

WP66

### Performance Simulation and Design Optimization of the SNS FNP

T. M. Ito (Los Alamos National Laboratory), P. R. Huffmann (North Carolina State University and Oak Ridge National Laboratory), C. B. Crawford (University of Tennessee)

The Fundamental Neutron Physics Beamline (FNPB) is one of 24 neutron beamlines in the target hall of the Spallation Neutron Source (SNS), and has two sub-lines dedicated to fundamental physics using cold and ultracold neutrons: The Cold Neutron Beamline will be used for experiments in the wave length range of 0.2-1.0 nm, including precision neutron beta decay correlation measurements and studies of the hadronic weak interaction. A 0.89 nm line is extracted from the Cold Beamline for experiments using ultracold neutrons generated by superthermal processes in superfluid helium, including a search for the electric dipole moment of the neutron. We have performed a detailed performance study using Monte Carlo simulations of both the Cold Beamline and the 0.89 nm Line, and have optimized the design using these results. In this talk, we will discuss the performance simulation and the design optimization of these two beamlines.

WP67

### The cold TAS PANDA - performance and prospects after a year of operation

P. Link<sup>1</sup>, A. Schneidewind<sup>2</sup> and M. Loewenhaupt<sup>2</sup>

<sup>1</sup>Forschungszentrum für Neutronenphysik und -technik, TU München, Lichtenbergstr. 1, D-85747 Garching, Germany

<sup>2</sup>Institut für Festkörperlphysik, TU Dresden, D-01062 Dresden, Germany

After a year of operation we report about the excellent performance of the cold three-axis spectrometer PANDA located at the new German research reactor FRM2. Emphasis will be laid on the specific instrument design, which combines high neutron flux together with a very good resolution for both, energy and momentum transfer, low background and a large dynamic range.

The typical applications of cold neutron three-axes spectrometers (TAS) with polarisation analysis are magnetic and also lattice excitations. Ideally suited for single crystal studies three-axis spectrometers allow measurements at almost any point of the Q-space.

Scientific applications comprise studies of spin dynamics and lattice dynamics as there are magnon and phonon dispersion relations, crystal-field excitations, anharmonic effects and magnon-phonon interaction. The high resolution in Q-space allows experiments related to dynamics of phase transitions, critical scattering, soft-modes, central-peaks, spin-relaxation-effects and modulated phases.

We will present instrument parameters as well as data obtained during the commissioning time and about 15 user experiments. It will be shown that PANDA fulfills the expectations from the design studies. Further development of the instrument in the near future (polarization analysis; perfect bent Si monochromator) will also be addressed.

### Lunch Session (12:30 – 1:45 pm) (St. Charles Ballroom)

- Student Research Award Presentation
- Neutron Advocacy Discussion,  
Chair: R. Pynn  
**S. Pierson:** *Grassroots Advocacy: Can scientists make a difference?*  
**J. Rush** (to be confirmed)  
**D. Koolbeck** (to be confirmed)

W2-A (2:00 – 3:45 pm)

### Nanoclusters and Nanostructured Materials Chair: J. Eckert (New Orleans Ballroom)

W2-A1 (2:00 pm)

### Single-molecule magnets and their supramolecular aggregates: a molecular approach to nanomagnetism (Invited)

G. Christou (University of Florida)

Many present and future specialized applications of magnets require monodisperse, nanoscale magnetic particles, and the discovery that individual molecules can function as nanoscale magnets was therefore a significant development. Each molecule functions as a nanoscale, single-domain magnetic particle that, below its blocking temperature, exhibits the classical macroscale property of a magnet, namely magnetization hysteresis. SMMs thus represent a molecular (or 'bottom up') approach to new nanoscale



magnetic materials, offering all the advantages of molecular chemistry (room temperature synthesis, purity, solubility in many solvents, a well defined periphery of organic groups, a crystalline ensemble of monodisperse units) as well as displaying the superparamagnetism of a much larger, classical magnetic particle. SMMs are also true mesoscale materials, straddling the interface between classical and quantum behavior by also exhibiting quantum tunneling of magnetization (QTM).

As a result, SMMs have potential applications in high-density information storage, with each molecule storing one bit, as well as in quantum computing as quantum bits (qubits), since the QTM allows each molecule to exist in a quantum superposition of states. The first SMMs were the  $[\text{Mn}_{12}\text{O}_{12}(\text{O}_2\text{CR})_{16}(\text{H}_2\text{O})_4]$  compounds with a spin ground state of  $S = 10$ . This large spin value and a significant easy-axis (Ising-type) anisotropy (negative axial anisotropy parameter,  $D$ ) lead to a significant barrier to magnetization reorientation and are thus the origin of the SMM property. Another well-studied SMM family are the related  $[\text{Mn}_4\text{O}_3\text{X}(\text{O}_2\text{CR})_4(\text{dbm})_4]$  compounds. These  $\text{Mn}_{12}$  and  $\text{Mn}_4$  molecular nanomagnets have been a particularly rich source of data on the sensitivity of the QTM to small structural perturbations, the environment and site-symmetry of the molecules within the crystal, and exchange interactions with neighboring molecules. The talk will present some recent progress in this area, both on new structural types of SMMs and on new developments within already established types, as well as summarizing the very limited neutron-based studies on such materials to date.

W2-A2 (2:30 pm)

### Self-Assembly of Nanoparticle/Diblock Copolymer Complexes in a Selective Solvent

C. Lo, B. Lee, R. E. Winans, P. Thiyagarajan (Argonne National Laboratory)

Self-assembly of complexes of polystyrene-*b*-poly(2-vinylpyridine) (PS-PVP) diblock copolymer and thiol-terminated PS stabilized Au nanoparticles in *d*-toluene was investigated using small-angle neutron scattering. Results reveal that the phase behavior is strongly influenced by the polymer concentration, Au nanoparticle loading and temperature. At high loading of nanoparticles in a dilute copolymer solution, both nanoparticles and toluene expand the PS blocks, leading to the order-order transition.

Upon heating, the solvent selectivity reduces, and dramatic shifts occur in both the order-disorder and order-order transition temperatures. The phase transformations can be understood in terms of change in interfacial curvature caused by the selective swelling of one of the domains by the solvent and the nanoparticles. The understanding from these studies on the effect of nanoparticles and temperature on the phase behavior of polymer/nanoparticle complexes in solution will greatly aid in tailoring novel nanocomposites with defined morphologies.

*This work was supported by the LDRD and benefited by the use of APS and IPNS funded by DOE-BES under contract #W-31-109-ENG-38.*

W2-A3 (2:45 pm)

### Dynamic PDF from TOF inelastic neutron scattering: study of relaxor behavior in PMN

W. Dmowski (University of Tennessee), S. B. Vakhrushev (Ioffe Physico-Technical Institute, St. Petersburg, 194021, Russia), I. K. Jeong (Los Alamos National Laboratory), M. Hehlen, F. Trouw (Los Alamos Neutron Science Center, Los Alamos National Laboratory), T. Egami (University of Tennessee)

We have used inelastic neutron scattering to determine dynamic structure factor for powder sample of ferroelectric lead magnesium niobate (PMN). The measurements were done with the pulsed neutron time-of-flight method using the PHAROS spectrometer at the LNANCE, Los Alamos National Laboratory, on a powder PMN sample of about 100 grams. The incoming neutron beam was monochromatized by a mechanical chopper, and scattered neutrons were detected by an array of position sensitive detectors placed over a wide range of scattering angles up to  $160^\circ$ . The measurements were performed at temperatures, 680K, 590K ( $\sim T_d$ ), 450 K, 300K, 230 K ( $\sim T_f$ ) and 35 K. High incident energy of 250 meV was selected to access a wide range of  $Q$  and  $E$  space. The dynamic structure factor was Fourier-transformed over  $Q$  to examine the real space dynamic correlation. By selecting different energy range during transformation we were able to examine same-time correlations, time-averaged correlations and correlations with a characteristic frequency related to the local atomic dynamics. The temperature study revealed that local atomic dynamics is responsible for dynamic ferroelectric polarization and anomalous dielectric properties of PMN above the freezing temperature.



W2-A4 (3:00 pm)

**Single Crystal Neutron Diffraction of Two Late Transition Metal Terminal Oxo Complexes**

P. M. Piccoli (Intense Pulsed Neutron Source, Argonne National Laboratory), T. M. Anderson (Emory University), W. A. Neiwert (Bethel University), M. L. Kirk (University of New Mexico), A. J. Schultz, T. F. Koetzle (Intense Pulsed Neutron Source, Argonne National Laboratory), D. G. Musaev, K. Morokuma, R. Cao, C. L. Hill (Emory University)

Isolable late transition metal terminal oxo complexes are rare owing to their extreme reactivity and tendency to disproportionate, and are proposed intermediates in catalytic processes. By employing polyoxometalate (POM) cluster ligands, which draw electron density away from the metal center, late transition metal terminal oxo complexes have been successfully synthesized and isolated. The large POM ligands are good  $\pi$ -acceptors that are able to reduce the electron density on the metal and thus to stabilize the metal-oxo bond. Two such complexes, containing Pt(IV) [1] and Au(III), were examined using single crystal neutron diffraction using the Single Crystal Diffractometer (SCD) at the Intense Pulsed Neutron Source at Argonne National Laboratory to confirm the length of the M=O bond and rule out the possibility that the terminal moiety was instead a terminal M-OH species. The structural results will be presented.

[1] Anderson, T. M.; Neiwert, W. A.; Kirk, M. L.; Piccoli, P. M. B.; Schultz, A. J.; Koetzle, T. F.; Musaev, D. G.; Morokuma, K.; Cao, R.; Hill, C. L. *Science* **2004**, 306, 2074-2077.

Work at ANL supported by the U.S. DOE, Basic Energy Sciences-Materials Sciences, under Contract W-31-109-ENG-38.

W2-A5 (3:15 pm)

**A Neutron Scattering and Molecular Dynamics Study of Glucoside Micelles**

F. Trouw (Los Alamos Neutron Science Center, Los Alamos National Laboratory)

The characteristic motions of micelles encompass a wide range of length and time scales, ranging from the vibrational motion of the interatomic bonds to micellar shape fluctuations. Quasielastic neutron scattering is well-suited to probing diffusive motions over those length and time scales, although a variety of instrumentation is required.

This talk will present inelastic scattering results for three beta-glucosides which differ by having 7, 8, or 9 carbon atoms in their hydrophobic tails. In spite

if such small structural differences, these three glucosides exhibit strikingly different behaviour in solution. Results will be presented from neutron spin echo, backscattering, and time-of-flight spectrometers. Molecular dynamics simulations will also be presented and compared with the neutron scattering results.

W2-A6 (3:30 pm)

**SANS Study of the Order in Vertically Aligned Carbon Nanotubes**

H. Wang, Z. Xu (Michigan Technological University), G. Eres (Oak Ridge National Laboratory)

Vertically aligned carbon nanotube (CNT) arrays can exploit the remarkable properties of individual nanotubes in macroscopic applications. Here we report the first measurements of the degree of alignment order in as-grown vertically aligned CNT arrays using small angle neutron scattering. The scattering patterns reveal continuously varying alignment order along the growth and two distinctly different morphologies of CNTs. The observations are discussed in the light of the root-growth mechanism, where the evolution of the macroscopic CNT morphologies is driven by the competing factors of collective growth and spatial constraints.

W2-B (2:00 – 3:45 pm)

**Exotic Magnetism**

Chair: C. Broholm (Amphitheater)

W2-B1 (2:00 pm)

**Exploring novel quantum magnets – examples and prospects for multiplexing triple axis spectrometry (Invited)**

H. M. Ronnow (Laboratory for Neutron Scattering, ETH Zurich and PSI Village, Switzerland)

The exploration of novel quantum magnets is a significant challenge for inelastic neutron scattering: Intensity from spin 1/2 is weak; the excitation spectra are distributed over large ranges of momentum-energy space; and novel materials are often only available as small crystals. The advent and upcoming proliferation of hugely pixelated direct time-of-flight spectrometers revolutionize possibilities for momentum-energy mapping, yet require large samples and remain

essentially incompatible with parametric studies as function of temperature, field or pressure. Multiplexing triple axis spectrometers offer a compromise between 'global mapping' and 'point-by-point' scanning. We present recent results from emerging quantum magnets obtained using a 47 channel multi-TAS, and present the plans for continuous angle multiple energy analysis (CAMEA) at PSI.

W2-B2 (2:30 pm)

### Quantum Criticality in an Organometallic Magnet

(Invited)

M. B. Stone (Oak Ridge National Laboratory), C. L. Broholm, D. H. Reich, O. Tchernyshyov (Johns Hopkins University), P. Vorderwisch (Hahn-Meitner Institut), N. Harrison (National High Magnetic Field Laboratory)

Exchange interactions in piperazinium hexachlorodocuprate (PHCC) produce a frustrated bilayer antiferromagnet with a zero field disordered singlet (spin-liquid) ground state [1]. We report the magnetic field versus temperature phase diagram of this system as determined via pulsed field magnetic susceptibility measurements and both elastic and inelastic neutron scattering ( $H = 14.2$  T) experiments [2]. We observe two quantum critical points. The lower critical field,  $H_{c1} = 7.5$  T, separates the singlet phase from a three dimensional spin-ordered state while the upper critical field,  $H_{c2} = 37$  T, marks the onset of a saturated ferromagnetic phase. The long range ordered phase, which we describe as a magnon Bose-Einstein condensate (BEC), is embedded in a gapless quasi-two-dimensional paramagnetic regime with short range spin correlations. Close to the low field quantum critical point, a reentrant phase transition between long range order and the singlet phase indicates that weak interactions with lattice or nuclear spin degrees of freedom become important.

*Work at JHU was supported by the NSF through DMR-0074571, DMR-0306940, DMR-0348679 and by the BSF through grant No. 2000-073. ORNL is managed for the US DOE by UT-Battelle Inc. under contract DE-AC05-00OR2272.*

[1] M. B. Stone, I. Zaliznyak, Daniel H. Reich, and C. Broholm, *Phys. Rev. B* **64**, 144405 (2001).

[2] M. B. Stone, C. Broholm, D. H. Reich, O. Tchernyshyov, P. Vorderwisch, and N. Harrison, *cond-mat/0503450* and in review.

W2-B3 (3:00 pm)

### The approach to order in a quantum critical system

W. Montfrooij, J. Lamsal (University of Missouri), M. C. Aronson (University of Michigan), A. de Visser, H. Ying Kai, N. Thanh Huy (van der Waals-Zeeman Institute), Y. Qiu (National Institute of Standards and Technology), M. Yethiraj, M. Lumsden (Oak Ridge National Laboratory)

We present neutron scattering experiments on single crystal  $\text{Ce}_2(\text{Fe}_{0.76}\text{Ru}_{0.24})_2\text{Ge}_2$ , prepared to be at the Quantum Critical Point. We show that the ground state of this system is an incommensurate spin density wave with the moments residing on the cerium ions. However, this spin density wave does not span the entire sample owing to the random zero-point-motion of the cerium ions.

W2-B4 (3:15 pm)

### Neutron scattering study of novel magnetic order in $\text{Na}_{0.5}\text{CoO}_2$

G. Gasparovic, R. A. Ott, J. H. Cho, F. C. Chou, Y. Chu (Massachusetts Institute of Technology), J. W. Lynn (National Institute of Standards and Technology), Y. S. Lee (Massachusetts Institute of Technology)

The layered sodium cobaltates,  $\text{Na}_x\text{CoO}_2$ , have attracted much recent attention, due to their unusual thermodynamic properties, as well as the recent discovery of superconductivity in the hydrated composition. These strongly correlated systems exhibit a rich electronic phase diagram as a function of sodium doping,  $x$ . A particularly intriguing insulating phase is realized at  $x=1/2$ , featuring a long range sodium order, a metal-insulator phase transition at 51 K, and a magnetic ordering transition at 88 K. We present polarized and unpolarized neutron scattering measurements of the magnetic order in single crystals of  $\text{Na}_{0.5}\text{CoO}_2$ . Our data indicate that below  $T_N = 88$  K the spins form a novel antiferromagnetic pattern within the  $\text{CoO}_2$  planes, consisting of alternating rows of ordered and non-ordered Co ions. The domains of magnetic order are closely coupled to the domains of Na ion order, consistent with such a two-fold symmetric spin arrangement. Magnetoresistance and anisotropic susceptibility measurements further support this model for the electronic ground state.

W2-B5 (3:30 pm)

**Multi-stage magnetic ordering in the frustrated, charge-ordered,  $\text{Mn}^{3+}/\text{Mn}^{2+}$  borate,  $\text{Mn}_2\text{BO}_4$** J. E. Greedan, H. Ghazi, A. S. Sefat (McMaster University),  
L. Cranswick (National Research Council Canada), M. H. Whangbo (North Carolina State University)

The structure of  $\text{Mn}_2\text{BO}_4$ , a  $\text{Mn}^{2+}/\text{Mn}^{3+}$  borate, is that of a distorted warwickite type featuring infinite slabs of four edge-shared Mn octahedra extending along the c-axis.[1] The Mn ions within the slab are site ordered with the sequence  $\text{Mn}^{2+}$ - $\text{Mn}^{3+}$ - $\text{Mn}^{3+}$ - $\text{Mn}^{2+}$  and the slabs are linked by corner sharing at the slab centre. The d.c. susceptibility is consistent with previous results, showing a sharp increase below 100K and a distinct zero field cooled/field cooled irreversibility below  $\sim 25\text{K}$ . Neutron diffraction data show that spin ordering in this material occurs in two stages. Long range order occurs only below  $T_{c1} = 70\text{K}$  with wave vector  $k = (000)$ , in spite of the susceptibility and prior heat capacity data which seem to indicate  $T_c = 100\text{K}$ . [2] The  $k = (000)$  order involves only the z-component of the  $\text{Mn}^{3+}$  spins and a total moment of  $\sim 0.9\text{ BM}$ , the  $\text{Mn}^{2+}$  spins do not order. This is consistent with a frustrated interslab linkage and is supported by analysis of the exchange interactions using the method of magnetic dimers.[3] A prominent diffuse scattering component with a maximum near  $Q \sim 1.3\text{ \AA}^{-1}$  develops with decreasing temperature until a second ordering, described by wave vector  $k = (1/2\ 0\ 1/2)$ , sets in below  $T_{c2} = 24\text{K}$  involving, apparently, all of the spins. New heat capacity data show a lambda anomaly at this temperature. Efforts to find an unique model for the  $k = (1/2\ 1/2\ 0)$  structure using representation analysis are ongoing. The susceptibility and specific heat anomalies at 100K are attributed to short range intraslab ferrimagnetic correlations.

[1] R. Norrestam, M. Kritikos and A. Sjödin, *J. Solid State Chem.* **114** (1995) 311.

[2] M.A. Continentino, A.M. Pedreira, R.B. Guimaraes, M. Mir, J.C. Fernández R.S. Freitas and L. Ghivelder, *Phys. Rev.* **B64** (2001) 014406-1; R.B. Guimaraes, J.C. Fernandes, M.A. Continentino, H.A. Borges, C.S. Moura, J.B.M da Cunha and C.A. dos Santos, *Phys. Rev.* **B56** (1997) 292.

[3] M-H. Whangbo, H-J. Koo and D. Dai, *J. Solid State Chem.* **176** (2003) 417.

W2-C (2:00 – 3:30 pm)

**Software and Methods**

Chair: M. Aivazis (Ruby Room)

W2-C1 (2:00 pm)

**DANSE (Distributed Data Analysis for Neutron Scattering Experiments): Extending the Scientific Toolkit for the Neutron Community (Invited)**

M. M. McKerns (California Institute of Technology)

The DANSE system will merge the various computational tasks of neutron scattering into a unified, component based run-time environment. Standard components will implement data analysis, visualization, modeling, and instrument simulation for all areas of neutron scattering. A core technology of DANSE is an open source framework that supports the software components and mediates their interactions. DANSE will provide tools to help instrument scientists and expert users migrate their existing routines to components, and allow new and casual users to access a stock set of standard analysis applications or configure their own new computing procedures for novel experiments. The modular structure of DANSE parallels the steps of data analysis performed by scientists, thus making it a natural environment for creating flexible computing procedures. DANSE will lower barriers to sharing software, and extend the experimentalist's toolkit with capabilities of analysis and interpretation such as high-performance simulations (band structure, molecular dynamics, etc.), co-analysis of data from multiple experiments, and real-time feedback for experimental control.

W2-C2 (2:30 pm)

**McStas 1.10 - new release of the flexible neutron ray-tracing package - improved support for virtual experiments**

P. K. Willendrup (Riso National Laboratory, Denmark), E. Farhi, K. Lieutenant (Institut Laue-Langevin, France), P. Christiansen, K. Lefmann (Riso National Laboratory, Denmark)

The new release 1.10 of the McStas neutron ray-tracing simulation package has many new features providing enhanced support for virtual neutron scattering experiments.

New language keywords supports newly added advanced sample models, enabling the user to simulate effects of sample environment and allows

to combine elastic, inelastic, phonon, powder and single crystal scattering effects. A detailed example of the use of these very important new features will be given.

In regard to simulation of neutron polarisation, McStas 1.10 is an important milestone, since the first basic polarisation-capable components will be added to the software distribution.

Finally, important work has been made to make McStas run more easy on large machine grids and clusters, and tools have been added to merge multiple datasets in a statistically correct manner.

W2-C3 (2:45 pm)

### **Neutron Holography: Continuing to Break New Ground**

R. B. Rogge (National Research Council Canada), B. Sur, V. N. Anghel (Atomic Energy of Canada Ltd.), J. Katsaras (National Research Council Canada)

The initial work [1] of the Chalk River Neutron Holography group represented the first experimental demonstration of atomic resolution holography using thermal neutrons and generated a great deal of interest. Further experimental results [2] were published soon after and both were presented at the 2002 ACNS. Since that time the Chalk River group has developed a kinematical formulation for the diffraction pattern of monochromatic plane waves scattering from a mixed incoherent and coherent scattering length distribution [3]. The formulation demonstrates the conditions under which one can reconstruct thermal neutron holographic data from samples with either a single incoherent scatterer per unit cell, or with numerous incoherent scatterers per unit cell. The Chalk River group has also acquired thermal neutron holograms from a variety of samples, demonstrating both the internal source, and the internal detector modes. The ongoing experimental effort has yielded some exciting new results with the potential to expand applications of this new technique. Some of these data, and problems encountered in data analysis will be presented.

[1] B. Sur, R. B. Rogge, R. P. Hammond, V. N. P. Anghel and J. Katsaras, *Nature* **414** (2001) 525.

[2] B. Sur, R. B. Rogge, R. P. Hammond, V. N. P. Anghel, and J. Katsaras, *Phys. Rev. Lett.* **88**(6) 065505 (2002).

[3] B. Sur, V. N. P. Anghel, R. B. Rogge, and J. Katsaras, *Phys. Rev. B*, **71**, 014105 (2005).

W2-C4 (3:00 pm)

### **Statistical Analysis of Neutron Specular Reflection Phase-Inversion**

N. F. Berk (NIST Center for Neutron Research)

Neutron specular reflection probes the laterally averaged scattering length density (SLD) depth profile of thin films. The power of the technique stems from its underlying mathematical coherence. Because specular reflection can be cast formally as a one-dimensional wave mechanics problem, it admits to exact solutions of both the “direct” problem of calculating the reflection amplitude spectrum from any SLD profile, and of the “inverse” problem of retrieving the SLD profile from the amplitude spectrum. For perfect data, these formalities establish a one-to-one correspondence between the amplitude spectrum and the profile (for a broad class of SLD profiles). Moreover, practical methods exist for determining the complex reflection amplitude from one or more reflectivity measurements, thus enabling reliable interpretations of neutron measurements.

Here we address the statistical analysis of the phase-inversion program. By realistically simulating phase-inversion measurements, we show that standard error propagation formulas do not work well for thin film samples. We identify high and low frequency components of a noisy reflection amplitude spectrum for films of known thickness. We distinguish between measurement noise and data truncation effects and demonstrate how bootstrap methods can provide good estimates of uncertainties for SLD profiles. Finally, we advance the principle that phase-inversion sets the limits of information from real neutron specular reflection data.

W2-C5 (3:15 pm)

### **Continuous White Beam Reflectometer/ Diffractometer**

C. F. Majkrzak (National Institute of Standards and Technology)

Plans for a broad wavelength band neutron reflectometer/diffractometer, to be installed at an end-guide position at the NCNR, are presented. Conventional reflectometers/diffractometers at continuous neutron sources typically employ nominally monochromatic beams with wavelength spreads of the order of one percent. In general, incident beams with significantly greater bandwidths, e.g., extending from 4 to 10 Angstroms,



can be used without sacrificing wavevector transfer ( $Q$ ) resolution if wavelength analysis of the elastically reflected beam is performed. This can be accomplished at a pulsed neutron source via time of flight. At a continuous source, a set of single crystals can be arranged to do the wavelength analysis instead. Alternatively, for the case of specular reflection (measurements of which ultimately yield the scattering length density [SLD] depth profile), multiple polychromatic beams of appropriate wavelength distributions and angles of incidence on a planar sample can be collected in an array of detectors in such a way that the specular reflectivity can be extracted without analysis of every individual neutron's wavelength. That is, a system of linear equations can be solved in which the measured quantities are the wavelength-integrated intensities at different angles of reflection and the coefficients of the desired reflectivity (as a function of  $Q$ ) are determined by the wavelength-dependent incident intensity distributions. Thus, in either case, continuous incident beams with broad angular and wavelength spreads can be incident on the sample for measurements of the specular reflectivity without compromising resolution. In principle, the higher resulting efficiencies would be comparable to what is achievable at a pulsed source with an equivalent time-averaged flux. For other scattering processes, namely nonspecular reflection in which in-plane structures are probed, broad wavelength bands can still be utilized in a single incident beam having a relatively narrow angular divergence, but a series of crystal analysers, one for each wavelength resolution width, would then be required. Possibilities for doing phase-sensitive reflectometry, which enables one-dimensional real space imaging of the SLD depth profile, with a continuous white beam instrument are discussed.

W2-D (2:00 – 3:30 pm)

## **Self-Assembled Nanoscopic Systems**

*Chair: J. Katsaras (Turquoise A-B Room)*

W2-D1 (2:00 pm)

### **Important parameters controlling size, polydispersity and shape of self-assembled unilamellar vesicles** (Invited)

M. Nieh (NRC Chalk River Laboratories, Canada)

Spontaneously forming unilamellar vesicles (ULV) have been found in some surfactant and lipid systems. Our research has been focused on the mixtures composed of long- and short-chain phospholipids, where stable, low-polydispersities ULV are obtained. Using small angle neutron scattering, we are able to investigate the effects of some important parameters on the polydispersity, size and shape of the ULV, including the molar ratio of long- to short-chain lipids, charge density, salinity of the solutions, chain length of the long-chain lipid, temperature cycling, lipid concentration, bilayer rigidity and so on. Experimental result also supports our proposed model for the formation mechanism of these self-assembled ULV. Moreover, under the condition of low lipid concentration, ULV can be locked in the vesicular morphology for hours.

W2-D2 (2:30 pm)

### **Structural Studies of Proton-Conducting Fluorous Block Copolymer Membranes** (Invited)

B. J. Frissen (Simon Fraser University)

We use diblock copolymers as a model system to investigate the correlation between morphology and transport properties in ionomer materials. Diblock copolymers with a fluorinated block and a sulfonated polystyrene block allow control of the ionic exchange capacity by adjusting either the length of the sulfonated polystyrene chains or their degree of sulfonation. We have studied the structure of membranes made from various polymer configurations by small angle neutron scattering using contrast variation. Analysis shows that there is phase separation at length scales of the order of a few tens of nanometers due to the immiscibility of the two polymer blocks; and that there is substructure within the sulfonated polystyrene domains due to separation between the hydrated ionic groups and the hydrophobic



polystyrene. We compare these results to transmission electron microscopy images and with proton conductivity and water content measurements.

W2-D3 (3:00 pm)

### **Effect of Hydrophobic Alcohols on the Phase Behavior of Pluronic Micelles**

P. Thiagarajan (Argonne National Laboratory, Intense Pulsed Neutron Source), L. Guo (Argonne National Laboratory), R. Colby (The Pennsylvania State University)

Water-soluble nonionic triblock copolymer surfactants PEO-PPO-PEO (Pluronics) are extensively used by industries for a wide range of applications. We investigated the effects of temperature and concentration of two hydrophobic alcohols (DL-1-phenylethanol and Surfynol 104, a C14 diol) on the phase behavior of aqueous solutions of Pluronic P84 and P105. Results reveal that morphological changes from spherical to cylindrical and then to lamellar micelles occur with either increasing temperature or concentration of added DL-1-phenylethanol. Furthermore, above the solubility limit, the alcohol gets distributed throughout the micelles (core and shell). Interestingly, the P105 solution with added Surfynol forms high viscosity solutions consisting of large cylindrical micelles at room temperature, but at about 10 K above or below room temperature, disk-like micelles are formed. Unlike DL-1-phenylethanol, the more hydrophobic Surfynol sequesters within the core of the micelles. We will discuss the phase behavior and the distribution of the two systems in the Pluronic dispersions and correlate the mechanism of these structural changes. The rich micellar phases of Pluronics with added hydrophobic alcohols provide potential applications in controlled drug delivery, and the temperature-induced phase change broadens the application of Pluronics in other areas.

*This work benefited from the use of IPNS at Argonne National Laboratory, which is funded by the Office of BES, US DOE under contract #W-31-109-ENG-38 to the University of Chicago.*

W2-D4 (3:15 pm)

### **Magnetic contrast in neutron reflection from Soft Condensed Matter films**

D. J. McGillivray, F. Heinrich (Carnegie Mellon University and CNBT at the NIST Center for Neutron Research), U. A. Perez-Salas (University of California, Irvine), N. F. Berk, C. F. Majkrzak (NIST Center for Neutron Research), M. Loesche (Carnegie Mellon University and CNBT at the NIST Center for Neutron Research)

We have developed a robust implementation in neutron reflectometry of thin magnetic reference layers underneath gold films (both iron and a nickel-rich “ $\mu$ -metal” alloy) to provide independent contrast measurements of systems of interest using polarized neutron beams. This technique not only reduces the inherent ambiguity which arises from the loss of phase information, but also serves to enhance the reflectivity of the system without perturbing the sample - a feature particularly important in the characterization of delicate biological systems. Moreover, the two contrasts can be measured practically simultaneously, ensuring that the system itself has not undergone physical changes between contrast measurements. In exemplary applications, we show that the polarization-dependent contrast variation helps resolve structural features that are otherwise difficult to determine. Finally, we demonstrate that the implementation of the phase inversion method developed by Berk and Majkrzak based on magnetic contrast variation yields results in accord with those expected from conventional modelling. The technique thus provides a basis for structural investigations of complex systems where there is little prior physical knowledge.

W3-A (4:15 pm)

## Breakout Sessions

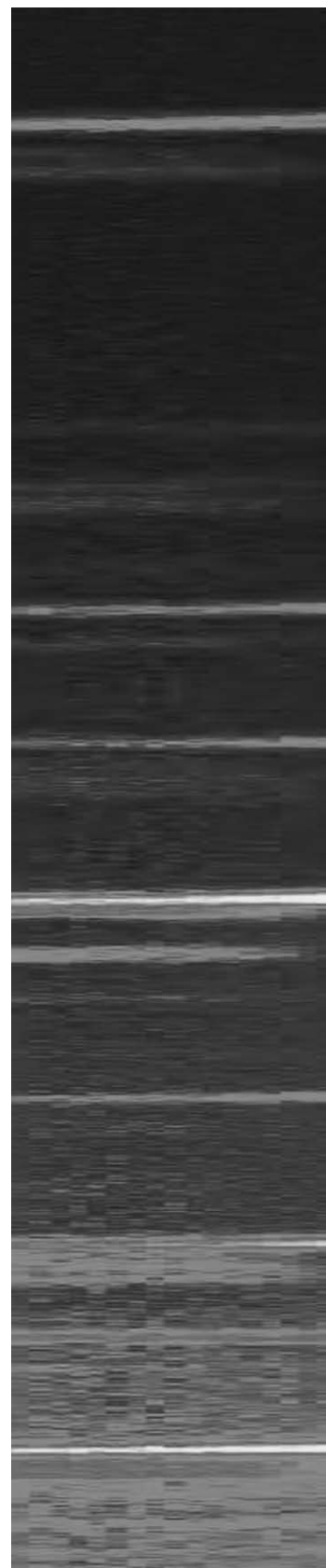
- SHUG Meeting  
*Organizer: D. Louca* (New Orleans Ballroom)
- The Very Cold Neutron Source  
*Organizers: B. Micklich, J. Carpenter*  
(Ruby Room)
- Topaz IDT Meeting  
*Organizer: C. Hoffmann* (Sapphire Room)
- SEQUOIA IDT Meeting  
*Organizer: G. Granroth* (Coral Room)
- Sample Environment at Neutron Scattering  
Facilities  
*Organizers: K. Volin, D. Dender, L. Santodonato*  
(Turquoise A-B Room)

## Thursday, June 22

- |          |   |
|----------|---|
| 8:45 am  | Buses depart to Argonne National Laboratory     |
| 9:30 am  | Tour of the IPNS at Argonne National Laboratory |
| 11:00 am | IPNS 25th Anniversary Ceremony                  |
| 12:00 pm | Lunch at Argonne National Laboratory            |
| 1:30 pm  | Buses depart for Pheasant Run and airports      |



## Author Index







**A**

Abbas, S.: MP41  
 Abernathy, D. L.: TP10  
 Abraham, T.: TP29  
 Acatreinei, A. I.: TP13  
 Acatrinei, A. I.: T3-B4, TP02  
 Adams, M. A.: T3-B3  
 Adroja, D. T.: T2-A4, T4-B3, WP10  
 Agamalian, M.: TP31  
 Agnew, S. R.: M3-D2  
 Agrawal, S. K.: MP14  
 Aivazis, M.: WP55  
 Akgun, B.: M4-D4  
 Allis, D. G.: MP18, TP24, WP25  
 Alonzo, J.: TP18  
 Amoretti, G.: MP20  
 An, K.: M4-B2, MP21, MP51, WP09, WP46  
 Andersen, N. H.: WP56  
 Anderson, I. E.: WP24  
 Anderson, T. M.: W2-A4  
 Anghel, V. N.: W2-C3  
 Ankner, J. F.: TP30  
 Annis, B. K.: TP64  
 Antonio, D.: WP06  
 Arias, D.: T3-C2  
 Arif, M.: MP06, T4-C3  
 Armes, S. P.: M4-D3  
 Armstrong, A. R.: WP51  
 Armstrong, N. L.: M3-A3, MP06, WP14  
 Arnold, T.: MP29, TP59  
 Aronov, M. A.: TP53  
 Aronson, M. C.: M4-A2, T2-A4, W2-B3  
 Aso, N.: TP08  
 Autrey, T.: M3-B3, M3-B5, MP55, WP05  
 Avci, S.: MP32  
 Avdeev, M.: MP42, WP49  
 Azuah, R. T.: MP38, WP44  
 Azzam, S.: MP12  
 Azzoni, C. B.: TP44

**B**

Badyal, Y. S.: TP64  
 Baglioni, P.: M3-A5, MP33  
 Bailey, W. B.: M3-D4, MP51  
 Baldrian, J.: TP40  
 Balsara, N.: M4-D2, MP24  
 Banishki, N.: M3-B2  
 Banuelos, J. L.: TP14  
 Banuelos, L. J.: TP02

Bao, W.: MP46, T2-A1  
 Barabash, R.: M4-B3  
 Barbour, A. M.: MP29  
 Barnes, P. W.: MP42, WP21, WP49  
 Bauer, E.: T2-A1  
 Bauer, E. D.: T2-A2  
 Baxter, D. V.: M2-C2, MP09, WP14, WP35  
 Belanger, D. P.: WP23, WP24  
 Benmore, C. J.: MP58, T3-B1, TP14, WP22, WP48  
 Bennett, B.: T4-A2  
 Benson, M. L.: M4-B4, M4-B5, MP16, MP19  
 Bera, T.: WP18  
 Berk, N. F.: W2-C4, W2-D4, WP26  
 Berliner, R.: TP35, TP60  
 Beveridge, T.: TP29  
 Beyermann, W.: MP25  
 Bhatia, S. R.: MP14  
 Bilheux, H. Z.: TP26  
 Billinge, S.: MP28, WP11, WP40  
 Billinge, S. J.: WP16, WP17, WP57, WP63, WP50  
 Black, T. C.: MP06  
 Blackburn, E. R.: TP48  
 Bleuel, M.: T4-D5, TP45, WP41  
 Bline, R.: MP65  
 Bloch, J.: WP40  
 Block, R.: M4-C6  
 Blokland, W.: WP64  
 Blumenthal, W. R.: M3-D2  
 Bonca, J.: MP04  
 Bond, G. M.: M2-A5, TP32  
 Booth, C. H.: WP06  
 Borchers, J. A.: M4-A1, M4-A2, T3-C3, TP39, TP57  
 Bossev, D.: M3-A3, WP14  
 Bossev, D. P.: M2-D4, M4-A4, TP37, W2-D5  
 Bourges, P.: MP62  
 Bourke, M. A.: M3-D2  
 Bozin, E.: WP40  
 Bozin, E. S.: MP28, WP11  
 Bradshaw, J. P.: M2-D2  
 Bramwell, S. T.: WP06  
 Bribe, R. M.: MP10  
 Britt, P. F.: T3-D4  
 Brittain, W. J.: M4-D4  
 Bocker, C.: WP02  
 Broholm, C.: MP40, MP47, T2-A3, T4-B5  
 Broholm, C. L.: W2-B2  
 Brown, C.: M3-B5, WP05  
 Brown, C. M.: M3-B4, MP55, T3-C4  
 Brown, D.: M4-B5  
 Brown, D. E.: TP52

Brown, D. W.: M3-D2, M4-B2, M4-B3, M4-B4, MP21, T4-C5  
 Browning, J. F.: M2-A5, TP32, WP32  
 Bruce, P. G.: WP51  
 Bruno, P.: TP45  
 Bryndin, D.: WP40  
 Bu, Z.: WP03  
 Buchanan III, A. C.: T3-D4  
 Bunick, G. J.: T4-A1  
 Bunz, U. H.: M4-D5  
 Burnham, C. J.: T3-B3  
 Butch, N. P.: T2-A4  
 Butler, P. D.: MP26, TP46, WP42  
 Butzek, M.: TP56  
 Bychkov, E.: MP58

## C

Caciuffo, R.: MP20  
 Cadene, A.: TP49  
 Callaway, D. J.:  
 Cao, R.: W2-A4  
 Carey, M. J.: T3-C3  
 Carlile, C. J.: M2-C4  
 Carpenter, J. M.: M2-C3  
 Carrell, H. L.: T4-A1  
 Carretta, S.: MP20  
 Cava, R.: M2-A1  
 Chae, T.: TP65, TP30  
 Chaffee, A.: T3-D4  
 Chakoumakos, B. C.: TP09, TP41  
 Chan, J.: WP09  
 Chan, J. Y.: T2-A1  
 Chanaa, S. Z.: MP29  
 Chandra, D.: TP34  
 Chang, S.: M2-B5, MP25, T2-A5, WP36  
 Chapon, L. C.: WP54  
 Chatterji, T.: MP37  
 Chen, M. L.: WP31, WP53  
 Chen, S.: M3-A5, MP22, MP33, T3-B2  
 Chen, W.: M2-B3  
 Chen, W. C.: TP39, TP50, TP57, WP39  
 Chen, Y.: MP46, T2-A1, T4-B4, TP39, TP57, WP02  
 Cheng, S.: TP11  
 Cheong, S.: WP27  
 Cheong, S. W.: M2-B2, T4-B4  
 Chi, S.: MP52  
 Chien, W.: TP34  
 Childers, W. S.: M3-A2  
 Chmaissem, O.: MP32, TP52, WP21, WP61

Cho, J. H.: W2-B4  
 Cho, S.: WP13  
 Cho, Y.: MP62  
 Choo, H.: M4-B3, M4-B5, MP05, MP16, MP19, MP21, MP51, T4-C1, TP11, TP21, WP46, WP50  
 Chou, F. C.: W2-B4  
 Chowdhuri, Z.: MP12  
 Christensen, N. B.: WP56  
 Christiansen, P.: MP31, W2-C2  
 Christianson, A. D.: T2-A2, WP30  
 Christou, G.: W2-A1  
 Chu, X.: MP33  
 Chu, Y.: W2-B4  
 Chung, J.: MP61, WP27  
 Chung, J. H.: MP50, WP56  
 Clapham, L.: M3-D1  
 Clarke, S.: MP29  
 Claus, H.: WP49  
 Clausen, B.: M4-B2, M4-B4, MP19, MP21  
 Clearfield, A.: MP17  
 Coates, L.: T4-A1, T4-A2, T4-A3  
 Cobb, J. W.: WP31, WP53  
 Colby, R.: W2-D3  
 Collett, B.: WP39  
 Conlon, K. T.: T4-C4, TP20  
 Cook, R.: TP59  
 Cook, R. E.: MP29  
 Cooley, L. D.: WP34  
 Cooper, R. G.: WP20  
 Copley, J. R.D.: MP20  
 Cornelius, A. L.: WP06  
 Cotton, F. A.: WP10  
 Cranswick, L.: T4-D1, W2-B5  
 Cranswick, L. M.: TP20  
 Crawford, C. B.: M4-C5  
 Crow, L.: MP53  
 Cubitt, R.: WP18  
 Cuesta-Ramirez, A.: TP59  
 Curtis, J. E.: M3-A1, MP12, WP26, WP28

## D

Dabkowska, H. A.: MP04  
 Dabrowski, B.: M2-A3, MP32, T3-C4, TP52, WP04, WP21, WP61  
 Dadmun, M.: WP45  
 Dadmun, M. D.: TP18, TP54  
 Daemen, L.: M3-B3, TP07  
 Daemen, L. L.: M3-B5, MP55, T3-B4, TP02, TP33, TP42, WP05

Dai, P.: M3-C4, M4-A3, MP52, MP59  
 Dalal, N.: WP10  
 Danagouliau, G.: MP03  
 Daniel, M.: WP06  
 Danon, Y.: M4-C6  
 David, S. A.: M4-B2, MP21  
 Daymond, M. R.: M4-B4, MP16  
 de Souza, N. R.: T3-B3  
 de Visser, A.: W2-B3  
 Dealwis, C.: T4-A2  
 DeBeer-Schmitt, L.: WP18  
 DeBeer-Schmitt, L. M.: MP11  
 DeConinck, A.: WP11  
 Delaire, O.: M2-A6  
 Delaire, O.: MP44, WP47, WP55  
 Demmel, F.: MP37  
 Desmond, K.: M3-A4  
 Dewhurst, C. D.: MP11, WP18  
 Diallo, S.: MP38  
 DiJulio, D.: TP60  
 Dmowski, W.: W2-A3  
 Dolgos, M. R.: WP48  
 Donaberger, R. L.: TP20  
 Dong, J.: M3-A2  
 Dosch, H.: T4-D2  
 Doucet, M.: T3-C3, WP44  
 Dove, M.: M2-B4  
 Dubois, E.: TP49  
 Dufour, C.: M4-A1  
 Dumesnil, K.: M4-A1  
 Dunker, A. K.: M3-A3  
 Dunsiger, S. R.: MP04  
 Durodola, J. F.: M3-D5  
 Durstock, M. F.: TP19  
 Duxbury, P. M.: WP57  
 Dye, D.: T4-C4

## E

Eckert, J.: MP65, T3-C3  
 Egami, T.: MP30, W2-A3  
 Ehlers, G.: MP56, WP06  
 El Shawish, S.: MP04  
 El-Khatib, S. T.: MP64  
 Engelhardt, L.: M4-A5  
 Erdemir, A.: M2-A2  
 Eres, G.: W2-A6  
 Erwin, R. W.: TP39, TP57  
 Eryilmaz, O. L.: M2-A2  
 Eskildsen, M. R.: M3-C1, MP11, WP18

## F

Fakra, S.: TP34  
 Falus, P.: T4-D2  
 Falvello, L.: TP02  
 Falvello, L. R.: TP13, TP28  
 Fan, C.: WP50  
 Fanelli, V. R.: T2-A2  
 Faraone, A.: M3-A5, MP33, MP47, T3-B2, T4-D3  
 Farhi, E.: W2-C2  
 Farinelli, M. J.: MP29  
 Farrell, S. P.: M4-B1  
 Farrow, C. L.: WP40  
 Felcher, G. P.: M2-C5, T4-D2  
 Fellows, N. A.: M3-D5  
 Feng, Z.: M4-B2, MP21  
 Ferguson, B. L.: TP53  
 Ferguson, P. D.: WP64  
 Fernandez-Alonso, F.: MP50, WP10  
 Fernandez-Baca, J. A.: M4-A3, MP52, WP23, WP24  
 Fieramosca, J.: WP61  
 Filges, U.: MP31  
 Fishman, R. S.: WP19  
 Fisk, Z.: T2-A1  
 Fitzsimmons, M.: M2-C5  
 Fitzsimmons, M. R.: M4-A1, T3-C2  
 Flor, G.: TP44, WP17  
 Forgan, E. M.: M3-C3  
 Foster, L. J.: T4-A5  
 Foster, M. D.: M4-D4  
 Fox, J.: TP20  
 Franklyn, C. B.: TP03  
 Fratini, E.: M3-A5, MP33  
 Frazier, L.: MP29, TP59  
 Freeman, D. W.: WP64  
 Frisken, B. J.: W2-D2  
 Frost, C. D.: MP49, T2-A2  
 Fujita, M.: MP49  
 Fultz, B.: M2-A6, MP44, TP10, WP47, WP55  
 Furdyna, J. K.: T3-C4

## G

Gagliardo, J.: T4-C3  
 Gahler, R.: T4-D5, TP05  
 Gallmeier, F. X.: WP64  
 Gannett, W.: T3-C3  
 Gao, Y.: WP50  
 García Hernández, M.: T3-C2  
 Garcia Sakai, V.: M4-D1

Garcia-Sakai, V.: MP12  
 Gardner, J.: MP47  
 Gardner, J. S.: MP56, WP06  
 Garlea, E.: MP05  
 Garlea, V. O.: M4-A5, MP05, T2-A5, WP38, WP39  
 Garvey, C. J.: T4-A5  
 Gasparovic, G.: W2-B4  
 Gaulin, B. D.: MP04  
 Gehring, P. M.: M2-B1, M2-B3  
 Gentile, T. R.: TP39, TP50, TP57, WP34, WP39  
 Geselbracht, M. J.: MP08  
 Ghalsasi, P.: WP22  
 Gharghouri, M. A.: M4-B1, T4-C4, WP33  
 Ghazi, H.: W2-B5  
 Ghosh, V.: WP34  
 Giebultowicz, T. M.: T3-C1, T3-C4  
 Glushkov, I. S.: WP37  
 Glusker, J. P.: T4-A1  
 Glyde, H.: M3-C5  
 Glyde, H. R.: MP38  
 Goka, H.: WP62  
 Goldman, A. I.: T2-A5  
 Golub, R.: TP05  
 Goodwin, A.: M2-B4  
 Goremychkin, E.: WP54  
 Goremychkin, E. A.: T2-A2  
 Gourdon, O.: TP04, TP47  
 Gourdon, O. A.: MP35  
 Gout, D.: TP04, TP47  
 Goyette, R. J.: TP30, TP65  
 Granroth, G. E.: MP50, WP08, WP53  
 Gray, K.: WP59  
 Graziano, J.: WP09  
 Grech, E.: WP12  
 Greedan, J. E.: W2-B5, WP16  
 Gregory, R.: MP12  
 Greven, M.: MP62  
 Grosse, M.: M3-D3  
 Gruen, D.: TP45  
 Gu, G. D.: MP49, MP57, WP62  
 Guidi, T.: MP20  
 Guo, L.: W2-D3  
 Gutberlet, T.: TP15  
 Gutowski, M.: M3-B5, WP05

## H

H.Y. Yan, X. Tong, M. Snow, .: WP39  
 Haeussler, W.: WP06  
 Hagen, M.: WP34

Hagen, M. E.: M2-B4, WP53  
 Haile, S.: MP28  
 Hall, J. E.: T3-A4  
 Ham-Su, R.: M4-B1  
 Hamilton, W. A.: MP07, MP26, TP27  
 Hammerton, K. M.: T4-A5  
 Hammonds, J. P.: TP28  
 Hammouda, B.: M3-A3, WP03  
 Han, X.: T3-A5  
 Hannan, B.: MP53  
 Hanson, B. L.: T4-A1  
 Haravifard, S.: MP04  
 Harrison, N.: MP50, W2-B2  
 Harroun, T.: TP29  
 Harroun, T. A.: M2-D2, M2-D3  
 Hart, R. T.: T3-B1  
 Hartl, M.: M3-B3, M3-B5, WP05  
 Hartl, M. A.: T3-B4, TP02  
 Hartman, M. R.: WP29  
 Hawari, A. I.: TP35, TP60  
 Hawker, C. J.: MP13  
 He, D.: TP07  
 Hehlen, M.: W2-A3  
 Hehlen, M. P.: MP25, WP36  
 Heinrich, F.: T3-A4, TP36, W2-D4  
 Heller, W. T.: T4-A4, TP17, TP27, WP01  
 Hemley, R. J.: WP15  
 Heroux, L.: MP53  
 Herwig, K. W.: T3-D4  
 Hess, N.: M3-B3, M3-B5, WP05  
 Hess, N. J.: MP55  
 Heuser, B. J.: MP01, MP03  
 Hill, C. L.: W2-A4  
 Hill, J. M.: M2-A3  
 Hinde, R. J.: TP59  
 Hinks, D. G.: MP42, WP49  
 Hirota, K.: M2-B3, TP08  
 Hjelm, R. P.: M2-A5  
 Hjøllum, J.: MP31  
 Ho, D. L.: MP46  
 Hodges, J.: MP53  
 Hodges, J. P.: TP61  
 Hoffmann, A.: T3-C2  
 Hoffmann, C.: WP39  
 Holden, P. J.: T4-A5  
 Holden, T. M.: TP21  
 Holderna-Natkaniec, K. Z.: MP54, TP51, WP12  
 Holoubek, J.: TP40  
 Holt, S. A.: T3-A3

Holzapfel, M.: WP51  
 Homouz, D.: MP65  
 Hong, K.: WP13  
 Hong, T.: MP40, T4-B5  
 Honig, J.: M2-B5  
 Hoogenboom, B. W.: MP11  
 Howell, E.: T4-A2  
 Hristova, K.: T3-A5  
 Huang, E.: MP19  
 Huang, Z.: TP18  
 Hubbard, C.: M4-B2  
 Hubbard, C. R.: M3-D4, MP05, MP21, MP51, TP11, TP21, TP53, WP09, WP46  
 Huber, M.: MP06  
 Hudis, J.: T2-A3  
 Hudson, B. S.: MP18, TP24, TP25, WP25  
 Huffman, P. R.: M4-C2  
 Huffmann, P. R.: M4-C5  
 Humphreys, M. W.: TP48  
 Huq, A.: TP34  
 Hurd, A. J.: TP63  
 Hussey, D. S.: T4-C3

## I

Ice, G.: M4-B3  
 Ice, G. E.: T4-D1  
 Ignatjev, I.: TP36  
 Ignatovich, V. K.: TP05  
 Inderhees, S. E.: M4-A2  
 Iolin, E.: MP48, TP38, TP58  
 Ito, T. M.: M4-C5  
 Iverson, E. B.: wp64

## J

Jacobson, D. L.: MP06, T4-C3  
 Jakubas, R.: MP54, WP12  
 Janssen, Y.: T2-A5  
 Jeng, U.: TP15  
 Jenkins, T. A.: WP15  
 Jensen, T. B.: WP56  
 Jeong, I. K.: W2-A3  
 Ji, H.: TP18  
 Jiang, Y.: M4-D5  
 Jin, R.: MP45, MP59, T4-B3  
 Johnson, C. S.: WP51  
 Johnson, J. A.: M2-A2  
 Jonas, S.: MP47  
 Jones, C. Y.: M3-B2  
 Jones, G. L.: M4-C4, TP50, WP39

Jorgensen, J. D.: MP32, MP42, TP52, WP04, WP21, WP49, WP61  
 Ju, H.: MP01  
 Juhas, P.: WP40, WP57

## K

Kaiser, H.: M3-A3, MP06, MP09, WP14, WP35  
 Kakurai, K.: MP61  
 Kamath, S. Y.: TP54  
 Kamazawa, K.: MP23  
 Kang, H. J.: M3-C4  
 Kang, S. H.: WP51  
 Kareev, Y. A.: WP37  
 Karen, P.: WP36  
 Karpinski, J.: WP18  
 Kasianowicz, J. J.: TP36  
 Katsaras, J.: M2-D2, M2-D3, TP29, W2-C3  
 Katz, A. K.: T4-A1  
 Kent, M. S.: T3-A2  
 Kenzelmann, M.: M2-B2, WP56  
 Kepa, H.: T3-C1, T3-C4  
 Kidder, M. K.: T3-D4  
 Kilbey, S. M.: TP18  
 Kim, H.: MP10, MP28, WP13  
 Kim, H. J.: WP17  
 Kim, J.: WP27  
 Kim, M. H.: TP31  
 Kim, S. B.: M2-B2  
 Kintzel, E. J.: T3-D4  
 Kirby, B.: M2-C5, T3-C2  
 Kirk, M. L.: W2-A4  
 Kirumakki, S. R.: MP17  
 Kiryukhin, V.: T4-B4  
 Kivelson, S.: M3-C2  
 Kiyanagi, R.: WP61  
 Klarstrom, D. L.: MP16, MP19  
 Klausen, S.: MP23  
 Klose, F. R.: TP65  
 Klueh, R. L.: TP31  
 Klug, D. D.: T3-B1  
 Ko, H.: MP35  
 Kobasko, N. I.: TP53  
 Koetzle, T. F.: W2-A4  
 Kogan, V. G.: WP18  
 Kögerler, P.: M4-A5  
 Kohl, J. A.: WP53  
 Kohlbrecher, J.: M3-D3  
 Kolesnik, S.: MP32, T3-C4, TP52, WP21  
 Kolesnikov, A.: T3-B2



Kolesnikov, A. I.: MP63, T3-B3, WP30  
 Komives, A.: M4-C4  
 Könnecke, M.: MP31  
 Koza, M. M.: MP37  
 Kozlowski, P. M.: TP24  
 Kramer, M. J.: M2-A4  
 Kresch, M.: M2-A6, MP44, WP47  
 Kreyssig, A.: T2-A5  
 Krishnamurthy, V. V.: T2-A4, WP19  
 Krist, T.: T4-D4, W2-C6, WP41  
 Krueger, S.: TP16, WP26, WP28  
 Kucerka, N.: M2-D1  
 Kuhl, T. L.: MP07  
 Kulan, S. J.: TP27  
 Kunz, M.: TP34  
 Kurzman, J. A.: MP08  
 Kuzmenko, I.: T3-A2

## L

Lago, J.: WP06  
 Lakey, J. H.: T3-A3  
 Lal, J.: T4-D5, TP40, TP45, WP41  
 Lamsal, J.: W2-B3  
 Landee, C. P.: T4-B5  
 Lang, E. A.: WP41  
 Langan, P.: T4-A1, T4-A2, T4-A3, TP61  
 Lantzky, K. M.: MP63  
 Lara-Curzio, E.: WP09  
 Larese, J. Z.: MP29, TP42, TP59  
 Larkins, B. K.: TP27  
 Lathrop, S.: WP31  
 Laub, C. F.: MP07  
 Lavelle, C. M.: MP09  
 LaVelle, C. M.: WP35  
 Laver, M.: M3-C3  
 Lawrence, J. M.: T2-A2, WP30  
 Lay, M.: TP18  
 Leao, J.: T3-B2, T3-C4, WP15  
 Lee, B.: W2-A2  
 Lee, C.: T3-A1, WP13  
 Lee, H.: TP65, T2-A1, TP15  
 Lee, J.: WP13  
 Lee, S.: MP61, T4-B2, WP27  
 Lee, S. H.: MP23, MP40, WP60  
 Lee, W. T.: TP50, WP34, WP39  
 Lee, Y. S.: W2-B4  
 Lefmann, K.: MP31, W2-C2, WP56  
 Lehmann, E.: M3-D3  
 Leon, C.: T3-C2  
 Leonhardt, W.: WP34  
 Leuschner, M.: M4-C4, WP35  
 Leuschner, M. B.: MP03, MP09, WP14  
 Li, H.: TP11  
 Li, J.: M4-A5, WP38, WP56  
 Li, P.: M4-D3  
 Li, Q.: WP59, WP62  
 Li, X.: T4-A1  
 Li, Z.: TP53  
 Liang, Y.: M3-A2  
 Liaw, P. K.: M4-B3, M4-B4, M4-B5, MP05, MP16,  
 MP19, TP11, TP21, WP46, WP50  
 Lieutenant, K.: W2-C2  
 Lin, J.: WP55  
 Lin, M. Y.: MP24, MP46  
 Lin, T.: TP15  
 Lin, Z.: MP10  
 Link, P.: WP67  
 Littrell, K. C.: M2-C5, WP30, WP52  
 Liu, C. T.: WP50  
 Liu, D.: MP22  
 Liu, J.: WP40  
 Liu, L.: M3-A5, MP33, T3-B2  
 Liu, M.: TP18  
 Liu, P.: M3-A2  
 Liu, Y.: M3-B5, WP29  
 Liu, Y. D.: M4-B4  
 Llobet, A.: MP34, MP64, TP55  
 Lo, C.: W2-A2  
 Locke, D.: T4-D1  
 Loesche, M.: T3-A2, T3-A4, TP36, W2-D4  
 Loewenhaupt, M.: WP67  
 Loguillo, M. J.: TP10  
 Lohse, D. J.: MP24  
 Loizou, E.: TP46  
 Lokshin, K.: TP07  
 Lone, M. A.: MP09  
 Loong, C. K.: T3-B3  
 Lorenzo, J. E.: MP46  
 Louca, D.: MP23, T3-D2  
 Love, L. J.: TP41  
 Lozano-Gorrin, A. D.: WP16  
 Lozowski, W. R.: MP09, WP35  
 Lu, K.: M3-A2  
 Lu, W.: WP64  
 Lu, Y.: MP27  
 Lu, Y. L.: M4-B3, WP46  
 Lu, Z. P.: MP15  
 Luban, M.: M4-A5  
 Lucas, M.: M2-A6

Lumsden, M.: W2-B3  
 Lumsden, M. D.: MP45, MP50, MP59, TP27, WP19  
 Luo, X.: T4-C5  
 Lynch, V. E.: WP31  
 Lynn, D. G.: M3-A2  
 Lynn, G.: MP26  
 Lynn, G. W.: T4-A4, TP17  
 Lynn, J.: T4-B4  
 Lynn, J. W.: M2-B2, M3-C4, TP39, TP57, W2-B4, WP02  
 Lynn, Z.: T2-A1

## M

Ma, D.: M2-A4, MP15  
 Ma, J.: MP25  
 Macaluso, R.: WP54  
 Macaluso, R. T.: T2-A1  
 Mackay, M. E.: MP13  
 Madden, M. E.: TP41  
 Maeno, Y.: MP47  
 Magid, L. J.: TP17  
 Maierhafer, D. L.: TP27  
 Mais, J.: TP52, WP04  
 Majewski, J.: T3-A2  
 Majkrzak, C.: T3-A1  
 Majkrzak, C. F.: M4-D4, T3-A2, T3-A3, TP39, TP57, W2-C5, W2-D4  
 Major, J.: T4-D2  
 Majumdar, B. S.: MP27  
 Malavasi, L.: TP44, WP17  
 Malikova, N.: TP49  
 Maliszewskyj, N.: WP02, WP44  
 Malkova, S.: TP40  
 Mamontov, E.: M3-A5, MP33, MP55, T3-B3, T3-B5, WP05, WP53  
 Mandrus, D.: MP30, MP59  
 Mandrus, D. G.: MP45, MP50, T4-B3  
 Mangin, P. H.: M4-A1  
 Mankey, G. J.: T3-C5  
 Mao, H. K.: WP15  
 Mao, W.: WP15  
 Maple, M. B.: T2-A4  
 Maples, R.: TP08  
 Marry, V.: TP49  
 Martínez, J. L.: T3-C2  
 Masadeh, A. S.: WP50  
 Mason, T. E.: T1-A4  
 Mathieu, R.: MP52  
 Matsuda, M.: MP61  
 Matsuura, M.: M2-B3  
 Maxey, E.: TP34  
 Maxey, E. R.: TP23, WP04, WP50  
 Mayers, J.: MP65, T3-B3  
 Mays, J. W.: TP18  
 McCall, S. H.: TP26  
 McEwan, L.: TP20  
 McGillivray, D.: T3-A2  
 McGillivray, D. J.: T3-A3, T3-A4, TP36, W2-D4  
 McHargue, T. A.: TP30  
 McKenney, S.: TP39, TP57  
 Mckerns, M.: WP55  
 McKerns, M. M.: W2-C1  
 McLain, S. E.: WP48  
 McQueeney, R. J.: M2-B5, MP25, T2-A5, WP36  
 Mehta, A.: M3-A2  
 Mehta, R.: WP45  
 Mei, Q.: WP22  
 Melnichenko, Y. B.: TP17  
 Mesecar, A. D.: TP61  
 Metallo, C.: MP30  
 Metcalf, P.: M2-B5  
 Mezei, F.: MP48, TP62, WP43  
 Micklich, B. J.: M2-C3  
 Mihailescu, E.: T3-A1  
 Mikkelsen, D.: TP02, TP13  
 Mikkelsen, D. J.: TP28  
 Mikkelsen, R.: TP02, TP13  
 Mikkelsen, R. L.: TP28  
 Mikula, P.: TP58  
 Miltzer, B.: WP15  
 Miller, G. J.: MP35, TP47  
 Miller, M. E.: WP39  
 Miller, R. D.: MP10  
 Miller, S. D.: WP31, WP53  
 Mitcehl, J. F.: WP19  
 Mitchell, J.: WP59  
 Mitchell, J. F.: M2-A3, MP23, MP34, WP11  
 Mitsui, Y.: WP60  
 Moglianetti, M.: M4-D3  
 Molaison, J. J.: WP48  
 Moncton, D. E.: M2-C1  
 Moner, I.: T4-C4  
 Monkenbusch, M.: TP56  
 Montfrooij, W.: M2-B5, W2-B3  
 Moodenbaugh, A. R.: WP62  
 Mook, H. A.: M3-C4  
 Moon, J. W.: TP41  
 Moore, S.: TP08  
 Moore, S. A.: TP48

Moreh, R.: M4-C6  
 Moritomo, Y.: MP23  
 Morokuma, K.: W2-A4  
 Motome, Y.: MP23  
 Motoyama, E.: MP62  
 Mou, C.: T3-B2  
 Moyerman, S. M.: T3-C3  
 Mozzati, M. C.: TP44  
 Mulder, D. J.: MP07  
 Muralidharan, G.: TP31  
 Murbach, M.: WP02  
 Murton, J. K.: T3-A2  
 Musaev, D. G.: W2-A4  
 Mustyakimov, M.: T4-A2, T4-A3  
 Myles, D. A.: T4-A4, TP17, TP61

## N

Nagao, M.: T3-D3  
 Nagler, S.: TP08  
 Nagler, S. E.: M4-A5, MP45, MP50, MP59, T4-B3, WP10, WP39  
 Nakatsuji, S.: MP47, T2-A1  
 Nakotte, H.: MP64  
 Nambu, Y.: MP47  
 Nanda, H.: M3-A1, WP28  
 Nandi, S.: T2-A5  
 Natkaniec, I.: MP54, TP51, WP12  
 Neiwert, W. A.: W2-A4  
 Nemes, N. M.: T3-C2  
 Neuefeind, J.: M2-A4, TP14  
 Neuman, M.: M4-C6  
 Neumann, D. A.: M3-B4, TP57  
 Niedermayer, C.: MP31, WP56  
 Nieh, M.: TP29, W2-D1  
 Nieh, M. P.: M2-D3  
 Nojiri, H.: WP24  
 Novak, P.: WP51  
 Novikov, V. N.: MP12  
 Nowak, D.: MP54, TP51  
 Nyborg Ancona, S.: WP59

## O

O'Donovan, K. V.: TP39, TP57  
 Ohl, M.: TP56  
 Oldfield, E.: T3-A1  
 Osborn, R.: MP23, MP43, T2-A2, T2-A4, WP30, WP54, WP59  
 Ott, R. A.: W2-B4  
 Owejan, J. P.: T4-C3

## P

P. Winpenny, R. E.: MP20  
 Pabst, U.: TP56  
 Paglia, G.: WP11  
 Pal, D.: WP18  
 Pantea, C.: TP07  
 Parikh, T. S.: M3-D5  
 Parise, J. B.: T4-D1  
 Parizzi, A.: TP65  
 Park, S.: M2-A2, M2-C5, M4-A1, T3-C2, T4-B4, MP66, WP27  
 Park, T.: T2-A1  
 Parsegian, V. A.: TP16  
 Passell, L.: WP34  
 Payzant, E. Z.: MP15  
 Pearce, J. V.: MP38  
 Pedersen, B. L.: TP09  
 Peña, V.: T3-C2  
 Pencer, J.: TP29  
 Penumadu, D.: T4-C5  
 Perahia, D.: M4-D5  
 Peral, I.: MP12  
 Perez-Salas, U.: MP26, W2-D4  
 Perring, T.: T4-B3  
 Perring, T. G.: M2-B5, MP49  
 Perry, H. P.: MP17  
 Petersen, V. K.: WP29  
 Petrov, S.: MP40  
 Petrovic, C.: MP11  
 Pheiffer, S.: WP44  
 Phelan, D. P.: MP23  
 Phelps, T. J.: TP41  
 Piccoli, P.: T4-B4  
 Piccoli, P. M.: TP28, W2-A4, WP39  
 Pingali, S. V.: M3-A2, MP17  
 Plummer, E. W.: M4-A3  
 Pomjakushin, V.: TP44  
 Porcar, L.: MP26, TP46  
 Porter, R. R.: TP43  
 Porter, W. D.: MP15  
 Powell, J. A.: TP53  
 Price, D. L.: MP58  
 Proffen, T.: M2-A4, MP15, MP30, MP34, MP36, TP04, TP47, TP55, WP05, WP07, WP11, WP16, WP17, WP50  
 Purcell, J. D.: WP64  
 Purwanto, A.: MP64  
 Pynn, R.: M4-A1, MP03

**Q**

Qian, J.: T3-B4, TP07  
 Qiu, X.: WP11  
 Qiu, Y.: M4-A2, M4-A5, MP20, MP46, T4-B4, W2-B3

**R**

Radaelli, P. G.: WP11  
 Raghavan, A. N.: T4-A4  
 Raghunathan, V. A.: M2-D3  
 Rainford, B. D.: WP54  
 Rajewska, A. G.: TP01  
 Ramesha, K.: TP55  
 Ratcliff, W. D.: T4-B4  
 Ratcliff II, W.: WP26  
 Rau, D. C.: TP16  
 Rawn, C. J.: TP09, TP41  
 Rehm, C.: TP61  
 Reich, D.: MP40  
 Reich, D. H.: W2-B2  
 Reiche, H. M.: MP02  
 Reiter, G.: MP65, T3-B3  
 Remmes, N. B.: MP09, WP14, WP35  
 Remsen, S.: WP04  
 Ren, W.: TP31  
 Ren, Y.: M4-B5, TP52  
 Rennich, G. Q.: TP11, TP21  
 Reynolds, B. J.: MP24  
 Rhyne, J. J.: M4-A1, MP34  
 Richards, J. D.: WP20  
 Richardson, J. W.: WP50, WP61  
 Richardson Jr., J. W.: WP04  
 Richardson, Jr, J. W.: TP34  
 Richter, D.:  
 Riedel, R. A.: WP20  
 Rinckel, T.: MP09, WP35  
 Ritter, C.: TP44  
 Rivera, S.: TP24  
 Rivera, S. A.: MP18  
 Robertson, J. L.: T2-A4, TP27, TP48, WP19  
 Robertson, L.: TP08  
 Rodgers, S. M.: TP26  
 Rodriguez, E. E.: MP34  
 Rodriguez, Y. W.: WP23, WP24  
 Roennow, H.: WP56  
 Rogge, R.: T4-D1, TP20  
 Rogge, R. B.: W2-C3  
 Roh, J. H.: MP12  
 Ronnow, H. M.: W2-B1  
 Rosenblad, P. M.: TP30

Rosenkranz, S.: MP23, MP43, WP59  
 Ruegg, M. L.: M4-D2, MP24  
 Rusevich, L.: MP48, TP58  
 Russell, R. A.: T4-A5  
 Russina, M.: TP62

**S**

Sahyun, S. C.: TP22  
 Sakai, O.: MP47  
 Sakiyama, N.: WP60  
 Saleh, T. A.: MP16  
 Sales, B.: MP30  
 Sales, B. C.: MP45, T4-B3, WP39  
 Sampath, S.: MP63  
 Sanabria-DeLong, N.: MP14  
 Santamaria, J.: T3-C2  
 Santella, M. L.: TP31  
 Santini, P.: MP20  
 Sarin, V. A.: WP37  
 Sarrao, J. L.: MP46, T2-A2, WP30  
 Sartbaeva, A.: WP63  
 Satija, S.: T3-A2  
 Sato, T.: MP61  
 Savici, A. T.: MP57  
 Schmidt, G.: TP46  
 Schmidt, M.: WP11  
 Schneidewind, A.: WP67  
 Schoenborn, B.: T4-A2, T4-A3  
 Schoenborn, B. P.: T4-A1  
 Schooling, S.: TP29  
 Schultz, A.: T4-B4  
 Schultz, A. J.: TP28, TP61, W2-A4, WP39  
 Schurtenberger, P.: M3-A4  
 Sears, D.: TP20  
 Sediako, D.: TP20, WP33  
 Seeger, P. A.: TP42  
 Sefat, A. S.: W2-B5  
 Sefrioui, Z.: T3-C2  
 Seong, B.: WP13  
 Seto, H.: T3-D3  
 Sha, H.: M4-A3  
 Shams, A.: M3-C5  
 Shapiro, S. M.: M2-B4, TP08, WP34  
 Shaw, K. M.: TP10  
 Shea, T. J.: wp64  
 Shi, D.: MP15  
 Shin, K.: WP13  
 Shingledecker, J. P.: TP31  
 Shirane, G.: M2-B3

Short, S.: MP42, WP49  
 Siewenie, J.: WP22  
 Simonson, J. M.: TP64  
 Singh, D.: MP26  
 Sinha, S. K.: T2-A4  
 Smith, G.: TP18  
 Smith, G. D.: T3-D1  
 Smith, G. S.: MP07, TP32, WP32  
 Snow, C. S.: WP32  
 Snow, W. M.: M4-C1, MP03, WP35, WP39  
 Snyder, G. J.: MP28  
 Sokol, P. E.: M3-A3, MP09, WP14, WP35  
 Sokolov, A. P.: MP12  
 Sokolov, d.: MP60  
 Soltner, H. P.: TP56  
 Soper, A. K.: WP48  
 Sparks, P. D.: T3-C3  
 Stalick, J. K.: TP09  
 Stanley, C.: TP16  
 Stevens, R.: WP47  
 Stillwell, B.: WP04  
 Stock, C.: M2-B1, MP47, T2-A3, T4-B5  
 Stoica, A. D.: M2-A4, M4-B4, MP15, MP16, MP51, TP21  
 Stone, M.: MP40  
 Stone, M. B.: MP45, MP50, T4-B3, W2-B2, WP10  
 Stowe, A.: M3-B3  
 Stowe, A. C.: M3-B5, WP05  
 Stowe, A. S.: MP55  
 Stradner, A.: M3-A4  
 Strobl, M.: MP41, MP48, TP58  
 Struzhkin, V.: WP15  
 Strycker, G. L.: M4-A2  
 Suescun, L.: MP32, WP04  
 Summers, P. R.: TP26  
 Sun, Y.: M4-B3, WP46  
 Sundaram, N. G.: WP07  
 Sur, B.: W2-C3  
 Swainson, I.: T4-D1  
 Swainson, I. P.: TP12, TP20  
 Swan-Wood, T.: M2-A6  
 Swiergiel, J.: WP12

## T

Tait, K.: TP07  
 Takagi, H.: MP61  
 Tang, F.: M3-D4, MP51, TP53, WP46  
 Tao, K.: MP19  
 Taylor, D. J.: M3-D4

Taylor, G. B.: TP48  
 Tchernyshyov, O.: W2-B2  
 te Velhuis, S. G. E.: M2-C5, T3-C2, T4-D2, W2-C6  
 Tealdi, C.: TP44, WP17  
 Telling, M. T.: MP04  
 Tew, G. N.: MP14  
 Thackeray, M. M.: WP51  
 Thanh Huy, N.: W2-B3  
 Thiagarajan, P.: M3-A2, MP17, MP22, TP61, W2-A2, W2-D3  
 Thomas, R. K.: M4-D3  
 Thompson, J. D.: T2-A2, WP30  
 Thurston, G. M.: M3-A4  
 Tian, W.: MP50, T4-B3  
 Timco, G.: MP20  
 Titmuss, S.: M4-D3  
 Tjebane, T.: TP03  
 Tobias, D. J.: WP28  
 Tokura, Y.: M4-A3, MP52  
 Tome, C. N.: M3-D2  
 Tomioka, Y.: M4-A3  
 Tong, X.: WP39  
 Tonomura, H.: MP47  
 Torikai, N.: TP15  
 Trabold, T. A.: T4-C3  
 Tranquada, J.: TP08  
 Tranquada, J. M.: MP49, W1-A1, WP62  
 Treimer, W.: MP41, MP48, TP58  
 Tremelling, G.: T4-B5  
 Trouw, F.: W2-A3, W2-A5  
 Trouw, F. R.: MP25, WP36  
 Tulk, C. A.: T3-B1, T4-D1  
 Turnbull, M. M.: T4-B5  
 Turner, J. F.: WP48  
 Turq, P.: TP49  
 Tuteja, A.: MP13

## U

Udby, L.: MP31  
 Udovic, T.: M3-B5, WP05  
 Ueda, H.: MP61  
 Urban, V. S.: T4-A4, TP17  
 Urquidi, J.: TP02, TP13, TP14, TP28  
 Uversky, V. N.: M3-A3

## V

Vaia, R. A.: TP19  
 Vajk, O.: MP62  
 Vajk, O. P.: M2-B2



Vakhrushev, S. B.: W2-A3  
 Vaknin, D.: M4-A5, WP38, WP56  
 Valincius, G.: TP36  
 Vanderah, D. J.: TP36  
 Varela, M.: T3-C2  
 Vaughey, J.: WP51  
 Verdal, N.: TP24, TP25, WP25  
 Villagran, D.: WP10  
 Vishik, I.: MP62  
 Visscher, T.: WP20  
 Vogel, S.: TP33  
 Vogel, S. C.: M3-D2, MP02  
 Volin, K. J.: TP23  
 Volksen, W.: MP10  
 Vorderwisch, P.: W2-B2  
 Vorobiev, A.: T4-D2

## W

W.T. Lee, C. Hoffmann, .: WP39  
 Wagh, A. G.: MP41  
 Wagner, W.: M3-D3  
 Wakimoto, S.: MP49  
 Wall, J. J.: MP02  
 Wall, J. J.: TP11  
 Wang, H.: TP09, W2-A6  
 Wang, J.: WP09  
 Wang, X.: M4-B2, TP21  
 Wang, X. L.: M2-A4, M4-B4, MP15, MP16, MP21, TP11  
 Wang, Y.: M4-B5, MP19  
 Warren, G. T.: M4-A4, WP65  
 Wassall, S. R.: M2-D2  
 Watkins, E. B.: TP32, WP32  
 Watkins, T.: M3-D4  
 Watkins, T. R.: TP53  
 Watson, M. J.: T4-C4, WP33  
 Watson, S. M.: T3-C3  
 Weiss, K. L.: T4-A4  
 Wells, S. A.: WP63  
 Wenk, R.: T4-C2  
 Werner, S. A.: MP06  
 Whan, T.: TP20  
 Whangbo, M. H.: W2-B5  
 Wietfeldt, F. E.: M4-C4, MP06  
 Wignall, G. D.: T4-A4, TP17  
 Wilde, K. L.: T4-A5  
 Wildgruber, U.: TP42  
 Willendrup, P. K.: MP31, W2-C2  
 Williams, D.: TP07  
 Williams, D. J.: TP33  
 Wilson, S.: MP59  
 Winans, R. E.: W2-A2  
 Winkler, B.: MP02  
 Winn, B. L.: TP06, TP08  
 Wiren, Z.: T3-C4  
 Woo, W.: M4-B2, MP21  
 Woodford, J. B.: M2-A2  
 Worcester, D.: T3-A1, WP03  
 Worlton, T. G.: TP28  
 Wozniak, D.: MP22  
 Wrenn, C.: WP02  
 Wright, M. C.: MP51  
 Wu, J.: TP15

## X

Xu, C.: TP11  
 Xu, G.: M2-B1, WP62  
 Xu, H.: TP07  
 Xu, J.: T4-D1  
 Xu, Z.: W2-A6

## Y

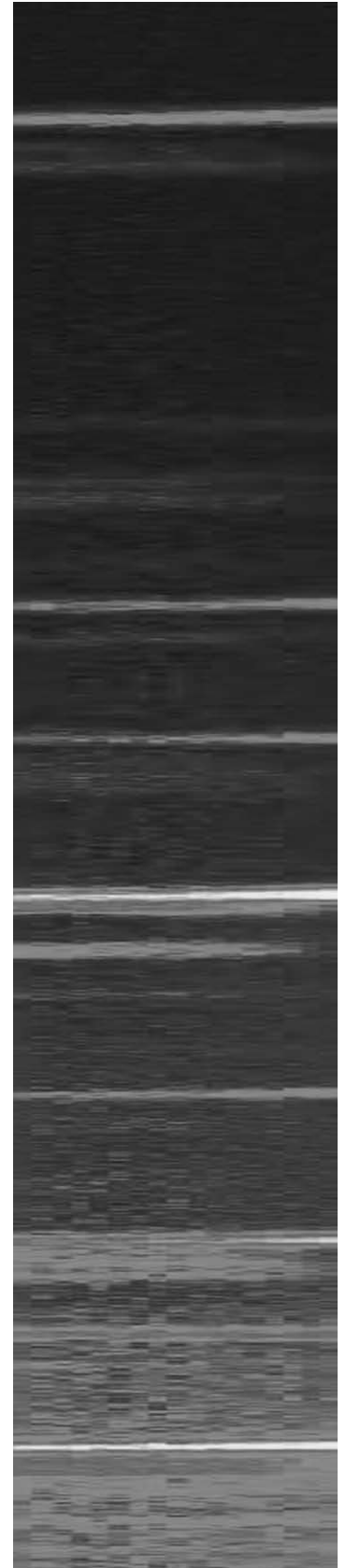
Yamada, K.: MP49, WP62  
 Yamada, N. L.: T3-D3  
 Yan, H. Y.: WP39  
 Yan, J.: MP25  
 Yang, J.: TP09  
 Yang, L.: M2-A4, MP15  
 Yarger, J. L.: MP63, WP22, WP48  
 Yaron, P. N.: MP29  
 Ye, F.: M4-A3, MP52, WP23  
 Ye, Z. G.: M2-B3  
 Yeary, L.: TP41  
 Yen, C.: T3-B2  
 Yeng, F.: WP24  
 Yeo, S.: T4-B4  
 Yethiraj, M.: M2-B5, TP27, W2-B3  
 Yi, Z.: M2-D4, TP37  
 Yildirim, T.: M3-B1, W1-A2  
 Yim, Y.: T3-A2  
 Ying Kai, H.: W2-B3  
 Yoonessi, M.: TP19  
 Yoshizawa, H.: TP08, WP60  
 Yu, G.: MP62

## Z

Zaliznyak, I.: MP40, WP34, WP60  
 Zaliznyak, I. A.: MP57

Zarestky, J.: T2-A5  
Zarestky, J. L.: T2-A2, WP38, WP56  
Zhang, J.: M4-A3, T3-B4, TP07  
Zhang, Y.: MP22, TP18  
Zhao, J. K.: TP26  
Zhao, X.: MP62  
Zhao, Y.: TP07  
Zheludev, A.: T4-B1  
Zhigadlo, N. D.: WP18  
Zhou, J.: WP26, WP42  
Zoto, I.: MP67  
Zuo, L.: M4-B5

## Vendor Ads







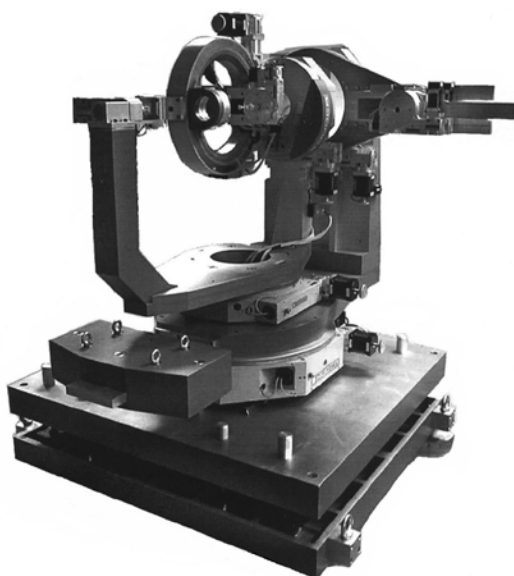
---

BLAKE INDUSTRIES, INC.

---

*Your complete source for:*

**Goniometer Heads  
Huber Components  
Complete Diffractometers  
Custom Designs**



6+2 - Circle PSI - Diffractometer

More than 4500 professionals at over 1400  
research locations have chosen Blake Industries  
for their X-ray diffraction instrumentation.

**Let us put our experience to work for you.**

---

**BLAKE INDUSTRIES, INC.**

660 Jerusalem Road  
Scotch Plains, New Jersey 07076 USA

Tel: +1 908 233 7240

Fax: +1 908 233 1354

E-mail: [blake4xray@worldnet.att.net](mailto:blake4xray@worldnet.att.net)



# What's new from Oxford Instruments?

$^3\text{He}$       **Helium Dilution Refrigerators**      Kelvinox  
Teslatron      HelioxAC-V      7mK      High Field Magnets  
**Cryofree**      xray      Nanotechnology      **Spectroscopy**  
Liquid Helium Cryostats      Luminescence  
**Microscopy**            Heliox  
Microstat            **ULT**  
FTIR      Raman      **Superconducting Magnets**  
Liquid Nitrogen Cryostats      Custom Magnets      Magneto-Optical  
MicrostatB-T      Cryojet      Optistat       $^4\text{He}$   
ESR      Spectromag      **NMR**      **ICR**

**[www.oxford-instruments.com](http://www.oxford-instruments.com)**

Meet with Oxford Instruments at our exhibition booth  
and get the very latest news on our innovative products.

ANL and APS Researchers with  
Technical and Sales Questions please contact:

Rick Hapanowicz

(847) 590-9581

[hapanowicz@ma.oxinst.com](mailto:hapanowicz@ma.oxinst.com)



# TOSHIBA

TOSHIBA ELECTRON TUBES & DEVICES CO., LTD (TETD) is one of the leading radiation detector manufacture in the world such as X-ray / neutron proportional counters (PC), Ion chambers and Position Sensitive Detectors (PSD). And also we offer Beam Loss Monitors (BLM) for proton or electron beam accelerators. In addition, we have various kinds of microwave products, which are Klystrons, Gyrotrons and high power Couplers/Windows for scientific and industrial applications.

## **TOSHIBA ELECTRON TUBES & DEVICES CO.,LTD.**

Website:

[www.toshiba-tetd.co.jp/tetd/eng/](http://www.toshiba-tetd.co.jp/tetd/eng/)

Contact:

Hiroshi Saito

1-1-1 Shibaura, Minato-ku, Tokyo,105-8001, Japan

Tel: +81-(3) 3457-4870 Fax: +81-(3) 5444-9325

[hiroshi3.saito@toshiba.co.jp](mailto:hiroshi3.saito@toshiba.co.jp)

---

# **SwissNeutronics**

**Neutron Optical Components  
& Instruments**

Bruehlstrasse 28, CH-5313 Klingnau, Switzerland  
phone: +41 56 245 0202, fax: +41 56 245 0204  
tech@swissneutronics.ch, www.swissneutronics.ch



*focusing guides*



*guides*



*guide  
switches*



*complex truly  
curved guides*



*polarizing  
benders*



*monochromators/analyzers*



*monochromator shieldings*

*from ideas...  
...to solutions*

*Distributor for USA, Canada and China:*

**American Scientific Instrumentation**

213 Whippoorwill Dr., Oak Ridge, TN 37830

phone: +1 865 483 8460, cellular: +1 865 789 0899

american-si@comcast.net, <http://american-si.home.comcast.net>

## euro collimators



Euro Collimators is a UK based company that designs, develops and manufactures collimators for the scientific community.

The company has successfully designed, developed and produced Soller, Diverging, Double Diverging, Honeycomb, Radial and ORC collimators utilising a variety of materials and methods. These include foils made of Mylar, Peek and Stainless Steel with coatings of either Gadolinium Oxide or Boron.



We have developed and manufactured a system for the tensioning of small divergence radial collimators that enables blade spacing of less than 0.5mm to be accurately positioned.



The company offers a complete service that includes involvement with scientists and engineers at the earliest stage of development through to delivery and installation at the customer's premises.

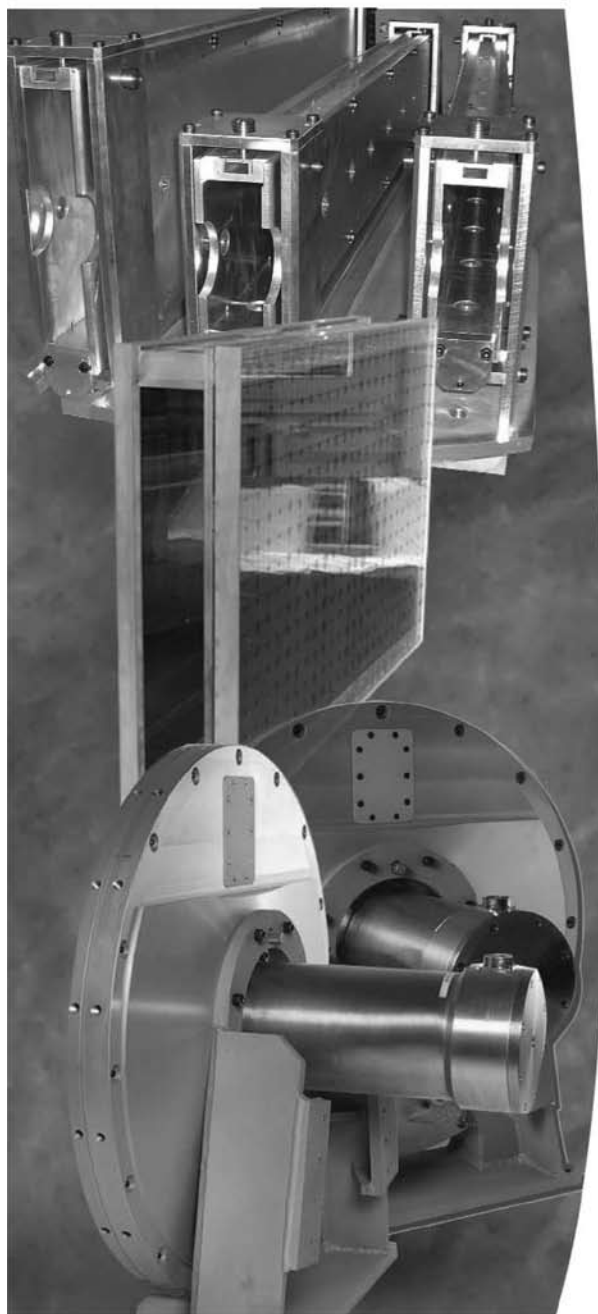
*Euro Collimators Ltd  
T Booth works  
Elmstone Hardwicke  
Cheltenham  
GL51 9TB  
United Kingdom*

*Tel : +44 (0) 1242 242806  
Fax : + (0) 1242 224176  
Email: [sales@eurocollimators.com](mailto:sales@eurocollimators.com)  
[www.eurocollimators.com](http://www.eurocollimators.com)*





## Partners in Neutron Science



### **Guides**

- Large capacity sputter coating capability
- Super mirror coatings to  $m=4.0$
- 100% quality inspection on each guide section on neutron reflectometer
- Specialized guide designs, converging/focusing

### **Guide Systems**

- Complete guide system design
- Specialized shielding, support structure & vacuum housing
- Expert installation & alignment teams
- Shutter guides, In pile guides, choppers & chopper housings
- Worldwide on-site installation capabilities

### **Choppers**

- BWL choppers
- Femmi choppers
- Tø choppers
- Single & dual blade chopper systems
- Customized sizes & geometries
- Magnetic bearing designs

***Contact us for consultation,  
quotation or proposals.***

06-045

**Kurt J. Lesker**  
Company

412.387.9200

1.800.245.1656

John Lubic

neutron@lesker.com

1925 Worthington Ave, Clairton PA 15025



- > Detector Electronics**
- > Readout Systems**
- > High Voltage**
- > VME & VME64x**
- > NIM & CAMAC**



**wieNER**

Plein & Baus Elektronik

Werk für  
Industrie-  
elektronik  
Nuclear-  
elektronik  
Regelungs-  
technik

[www.wiener-us.com](http://www.wiener-us.com)

